

AD-A202 520

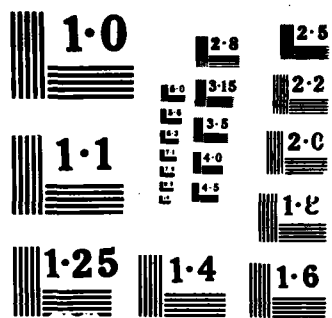
INTERNATIONAL CONFERENCE ON MULTIPHOTON PROCESSES (4TH)
HELD IN BOULDER CO. (U) JOINT INST FOR LAS ASTROPHYSICS
BOULDER CO JUL 88 AFOSR-IR-88-1278 AFOSR-87-0221

1/4

UNCLASSIFIED

F/G 7/5

NL



DTIC FILE COPY

2

PROGRAM AND ABSTRACTS

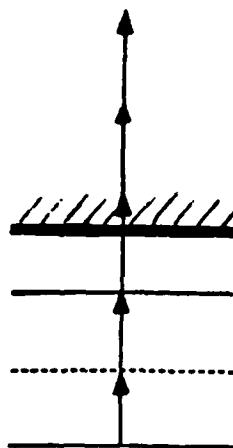
AD-A202 520

ICOMP IV

AFOSR-TR- 88 - 1278

International Conference on Multiphoton Processes

Joint Institute for Laboratory Astrophysics
July 13-17, 1987 • Boulder, Colorado USA



AIR FORCE OFFICE OF SCIENTIFIC RESEARCH (AFOSR)
NOTED FOR RELEASE TO DTIC
This document has been reviewed and is
approved for release in accordance with AFM 190-12.
Distribution is unlimited.
MATTHEW J. MILLER
Chief, Technical Information Division

Approved for public release;
distribution unlimited.

University of Colorado



DTIC
SELECTED
DEC 16 1988
OE

REPORT DOCUMENTATION PAGE

1a. REPORT SECURITY CLASSIFICATION UNCLASSIFIED			1b. RESTRICTIVE MARKINGS			
2a. SECURITY CLASSIFICATION AUTHORITY			3. DISTRIBUTION / AVAILABILITY OF REPORT Approved for public release; distribution is unlimited.			
2b. DECLASSIFICATION / DOWNGRADING SCHEDULE						
4. PERFORMING ORGANIZATION REPORT NUMBER(S)			5. MONITORING ORGANIZATION REPORT NUMBER(S) AFOSR-TR- 88 - 1278			
6a. NAME OF PERFORMING ORGANIZATION Univ of Colorado		6b. OFFICE SYMBOL (if applicable)	7a. NAME OF MONITORING ORGANIZATION AFOSR/NP			
6c. ADDRESS (City, State, and ZIP Code) Campus Box B-19 Boulder, CO 80309-0019			7b. ADDRESS (City, State, and ZIP Code) Building 410, Bolling AFB DC 20332-6448			
8a. NAME OF FUNDING / SPONSORING ORGANIZATION AFOSR		8b. OFFICE SYMBOL (if applicable) NP	9. PROCUREMENT INSTRUMENT IDENTIFICATION NUMBER AFOSR-87-0221			
8c. ADDRESS (City, State, and ZIP Code) Building 410, Bolling AFB DC 20332-6448			10. SOURCE OF FUNDING NUMBERS			
			PROGRAM ELEMENT NO. 61102F	PROJECT NO. 2301	TASK NO. A4	WORK UNIT ACCESSION NO.
11. TITLE (Include Security Classification) (U) FOURTH INTERNATIONAL CONFERENCE ON MULTIPHOTON PROCESSES						
12. PERSONAL AUTHOR(S)						
13a. TYPE OF REPORT FINAL		13b. TIME COVERED FROM 1 Jun 87 to 30 May 88		14. DATE OF REPORT (Year, Month, Day) 13 July 88		
15. PAGE COUNT 349						
16. SUPPLEMENTARY NOTATION						
17. COSATI CODES			18. SUBJECT TERMS (Continue on reverse if necessary and identify by block number)			
FIELD	GROUP	SUB-GROUP				
	20.08					
19. ABSTRACT (Continue on reverse if necessary and identify by block number) The Fourth International Conference on Multiphoton Processes was held on 13-17 July 1987 at the Joint Institute for Laboratory Astrophysics in Boulder, Colorado. Sixteen scientific sessions were held and approximately eighty papers were presented.						
20. DISTRIBUTION / AVAILABILITY OF ABSTRACT <input checked="" type="checkbox"/> UNCLASSIFIED/UNLIMITED <input checked="" type="checkbox"/> SAME AS RPT. <input type="checkbox"/> DTIC USERS			21. ABSTRACT SECURITY CLASSIFICATION UNCLASSIFIED			
22a. NAME OF RESPONSIBLE INDIVIDUAL R E KELLEY			22b. TELEPHONE (Include Area Code) (202) 767-4908		22c. OFFICE SYMBOL AFOSR/NP	

PROGRAM AND ABSTRACTS

**FOURTH INTERNATIONAL CONFERENCE
ON MULTIPHOTON PROCESSES**

July 13-17, 1987



Accession For	
NTIS GRA&I	<input checked="" type="checkbox"/>
DTIC TAB	<input type="checkbox"/>
Unannounced	<input type="checkbox"/>
Justification	
By	
Distribution/	
Availability Codes	
Dist	Avail and/or Special
A-1	

**Joint Institute for Laboratory Astrophysics
University of Colorado
Boulder, Colorado 80309**

Organizing Committee

L. Armstrong, Jr.
C. Clark
R. M. Compton
J. H. Eberly
C. Fotakis
P. L. Knight
M. Kroo
V. S. Latokhov
C. Manus
C. K. Rhodes
K. Rzaewski
M. J. van der Wiel
H. Walther
P. Zoller
S. J. Smith, Chairman

Program Committee

P. Agostini
L. Armstrong, Jr.
R. R. Freeman
P. L. Knight
V. S. Latokhov
J. P. Reilly

Local Committee

J. Cooper
S. Geltman
W. C. Lineberger
D. W. Norcross
M. F. Ramsey
S. J. Smith
V. Vaida
L. A. Westling

Sponsors

We gratefully acknowledge sponsorship from the following organizations:

International Union of Pure and Applied Physics
National Science Foundation
Air Force Office of Scientific Research
Office of Naval Research
Department of Energy Office of Basic Energy Sciences
National Bureau of Standards
University of Colorado

This work relates to Department of Navy Grant N00014-67-A-0004
awarded by the Office of Naval Research. The U. S. Government
owns a proprietary interest throughout the world in all copy-
rights in the above mentioned work.

PROGRAM

FOURTH INTERNATIONAL CONFERENCE ON MULTIPHOTON PROCESSES

Boulder, Colorado
July 13-17, 1987

Sessions in Duane G-030 are labeled with "G" (i.e. A-G).
Sessions in the JILA Auditorium are labeled with "J" (i.e. A-J).
Underline indicates invited speaker.

Monday, July 13

Page

Session A-G Above Threshold Ionization

9:00 a.m. (L. Armstrong, Jr., Chair)

- "The Role of Ponderomotive Potentials in Above-Threshold Ionization,"
R. R. Freeman (AT&T Bell Laboratories, Murray Hill) 1
- "Electron Energy Spectra in High Intensity Multiphoton Ionization,"
G. Petite (CEN/Saclay) 2
- "Quasi-Classical Approach to Multiphoton Ionization of Hydrogen Atoms,"
I. J. Bersons (Latvian SSR Academy of Sciences, Riga) 3
- "Numerical Experiments on Above-Threshold Ionization," J. Javanainen
(University of Rochester) 4
- "Essential States Approach to Above Threshold Ionization in Application
to Hydrogen Atoms," K. Rzaewski and M. Trippenbach (Polish
Academy of Sciences, Warsaw), and R. Grobe (Universität Essen) 7

Session A-J Multiphoton Processes in Molecules

11:00 a.m. (P. M. Dehmer, Chair)

- "Multiresonant Spectroscopy and the Dynamics of Nonradiative Decay in
Molecular Rydberg States," K. S. Haber, F. X. Campos,
J. W. Zwanziger, R. T. Wiedmann and E. R. Grant
(Purdue University) 10
- "High Resolution Multiphoton Spectroscopy of Rydberg States of NO,"
D. T. Biernacki, S. D. Colson and E. E. Eyler (Yale University) 13
- "Experimental Investigations of Circular Dichroism in Photoelectron
Angular Distributions," J. R. Appling and M. G. White (Brookhaven
National Laboratory) 16

Session B-G Above Threshold Ionization

2:00 p.m. (G. Menz, Chair)

- "Angular Distributions of Photoelectrons from Above-Threshold
Ionization of Hydrogen and Xenon Atoms," D. Feldmann,
B. Wolff, H. Rottke, M. Weshöner, and K. H. Welge
(Universität Siefeld) 18

Session B-G 2:00 p.m. - continued

Page

- "Limiting Cases of Excess-Photon Ionization," H. B. van Linden van den Heuvell and H. G. Muller (FOM Institute) 20
- "Electron Wave Packets, Multiphoton Absorption and Diffusion in a Continuous and Quasi-Continuous Atomic Spectrum," M. V. Fodorov (USSR Academy of Sciences, General Physics Institute, Moscow) 23
- "Model Theory of Pulse Shape Effects in Above Threshold Ionization," H. Huang, L. Roso-Franco and J. H. Eberly (University of Rochester) 24
- "High Order Multiphoton Ionization Without Tunneling," H. R. Reiss (The American University, Washington, DC) 27
- "Consequences of a Final State Model of Above-Threshold Ionization," W. Becker (University of New Mexico) R. R. Schlicher (Max-Planck Institut für Quantenoptik, Garching), M. O. Scully (University of New Mexico) and K. Wódkiewicz (Warsaw University, Poland) 30

Session B-J1 Multiphoton Processes in Molecules

2:00 p.m. (W. C. Lineberger, Chair)

- "Photoelectron Studies of Multiphoton Processes in Small Molecules," S. T. Pratt, M. A. O'Halloran, F. S. Tomkins, J. L. Dehmer, and P. M. Dehmer (Argonne National Laboratory) 33
- "Theoretical Resonant Multiphoton Ionization Studies in Molecules," S. N. Dixit (University of California), R. L. Dubs, H. Rudolph, and V. McKoy (California Institute of Technology) 35
- "Multiphoton Molecular Spectroscopy," M. N. R. Ashfold (University of Bristol) 38
- "Intramolecular Couplings Studied by Doppler-Free Two-Photon Processes," E. Riedle and H. J. Neusser (Technische Universität, München) 39
- "Dephasing Effects on Time-Resolved Multiphoton Transitions of Molecules," Y. Nomura, M. Hayashi, Y. Fujimura (Tohoku University, Japan), and S. H. Lin (Arizona State University) 42

Session B-J2 Atomic Hydrogen in Intense Laser Fields

4:30 p.m. (K. H. Welge, Chair)

- "Dressing and Photoionization of the H Atom in an Ultraintense Laser Field," M. Janjusević and M.H. Mittleman (City College, New York) 44
- "The Structure of Atomic Hydrogen in High-Intensity, High-Frequency Laser Fields of Linear Polarization," M. Pont, N. Walet, M. Gavrilu (FOM Institute) and C. W. McCurdy (Ohio State University) 47
- "Atomic Hydrogen in Circularly Polarized, High-Intensity and High-Frequency Laser Fields," M. Pont, M. J. Offerhaus and M. Gavrilu (FOM Institute) 50

Tuesday, July 14, 1987

Page

Session C-G Quantized Externally Driven Chaotic Systems

8:30 a.m. (J. E. Bayfield, Chair)

- "Experimental Signatures of Atomic Many-Photon Absorption in the Classically-Chaotic Regime," J. E. Bayfield (University of Pittsburgh) 53
- "Quantum-Mechanical Aspects of Classically Chaotic Driven Systems," P. W. Milonni (Los Alamos National Laboratory) 56
- "Exponential Photonic Localization and Chaos in the Hydrogen Atom in a Monochromatic Field," G. Casati (Universita di Milano) 58
- "Quantum Mechanical Approaches to Multiple-Photon Absorption: Computing with Thousands of States," R. E. Wyatt (University of Texas at Austin) 60
- "Vibrational Chaos in Infrared Multiphoton Excitation of Polyatomic Molecules," E. A. Ryabov (Institute of Spectroscopy, USSR Academy of Sciences, Troitzk, USSR) 61

Session C-J Collisions and Half-Collisions in Intense Fields

10:45 a.m. (K. Burnett, Chair)

- "Coupled Equations Approach to Half-Collisions in Intense Fields," A. Bandrauk (Université de Sherbrooke, Canada) 62
- "Femtosecond Dynamics of Multielectron Dissociative Ionisation Using a Picosecond Laser," L. J. Frasinski, K. Codling and P. Hatherly (University of Reading) 63
- "A New Class of Resonances in the $e\text{-H}^+$ Scattering in an Excimer Laser Field," L. Dimou and F. H. M. Faisal (Universität Bielefeld) 66
- "Laser-Assisted Potential Scattering. An Assessment of Recent New Results," B. Piraux (Imperial College of Science & Technology); F. Trombetta, G. Ferrante and G. Messina (Istituto di Fisica dell'Università, Palermo, Italy) 69

Session D-G Above Threshold Ionization

2:00 p.m. (J. E. Sharly, Chair)

- "Atomic Processes in Strong Laser Fields," H. O. Lutz (Universität Bielefeld) 71
- "ATI Polarization Experiments and Calculations for Xenon and Krypton," P. H. Bucksbaum, M. Bashkansky, and D.W. Schumacher (AT&T Bell Laboratories, Murray Hill, New Jersey) 72
- "Theory of Atoms in Strong Electromagnetic Fields," A. Szöke (Lawrence Livermore National Laboratory) 75
- "Multiphoton Ionization of Xenon from 570 nm to 600 nm," M. D. Perry (University of California, Berkeley), E. M. Campbell, O. L. Landen and A. Szöke (Lawrence Livermore National Laboratory) 78

- "Multiphoton Ion Production in Intense Fields: A Quantitative Approach," G. A. Kyrala, D. E. Casperson, P. H. Y. Lee, L. A. Jones, A. J. Taylor and G. T. Schappert (Los Alamos National Laboratory)

81

Session D-J Multiphoton Processes in Atoms

2:00 p.m. (P. Zoller, Chair)

- "Gaussian and Pre-Gaussian Laser Noise in Multiphoton Transitions," K. Wódkiewicz (Warsaw University, Poland) 82
- "Saturation of an Optical Transition by a Phase-Diffusing Laser Field," M. W. Hamilton, D. S. Elliott, K. Arnett and S. J. Smith (JILA, University of Colorado) 84
- "Theory of Double Optical Resonance: Collisional Broadening and Doppler Effects on ac Stark Splitting," A. M. F. Lau (Sandia National Laboratories, California) 87
- "Multistep Resonance Excitation of Autoionizing States in the Rare-Earth Elements," V. N. Fedoseyev (Institute of Spectroscopy, USSR Academy of Sciences, Troitsk, USSR) 89
- "Population Trapping and a Generalization of Fermi's Golden Rule for the Strong Bound-Continuum Transitions," K. Rzaewski, R. Kukliński and J. Mostowski (Polish Academy of Sciences, Warsaw) 90
- "Application of State-Multipole Heisenberg Equations to Multiphoton Excitation Dynamics," B. W. Shore and R. Sacks (Lawrence Livermore National Laboratory) 92
- "Abnormal Peak Structure in Doubly-Resonant Three-Photon Ionization of a Four-Level System with Two Near-Degenerated Intermediate Levels," M-Y Hou, Y-B Shi, B-H Feng and Y-L Shao (Academia Sinica, Beijing, China), Q-S Han (Central College of Nationalities, Beijing, China), Q-S Zhu (Academia Sinica, Dalian, China) 93

4:30 PM Poster Session - Kittredge Residence Hall Campus (see p. 183)

Wednesday, July 15, 1987

Session E-G Formation and Decay of Multiply Excited States

8:30 a.m. (J. Cooper, Chair)

- "Precise Calculations of Properties of Multiply-Excited States," C. F. Bunge (Universidad Nacional Autonoma de Mexico) 96
- "The Formation and Decay of Triply Excited States in e-He Scattering," R. S. N. Eldridge (Rijksuniversiteit Utrecht) 97
- "Hyperspherical Description of Multiply-Excited States: Triply-Excited States of He," A. Skrzypczak (CNRS, Observatoire de Paris-Meudon) 99
- "The Contribution of Autoionizing States to Multiphoton Ionization of Alkali earth atoms," Y. I. Izrael (University of Magerod, USSR) 102

Session E-G 8:30 a.m. - continued

Page

- "Two-Electron Excitation in an Intense Laser Pulse - The Outer Electron Shell of Magnesium," K. Burnett (Imperial College, UK) 103
- "Phase Space Approach to Two Electron Ionization," J. Mostowski (Polish Academy of Sciences, Warsaw), M. Trippenbach (Warsaw University) and C. L. Van (Polish Academy of Sciences, Warsaw) 104

Thursday, July 16, 1987

Session F-G Multiphoton Processes in Molecules

8:30 a.m. (J. P. Reilly, Chair)

- "Unimolecular Decay of Rotational-Selected Polyatomic Molecular Ions Prepared by Resonance-Enhanced Multiphoton Ionization," H. J. Neusser, H. Kühlewind, A. Kiermeier, E. W. Schlag (Technische Universität, München, FRG) 107
- "Structure and Dynamics of Isolated Molecules and Clusters," E. R. Bernstein (Colorado State University, Fort Collins) 110
- "Two-Photon Excitation of Dense Sodium Vapor near the $nd^2D_{5/2,3/2}$ ($n=3,4,5,7$) Levels: $Na_2b^3\Sigma_g^+ \rightarrow X^3\Sigma_u^+$ Excimer Emission," S. J. Bajic (University of Tennessee), R. N. Compton and J. A. D. Stockdale (Oak Ridge National Laboratory) 111
- "Linear Spectroscopy Using Non-Linear Optics," J. W. Hepburn, D.J. Hart and I. M. Waller (University of Waterloo, Canada) 114
- "Probing of Molecular Alignment Effects Using 'Saturated' Pulsed Laser Excitation," H. Meyer, R. Dressler, and S.R. Leone (JILA, University of Colorado) 117
- "MPD/MPI of Organometallic Molecules - The Role of Non-Radiative Processes in Determining Free Metal State Distributions," J. Chaiken (Syracuse University) 119
- "Resonant Multiphoton Laser-Surface Interaction," J. Reif, H. B. Nielsen, P. Tepper, O. Semmler, E. Matthias (Freie Universität Berlin), E. Fridell, E. Westin and A. Rosen (Chalmers University of Technology and University of Goteborg, Sweden) 120
- "Laser Excitation of Electronic States of Atoms Near Surfaces," A. C. Greenfield and K. Burnett (Imperial College); P. T. Greenland (Harwell) 123

Session F-I Interference and Competition in Multiphoton Excitation

8:30 a.m. (R. E. Garton, Chair)

- "Influence of Internally Generated Sum-Frequency Fields on Odd-Photon Excitations of Dipole-Allowed Transitions in Atomic Gases," R. E. Garton (Oak Ridge National Laboratory) 124
- "Nonlinear Optical Solitons," J. L. Ryan (IBM Thomas J. Watson Research Center) 125
- "IR and UV Ultrashort Pulse Generation by Hyper-Raman Scattering and Four-Wave Mixing in Metal Vapors," Yu. P. Malakian (Armenian Academy of Sciences, USSR) 128

Session F-J 8:30 a.m. - continued

Page

- "Suppression of N-Photon Absorption by the Four-Wave Mixing Process,"
D. J. Gauthier, M. S. Malcuit and R. W. Boyd (University of
Rochester) 129
- "Multiphoton Ionization Induced by 3rd Harmonic Internally Generated
in Kr," P. Lambropoulos and X. Tang (University of Southern
California) 132
- "Investigations of Electron Correlations Using Residual Ion
Fluorescence Detection," L. D. Van Woerkom, J. G. Story and W. E.
Cooke (University of Southern California) 134
- "Influence of Different Exit Channels on the Interference Effects in
the Autoionization of Two Strongly Coupled States," S. Ravi and
G. S. Agarwal (University of Hyderabad, India) 137
- "Interference Between the Two-Level Dressed Atom and Three-Level Free
Induction Decay in Cesium," H. W. H. Lee and J. E. Wessel (The
Aerospace Corporation) 139

Session G-G Infrared Multiphoton Processes

2:00 p.m. (G. Fotakis, Chair)

- "Vibrational Relaxation of Highly Excited Molecules," R. J. Gordon,
K. M. Beck, and M. Koshi (University of Illinois at Chicago) 142
- "Non-Thermal Intramolecular Vibrational Energy Distribution in
Isolated Infrared Multiphoton Excited CF_2Cl_2 Molecules," E.
Mazur, K-H Chen and J. Wang (Harvard University) 144
- "Characterization and Exploitation of Vibrationally Excited
Populations Produced by IRMPA," J. R. Barker, T. C. Brown,
J.-M. Zellweger, and M. Yerram (University of Michigan) 147
- "Multiphoton Absorption and Luminescence of Chromyl Chloride,"
M. Ivancic, D. K. Evans and R. D. McAlpine (Chalk River Nuclear
Laboratories, Canada) 150
- "Multiple Photon Absorption and Self-Focusing in CDF_3 ," S. L. Chin
(University of Laval) 153
- "IR Multiphoton Absorption with a High Pressure CO_2 Laser: Role of
the Laser Linewidth," G. Angelis, R. Capitini, and P. Girard
(CEN/Saclay, France) 154
- "Rates, Recurrences and Population Trapping in Quasi-Continuum and
Structured Continuum Photoexcitation," P. Radmore (University
College, London) P. Knight and S. Tarzi (Imperial College) 155

Session G-J Theory: Applications to Multiphoton Processes

2:00 p.m. (S. Galtman, Chair)

- "Finite Fermi Systems Method for the Multiphoton Processes in Many-
Electron Atoms," L. E. Baganoff (Voronezh State University, USSR) 157
- "Theory of Multiphoton Ionization of Atoms by Strong, Short Pulsed
Lasers," E. C. Hulander (Lawrence Livermore National Laboratory) 158

Session G-J 2:00 p.m. - continued

Page

- "Two- and Three-Photon Double Ionization and Excitation of Xenon,"
A. L'Huillier (CEN/Saclay, France) and G. Wendin (Chalmers
University of Technology, Sweden) 160
- "Two-Photon Ionization of Rare Gas Atoms: A Relativistic Time-
dependent Hartree-Fock Approach," M. G. J. Fink and W. R. Johnson
(University of Notre Dame) and P. Zoller (Universität Innsbruck) 163
- "Multiphoton Detachment in Negative Ions of Halogens," M. Grance (CRNS,
Orsay, France) 166
- "Rydberg Electrons in Laser Fields: A Finite Range Interaction
Problem," A. Giusti (CNRS, Orsay, France) and P. Zoller
(Universität Innsbruck) 169
- "Two and Three Photon Ionization of Helium with a Resonant Autoionizing
State," H. Bachau (Université de Bordeaux I) and P. Lambropoulos
(University of Southern California) 172

Friday, July 17, 1987

Session H-G Closing Session

9:30 a.m. (P. Lambropoulos, Chair)

- "State-resolved Study of Collisional Energy Transfer Studied by Laser
REMPI Spectroscopy," G. Sha, D. Proch, and K. L. Kompa
(Max-Planck Institut für Quantenoptik, Garching). 175
- "Laser Spectroscopy of Core-Excited Levels of Neutral Rubidium,"
S. E. Harris, J. K. Spong, and J. F. Young (Stanford University) 176
- "Nonclassical Radiation Generators," H. Walther (Max Planck Institut
für Quantenoptik, Garching) 177
- "En Route to One Petawatt," G. A. Mourou (University of Rochester) 178
- "Studies of Soft X-Ray Fluorescence from Excited States Produced by
Multiphoton Processes," C. K. Rhodes (University of Illinois at
Chicago) 179
- "Highly Excited Hydrogen Atoms in Strong External Fields," K. H. Welge
(Universität Bielefeld) 180

Summary Discussion and Overview

- P. Lambropoulos (University of Southern California and The Research
Center of Crete) 181

Invited Paper

THE ROLE OF PONDEROMOTIVE POTENTIALS IN ABOVE-THRESHOLD IONIZATION

R. R. Freeman

AT&T Bell Laboratories

Murray Hill, NJ 07974

This talk will summarize the phenomenology of Above-Threshold Ionization (ATI) with special emphasis on the role of final state interactions: specifically the effects of the elastic and inelastic scattering of the ionized electrons by the ponderomotive forces arising from the intense laser fields. There are now several important experimental results that show the diverse breadth of the effects: the suppression of low energy ATI using circularly polarized light, the dependence of the angular distributions upon light intensity and electron energy, and the recent results showing how electrons gain and lose energy from high intensity laser beams. These experimental results will be reviewed, and comparisons with classical computer trajectories will be presented. In addition, new, unpublished results of ATI using sub-picosecond pulse lengths will be presented that show how significantly the ponderomotive potentials can determine the shifts of peaks, their widths and shapes.

Invited Paper

ELECTRON ENERGY SPECTRA IN HIGH INTENSITY MULTIPHOTON IONIZATION

G. Petite

CEN/Saclay

DPh.G/S.P.A.S.

91191 Gif-sur-Yvette Cedex

France

Invited Paper

QUASI-CLASSICAL APPROACH TO MULTIPHOTON IONIZATION OF HYDROGEN ATOMS

I. J. Bērsons

Institute of Physics
Latvian SSR Academy of Sciences
229021 Riga, SALASPILS, USSR

Multiphoton ionization of hydrogen atoms both at small and large ratio of the frequency of the external field to that of the Rydberg electron is considered. For high field frequencies the high-order quasi-classical perturbation theory is developed and comparison with quantum mechanical calculations is presented. At low frequencies a one-dimensional hydrogen atom is considered. The penetration through the periodically varying potential barrier at energies near the top of the barrier is discussed and some of the experimental results of ionization of hydrogen atoms in a microwave field are explained.

NUMERICAL EXPERIMENTS ON ABOVE-THRESHOLD IONIZATION

Juha Javanainen
Department of Physics and Astronomy
University of Rochester
Rochester, NY 14627

The objective of this work is to elucidate the mechanism of Above-Threshold Ionization (ATI) by means of numerical model experiments.

I integrate the time dependent Schrödinger equation of a one-dimensional atom using the Crank-Nicholson space-time algorithm. The full Hamiltonian in the external field reads

$$H = -\frac{1}{2} \frac{\partial^2}{\partial x^2} - \frac{1}{\sqrt{1+x^2}} + xE \sin \omega t. \quad (1)$$

The integration is started at time $t = 0$ from the ground state of the time independent Hamiltonian, and at time t the photoelectron spectrum $P(W;t)$ is formed by projecting the state vector onto the energy eigenstates $|W\rangle$.

At the time scale of one cycle of the field, the photoelectron spectrum exhibits a variation exactly analogous to the forced motion of a classical electron. The quivering motion comes to a standstill at $n + 1/4$ and $n + 3/4$ cycles of the field. Accordingly, only for such times do I obtain photoelectron spectra with peak separation equal to the photon energy. I have not been able to ascertain any longer-term systematic variation of the positions and areas of the photoelectron peaks once they are resolved after about two cycles of the field, and thus I present the results for times corresponding to 4.25 cycles of the field.

The widely accepted explanation¹ for the vanishing of the lowest photoelectron peaks in the ATI spectrum combines two notions. First it is assumed that the continuum threshold shifts upward with intensity by an amount which (almost) equals the ponderomotive potential $W_p = E^2/4\omega^2$. Second, the released electrons gain the kinetic energy W_p as they leave the laser focus. The photoelectron energy peaks thus emerge at (nearly) the unperturbed zero-field energies, except that the peaks corresponding to the channels which are closed because of the dynamic raising of the continuum threshold, are absent.

This description is not² fully consistent with experiments, and, because I do not incorporate spatial inhomogeneity of the field intensity responsible for the ponderomotive

JOINT INSTITUTE FOR LABORATORY ASTROPHYSICS



UNIVERSITY OF COLORADO

UNIVERSITY OF COLORADO
BOULDER, COLORADO 80309-0440



NATIONAL BUREAU OF STANDARDS

June 15, 1988

Dr. Ralph Kelly
USAF Office of Scientific Research
Building 410
Bolling Air Force Base
Washington, DC 20332

AFOSR-87-0221

Dear Ralph:

This is a brief report on the Fourth International Conference on Multiphoton Processes (Boulder, Colorado, 13-17 July 1987) which was supported in part by grant AFOSR-87-0221 entitled "Fourth International Conference on Multiphoton Processes." Attachments to this report include:

- (1) a list of participants in the conference;
- (2) the Program and Abstracts, which includes in particular, the abstracts of orally presented contributed papers as well as of the poster presentations; and
- (3) the printed proceedings of the conference entitled "Multiphoton Processes," S. J. Smith and P. L. Knight, editors, Cambridge University Press, 1988, which consists of papers by invited speakers.

There were about 200 registrants. Of the 200 registrants, 86 were from fifteen countries other than the United States, including from: Australia (1), Austria (4), Canada (5), England (18), France (12), Greece (4), Hungary (2), Israel (3), Italy (11), Japan (2), the Netherlands (5), People's Republic of China (2), Poland (5), Russia (6) and West Germany (14). In addition, there were a number of foreign student participants from U.S. universities, notably those from the People's Republic of China.

The conference program included thirty-six invited speakers, twenty from foreign countries; forty-five orally presented contributed papers; and approximately one hundred posters.

Travel support was provided, as needed, for invited speakers. All speakers were asked to minimize their requests by obtaining support from their own institutions. Travel support was provided only in response to specific


requests and only where speakers asserted that they could not otherwise participate.

We were also able to respond to requests for support from a number of young scientists with records of accomplishment in multiphoton research, who otherwise could not have come or who would have had to pay entirely out of personal funds; and graduate students, mostly from U.S. universities, upon requests endorsed by their thesis advisors. We were able to respond significantly to all such requests, approximately fifteen in all. Travel support from the AFOSR grant was provided only to applicants from U.S. institutions. Air Force and other Government personnel were excluded from consideration.

The conference was sponsored by IUPAP, the University of Colorado, NBS, NSF, AFOSR, ONR and the DoE Office of Basic Energy Sciences. Contributions to the non-scientific program were received from Coherent, Inc.; Lambda Physik; Lumonics, Inc; Quantel International; Questek, Inc; and Spectra Physics.

The meeting seemed to be regarded by participants as an outstanding success. The Fifth International Conference on Multiphoton Processes will be held in France in 1990, with G. Mainfray serving as chairman of the international committee. This three year cycle was felt to be appropriate to this field. More frequent meetings would contribute unnecessarily to the problem of conference proliferation.

Sincerely,


Stephen J. Smith
Principal Investigator

SJS:jm

Enc.

Department of Housing

Participant Roster

Varda Ahiman,	Bar-Ilan University, Chemistry Dept., Ramatgan, Isreal 52100 (03) 718313
Gernot Alber,	University of Innsbruck, Inst. f/Theoret. Physic, Innsbruck, Austria A-6020 522/748-5155
Mike Anderson,	University of Colorado-JILA, Campus Box 440, Boulder, CO 80309
Jeff Appling,	Brookhaven National Lab., Bldg. 555, Upton, NY 11973 516/282-4346
Kenn Arnett,	University of Colorado-JILA, Campus Box 440, Boulder, CO 80309
C.P. Arrighini,	University of Pisa, Dept. of Chemistry, Pisa, Italy
Michael Ashfold,	University of Bristol, School of Chemistry, Bristol, U.K. BS81T5 0272-303030x4714
Henri Bachau,	Univ. Bordeaux I, Lab des Coll. Atom., 351 Cours de la Liberation Talence, France 33400 (56) 80-53-80
Stan J. Bajic,	Oak Ridge National Lab., P.O. Box X, Oak Ridge, TN 37831 615/574-6233
John R. Barker,	University of Michigan, Dept of Atms & Ocnc Sci, Ann Arbor, MI 48109 313/763-6239
James E. Bayfield,	University of Pittsburgh, 100 Allen Hall, Pittsburgh, PA 15260 412/624-9280
Roger Beaman,	Lambda Physik, Inc., 289 Great Road, Acton, MA 01720 617/263-1100
Yves Beaudoin,	University of Laval, Dept of Physics, LROL, Quebec, Canada Q1K7P4 418/656-5791
Wilhelm Becker,	University of New Mexico, Dept of Physics, Albuquerque, NM 87131 505/277-4307
Robert Bernheim,	152 Davey Lab, University Park, PA 16802, 814/865-3642
Elliot Bernstein,	Colorado State University, Dept. of Chemistry, Fort Collins, CO 80523 303/49-6347
Imants Bersons,	Institute of Physics, Latvian SSR, 229021 Riga, Salaspils Riga, Salaspils, USSR 947188
Rajeshree Bhatt,	Flat 1, Gunnersbury, Park Mansions, Popes Lane, London, U.K. W5 4LY 01-589-5111 x6838
Dorothea T Biernacki,	Yale University, Chemistry Dept., 225 Prospect St. New Haven, CT 06511 203/432-3979
Philip Buckbaum,	AT&T Bell Labs, 600 Mountain Avenue, Murray Hill, NJ 07974 201/582-3793
Roberto Buffa,	Stanford University, Stanford, CA 94305 415/723-1945
Keith Burnett,	Blackett Laboratory, Imperial College, London, United Kingdom SW72B2 01-589-5111 x6935
Giulio Casati,	Dipartimento di Fisica, Vel Celoria 16, Milano, Italy 20133,3931552563
Joseph Chaiken,	Syracuse University, Dept. of Chemistry, Syracuse, NY 13224-1200 315/423-4285
Yat Chan,	12340 Santa Monica Blvd, Los Angeles, CA 90025, 213/820-2200
S.L. Chin,	Laval University, Dept. of Physics, Quebec, G1K 7P4 Canada 418/656-3418
Wolfgang Christian,	Davidson College, Physics Dept., Davidson, NC 28036 704/892-2000
Shih--I Chu,	University of Kansas, Dept of Chemistry, Lawrence, KS 66045 913/864-4094
Keith Codling,	University of Reading, Whiteknights, Dept of Physics Reading, Berks, England RG62AF
Robert M. Compton,	Oak Ridge National Lab. , Oakridge, TN 37831, 615-574-6233
William E. Cooke,	Univ. of Southern California, Physics Dept., Los Angeles, CA 90089 213/743-6211
John Cooper,	University of Colorado-JILA, Campus Box 440, Boulder, CO 80309
Julian Coutts,	University of Colorado-JILA, Campus Box 440, Boulder, CO 80309
Micheli Crance ,	29 rue de la Garenne, Sevres, France 92310, (1) 46266165
C.A. de Lange,	Free University, Dept of Physical Chem., De Boelelaan 1083 Amsterdam, Netherlands 1081HV
Patricia M Dehmer,	Argonne National Lab, Bldg. 203, Argonne, IL 60439 312/972-4187

Department of Housing

Participant Roster

John Delos,	University of Colorado-JILA, Campus Box 440, Boulder, CO 80309
Paul L. DeVries,	Miami University, Dept of Physics, Oxford, OH 45056 513/529-2234
J.H. Eberly,	University of Rochester, Dept of Physics & Astro, Rochester, NY 14627 716/275-4576
J.G. Eden,	University of Illinois, 1406 W. Green St., Urbana, IL 61801 217/333-2481
Tom Efthimiopoulos,	University of Crete, Physics Dept., Iraklion, Crete Greece (081)238480
Daniel S. Elliott,	Purdue University, School of Elec. Engr., W. Lafayette, IN 47907 317/494-3442
John C. Englund,	Southern Methodist Univ., Physics Dept., Dallas, TX 75275 214/692-4075
Prof. Faisal,	University of Bielefeld, Dept. of Physics, 4800 Bielefeld, West Germany 0521-103936
Gyozo Farkas,	Central Rsrch. Inst. of Phy., P.O. Box 49, Budapest, Hungary H-1525 696-575
Valentin Fedoseyev,	Inst. of Spectroscopy, Acad. Sci. USSR, Troitzk Moscow, USSR 142092
Dirk Feldmann,	Universitat Bielefeld, Fakultat Physik, D4800 Bielefeld 1 West Germany 0521 106 5436
Gaetano Ferrante,	Istituto Di Fisica, Via Archirafi 36, Palermo, Italy 90123 91-283468
Michael Fink,	University of Notre Dame, Dept of Physics, Notre Dame, IN 46556 219/239-6590
Emilio Fiordilino,	Istituto Di Fisica, Via Archirafi 36, Palermo, Italy 90123 91-283468
Joseph A. Fleck, Jr.,	Lawrence Livermore Natl Lab, Livermore, CA 94550, 415/422-4127
Gary Fletcher,	Lawrence Livermore Natl Lab, L-401, P.O. Box 808, Livermore, CA 94550 415/422-9519
Costas Fotakis,	Research Center of Crete, Iraklion, P.O.B. 1527, Crete, Greece (081)238480
Richard R. Freeman,	AT&T Bell Labs, IE-338, Murray Hill, NJ 07974 201/582-4558
Mary Fullenkamp-Essary	Lambda Physik, Inc., 289 Great Road Acton, MA 01720 617/263-1100
Alan Gallagher,	University of Colorado-JILA, Campus Box 440, Boulder, CO 80309
Jean Gallagher,	University of Colorado-JILA, Campus Box 440, Boulder, CO 80309
W. Ray Garrett,	Oak Ridge National Lab, Oak Ridge, TN 37831, 615/574-6231
Daniel Gauthier,	The University of Rochester, The Institute of Optics, Rochester, NY 14627 716/275-5030
M. Gavrila,	FOM Inst f/Atomic & Mol. Phy, Postbus 41883, 1009 DB Amsterdam The Netherlands 31-20-946711
Sydney Geltman,	University of Colorado-JILA, Campus Box 440, Boulder, CO 80309
A.T. Georges,	University of Crete, Research Center of Crete, Heraklion, Greece 081/235-014
Annick Giusti,	Universite Paris - Sud, Labor. PPM - Baf 213, Orsay, France 91405 16-941-74-68
Michael Goggin,	Los Alamos National Lab, MS J569, Los Alamos, NM 87545 505/667-7799
Lionel Goodman,	Rutgers University, Chemistry Dept., New Brunswick, NJ 08903 201/932-2603
Thomas Gorczyca,	University of Colorado-JILA, Campus Box 440, Boulder, CO 80309
Silvia Gozzini,	Ist. Fisica Molecolare, Pisa, Italy
Edward Grant,	Purdue University, Dept. of Chemistry, W. Lafayette, IN 47907 317/494/9006
Anthony Greenfield,	Blackett Laboratory, London, United Kingdom, SW72B2 01-589-5111 x6947
P.T. Greenland,	AERE Harwell, Theoretical Physics Div, Didcot Oxon, England OX110R
Rainer Grobe,	Borkstr. 26, 4300 Essen 1, Essen, West Germany 011 49 201 710591
Stan Haan,	Calvin College, Physics Dept., Grand Rapids, MI 49506 616/957-6339



Department of Housing

Participant Roster

Gregory Hall,	Savannah River Laboratory, Bldg. 735A, Aiken, SC 29808 803/725-5451
Xianming Han,	University of Colorado-JILA, Campus Box 440, Boulder, CO 80309
G. Hazak,	Nuclear Research, P.O. 9001, Beer Sheva, Israel 57-68308
Michael Harris,	University of Colorado-JILA, Campus Box 440, Boulder, CO 80309
H.G.M. Heideeman,	Fysisch Laboratorium, Ryksuniversiteit, Princetonplein 5, 3584 CC Utrecht, The Netherlands 030-532925
Ritsch Helmut,	Inst. f/ Theoretical Physics, Innsbruck, Austria
John W. Hepburn,	University of Waterloo, Dept of Chemistry, Waterloo Ontario, Canada N2L3G1
Mark Hermann,	Lawrence Livermore Natl Lab, Livermore, CA 94550, 415/423-8672
Jeanne M. Hossenlopp,	Syracuse University, Chemistry Dept., 108 Bowne Hall Syracuse, NY 13244 315/423-4285
Mei Ying Hou,	P.O. Box 603, Beijing, China, 861 2032606
Michael Ivanco,	Chalk River Nuclear Labs, Chalk River, Ontario, Canada K0J1J0 613/584-3983
Maurice Jarzembki,	New Mexico State University, Dept. of Physics, Box 3D, Las Cruces, NM 88003 1494-2129
Miodrag Janjusevic,	CCNY, Physics Dept., Convent Ave. at 138th St. New York, NY 10031 212/690-8310
Juha Javanainen,	University of Rochester, Dept of Physics & Astro, Rochester, NY 14627 716/275-4841
Siegfried Jetzke,	Universitat Bielefeld, Fak. F. Physik, D-4800 Bielefeld Fed. Rep. of Germany 0521-1066163
Philip M. Johnson,	State University of New York, Dept. of Chemistry, Stony Brook, NY 11794 516/632-7912
Lars Jonsson,	University of Illinois, Dept. of Physics, Box 4348, Chicago, IL 60680 312/413-2108
Jim Kelly,	University of Idaho, Physics Dept., Moscow, ID 83843 208/885-7469
A. Kiermeier,	Inst. f/Phys. Chemie I, Lichenbergstr. 4, 8046 Garching Munchen, West Germany 8000 089-3209-3412
Katsumi Kimura,	Institute for Molecular Sci., Okazaki 444, Okazaki, Japan 0564-53-7327
Paul Kleiber,	University of Iowa, Dept of Physics, Iowa City, IA 52242 319/335-18415
P.L. Knight,	Imperial College, Blackett Laboratory, London, England SW72BZ
Randy Knight,	Ohio State University, Physics Department, Columbus, OH 43210 614/292-8798
Kenneth C. Kulander,	Lawrence Livermore Natl. Lab, Livermore, CA 94550, 415/422-5400
George A. Kyrala,	Los Alamos National Lab, P.O. Box 1663, MS E526, Los Alamos, NM 87545 505/667-7649
Anne L'Huillier,	DPHG-PAS, CEN Saclay 91191, Gif-sur-Yvette France 91191 (1) 69082113
Albert MF Lau,	Sandia National Laboratories, P.O. Box 969, Livermore, CA 94550 415/422-2541
Howard MH Lee,	The Aerospace Corporation, M2/253, P.O. Box 92957 Los Angeles, CA 90009 213/336-4535
Vladimir Lengyel,	Uzhgorod University, Gorky St.46, Uzhgorod, USSR 294000
Maciej Lewenstein,	Harvard University, Physics Department, Lyman Laboratory Cambridge, MA 02138 617/495-4349
Meng Li Du,	University of Colorado-JILA, Campus Box 440, Boulder, CO 80309
Ting Shan Luk,	University of Chicago, 829 W. Taylor St., Chicago, IL 60680 312/996-5443
Hans O. Lutz,	Universitat Bielefeld, Fakultat fur Physik, 4800 Bielefeld 1 Bielefeld, F.R.G. 521-106 5362
Gerard Mainfray,	CEA, PA:S, Cen Saclay, 91191 Gif-sur-yvette, France
Yuri P. Malakian,	Armenian Academy of Sciences, Inst. f/ Phy. Research, Ashtarak-2 Armenia, USSR 378410

Department of Housing

Participant Roster

Alfred Maquet,	Lab. de Chimie Physique, 11, Rue Pierre M. Curie, F75231 Paris, Cedex 05 Paris, France
Mazzoni Marina,	Ist. di Elet. Quantistica, Via Panciatichi 56/30, Florence, Italy 50127 055-416128
Manlio Matera,	Ist. di Elet. Quantistica, Via Panciatichi 56/30, Florence, Italy 50127 055-416128
Eric Mazur,	Harvard University, Div. of Applied Science, 225 Pierce Hall Cambridge, MA 02138 617/495-8729
Ulrich Meier,	DFVLR, Institut 442, Pfaffenwalding 38-40, Stuttgart 80 West Germany 7000 0711/6862-385
Menning Meyer,	University of Colorado-JILA, Campus Box 440, Boulder, CO 80309
Paul J. Miller,	Yale University, Chemistry Dept., 225 Prospect St. New Haven, CT 06511 203/432-3979
Peter W. Milonni,	Los Alamos National Lab., MS J-569, Los Alamos, NM 87545 505/667-7763
James Mitroy,	University of Colorado-JILA, Campus Box 440, Boulder, CO 80309
Marvin Mittleman,	The City College of NY, Physics Dept., New York, NY 10031 212/690-6908
Jan Mostowski,	Max-Planck-Institut, Postfach 1513 8046, Garching, West Germany 089/32905732
M.G. Muller,	FOM Inst f/Atomic & Molc Phy, P.O. Box 41003, 1006 DB Amsterdam The Netherlands 020-946711
Munir M. Nayfeh,	Univ. of Illinois, Dept. of Physics, 1110 W. Green St., Urbana, IL 61801 217/333-3774
Jeffrey T. Needels,	University of Kansas, Chemistry Dept., Malott Hall Lawrence, KS 66045 913/864-3053
H. Jurgen Neusser,	Technische Universitat Munch, Inst. f/Physik. Chemie, Lichenbergstr. 4 Garching, West Germany D-8046
David Norcross,	University of Colorado-JILA, Campus Box 440, Boulder, CO 80309
Maureen A. O'Halloran,	Argonne National Laboratory, 203 C-161, Argonne, IL 60439 312/972-6524
Thomas Olsen,	Lewis & Clark College, Dept of Physics, CB 15, 0615 SW Palatine Hill Road Portland, OR 97219 503/293-2751
Jonathan Parker,	University of Rochester, Wilmot Hall, Rochester, NY 14627 716/275-2471
Robert Parson,	University of Colorado-JILA, Campus Box 440, Boulder, CO 80309
J.D. Perez,	3881 Corina Way, Palo Alto, CA 94303, 415/424-2021
Michael D. Perry,	Lawrence Livermore Nat'l Lab, Mail Code L-473, Livermore, CA 94550 415/423-4915
Guillaume Petite,	DPHG-SPAS, CEN Saclay, Gif sur Yvette, France 91191 (1) 69-08-44-93
Stephen Pratt,	Argonne National Lab, Bldg. 203, C-141, Argonne, IL 60439 312/972-4199
Naseem Rahman,	University of Trieste, Dept. Chemical Sciences, Trieste, Italy
Norman F. Ramsey,	JILA, University of Colorado, Boulder, CO 80309 303/492-7839
Gene P. Reck,	Wayne State University, Dept of Chemistry, Detroit, MI 48202 313/577-2602
Jurgen Reif,	Freie Universitat Berlin, FB Physikal Physics Div, Berlin Fed. Rep. of Germany 49.30.838.21.57
Howard R. Reiss,	The American University, Physics Department, Washington, D.C. 20016 202/885-2749
E. Riedle,	Inst. f/Phys. Chemie I, Lichenbergstr. 4, 8046 Garching Munchen, West Germany 8000 089-3209-3397
Leonard Rosenberg,	New York University, Physics Dept., New York, NY 10003 212/598-7635
Eugene A. Ryabov,	Inst. of Spectroscopy, Acad. Sci. USSR, Troitzk Moscow, USSR 142092
Kazimierz Rzazewski,	Polish Academy of Sciences, Inst f/ Theoretical Phy, Warsaw, Poland 02-668 (48) (22) (470520)
R.J. Sandeman,	Australian National Univ., Dept of Phy & Theo Phy, Box 4, P.O. Canberra A.C.T., Australia 2601 (062) 492747
Gottfried Schappert,	Los Alamos National Lab, P.O. Box 1663, MS E526 Los Alamos, NM 87545 505/667-1294



University of Colorado at Boulder

International Conference on Multiphoton Processes
July 13-17, 1987

Office of Conference Services

Department of Housing

Participant Roster

Gregory Schian,	University of Colorado-JILA, Campus Box 440, Boulder, CO 80309
Mehul Shah,	Blackett Laboratory, Imperial College, London, United Kingdom SW72B2 01-589-5111 x6947
Bruce W. Shore,	Lawrence Livermore Nat. Lab., Livermore, CA 94550, 415/422-6204
David Skutrud,	U.S. Army Research Office, P.O. Box 12211, Research Triangle, NC 27709 919/549-0641
Arlee V. Smith,	Sandia National Laboratories, Division 1124, Albuquerque, NM 87185 505/846-6308
Stephen Smith,	University of Colorado-JILA, Campus Box 440, Boulder, CO 80309
John Stockdale,	Oak Ridge National Lab., Oak Ridge, TN 37831, 615/574-6238
Donna Strickland,	University of Rochester, 250 East River Road, Rochester, NY 14623 716/275-5101
Qichang Su,	University of Rochester, Dept of Physics & Astro, Rochester, NY 14627 716/275-8537
Gilbert Sultan,	18 Rue de Valois, Les Ulis, France 91940, 69072841
Abraham Szoke,	P.O. Box 808, L-297, Livermore, CA 94550, 415/422-4099
Xian Tang,	Univ. of Southern California, Dept of Physics, Los Angeles, CA 90089 213/743-5659
Sam Tarzi,	14 Warwick Road, Ashford, Middlesex, England TW153P 07842-41007
Tom Taylor,	Los Alamos National Lab, MS E43, CL5-5, Los Alamos, NM 87545 505/665-0030
R. Trainham,	University of Virginia, McCormick Rd., Charlottesville, VA 22901 804/924-7591
Marek Trippenbach,	ul. Gilariska 115, Warsaw 03589, Warsaw, Poland
Fabio Trombetta,	Istituto Di Fisica, Via Archirafi 36, Palermo, Italy 90123 91-283468
H. Ben van Linden,	Fom Institute, Kruislaan 407 Amsterdam The Netherlands
Sandor Varro,	Central Research Institute, P.O. Box 49, Budapest, Hungary 1525 699-499/26-22
H. Walther,	Max-Planck-Institut, fur Quantenoptik, 8046 Garching Garching, FRG 089/32905-704
Kuanghsi Wang,	University of Kansas, Chemistry Dept., Lawrence, KS 66045 913/864-3053
Shinichi Watanabe,	Observatoire de Paris-Meudon, Paris, France 92190, 45 34 75 70 x933
A. Bruce Wadding,	University of Colorado/JILA, Campus Box 440, Boulder, CO 80309
Lynn Westling,	University of Colorado-JILA, Campus Box 440, Boulder, CO 80309
H.V. Weyssenhoff,	U. Frau, Rehmerfeld 21, 3000 Hannover 51 Fed. Republic of Germany
Michael G. White,	Brookhaven National Lab., Chemistry Dept., Upton, NY 11973 516/282-4345
Arlene Wilson-Gordon,	Bar-Ilan University, Dept of Chemistry, Ramatgan, Isreal 52100 (03) 718313
Krzysztof Wodkiewicz,	Warsaw University, Inst. of Theoretical Physc, Warsaw, Poland 00-681 283396
Robert E. Wyatt,	University of Texas, Dept of Chemistry, Austin, TX 78712 512/471-3114
James Wynne,	IBM, Research 26-114, P.O. Box 218 Yorktown Hts., NY 10598 914/945-1575
Francois Yergeau,	Laval University, Dept of Physics, Quebec, Canada G1K7P4 418/656-3379
Jakub Zakrzewski,	Univ. of Southern California, Dept of Chemistry, SSC 702 Los Angeles, CA 90089 213/743-7142
Bino Zet,	Ripon College, P.O. Box 248, Ripon, WI 54971 414/748-2791
Hsiao-Ling Zhou,	University of Colorado-JILA, Campus Box 440, Boulder, CO 80309
Peter A. Zoller,	University of Innsbruck, Physics Dept., 6020 Innsbruck Innsbruck, Austria 5222-748x5154

forces, I cannot test it completely in the simulations either. However, with increasing intensity the photoelectron peaks move down in energy as if the continuum threshold moved up by an amount which for large multiphoton orders is close to W_p . Figure 1 illustrates the peak motion, as well as dynamic closing of an ionization channel.

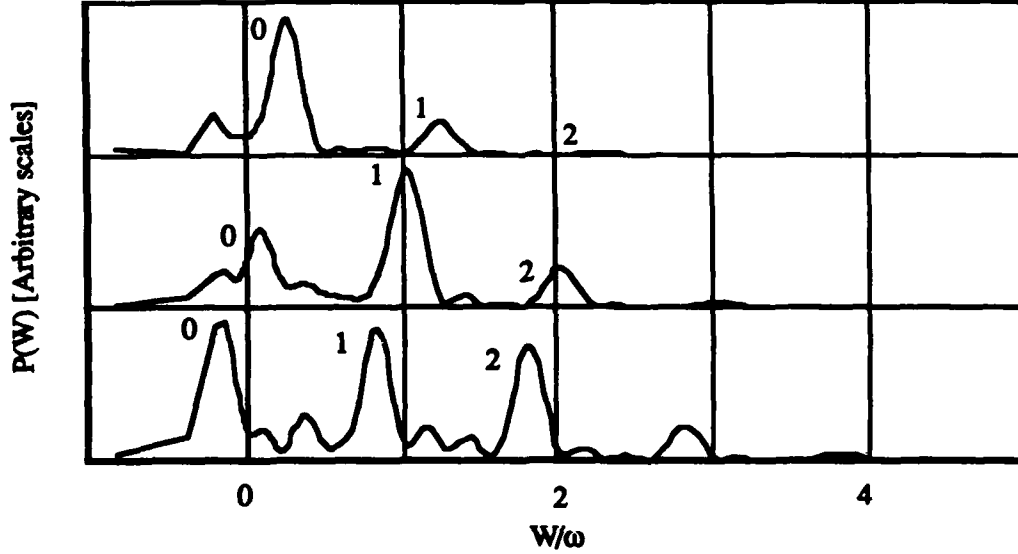


Fig. 1 The photoelectron spectra with $\omega = 0.14$ (5-photon ionization), for the field strengths $E = 0.05, 0.07071$ and 0.085 (from top to bottom). The numbers label peaks which transform into each other. For $E = 0.085$ the peak 0 has fallen below the continuum limit $W = 0$.

Two basic non-perturbative mechanisms of ATI have been advocated. Some authors³ regard ATI as transitions between continuum states analogous to dipole transitions between bound levels. Others⁴ attribute ATI to a dressing of the continuum states by the external field, associated with those dipole moment matrix elements which by a suitable choice of the continuum states can be rendered diagonal. As the former mechanism is absent with free electrons, a free-electron scaling of ATI suggests the continuum dressing mechanism.

To study the scaling I first define in terms of the photoelectron spectrum and the position of the lowest peak W_0 a quantity roughly representing the number of ATI peaks,

$$N = \frac{1}{\omega} \left[\int_0^{\infty} W P(W;t) dW - W_0 \right]. \quad (2)$$

In Fig 2. I plot N for several field intensities and frequencies as a function of the free-electron parameter $\eta = E^2/\omega^3$, essentially the ratio of the ponderomotive potential to the photon energy. For all three frequencies the onset of ATI, $N \sim 1$, takes place at $\eta \sim 1$, and a rough scaling of ATI with the parameter η is recognized.

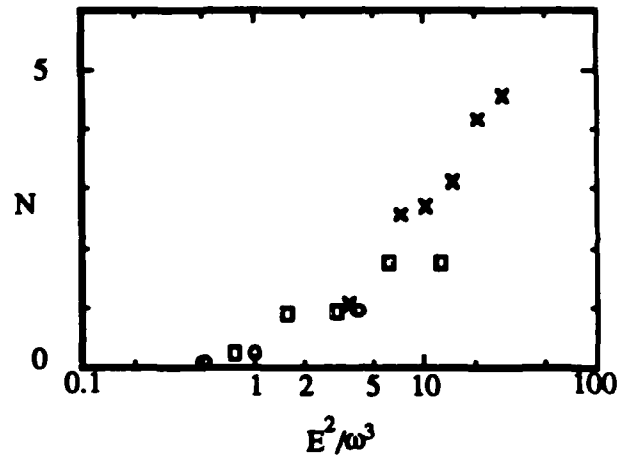


Fig. 2. The quantity N , essentially a measure of the number of ATI peaks, plotted as a function of the parameter E^2/ω^3 for the three field frequencies $\omega = 0.07$ (crosses), 0.14 (squares) and 0.27 (circles). These frequencies correspond to 10, 5 and 3-photon ionization.

My simulations support the interplay of the threshold shift and ponderomotive acceleration as the explanation for the vanishing of the lowest ATI peaks with increasing intensity, and suggest that diagonal continuum dressing is the dominant mechanism of ATI. To gain further insight, simulations of the scattered radiation are presently under way.

References:

1. H. G. Muller, A. Tip and M. J. van der Wiel, J. Phys. B. 16, L679 (1983).
2. L. Pan, L. Armstrong, Jr., and J. H. Eberly, J. Opt. Soc. Am B 3, 1319 (1986).
3. Z. Bialynicka-Birula, J. Phys. B 17, 3091 (1984); M. Edwards, L. Pan, and L. Armstrong, Jr., J. Phys. B 18, 1927 (1985); Z. Deng and J. H. Eberly, J. Opt. Soc. Am. B 2, 486 (1985).
4. M. Lewenstein, J. Mostowski, and M. Trippenbach, J. Phys. 18, L461 (1985); A. Dulcic, Phys. Rev. A 35, 1673 (1987); W. Becker, R. R. Schlicher, and M. O. Scully, J. Phys. B 19, L785 (1986).

**ESSENTIAL STATES APPROACH TO
THE ABOVE THRESHOLD IONIZATION
IN APPLICATION TO HYDROGEN ATOM**

Kazimierz Rzażewski, Institute for Theoretical Physics, Polish
Academy of Sciences, 02-668 Warsaw, al. Lotników 32/46,
Poland.

Marek Trippenbach, Institute of Experimental Physics, Warsaw
University, 00-681 Warsaw, ul. Hoza 69, Poland.

Rainer Grobe, Fachbereich Physik, Universität Essen, 43 Essen
West Germany.

Over the past several years, the experimental study of nonresonant multiphoton ionization of neutral atoms has led to a discovery of above-threshold ionization¹ (ATI). The phenomenon of ATI is an absorption of additional photons over a minimal number required for ionization. It manifests itself in an energy spectrum of the outgoing photoelectrons. This spectrum consists of a series of maxima displaced by the single photon energy $\hbar\omega$ of the light used for ionization. The relative sizes of the peaks or the populations of the consecutive maxima depend on the intensity of the laser light and in the region of 10^{12} - 10^{13} W/cm² become inverted. It means that higher than the first peak is most populated.

Our line of thought follows that represented by a series of papers pointing to the saturation of free-free dipole transitions^{2,3}. The important ingredient of these papers is an identification of the subspace of essential states of the atom. Essential states are those which get populated during the evolution. The total hamiltonian is then restricted to the subspace of relevant states. A number of qualitative results were obtained using this framework which are in a rough agreement with the observed peak switching in the photoelectron spectra. Staying within the framework of essential states, we have made the first calculations without adjustable

parameters^{4,5}. They are performed for the simplest possible system: the hydrogen atom. We stress that all the existing calculations of the ATI performed for the hydrogen atom were done with the help of the perturbative methods.

As emission and absorption of photons can only occur in a presence of accelerations, only relatively small number of partial waves should be present in the angular momentum decomposition of the ATI peaks. The first results on this problem has recently been published⁶ and they indeed show that only roughly a half of angular momenta permitted by the dipole selection rule are present.

In our model, the relevant states are the initial bound state and a matrix of narrow bands in the continuum corresponding to the definite orbital momentum components of the consecutive peaks of ATI. The scheme is for the 12 photon ionization by the powerful linearly polarized pulse of the nd:YAG laser. The 12-photon bound-free transition is assumed to be entirely nonresonant and a perturbative matrix element is used here. The standard analytically available⁷ free-free matrix dipole elements for the hydrogen atom are used to link the narrow bands in the continuum. The major simplification of such a multichannel dynamics has been made in Ref.8. As a result the dynamical equations of the model take a form of kinetic equations. It follows from them that, to a good approximation the relative sizes of peaks do not depend on the duration of the pulse.

The earlier results are now extended to laser intensities of the order of 10^{12} - 10^{13} W/cm². The description of the final scattering states as the Coulomb field continua is no longer adequate. The motion of the electron in the laser field, described by the, so called, Volkov solution is more appropriate. Technically this corrections appear as diagonal, singular parts of the free-free matrix element. The method of dealing with this terms is described in Ref.10.

The corrections coming from the diagonal parts of the coupling modify the weak field linear dependence of the single photon couplings of the model. They also introduce new direct multiphoton couplings between distant continua. They tend to increase somewhat a probability of higher angular momenta in the ATI peaks.

As in all the other calculations of single atom ATI in hydrogen, it seems to be very difficult to achieve the peak switching.

In our talk we plan to comment also about the ATI phenomenon with circularly polarized light and about the ATI starting from a Rydberg level.

REFERENCES

1. P. Agostini, F. Fabre, G. Mainfray, G. Petite, and N. Rahman, Phys. Rev. Lett. **42**, 1127 (1979); P. Kruit, J. Kimman, and M. van der Wiel, J. Phys. B **14**, L597 (1981); F. Fabre, G. Petite, P. Agostini, and M. Clement, J. Phys. B **15**, 1353 (1982).
2. Z. Bialynicka-Birula, J. Phys. B **17**, 3091 (1984).
3. M. Edwards, L. Pan, and L. Armstrong jr J. Phys. B **17**, L515 (1984), and J. Phys. B **18**, 1927 (1985); Z. Deng, and J. H. Eberly, Phys. Rev. Lett. **53**, 1810 (1984) and JOSA B **2**, 486 (1985).
4. K. Rzażewski, and R. Grobe, Phys. Rev. Lett. **54**, 1729 (1985).
5. K. Rzażewski, and R. Grobe, Phys. Rev. A **33**, 1855 (1986).
6. H. J. Humpert, H. Schwier, R. Hippler, and H. O. Lutz, Phys. Rev. A **32**, 3787 (1985).
7. W. Gordon, Ann. Phys. (Leipzig) **2**, 1031 (1929).
8. M. Crance, and M. Aymar, J. Phys. B **13**, L421 (1980).
10. M. Lewenstein, J. Mostowski, and M. Trippenbach, J. Phys. B **18**, L461 (1985).

Invited Paper

**Multiresonant Spectroscopy and the Dynamics of Nonradiative Decay
in Molecular Rydberg States**

Kenneth S. Haber, Francis X. Campos, Josef W. Zwanziger,
Ralph T. Wiedmann and Edward R. Grant

Department of Chemistry
Purdue University
West Lafayette, IN 47907

Nonradiative processes are well known to affect the course of molecular multiphoton processes.¹⁻³ Intermediate nonradiative decay diverts the direct ionization of excited molecules, and can thus reduce the yield of parent ions as well as affect vibronic overlaps for subsequent neutral-neutral and neutral-ion transitions. Products of nonradiative decay can consist of vibrationally excited levels built on lower electronic states of parent molecules,^{4,5} as well as photodissociation fragments.⁶⁻⁸ Such effects are observed for both valence and Rydberg intermediate levels, with characteristic timescales, as inferred from line shapes,⁹ power dependencies,⁸ and a few direct measurements,¹⁰ ranging from nanoseconds to femtoseconds. For polyatomic Rydberg states in particular, where fast to ultrafast nonradiative relaxation is regarded as axiomatic, information on specific decay paths is sparse. This situation persists despite the attractive opportunities for photophysics presented by Rydberg systems in general as series of systematically related electronic states. Moreover, Rydberg states offer a possible simplification through the close connection between electron-ion scattering and Rydberg-core interaction, as made evident by descriptions that conceptually divide Rydberg molecules into Rydberg-electronic and core-ionic subsystems coupled by interaction terms.¹¹

With the above factors in mind we have undertaken a systematic study of the observable properties of Rydberg states in triatomic and small polyatomic molecules. Our observations thus far have been confined to determinations of global lifetimes and specific interactions in the frequency domain. Experiments under development will probe relaxation directly by time-resolved pump-probe methods. In all cases, systems under study are seeded in a pulsed free-jet expansion. Rydberg states are then accessed either by conventional one-color two-photon or three-color multiresonant

three-photon excitation. Absorption is detected by subsequent photoionization, or, in some cases, by autoionization. Ions are collected and filtered by a quadrupole mass spectrometer. Under jet-cooled conditions, and particularly for multiresonant stepwise excitation, inhomogeneous contributions to linewidths from rotational and low-frequency vibrational congestion is greatly reduced so that observed band profiles give information on the lifetime of the optically bright (ionizable) state with respect to decay into a manifold of dark states. Above adiabatic ionization thresholds, resonance profiles additionally contain information on autoionization linewidths.

We find that decay rates obtained in this fashion vary enormously from one molecule to another, and, for any given molecule, among Rydberg states in a series. We will summarize results already published on benzene⁹ toluene,¹² triazine¹³ and cyclohexane,¹⁴ in combination with more recent data on cyclopropane.¹⁵ Against this background, the discussion will emphasize new results on the rovibrational state selected multiresonant spectroscopy and dynamics of high-Rydberg states near and above the adiabatic ionization threshold of NO_2 .

These latter states are accessed by the three-color multiresonant excitation method mentioned above. As presently configured, this technique uses two lasers, one of which is set, by use of an appropriate doubling crystal, to a fundamental frequency combined with its first harmonic. This bichromatic output is tuned to double-resonance with a selected rotational level (at ω_1) in the dense optical absorption spectrum of NO_2 , and a rotational level to which it connects by subsequent UV absorption ($2\omega_1$) in a chosen vibrational member of the $3p\sigma$ Rydberg State.¹⁶ The first laser thus nominally selects a molecular Rydberg level of well defined rotational and vibrational quantum numbers. From such gateway states the Franck-Condon allowed spectrum of higher Rydberg states is acquired via resonant ionization by scanning the output of a second dye laser. For vibrationally excited gateway states, the spectrum extends above the adiabatic ionization threshold to exhibit structure converging to corresponding vertical thresholds. Below the adiabatic IP, homogeneous widths reflect neutral decay pathways. Higher up, autoionization becomes an additional possibility, and we see distinct changes in lifetimes that appear to be correlated with thresholds for mode-specific vibrational-autoionization channels.

References

1. P. M. Johnson and C. E. Otis, *Ann. Rev. Phys. Chem.* **60** 161, (1985); K. Kimura *Adv. Chem. Phys.* **60**, 161, (1985); H. Reisler and C. Wittig, *Adv. Chem. Phys.* **60**, 1 (1985).
2. H. Sato, M. Kawasaki, K. Toya, K. Sato and K. Kimura, *J. Phys. Chem.*, **91**, 751 (1987); S. T. Pratt, P. M. Dehmer, *J. Chem. Phys.* **81**, 3444 (1984); J. B. Pallix and S. D. Coulson, *J. Phys. Chem.* **90**, 1499 (1986); M. G. White, W. A. Chupka, M. Seaver, A. Woodward and S. D. Colson, *J. Chem. Phys.* **80**, 678 (1984).
3. L. Bigio and E. R. Grant, *J. Chem. Phys.* **83**, 5361 (1985); L. Bigio, G. S. Ezra and E. R. Grant, *ibid* **83**, 5369 (1985).
4. C. E. Otis, J. L. Knee and P. M. Johnson, *J. Chem. Phys.* **78**, 2232 (1983).
5. T. G. Dietz, M. A. Duncan, A. C. Puiu and R. E. Smalley *J. Phys. Chem.* **86** 4026 (1982).
6. R. J. S. Morrison, B. H. Rockney and E. R. Grant, *J. Chem. Phys.* **75**, 2643 (1981); R. J. S. Morrison and E. R. Grant, *J. Chem. Phys.* **77**, 5994 (1982).
7. R. L. Whetten, K. J. Fu and E. R. Grant, *J. Phys. Chem.* **87**, 1484 (1983).
8. R. L. Whetten, K. J. Fu and E. R. Grant, *J. Chem. Phys.* **79**, 4899 (1983).
9. See for example: R. L. Whetten, S. Grubb, C. E. Otis, A. C. Albrecht and E. R. Grant, *J. Chem. Phys.* **82**, 1115 (1985).
10. J. M. Wiesenfeld and B. I. Green, *Phys. Rev. Lett* **51**, 1745 (1983).
11. See for example: C. H. Greene and Ch. Jungen, *Adv. At. Mol. Phys.* **21**, 51 (1985).
12. R. L. Whetten, K. J. Fu and E. R. Grant, *Chem. Phys.* **90**, 155 (1984).
13. R. L. Whetten and E. R. Grant, *J. Chem. Phys.* **81**, 691 (1984); R. L. Whetten, K. S. Haber and E. R. Grant, *J. Chem. Phys.* **84**, 1270 (1986).
14. R. L. Whetten and E. R. Grant, *J. Chem. Phys.* **80**, 1711 (1984).
15. J. W. Zwanziger and E. R. Grant, to be published.
16. L. Bigio and E. R. Grant, *J. Chem. Phys.* **83**, 5361 (1985).

High Resolution Multiphoton Spectroscopy of Rydberg States of NO.^{*}

D.T. Biernacki and S.D. Colson
Chemistry Department
Yale University
New Haven, CT 06511

E.E. Eyler
Physics Department
Yale University
New Haven, CT 06511

Two experiments on the Rydberg states of nitric oxide (NO) have been performed using very high resolution laser spectroscopy. In the first, the A+X transition has been measured to an accuracy of 0.01 cm^{-1} using both 2-photon resonant 4-photon ionization and 1-photon resonant 2-photon ionization. In the second, autoionizing Rydberg states are studied using stepwise excitation; states with $\ell > 2$ can be accurately described using a simple long-range interaction model. The autoionization rates vary dramatically with ℓ and with N , the total angular momentum exclusive of spin.

The $A(3s\sigma) \ ^2\Sigma^+ + X^2\Pi(1,0)$ transition near 214.8 nm is excited using a pulse-amplified continuous wave dye laser system with a resolution of $.002 \text{ cm}^{-1}$. For the measurements using 2-photon ionization the laser is frequency doubled by a $\beta\text{-BaB}_2\text{O}_6$ crystal. The A state is resonant at the one photon energy, and an additional photon from the same laser induces ionization. The experiment is performed in a pulsed supersonic molecular beam formed by the expansion of a 5% mixture of NO in argon. The free jet expansion yields a collision-free beam with a rotational temperature of about 2K. The beam is collimated by a 1-2 mm skimmer to reduce the Doppler broadening of the line width. An electric field of 350 V/cm created by the voltage applied to the electron multiplier tube collects the photoions. A typical spectrum is shown in Figure 1. Using the absorption spectrum of Te_2 as a reference, the energies of several branches of the A+X(1-0) transition have been measured to an accuracy of about 0.01 cm^{-1} . Together with the spectra of the Rydberg nf states, these transition energies yield accurate values for the quadrupole moment and polarizability of NO^+ , and the ionization potential of NO.

The higher Rydberg states can be studied by stepwise excitation using the same levels of the A state as intermediate states. For these experiments a pulsed

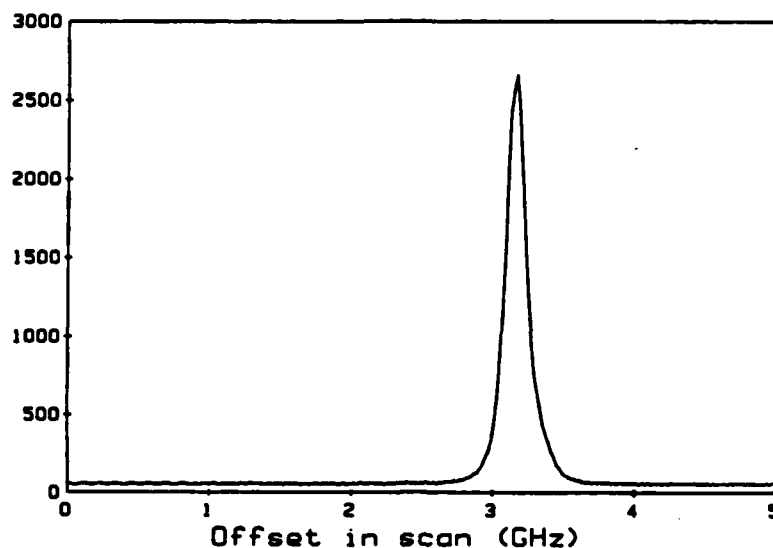


Figure 1. Scan over the $R_{11}(0.5)$ branch of the $A \rightarrow X(1,0)$ transition.

dye laser of about $.1 \text{ cm}^{-1}$ resolution populates the $v=1$ levels of the A state by a two photon absorption. The high resolution pulse-amplified cw dye laser then populates autoionizing $v=1$ Rydberg states. The gas sample is prepared as a 5% mixture of NO in helium. The ions produced by autoionization are collected by pulsed ion optics to reduce stray electric fields which may perturb the energies and widths of the Rydberg states studied. Natural linewidths are resolved for most of the lines of the Rydberg states studied, allowing a direct determination of the decay rates. The Rydberg ns, np and nf states can all be observed. The transition energies of the lines and their corresponding widths are determined by a least squares fit to a Lorentzian line shape function. Figure 2 shows a typical fit. For Rydberg states with $\lambda > 2$, the energy levels can be reproduced accurately using a long range interaction model.¹ Since there is little core penetration by these states, they can be described as a molecular ion core orbited by a single electron. This model incorporates corrections to the hydrogen atom wave function for the dipole moment, quadrupole moment, and polarizabilities of the molecular core.

¹E.E. Eyler, Phys. Rev. A 34, 2881 (1986), and references therein.

*Supported by Air Force Office of Scientific Research, grant number AFOSR-85-0054.

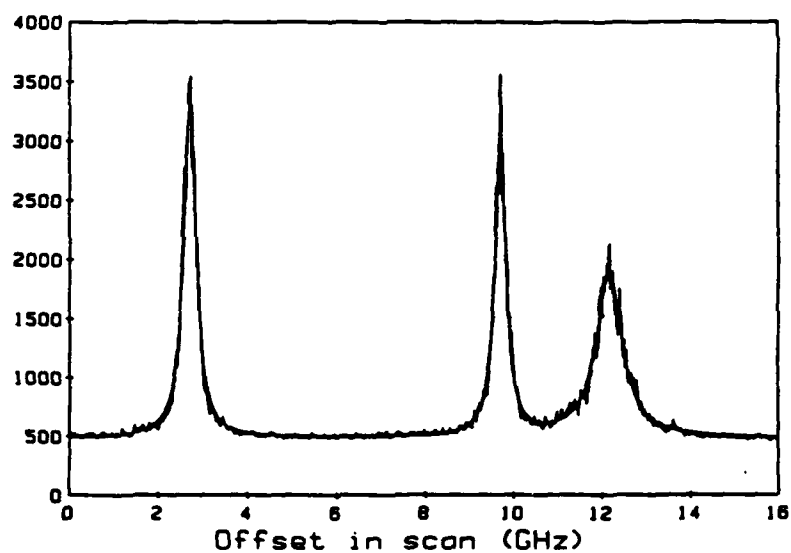


Figure 2. The $12f+A(1,1)$ transition from $N'=3$ is shown with P,Q,R branches to levels with core rotation $R=3$. The solid line is a least squares fit to a sum of three Lorentzians.

**Experimental Investigations of Circular Dichroism
in Photoelectron Angular Distributions***

Jeffrey R. Appling and Michael G. White

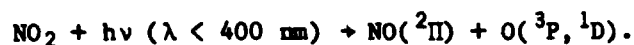
Chemistry Department, Brookhaven National Laboratory, Upton, NY 11973

The first observations^{1,2} of dichroic effects in photoelectron angular distributions are reported for photoionization from aligned molecular excited states. Optically aligned excited states, prepared with linearly polarized photons in two-color multiphoton ionization (REMPI) of NO, are probed through ionization by circularly polarized light. Resultant photoelectron angular distributions exhibit significant left-right asymmetry indicative of the excited state alignment. These experimental circularly dichroic angular distributions (CDAD) are found to be well described by the general theoretical framework recently developed by Dubs, Dixit and McKoy,³ and are in good qualitative agreement with their calculated REMPI-CD distributions.

Two cases of CDAD measurements are presented for the $(n + 1)$ REMPI of rotationally cooled nitric oxide. Initial observation¹ of circular dichroism resulted from study of two-color $(2 + 1)$ REMPI via $A^2\Sigma^+$, $v = 0, J = 3/2, 5/2$ excited states corresponding to the $R_{21} + S_{11}(1/2)$ and $S_{21}(1/2)$ rotational branch transitions. The experimental CDAD signal for these transitions approaches 20% of the circularly polarized differential cross section. A more extensive investigation² of CDAD from optically prepared levels of the A state was performed using a two-color $(1 + 1)$ REMPI scheme. For the $Q_{21} + R_{11}(1/2, 3/2)$ and $R_{21}(1/2, 3/2)$ rotational transitions, the CDAD intensities were found to be relatively small (typically, 5-10% of the circularly polarized cross section) in general accord with the smaller alignments expected for one-photon excitation. The P_{11} branch lines exhibit even smaller CDAD intensities (the $P_{11}(3/2)$ line shows no experimentally observable left-right asymmetry as expected

for an isotropic $J = 1/2$ upper state) but more interestingly, the extracted alignment parameters have the opposite sign. This result suggests that excited state alignments produced via the P_{11} branch have M_J sublevel populations skewed to higher $|M_J|$. Such distributions are not expected from simple one-photon excitation cross sections and the origin of this alignment is presently being sought.

The CDAD study of NO with (1 +1) REMPI was initiated as a preamble to the ongoing investigations of NO fragments released in the photodissociation of NO_2 :



Current work on NO_2 will be followed by future studies of NO-containing molecules by the photoelectron angular distribution measurement techniques described herein. Our goal is the elucidation of ground state alignment of NO fragments induced by the unimolecular photodissociation process.

- ¹ J. R. Appling, M. G. White, T. M. Orlando and S. L. Anderson, J. Chem. Phys. 85, 6803 (1986).
- ² J. R. Appling and M. G. White, in preparation.
- ³ R. L. Dubs, S. N. Dixit and V. McKoy, J. Chem. Phys. 85, 656 (1986).

* This research was performed at Brookhaven National Laboratory under contract DE-AC02-76CH00016 with the U.S. Department of Energy and supported by its Division of Chemical Sciences, Office of Basic Energy Sciences.

Invited Paper

Angular Distributions of Photoelectrons from Above-Threshold
Ionization of Hydrogen and Xenon Atoms

D. Feldmann, B. Wolff, H. Rottke, M. Wemhöner, and K.H. Welge
Fakultät für Physik, Universität Bielefeld, FRG

1. Hydrogen:

Above-threshold ionization (ATI) of atomic Hydrogen is of fundamental interest as a test case for theoretical calculations. Up to now only one experimental observation of ATI in Hydrogen has been reported in which either a three-photon-resonant process or the more complicated situation of two frequencies has been studied. (1)

We have measured angular distributions of the first few above-threshold -electron peaks at the off-resonant wavelengths 532 nm and 355 nm.

532 nm:

At estimated effective intensities of some 10^{12} Wcm^{-2} the electron energy spectrum shows peaks corresponding to the absorption of up to ten photons. A minimum of six photons is necessary for ionization at this wavelength. For the first three peaks angular distributions have been determined, using linearly polarized light.

A fit of the experimental values to a sum of spherical harmonics shows that partial waves of relatively low angular momentum contribute. The relative contributions of partial waves with different angular momentum are intensity dependent.

355 nm:

At this wavelength we have applied estimated effective intensities of the order of 10^{12} Wcm^{-2} .

The angular distributions of the electrons from four- and five-photon ionization contain strong d- and f-wave contributions respectively.

At the moment, the results for higher order processes suffer from low signal levels.

We hope that these results will stimulate theoretical calculations of angular distributions at these wavelengths.

2. Xenon:

The angular distributions of electrons from high order ATI-processes at 1064 nm at intensities above 10^{13} Wcm^{-2} show significant modifications when the total energy absorbed from the radiation field lies in the region of the autoionizing states of the atom which begins at an energy corresponding to seven photons above the ionization limit. This indicates that higher order ATI-processes in such a multi-electron atom cannot be described properly in a one-electron picture.

References:

- 1) H.G. Müller, H.B. van Linden van den Henvell, and M.J. van der Wiel, Phys. Rev. A 34, 236 (1986)

This research is supported by the Deutsche Forschungsgemeinschaft - Sonderforschungsbereich 216

Invited Paper

LIMITING CASES OF EXCESS-PHOTON IONIZATION

H.B. van Linden van den Heuvell and H.G. Muller

FOM-Institute for Atomic and Molecular Physics

Kruislaan 407, 1098 SJ Amsterdam, the Netherlands

In the last couple of years, much work has been done on the field of 'atoms in strong laser fields', both experimentally and theoretically. Two main streams of experiments can be distinguished: the observation of the energy distribution of the ionized electrons, and the observation of the charge state of the remaining ions. Here, we want to concentrate on experiments of the first type.

The first restricting on the topic is that it is assumed that the ions, formed by multiphoton ionization (MPI), are always singly ionized. As is very well known by now, the number of absorbed photons is not necessarily the minimum number one would expect based on an energy argument. For this phenomenon the names excess-photon ionization (EPI) and above threshold ionization (ATI) are in use.

The interpretation of EPI experiments is usually difficult, because a large number of effects cooperate to produce the observed behaviour. Disentangling this complex often leads to ambiguous results and confusion. In order to increase our understanding it is therefore desirable to study the various effects separately, in systems where they manifest themselves in their purest form, i.e. to study judiciously chosen limiting cases.

The most obvious reasons that comparison between theory and experiment is difficult are the following: Firstly, most target atoms are too complicated to tackle their multiphoton processes theoretically. Obviously, this can be overcome by going to a simplifying limiting cases through choice of the target atom. By using atomic hydrogen, a comparison is made much easier.^{1,2} Secondly, it is hard, and up to now in fact impossible to irradiate the atom with a strong field of constant amplitude. Both over space and in time the amplitude of the light field is varying, so the observations are averaged over a distribution of laser-field intensities. Since the observed processes are highly non-linear, this is an unwanted situation.

Another simplification is the disentangling of the ionization process and the absorption of excess photons, by using separate lasers for each of these processes.³ This shows the effects due to coupling between the EPI continua undisturbed by the often complicated ionization effects. The effect of the photoelectron being subject to the influence of both the laser and atomic field during the initial period of its voyage to infinity, is most pronounced in the situation where the energy of an excess-photonionized electron is as small as possible.⁴ This energy is roughly the energy of one photon. It is demonstrated that excess-photon ionization can be seen as a continuation of resonantly enhanced multiphoton ionization (REMPI).

Alternatively one could look to the multiphoton 'ionization', or more precisely multiphoton detachment, of negative ions. It is an interesting question through which mechanism the absorption of excess-photons can take place in this case, especially in connection with the above mentioned transition of EPI to REMPI. Such a transition is not possible in the case of negative ions since the lack of excited states preclude the occurrence of REMPI. Finally, a classical example of a limiting case, is the classical limit of the process, where the photon energy becomes so small that the quantized nature of the radiation field can be ignored.

Out of this list of five limiting cases, two will be discussed in a little more detail, namely the minimum-energy limit and the classical limit. The minimum-energy limit of EPI is strongly connected to the photoionization of Rydberg atoms. This last one is a phenomenon with many aspects. One of these is that the 'timing of a state', i.e. the inverse of energy separation between two adjacent n-states can be made comparable with the pulse duration of the laser pulse. In this way it is possible to measure the time dependence of photoionization. In order to increase this effect, we have performed measurements in a magnetic field. The elegance of the measurements is that they can be explained both in classical and in quantummechanical terms. Both treatments lead to the conclusion that:

- * the absorption of photons by a Rydberg or continuum electron is taking place in a localized area close to the nucleus.
- * a magnetic field is a convenient way to deform the time-evolution of wavefunctions on a time scale of the laser pulse duration.

As mentioned, in the situation treated above several classical aspects can be recognized. However the behaviour of the radiation field is still completely 'photon-like'. This indicates that the interaction between radiation field and electron is lasting long, at least during an oscillation period of the radiation field and therefore the interaction can be called weak. The classical interpretation is useful when the opposite is the case; i.e. when the interaction time is so short that the electric field is essentially constant during the process. This is the case if the distance over which the electron moves during one light oscillation is much more than the amplitude of the quiver motion.

Acknowledgement

This work is part of the research programme of the Stichting voor Fundamenteel Onderzoek der Materie (Foundation for Fundamental Research on Matter) and was made possible by financial support from the Nederlandse Organisatie voor Zuiver-Wetenschappelijk Onderzoek (Netherlands Organisation for Advancement of Pure Research).

References

1. H.G. Muller, H.B. van Linden van den Heuvell and M.J. van der Wiel
Phys. Rev. A 34 (1986)
2. D. Feldmann, private communication (1987)
3. H.G. Muller, H.B. van Linden van den Heuvell and M.J. van der Wiel
J. Phys. B L733 (1986)
4. H.B. van Linden van den Heuvell, H.G. Muller and M.J. van der Wiel
in: Photons and Continuum States to be published, Springer Verlag,
(1987)

Invited Paper

ELECTRON WAVE PACKETS, MULTIPHOTON ABSORPTION AND DIFFUSION IN A
CONTINUOUS AND QUASI-CONTINUOUS ATOMIC SPECTRUM

M. V. Fedorov

USSR Academy of Sciences
General Physics Institute
117942 Moscow, Vavilova 38, USSR

Field induced transitions between highly excited atomic levels and in the continuum are considered. Conditions under which the transition probabilities linearly depend on time are found. These are the conditions under which diffusion over energy can occur. Applicability of the diffusion equation is shown to depend on the initial width of the electron wave packet. The Fokker-Planck equation for stimulated bremsstrahlung is proposed.

MODEL THEORY OF PULSE SHAPE EFFECTS IN ABOVE THRESHOLD IONIZATION

H.Huang, L.Roso-Franco^{*} and J.H.Eberly

Department of Physics and Astronomy, University of Rochester,
Rochester, NY 14627, USA

In the intensity range where Above Threshold Ionization becomes important, the ATI spectrum has a well-defined peak structure.¹ The peaks are centered at $N+S$ times photon energy above the atomic ground state ($S=1,2,\dots$). The fact that off-resonant levels have very little population suggests that for a given continuum level, we can practically ignore the majority of C-C couplings with it. Thus the resonant C-C couplings deserve special consideration, and a resonant ladder can serve as a crude model for such processes.

A single level coupled to a ladder of "quasi-continuum" levels has been treated in rate equation² and Schrodinger's equation approaches³ in polyatomic molecular excitation studies, where the levels are truly discrete. To model a system with (non-degenerate) continuum levels, we must generalize these approaches to include a continuous ensemble of ladders.

Our model consists of a single discrete level $|0\rangle$ and an infinite set of ladders of levels $|\Delta, S\rangle$. Each continuum level is only connected to levels $\pm\Delta$ above and below it, so that a ladder of levels extended upwards is not coupled with other ladders. Such ladders are denoted by the detuning of their lowest step from the N -photon resonance from the ground state $|0\rangle$. The equations describing the system read:

$$i\dot{a}_0 = V_0(t) \int d\Delta \rho(\Delta) a_1(\Delta) \quad (1.a)$$

$$i\dot{a}_1(\Delta) = \Delta a_1(\Delta) + V_0(t) a_0 + V(t) a_2(\Delta) \quad (1.b)$$

$$i\dot{a}_S(\Delta) = \Delta a_S(\Delta) + V(t) [a_{S-1}(\Delta) + a_{S+1}(\Delta)]. \quad (1.c)$$

A general solution for arbitrary laser pulse shape was found by assuming V, V_0 real, and the continuum smooth. This solution is:

$$a_0(t) = \exp[-\int_{-\infty}^t \Gamma(t') dt'] \quad (2.a)$$

$$a_S(\Delta, t) = (-1)^S \int_{-\infty}^t dt' V_0(t') \exp\left[-\int_{-\infty}^{t'} \Gamma(t'') dt''\right] \exp[-i\Delta(t-t')] \\ \times \left\{ J_{S-1}\left[2\int_{t'}^t dt'' V(t'')\right] + J_{S+1}\left[2\int_{t'}^t dt'' V(t'')\right] \right\}. \quad (2.b)$$

Here $\Gamma(t) = \pi V_0^2(t) \rho$.

It is evident from the convolution form in (2.b) that the population reaches the S'th level by a two-step process. The first step, the depletion of the ground state, is unaffected by the presence of C-C couplings as shown by (2.a). So if the first continuum is connected with the ground state through an N-photon process, the power law $\Gamma \sim I^N$ holds for all intensity ranges.

In the second step, the electron will pick up photon energy at the rate $2V(t)$, since the ladder is exactly resonant. This process will continue all the time while the ground state is being depleted. After ground state depletion is complete, we will see the depletion of the first and subsequent "ionized" or "ATI" peaks. The number of peaks that have disappeared is proportional to the pulse length after ground state depletion.

In the case of non-constant pulse envelope, we define two new parameters of the pulse:

$$A_0 = \int_{-\infty}^{\infty} \Gamma(t) dt, \quad (3.a)$$

$$A = \int_{-\infty}^{\infty} 2V(t) dt. \quad (3.b)$$

The number of photons absorbed will depend on the "area" A after depletion, but the number of peaks that eventually emerge is determined by the ratio between V and V_0 before the ground state depletion. For a low intensity pulse, $A_0 \ll 1$, the rising edge doesn't pump much population into the first continuum, thus part of the area A is "wasted". In contrast, at the falling edge although the $|g\rangle \rightarrow |1, \Delta\rangle$ channel has been closed, the C-C channels are still open, so population in lower levels is pumped up without compensation from the ground state. If the tail of pulse is long enough, to be more definite if

$$2\int_{\text{tail}} V(t) dt > 1,$$

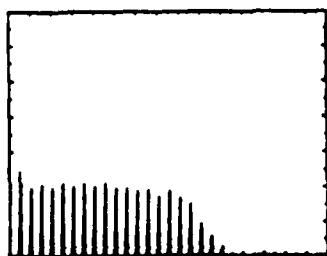
a shift of peak packet from the lowest continua will be significant. We note that this effect of pulse shape provides another explanation of the disappearance of the first peaks, even well below the depletion region.

In the figures we show the results obtained in the integration of eqs.(2) with $N=6$ for three representative pulse shapes: (a) square; (b) Gaussian; (c) random. The random pulse was generated by a simple pseudo random routine: $V(t) = \text{const} \times \sin^2((t+10)^2)$. Here the time unit equals $1/2V$, V is the square pulse amplitude. With step size $\Delta t = .05$, this formula simulates a near-uncorrelated amplitude fluctuation. Although the parameters A and A_0 were the same for the three (20 and .2 respectively), we see in Fig.2 the first few peaks almost disappear.

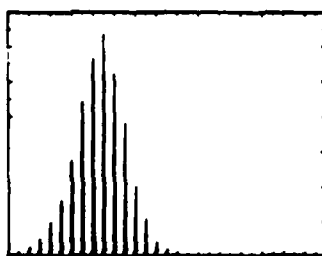
The experimental data in the references cited appear to belong to the latter case, below the depletion limit. When intensity is increased, the number of peaks suppressed and the number of remaining peaks both grow larger.

1. P.Kruit, J.Kimman, H.G.Muller, and M.J.van der Wiel, Phys. Rev. A 28, 248, (1983); L.A.Lompre, A.L'Huillier, G.Mainfray, and C.Manus, J. Opt. Soc. Am. B 2, 1906 (1985); C.K.Rhodes, Science 229, 1345 (1985)
2. J.R.Ackerhalt and B.W.Shore, Phys. Rev. A 16, 277 (1977); E.Thiele, M.F.Goodman and J.Stone, Chem. Phys. Lett. 72, 34 (1980)
3. A.A.Makarov, JETP 45, 918 (1977); G.L.Peterson, C.D.Cantrell and R.S.Burkey, Opt. Commun. 43, 123 (1982); E.Kyrola, Ph.D.Thesis, University of Rochester, (1984)

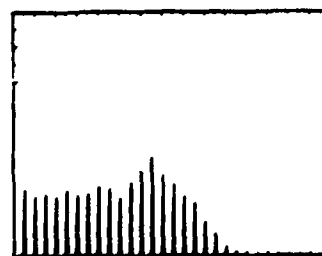
* Permanent address: Departamento de Fisica, Universidad Autonoma de Barcelona, Barcelona, Bellaterra, Barcelona, Spain.



(a) square



(b) Gaussian



(c) random

HIGH ORDER MULTIPHOTON IONIZATION WITHOUT TUNNELING

H. R. Reiss

Department of Physics
The American University
Washington, DC 20016

It is well known that for low frequency electromagnetic fields of very high intensity, the concept of ionization achieved by tunneling through a potential barrier is appropriate.¹ The observations by Yergeau, Chin, and Lavigne² of ionization of rare gases by a CO₂ laser are clearly in a tunneling region. Experiments³⁻⁵ with lasers of shorter wavelength than CO₂ give less extreme examples of high order photoionization in which the tunneling model may not be justified. An extended form⁶ of the Keldysh theory exists which gives good qualitative agreement⁷⁻⁹ with the experiments, gives criteria for distinguishing tunneling and non-tunneling domains in high order intense field processes, and provides explicit asymptotic forms for both domains. These results are used here to explore the limits, expressed in photon order and field intensity, of the region in which an ionization can be of high order and yet not be tunneling.

The extended theory⁶ involves two intensity parameters, a fundamental one, $z = e^2 E^2 / 4m\omega^3$, and a tunneling parameter $z_1 = 2z\omega/E_B$, where units with $\hbar = c = 1$ are used, E is the magnitude of the electric field of angular frequency ω , and E_B is the initial binding energy of the ionized electron. The quantity z_1 is the inverse square of the Keldysh parameter γ . Both z and z_1 must be large for tunneling to occur. Asymptotic results have been given for the intense field case $z \gg 1$, which do not require that z_1 be large as well. What is explored here is the degree to which these asymptotic forms will predict observable high order ionization subject to the limitation that $z_1 \leq 1$, i.e., that tunneling does not take place. Basic to this investigation is an asymptotic form for a generalized Bessel function of two variables, which can be simplified from a general expression given in Ref. 6 to the result

$$[J_n(u,v)]^2 \approx \left(\frac{ze}{2n} \right)^n \frac{\cos^2 \chi}{\pi(n^2 - z^2)^{1/2}}, \quad (1)$$

where z is the basic intensity parameter just defined, n is the multiphoton order, and χ is a complicated quantity whose definition is unimportant for the assessment of the magnitude of Eq. (1). The quantity n is bounded from below by $n_0 = (z + E_B/\omega)$, where the brace indicates the smallest integer containing the quantity within the brace, and Eq. (1) is valid when $n \approx n_0$. For explicitness, Eq. (1) can be incorporated into a transition rate expression based upon a hydrogen ground state as the initial state of the system, but the essential results flow from the use of Eq. (1) rather than any particular choice of initial state. The transition rate so generated is

$$W \approx \frac{4}{\pi^2} \omega \left(\frac{E_B}{\omega} \right)^{5/2} \sum_{n=n_0}^{\infty} \left(\frac{ze}{2n} \right)^n \frac{(n-z-E_B/\omega)^{1/2}}{(n+z)^{1/2}(n-z)^{5/2}}, \quad (2)$$

where the sum converges very rapidly after the first few terms. The number of independent physical quantities in Eq. (2) can be confined to two by demanding that $z_1 = 1$, which allows the greatest possible latitude while still excluding the tunneling regime. One notices in Eq. (2) factors equivalent to $(z/2)^n/n!$, which sharply limits the degree to which n can exceed z . The limitation on z_1 is indeed confining, but important possibilities for very high order processes do exist, as will be discussed.

REFERENCES

- ¹L. V. Keldysh, Sov. Phys. JETP 20, 1307 (1965).
- ²F. Yergeau, S. L. Chin, and P. Lavigne, J. Phys. B 20, 723 (1987).
- ³L. A. Lompré, A. L'Huillier, G. Mainfray, and C. Manus, J. Opt. Soc. Am. B 2, 1906 (1985).
- ⁴U. Johann, T. S. Luk, H. Egger, and C. K. Rhodes, Phys. Rev. A 34, 1084 (1986).

- ⁵T. J. McIlrath, P. H. Bucksbaum, R. R. Freeman, and M. Bashkansky, to be published.
- ⁶H. R. Reiss, Phys. Rev. A 22, 1786 (1980).
- ⁷H. R. Reiss, in Photons and Continuum States of Atoms and Molecules, edited by N. K. Rahman, C. Guidotti, and M. Allegrini (Springer-Verlag, Berlin, 1987).
- ⁸H. R. Reiss, J. Phys. B 20, L79 (1987).
- ⁹P. H. Bucksbaum, private communication, March 1987.

Consequences of a Final State Model of Above-Threshold Ionization
W. Becker^(a), R. R. Schlicher^(b), M. O. Scully^(a,b), and K.
Wódkiewicz^(a,c)

(a) Center for Advanced Studies and Dept. of Physics and Astronomy,
Univ. of New Mexico, Albuquerque, NM 87131

(b) Max-Planck Institut für Quantenoptik, D-8046 Garching bei München,
W. Germany

(c) Permanent address: Institute of Theoretical Physics, Warsaw
University, Warsaw 00-681, Poland

Calculating the rates and spectra of above-threshold multiphoton ionization (ATI) [1] from first principles is a next to impossible task. Even the simplest one-body problem - ionization of one bound electron in a monochromatic laser field - is very difficult due to the fact that no satisfactory wave function for the bound electron in the presence of the laser field is available. In addition, for the ionization of many-electron atoms collective effects such as the excitation of collective atomic modes or the simultaneous ejection of several electrons are likely to play a role. Finally, it is certain that the detailed structure of the laser pulse (which is poorly known to the experimenter) has to be taken into account before any quantitative comparison with the experimental data can be carried out. Given this situation it is very useful if some aspects of the entire problem can be separated off and studied more or less independently of the others. Such an aspect is the behavior of the electron in the laser field after it has been "created" by ionization. It will turn out that this final state interaction is responsible for most of the features observed in the ATI electron spectra.

With this motivation in mind we have modeled the ATI process in a very simple way [2,3]. We assume some effective interaction that just lifts the electron into the continuum via absorption of the minimum number N of photons. We further assume that as soon as the electron has been created it is only subject to the laser field and does no longer

feel the ionic potential. We thus decompose the entire ATI process into two subprocesses which add up incoherently. We leave the first part largely unspecified; the second part is then fully described by the so-called Volkov wave function, which is an exact solution for an electron in an external plane wave field. Thereby, we will be able to conclude that all features which we will derive for the ATI electron spectrum originate solely from the Volkov solution, and have little to do with the details of how exactly the electrons were created. Conversely, whatever features of the experimental ATI spectrum we do not recover in our model calculation, are then due to the details of the process of ionization.

The electron spectra derived from this model qualitatively exhibit most of the universal features of ATI, notably peak switching and peak suppression [2,3]. The latter is due to the presence of the ponderomotive potential when the electron leaves the pulse on one side. The reduced order of nonlinearity of the first peak of the spectrum is well reproduced [3]. The model makes definite predictions for the angular distributions in a monochromatic laser field. These will be distorted by the action of the ponderomotive force which depends on the pulse shape and the path along which the electron leaves the pulse. However, gross features of the angular distributions are immediately evident from the model, such as the predominant emission in the direction of the electric field which has been observed for linear polarization [4]. If the effective interaction is such that the electron is in the first step lifted up high into the continuum at a certain energy, the model predicts an electron energy distribution which is symmetric about this energy with a pronounced peak on either side. This is related to the classical limit discussed in [5] where $\hbar \rightarrow 0$ in as much as the Volkov solution is concerned. This situation could be achieved by a superposition of a high-intensity high-frequency laser which brings the electron in the continuum and a low frequency laser (possibly microwave) that induces continuum-continuum transitions (cp.

[6]). If we assume an effective interaction which contributes an intensity dependence I^N (with N the minimum number of photons), the model predicts a total ionization rate proportional to I^N as given by perturbation theory. In contrast, the electron energy spectrum is determined by the Volkov solution and beyond the reach of perturbation theory. To put it differently, ATI realizes a situation where perturbation theory is applicable for the total ionization rate while it is not for the differential rate with respect to the electron energy. The Volkov solution primarily effects a redistribution of electron energies which does not affect the total rate. This is a very general feature of the laser-particle interaction. It has, for example, been discussed in the context of nuclear beta-decay in a laser field [5,7] and has been clearly established experimentally in ATI [8].

REFERENCES

1. For a review, see M. Crance, Phys. Reports 144, 117 (1987).
2. W. Becker, R. R. Schlicher, and M. O. Scully, J. Phys. B 19, L785 (1986).
3. W. Becker, R. R. Schlicher, M. O. Scully, and K. Wódkiewicz, J. Opt. Soc. Am. B (to be published).
4. H. J. Humpert, H. Schwier, R. Hippler, and H. O. Lutz, Phys. Rev. A32, 3787 (1985).
5. W. Becker, R. R. Schlicher, and M. O. Scully, Proc. of the NATO ASI on Nonequilibrium Cooperative Phenomena in Physics and Related Fields, El Escorial, Spain, ed. by M. G. Velarde (Plenum, N.Y. 1984) p. 145.
6. H. G. Muller, H. B. van Linden van den Heuvell, and M. J. van der Wiel J. Phys. B 19, L733 (1986).
7. W. Becker, R. R. Schlicher, and M. O. Scully, Nucl. Phys. A426, 125 (1984); R. R. Schlicher, doctoral dissertation, Technical University of Munich (1985).
8. F. Yergeau, G. Petite, and P. Agostini, J. Phys. B 19, L663 (1986).

PHOTOELECTRON STUDIES OF MULTIPHOTON PROCESSES IN SMALL MOLECULES*

S. T. Pratt, M. A. O'Halloran,
F. S. Tomkins, J. L. Dehmer, and P. M. Dehmer
Argonne National Laboratory
Argonne, Illinois 60439

In the past few years we have used resonantly enhanced multiphoton ionization-photoelectron spectroscopy (REMPI-PES) to examine the photoionization dynamics of a number of atoms and small molecules in excited states.¹ REMPI-PES has been used to study photoionization processes in atoms produced by the photofragmentation of molecular species and to study photoionization and predissociation of excited states of rare gas dimers. In addition, we have used direct, nonresonant multiphoton excitation into the ionization continuum to probe autoionizing levels of the rare gas atoms and the nitric oxide molecule. The photoelectron branching ratios and angular distributions so obtained provide new information on the dynamics of autoionization in these systems.

One example that will be discussed in some detail involves the three photon resonant, four photon ionization of molecular hydrogen via the $C\ ^1\Pi_u$ electronic state. Experimental data for this system has been obtained for ionization via a number of individual rotational and vibrational levels of the $C\ ^1\Pi_u$ state. The data include photoelectron angular distributions² and angle-resolved² and angle-integrated³ vibrational branching ratios. Data obtained using a magnetic bottle electron spectrometer³ also provide information on the rotational branching ratios within individual vibrational bands of the photoelectron spectrum. In addition, photoelectron angular distributions and vibrational branching ratios have recently been recorded for the analogous bands in D_2 . The data will be compared with the detailed theoretical calculations of Dixit et al.⁴ The qualitative agreement between experiment and theory is quite good. Possible explanations for the quantitative discrepancies will be discussed.

References

1. P. M. Dehmer, J. L. Dehmer, and S. T. Pratt, Comm. in Atom. and Mol. Phys., in press.
2. S. T. Pratt, P. M. Dehmer, and J. L. Dehmer, J. Chem. Phys. 85, 3379 (1986).
3. M. A. O'Halloran, S. T. Pratt, P. M. Dehmer, and J. L. Dehmer, in preparation.
4. S. N. Dixit, D. L. Lynch, and V. McKoy, Phys. Rev. A 30, 3332 (1984).

*Work supported by the U.S. Department of Energy, Office of Health and Environmental Research, under Contract W-31-109-Eng-38 and by the Office of Naval Research.

THEORETICAL RESONANT MULTIPHOTON IONIZATION STUDIES IN MOLECULES

S. N. Dixit,[†] R. L. Dubs,^{††} H. Rudolph,^{††} and V. McKoy^{††}

[†]University of California, Lawrence Livermore National Laboratory*
Livermore, California 94550

^{††}Noyes Laboratory of Chemical Physics**
California Institute of Technology
Pasadena, CA 91125

In an (n+m) resonant enhanced multiphoton ionization (REMPI), a molecule in its initial state absorbs n photons to make a transition to an excited rovibronic state and is subsequently ionized out of this state by the absorption of additional m photons. The high intensity, narrow bandwidth and the tunability of modern dye lasers, together with high resolution photoelectron spectroscopy (PES) make REMPI-PES an extremely powerful probe of excited states and ionization dynamics. This technique offers several possibilities and advantages, including: i) high precision spectroscopy of highly excited states, ii) photoionization dynamics of fully quantum mechanically specific rovibronic states, iii) production of ions in well-defined rovibronic states, iv) study of the effects of collisions by varying the delay between pump and probe lasers and v) ultrasensitive detection. Several groups¹ have exploited one or more of these advantages to demonstrate ionic state selectivity,² non-Franck-Condon effects in ionic vibrational branching ratios,³ identification of new states,⁴ Rydberg valence mixing⁵ and autoionization.⁶ REMPI is also being used to probe rotational state population and alignment in molecules desorbed or scattered from surfaces.⁷

In spite of this considerable experimental activity, there has been limited theoretical analysis of molecular REMPI processes. The need for such an analysis is quite obvious as REMPI spectra are influenced not only by dynamical effects such as saturation, a.c. Stark shifts, and the spatio-temporal profiles of the laser pulses but also

by strictly molecular aspects such as the multi-center nature of the molecular field and the interaction among the rotational, vibrational and electronic states.

In the last two years, we have begun a theoretical analysis of REMPI processes in diatomic molecules.⁸ Our emphasis is on ab initio calculation of the molecular parameters and their subsequent incorporation into REMPI dynamics. Applications of the framework to analyze the observed rovibrational branching ratios in several REMPI experiments in H_2 (via the $B'\Sigma_u^+$, $C'\Pi_u$ and $E,F'\Sigma_g^+$ states)⁹ and rotational branching ratios in NO [via the $A^2\Sigma^+(3s\sigma)$ and the $D^2\Sigma^+(3p\sigma)$ states]^{10,11} have been fairly successful in explaining observed anomalies. For example, the experimental ionic rotational branching ratios in the (2+1) REMPI via the $D^2\Sigma^+$ state¹² point to the production of photoelectrons in the $l=1$ partial wave after ionization out of the predominantly 3p (>99%) Rydberg orbital! Studies taking into account the non-spherical nature of the molecular potential reproduce this anomaly and yield rotational branching ratios in good agreement with experiment.¹¹ This analysis has also lead to a rotational selection rule¹³ which offers possibilities for creating ions in specific rovibronic states by clever choices of REMPI schemes. We have recently shown¹⁴ that the alignment created by absorption of photons imparts a circular dichroic character to the photoelectron angular distributions (CDAD) resulting from the photoionization of these resonant intermediate states. This effect is present in non-chiral molecules and persists in the electric dipole approximation. The (n+1) CDAD spectra can be simply related to the state alignment and, as such, hold promise as a useful tool in investigating product state alignment. We will highlight these and other REMPI aspects in the presentation.

*Work performed under the auspices of the U.S. Department of Energy by Lawrence Livermore Nat'l. Lab. under contract #W-7405-Eng-48.

**Work supported by the National Science Foundation under Grant No. CHE-8521391 and by the Air Force Office of Scientific Research under Grant No. 87-0039.

REFERENCES

1. See, for example, the reviews by K. Kimura, Adv. Chem. Phys. 60, 161 (1985); R. N. Compton and J. C. Miller, to be published.
2. S. T. Pratt, et al., J. Chem. Phys. 80, 1706 (1984); 81, 3444 (1984).
3. S. T. Pratt, et al., Chem. Phys. Lett. 105, 28 (1984).
4. P. Chen, et al., J. Chem. Phys. 86, 516 (1987).
5. A. Sur, et al., J. Chem. Phys. 84, 69 (1986).
6. J. Kimman, et al., Chem. Phys. 97, 137 (1985).
7. A. Burns, Phys. Rev. Lett. 55, 525 (1985); D. Jacobs and R. N. Zare, J. Chem. Phys. 85, 5457 (1986); *ibid* 85, 5469 (1986).
8. S. N. Dixit and V. McKoy, J. Chem. Phys. 82, 3546 (1985).
9. S. N. Dixit, et al., Phys. Rev. A 30, 3332 (1984); D. L. Lynch, et al., Chem. Phys. Lett. 123, 315 (1986); H. Rudolph, et al., J. Chem. Phys. 84, 6657 (1986) and H. Rudolph, et al., to be published.
10. S. N. Dixit, et al., Phys. Rev. A 32, 1267 (1985).
11. H. Rudolph, et al., to be published.
12. K. Viswanathan, et al., J. Phys. Chem. 90, 5078 (1986).
13. S. N. Dixit and V. McKoy, Chem. Phys. Lett. 128, 49 (1986).
14. R. L. Dubs, et al., J. Chem. Phys. 85, 656 (1986), *ibid* 85 6267 (1986) and R. L. Dubs, et al., to be published.

Invited Paper

MULTIPHOTON MOLECULAR SPECTROSCOPY

M. N. R. Ashfold

School of Chemistry
University of Bristol
Bristol BS8 1TS
England

Intramolecular Couplings Studied by Doppler-Free Two-Photon Processes

E. Riedle and H. J. Neusser, Institut f. Physikalische u. Theoretische Chemie
TU München, Lichtenbergstr. 4, D-8046 Garching, West-Germany

One of the virtues of multi-photon processes is the capability to yield Doppler-free excitation. In particular we could show, that Doppler-free two-photon spectroscopy allows the resolution of the rotational structure of vibronic bands of the prototype organic molecule benzene (C_6H_6) /1/ and permits the precise investigation of intramolecular coupling /2/. Intramolecular couplings are well studied in the electronic spectra of small molecules. In large molecules such couplings are of particular interest, as they lead to dynamical processes due to the large number of coupling states. Often even coupling to a quasi-continuum of states within the bound level structure of the molecule is observed. However, in these large molecules, the observation of single rovibronic transitions was not possible hitherto, since the rovibronic lines are separated by less than the Doppler-width in the gas phase.

For the Doppler-free experiments a cw frequency-stabilized single mode dye laser is used as a light source for the excitation of the molecules. To increase the probability of the two-photon absorption by up to three orders of magnitude, the absorption cell is placed inside an external concentric resonator /3/. The UV-fluorescence is observed to monitor the excitation of the molecules. An example of the spectrum observed in this way is shown in the lower part of Fig. 1. It shows the blue edge of the 14^1_0 -band of 1,3,5- $C_6H_3D_3$ at the molecular frequency of 39758 cm^{-1} , corresponding to a laser wavelength of about 5030 Å. The spectrum is a pure line spectrum, with each of the lines corresponding to a single rovibronic transition. The Doppler-width of 1.7 GHz would not allow the resolution of any of these lines. The assignment of the lines according to a symmetric rotor model yields values of the rotational constants with an accuracy higher by two orders of magnitude than obtained from Doppler-limited spectroscopy. Even the exact determination of the centrifugal distortion constants is now possible. The spectrum calculated with these constants is shown for comparison in the upper part of Fig. 1. The deviations of less than 10 MHz in the line positions correspond to the present accuracy in the calibration of the spectrum.

In some parts of the band deviations from the calculated spectrum appear. This has been recently demonstrated for C_6H_6 /2/. A systematic analysis of

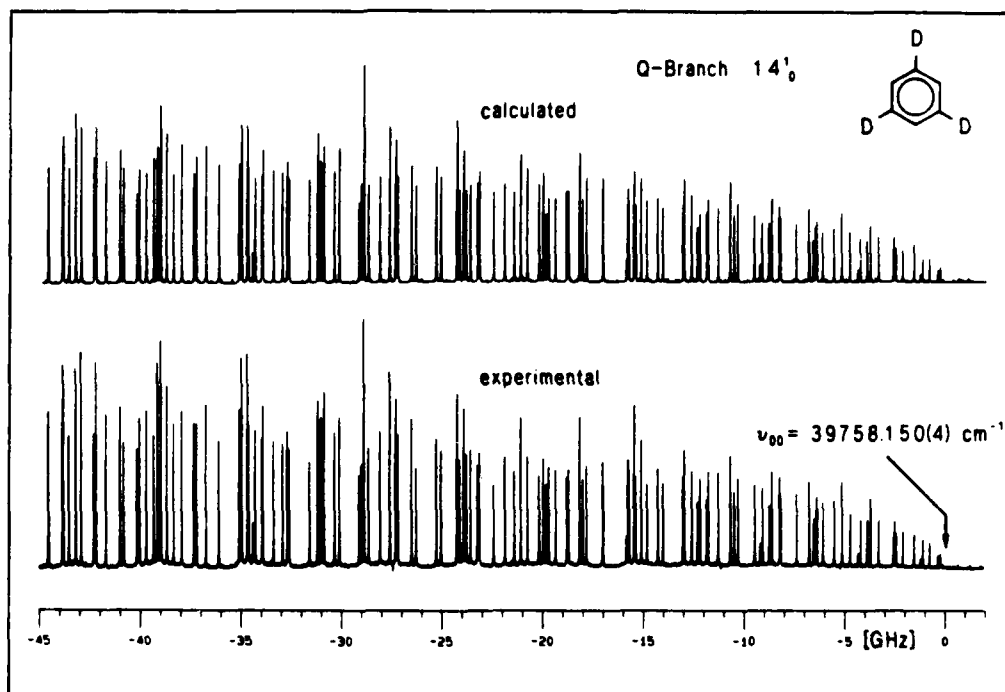


Fig. 1: Doppler-free two-photon spectrum of $C_6H_3D_3$. The upper trace shows the calculated spectrum, the lower one the experimental

these perturbations shows, that they are caused by rotational selective Coriolis-coupling of the light zero order states to a dark background state. From the deviations of the positions of the two resulting eigenstates from the expected position of the light state, the value of the coupling matrix element, the position of the unperturbed dark zero order state and the degree of mixing can be determined.

To investigate the dynamic behavior of the excited rovibronic states, pulsed laser light of extremely narrow band width is used /4/. This light is produced by pulsed amplification of the cw light in a three stage amplifier chain pumped by the light of an excimer laser. The resulting light pulses of up to 10 ns length have a Fourier limited bandwidth of only 50 MHz. For the observation of very fast decays the pulses can be shortened to a length of 2.5 ns with a corresponding increase in band width /5/. Investigation of the decay of a large number of rovibronic states with a wide range of the values of the rotational quantum numbers J and K shows, that the decay of unperturbed states does not depend on the rotation of the molecule /4/. On the contrary, for perturbed states there is a strong dependence of the decay on

the degree of the mixing. In this way the decay rate of the dark states can be determined.

While all results mentioned so far were obtained at low vibrational excess energy (about 1570 cm^{-1}), at higher vibrational energy (about 3400 cm^{-1}) a strong decrease of the number of rotational lines in the vibrational bands is observed. This is due to the rotational selective fast decay of most of the excited states, which only makes long lived states observable in our fluorescence excitation spectra. We were able to show, that this selective decay is due to Coriolis coupling of the light states to dark states which decay very rapidly due to the strong ISC and IC coupling /5/. The resolution of better than 10 MHz in the cw experiments made it possible to measure the homogeneous line width of some of the lines in this regime /3/. With the pulsed set up the decay time of the same states could be measured /5/. It is found to agree very well with the observed line widths.

Comparison of the observed decay rates with previously reported decay rates of single vibronic states of benzene is made difficult by the fact, that most experiments were performed on vibronic states which can be reached by one-photon transitions. Due to the high symmetry of the benzene molecule (D_{6h}) these states are different from the ones reached in our two-photon experiments. To obtain rotationally resolved spectra of such one-photon-bands, we recently frequency-doubled the light of our extremely narrow band pulsed light source and recorded spectra in a well collimated molecular beam apparatus. Instead of the detection of the molecular fluorescence, the resonance enhanced two-photon ionization signal was observed. A resolution of 150 MHz was obtained in the spectra. This proved to be sufficient for the resolution of most rotational transitions. For higher vibrational excess energy, perturbations were also identified in these one-photon bands.

The results reported show, that both one-photon and two-photon bands of the large molecule benzene can be observed with rotational resolution by Doppler-free two-photon methods. This leads to a dramatic increase in possible accuracy of the observation of intramolecular coupling and state-specific decay.

- /1/ E.Riedle, H.J.Neusser and E.W.Schlag, J.Chem.Phys. 75, 4231 (1981)
- /2/ E.Riedle, H.Stepp and H.J.Neusser, Chem.Phys.Letters 110, 452 (1984)
- /3/ E.Riedle and H.J.Neusser, J.Chem.Phys. 80, 4686 (1984)
- /4/ U.Schubert, E.Riedle and H.J.Neusser, J.Chem.Phys. 84, 5326 (1986)
- /5/ U.Schubert, E.Riedle, H.J.Neusser, E.W.Schlag, J.Chem.Phys. 84, 6182 (1986)

Dephasing effects on time-resolved multiphoton
transitions of molecules

Y. Nomura, M. Hayashi, and Y. Fujimura
Department of Chemistry, Faculty of Science

Tohoku University, Sendai 980, JAPAN

and

S. H. Lin

Department of Chemistry, Arizona State University
Tempe, Arizona 85287 U.S.A.

Recently nonexponential time-dependent behaviors such as biexponential and oscillatory decays have been reported in time-resolved multiphoton ionization¹ and coherent anti-Stokes Raman scattering (CARS) spectra of molecules.² These time-dependent behaviors originate from the coherent excitation of molecular eigenstates (molecular coherence) by pumping laser and the subsequent dephasing of the molecular coherence in the resonant state. By analyzing the time-resolved spectra, one can determine the rovibronic structure and characterize the molecule-perturber interactions. So far effects of the dephasing were neglected in most of the theoretical treatments on time-resolved multiphoton processes of molecules in vapor or solids.

The purpose of this paper is to theoretically investigate the dephasing effects on the multiphoton transitions in the time domain. Dephasing effects in the frequency domain have already been reported.³ For this purpose we consider time-resolved resonant three-photon ionization and CARS processes.

Expressions for the probability of the ionization and the intensity of the CARS as a function of time are

derived by using the density matrix method. A different role of the dephasing constant between the multiphoton ionization and CARS processes is explained. Model calculations of the time-resolved three-photon ionization spectra of pyrazine via $S_1(0-0)$ state in supersonic jet and CARS spectra of hydrogen bonded crystals including amino acids and peptides are performed to clarify the mechanism of the dephasing of the molecular coherence.

References

1. J. L. Knee, F. E. Doany, and A. H. Zewail, J. Chem. Phys. 82, 1042 (1985)
2. T. J. Kosic, R. E. Cline, and D. D. Dlott, J. Chem. Phys. 81, 4932 (1984)
3. (a) Y. Prior, A. R. Bogdan, M. Dagenais, and N. Bloembergen, Phys. Rev. Lett. 46, 111 (1981)
(b) Y. Fujimura and S. H. Lin, J. Chem. Phys. 78, 6468 (1983)

DRESSING AND PHOTOIONIZATION OF THE H ATOM IN AN UNTRAINTENSE LASER FIELD

M Janjušević and M. H. Mittleman

The City College of The City University of New York
Convent Avenue & 138th Street
New York, NY 10031

We used a projection operator formalism, described in (1) to analyze a state of a hydrogen atom in a very intense laser field. A starting Hamiltonian in dipole approximation is

$$H = \frac{\vec{p} + e/\omega \vec{E} \cos \phi}{2m}^2 + V + \hbar\omega(N + \frac{1}{i} \frac{\partial}{\partial \phi}) \quad (1)$$

the laser field being given in the phase representation (2).

This formalism leads to the Schrödinger equation

$$P[W + i\omega \frac{\partial}{\partial \phi} - h - \nu] P\psi = 0 \quad (2)$$

where

$$h = \frac{p^2}{2m} + U_p + V + \delta h \quad (3)$$

U_p being a ponderomotive potential, ν is the effective potential defined by the equation

$$PVP\psi = P\delta h \frac{Q}{i\omega \frac{\partial}{\partial \phi} + W - T - V - U_p - Q\delta hQ} \delta hP\psi \quad (4)$$

where in a high intensity limit V could be neglected with respect to $Q\delta hQ$. P and Q are projection operators $P=1-Q$, P projecting onto the state with initial number of photons.

This gauge gives a continuum edge shifted upward by the ponderomotive potential, U_p .

A variational principle is used to construct a ground state wave function $\Phi(k)$

$$E = \frac{\langle T \rangle}{\langle N \rangle} + \frac{\langle V \rangle}{\langle N \rangle} \quad (5)$$

where

$$\langle T \rangle = \int d^3k \Phi^2(k) \epsilon_k, \quad \langle N \rangle = \int d^3k \Phi^2(k)$$

and

$$\langle V \rangle = \int d^3k d^3k' \Phi(k) J_0(\alpha k_{\perp}) \tilde{V}(k-k') J_0(\alpha k'_{\perp}) \Phi(k') \quad (6)$$

is obtained from (4). A trial function has been given in the form

$$\Phi(k) = J_0(\alpha k_{\perp}) u(k) \quad (7)$$

with

$$u(k) = \frac{1}{k_{\perp}^2 + \beta^2} (k_z^2 + 1) \quad (8)$$

We found that for a circularly polarized field the H atom does not form a bound state.

For a linearly polarized field there exists a near stable bound state with its binding energy

$$E \sim \frac{c}{\lambda} (\ln \lambda)^2 \lambda \sim \frac{E}{\omega^2} \quad (9)$$

The width of a state is small in comparison to binding energy

$$\frac{\Gamma}{2\pi} = \text{Im} (\Phi(k), \delta h_k P \cos \phi G(k, \phi; k', \phi') \cos \phi' P \delta h_{k'}, \Phi(k')) \quad (10)$$

where the Green's function G could be expanded as

$$G = G^{(+)} + G^{(+)} V G^{(+)} + G^{(+)} V G^{(+)} V G^{(+)} + \dots \quad (11)$$

$G^{(+)}$ being defined as

$$(-i\epsilon_k \frac{\partial}{\partial \phi} + 1 + i\eta + a_k Q \cos \phi Q) G^{(+)}(\phi, \phi') = Q \delta(\phi - \phi') \quad (12)$$

A first nonvanishing term is a second order in Coulomb potential.

REFERENCES

1. J. I. Gersten and M. H. Mittleman, J. Phys. B 9, 2561 (1976).
2. I. Bialynicka-Birula and Z. Bialynicka-Birula, Phys. Rev. A 14, 1101 (1976); I. Bialynicka-Birula, Acta Phys. Austriaca Suppl. XVIII, 111 (1977).

THE STRUCTURE OF ATOMIC HYDROGEN IN HIGH-INTENSITY, HIGH-FREQUENCY LASER FIELDS OF LINEAR POLARIZATION

M. Pont^{*}, C.W. McCurdy^{**}, N. Walet^{*}, and M. Gavrilă^{*},

^{*}FOM-Institute for Atomic and Molecular Physics, Amsterdam, the Netherlands
^{**}Chemistry Department, Ohio State University, Columbus, Ohio, USA

Substantial effort is now being invested in the development of high-frequency lasers operated at high intensities. Intensities as high as 10^{17} W/cm² (several times the atomic unit = $3.51 \cdot 10^{16}$ W/cm²) have been achieved at wave lengths as short as 193 nm, and more progress is expected¹. Under these circumstances, atomic interactions are drastically modified. A nonperturbative theory was recently developed to deal with atoms placed in such radiation fields^{2,3}.

We present here the first highly accurate calculation of the structure of atomic hydrogen in a monochromatic, high-frequency (ω) laser field, of linear polarization (polarization vector \vec{e}) and arbitrary intensity. It was shown that the semiclassical, time dependent Schrödinger equation reduces in first approximation to a time independent Schrödinger equation, $H\Psi = E\Psi$, containing the "dressed potential":

$$V_0(\alpha_0; \vec{r}) = \frac{1}{\pi} \int_{-1}^{+1} V(\vec{r} + \alpha_0 \vec{e} u) \frac{du}{(1-u^2)^{1/2}}. \quad (1)$$

Here $V(r) = -Z/r$ is the original Coulomb potential and $\alpha_0 = I^{1/2} \omega^{-2}$ a.u. Since the equation $H\Psi = E\Psi$ has real eigenvalues, this shows that in, first approximation, the atom is stable in this regime, i.e. does not decay by multiphoton or excess-photon ionization. (These become possible only in the next approximation.) This agrees with a theory presented earlier in Ref.4.

V_0 of Eq.(1) is the electrostatic potential due to a linear charge distribution, extending from $-\alpha_0$ to $+\alpha_0$ along the direction of \vec{e} , of density $\sigma(\xi) = (\pi\alpha_0)^{-1} [1 - (\xi/\alpha_0)^2]^{-1/2}$. It is axially symmetric around \vec{e} and has even parity with respect to the center of the line of charges. The axial symmetry causes considerable difficulty in the solution of the eigenvalue problem, since only the magnetic quantum number m and the parity (g or u) remain good quantum numbers. Hence, a classification scheme can be introduced for the states, similar to that for homonuclear diatomic molecules.

We have computed the eigenvalues and eigenfunctions of the lower lying states of the type σ_g and σ_u . This was done by diagonalizing the Hamiltonian containing the dressed

potential Eq.(1) in a multicenter (cartesian) Gaussian basis. The location of the centers, their number, as well as the exponents of the Gaussians, were optimized for each value of α_0 separately over a large range ($0 < \alpha_0 < 100$). In Figs. 1 and 2 we present the values of the wave function of the ground state $(1s)\sigma_g$ for $\alpha_0=20$, in a plane passing through the symmetry axis \vec{e} (denoted Z in the Figures). They show how the hydrogen atom is stretched out along the line of charges (extending from -20 to +20 along the Z axis) and how the wave function tends to concentrate at its end points. The eigenvalue for $\alpha_0=20$ is $E = -0.1596$ Ry. Note the dramatic decrease of the binding energy of the atom at this value of α_0 . At still higher α_0 values, the field practically splits the atom into two distinct parts separated by a distance of the order of $2 \alpha_0$.

REFERENCES

1. C.K. Rhodes, Science 229, 1345 (1985).
2. M. Gavrilă, in: *Fundamentals of Laser Interactions*, ed. F. Ehlotzky (Lecture notes in physics, vol. 229, Springer, 1985), p.3.
3. M. Gavrilă and J.Z. Kaminski, Phys.Rev.Lett. 52, 613 (1984), and to be submitted for publication.
4. J.I. Gersten and M.H. Mittleman, J.Phys.B 9, 2561 (1976).

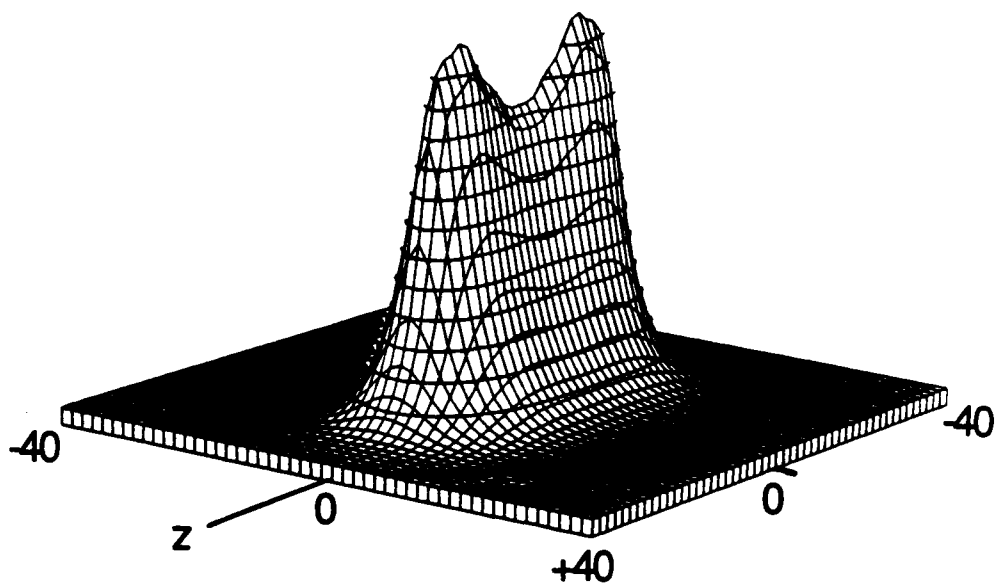


Figure 1. Values of the (normalized) ground state $(1s)\sigma_g$ wave function of hydrogen in a plane passing through the polarization vector \vec{e} , for $\alpha_0 = 20$, $Z = 1$. The maximum height is 0.022.

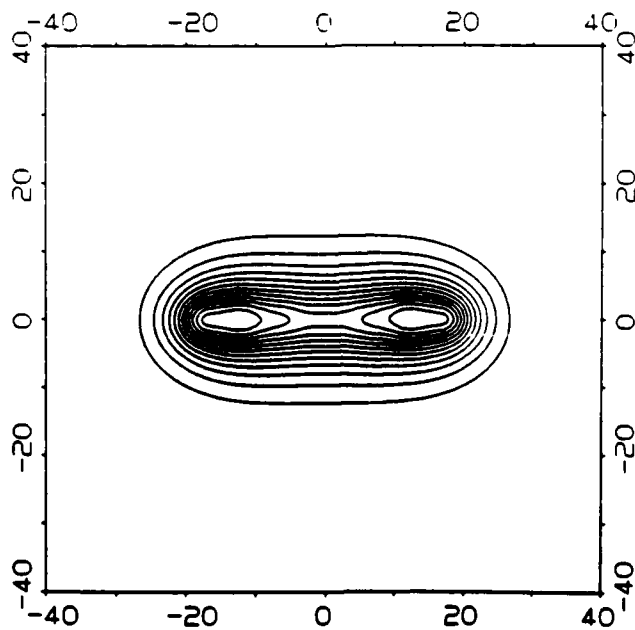


Figure 2. Contour plot of the wave function in Fig.1. The equidistance of the level lines is 0.002.

ATOMIC HYDROGEN IN CIRCULARLY POLARIZED, HIGH-INTENSITY AND HIGH-FREQUENCY LASER FIELDS

M. Pont, M.J. Offerhaus and M. Gavrilu

FOM-Institute for Atomic and Molecular Physics, Amsterdam, The Netherlands

The study of atoms in intense infrared and visible laser fields has been carried out extensively over the years. More recently, following impressive advances in the development of high-intensity lasers (yielding several atomic units of intensity) at high frequencies (VUV and beyond)¹ attention has been focused on atomic physics in this radiation regime. A nonperturbative theory was devised to describe atomic behaviour under such extreme conditions^{2,3}. We here present its application to the calculation of the structure (energy levels and average sizes) of a hydrogen atom placed in a circularly polarized field. The case of circular polarization has attracted considerable interest lately because of the different experimental features found with respect to the linearly polarized case. (Atomic hydrogen in a linearly polarized field is discussed, from a different point of view, in a separate abstract⁴.)

In the radiation regime we are considering, the semiclassical, time dependent Schrödinger equation describing the interaction with the field reduces in first approximation to a time independent Schrödinger equation $H\psi = E\psi$, containing the "dressed potential"^{2,3}:

$$V_0(\alpha_0; \vec{r}) = -\frac{1}{2\pi} \int_0^{2\pi} V(\vec{r} + \alpha_0 \vec{e}_1 \cos\phi + \alpha_0 \vec{e}_2 \sin\phi) d\phi \quad (1)$$

Here $V(r) = -Z/r$, \vec{e}_1 and \vec{e}_2 are unit vectors orthogonal to each other and to the direction of propagation of the radiation, and $\alpha_0 = I^{1/2}\omega^{-2}$, with I the intensity and ω the frequency in atomic units. As in the linear case⁴, the fact that the equation $H\psi = E\psi$ has real eigenvalues means that in first approximation the atom is stable towards decay by multiphoton ionization. This agrees with the theory presented earlier in Ref. 5.

$V_0(\alpha_0; \vec{r})$ of Eq.(1) represents the electrostatic potential generated by a homogeneously charged ring of radius α_0 , perpendicular to the direction of propagation. It is axially symmetric around the axis of the ring, and has even parity with respect to its center. Thus, as in the linear case⁴, the magnetic quantum number m and the parity (g or u) remain good quantum numbers, whereas the azimuthal quantum number ℓ ceases to be so. We therefore have adopted a classification scheme for the states similar to that for homonuclear diatomic molecules (although the potential has a quite different form in the

latter case), e.g. $(n\ell)\sigma_g$ will designate the state with $|m| = 0$, even parity, developing continuously from the unperturbed state n, ℓ .

The calculation of the energy levels was carried out by analyzing the Schrödinger equation for the dressed potential in a spherical harmonics basis, and by adopting the "decoupled ℓ -channels approximation" (nondiagonal, $\ell \neq \ell'$, matrix elements of V_0 neglected). We have computed the levels corresponding to principal quantum number $n \leq 4$ over an extended range of α_0 values ($0 < \alpha_0 < 100$). Further, in order to characterize the size of the atom in its various states, we have computed the average values \bar{r} , and their root-mean-squares Δr , over the same range of α_0 . In Fig. 1 we present eigenvalues for the lower-lying σ_g states, and in Fig. 2 the corresponding \bar{r} .

Fig. 1 shows a dramatic decrease with α_0 of some of the binding energies, in particular that of the ground state, at values now attainable in experiment (e.g. $\alpha_0 \approx 10$). This is of considerable consequence for the energy spectrum of the ionized electrons. A new peak pattern is predicted differing from that currently seen in multiphoton ionization experiments: no peak suppression occurs now, and substantial shifts of the peaks with respect to the weak field case may appear. Fig. 2 displays a quasi-linear increase of the averages \bar{r} with α_0 . Apparently, at large α_0 the atom in its lower states (e.g. the ground state) attains a size typical of Rydberg atoms. We have also made a comparison with the case of linear polarization.

References

1. C.K. Rhodes, Science **229**, 1345 (1985).
2. M. Gavrilă, in: *Fundamentals of Laser Interactions*, ed. F.Ehlotzky (Lecture notes in physics, vol. **229**, Springer, 1985), p. 3.
3. M. Gavrilă and J.Z. Kaminski, Phys.Rev.Lett. **52**, 613 (1984) and to be submitted for publication.
4. M. Pont, C.W. McCurdy, N. Walet and M. Gavrilă, contributed paper to ICOMP IV.
5. J.I. Gersten and M.H. Mittleman, J.Phys. **B9**, 2561 (1976).

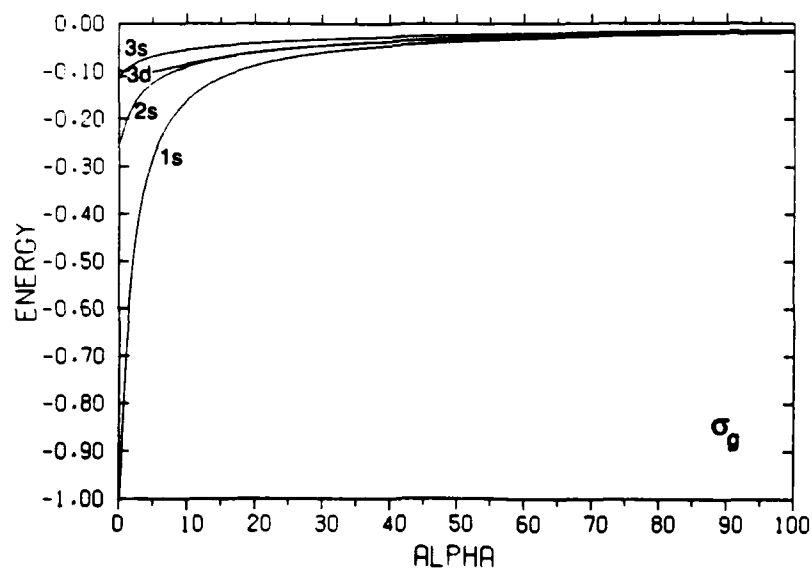


Fig.1. Dependence of energy levels (in Ry) on α_0 (in a.u.) for lower lying σ_g states ($Z=1$).

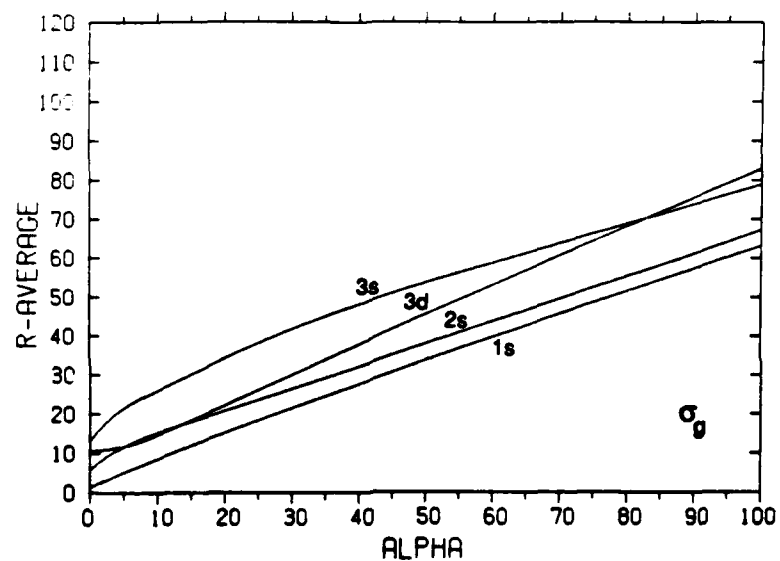


Fig.2. Dependence of averages \bar{r} on α_0 (both in a.u.) for lower lying σ_g states ($Z=1$).

Invited Paper

Experimental Signatures of Atomic Many-Photon
Absorption in the Classically-Chaotic Regime

James E. Bayfield
Department of Physics and Astronomy
University of Pittsburgh
Pittsburgh, Pennsylvania 15260 USA

Hydrogenic atoms and ions in excited states with large quantum numbers can be exposed to low frequency electromagnetic waves where one hundred photons must be absorbed for ionization. At sufficiently high external field intensities, classical treatments of the absorption of electromagnetic energy predict electron motion that exhibits deterministic chaos (1,2). The quantum dynamics of such classically chaotic systems involves a strong radiative coupling of all pairs of quantum states with nearly-resonant energy differences, starting from the initial state and extending all the way into the continuum. The radiative broadenings of these states must be comparable to or larger than their energy differences. All the two-state Rabi-flopping probability amplitudes for one-photon absorption are nearly equal to one (3).

Classically, the time evolution of the increasing energy of the chaotically-moving electron is that of a diffusion process in action space, with the square of the increase in action proportional to the elapsed time (4). Simple mathematical models that characterize a broad class of deterministic nonlinear systems qualitatively can explain the classical diffusive behavior (5,6). Mathematically, the onset of diffusion with increasing strength of the applied electromagnetic field is analogous to a phase transition (6). The quantum-mechanical time evolution mimics the classical diffusion with an increase in mean atom quantum number, with the square of the increase again proportional to time (4). This "quantum diffusion" persists only for a finite time interval. The

quantum dynamics is associated with an electron wavefunction delocalization that, after a time that can be of the order of one hundred external field oscillations, can produce exponential final bound state distributions and, for "quantum diffusion" into the continuum, nonzero ionization probabilities. When the number of absorbed photons needed for ionization becomes small, the quantum dynamics does not appear to closely mimic the classical behavior (4).

Exponential final bound state distributions have been observed for $n=63$ hydrogen atoms in partially-ionizing 7 GHz microwave electric fields (7), see Figure 1. Also, measured ionization probabilities agree with both quantum and classical numerical calculations, when the number of absorbed photons is large (8,9). These two observed signatures of classically-chaotic quantum dynamics can be supplemented with at least a third, the special time evolution of the system.

The results of the microwave experiments are expected to scale to the case of excited multiply-charged hydrogenic ions in intense short-pulse infrared laser fields (10).

Also, one may conjecture that classically chaotic many-photon absorption within excited atomic states may play some role in the multiple ionization of initially unexcited atoms in such infrared fields (11).

1. B. I. Meerson, E. A. Oaks and P. V. Sasorov, Sov. Phys.-JETP Lett. 29, 72 (1979).
2. R. V. Jensen, Phys. Rev. A 30, 386 (1984).
3. J. E. Bayfield, in Quantum Measurement and Chaos, edited by E. R. Pike, (Plenum Press, New York, 1987).
4. G. Casati, B. V. Chirikov, D. L. Shepelyansky and I. Guarneri, Physics Reports, to be published.
5. H. G. Schuster, Deterministic Chaos (Physik-Verlag,

Weinheim, 1984), page 26.

6. T. Geizel, in Nonequilibrium Cooperative Phenomena in Physics and Related Fields, (Plenum Press, New York, 1984), page 437.
7. J. N. Bardsley, B. Sundaram, L. A. Pinnaduwege and J. E. Bayfield, Phys. Rev. Lett. 56, 1007 (1986).
8. K. A. H. van Leeuwen, G. V. Oppen, S. S. Ewsnick, J. B. Bowlin, P. M. Koch, R. V. Jensen, O. Rath, D. Richards and J. G. Leopold, Phys. Rev. Lett. 55, 2231 (1985).
9. J. N. Bardsley and M. J. Comella, J. Phys. B 19, L565 (1986).
10. J. E. Bayfield, Proc. SPIE 664, 122 (1986).
11. F. Yergeau, S. L. Chin and P. Lavigne, Proc. SPIE 664, 229 (1986).

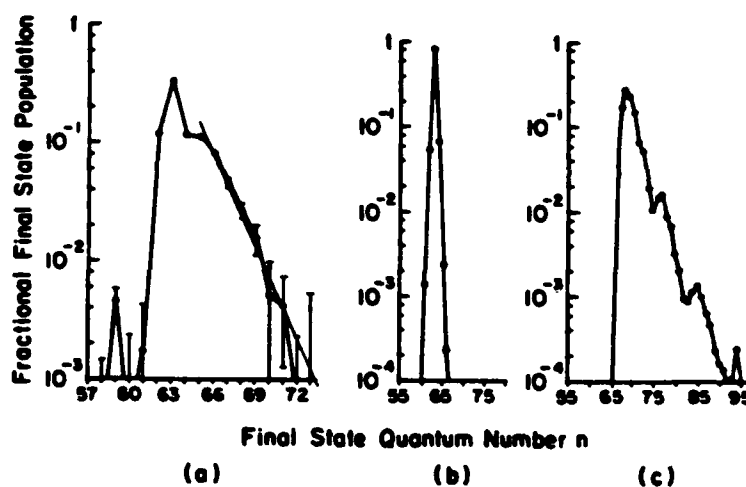


Figure 1. Part (a) shows an experimental final state quantum number distribution created by temporarily placing $n=63$, $n, m=0$ hydrogen atoms in a strong linearly polarized microwave field. Parts (b) and (c) are typical numerical quantum predictions for the atom initially below (b) and above (c) the quantum number threshold for classically chaotic behavior, respectively. The experimental curve reflects a superposition of regular and chaotic classical behavior. From references 3 and 7.

Invited Paper

Quantum-Mechanical Aspects of Classically Chaotic Driven Systems

P.W. Milonni

Theoretical Division (T-12)
Los Alamos National Laboratory
Los Alamos, New Mexico 87545

The onset of chaos in the interaction of laser radiation with atomic and molecular systems can lead to effectively statistical behavior even though the equations of motion are fully deterministic. Such behavior has been identified in lasers and other dissipative systems by the observation of well-characterized, universal routes to chaos. At the level of a single atom or molecule in a field, things are not as clear, mainly because of the difficulty in performing fully quantum-mechanical calculations.

After a brief, partly historical overview of the relevant ideas from classical and quantum chaos, I will discuss quantum-mechanical aspects of driven systems that are chaotic in the classical limit. These include models of multiple-photon excitation of molecular vibrations, the microwave ionization of Rydberg hydrogen atoms, and the artificial but instructive example of the kicked pendulum. Classical trajectory analyses indicate that overlapping resonance and the onset of "widespread chaos" can produce, among other things, statistical behavior in intramolecular energy transfer; the incoherent, fluence-dependent character of multiple-photon excitation of polyatomic molecules; and the similarly diffusive energy growth leading to microwave ionization of hydrogen.

Quantum effects like tunneling and Anderson-like localization can greatly weaken the degree of irregularity predicted classically. However, even though driven quantum systems appear to enjoy a greater degree of dynamical stability than their classical counterparts, they

can nevertheless exhibit effects - like decaying correlations and diffusive energy growth - that are typical consequences of classical chaos.

This work was performed in close collaboration with J.R. Ackerhalt. Support from the National Science Foundation under grant PHY-8308048 is also gratefully acknowledged.

Invited Paper

EXPONENTIAL PHOTONIC LOCALIZATION AND CHAOS IN THE HYDROGEN ATOM
IN A MONOCHROMATIC FIELD

Giulio Casati

Dipartimento di Fisica dell'Università di Milano
Via Celoria 16, 20133 Milano, Italy

Self-generated stochasticity is a very common occurrence in classical systems subject to time-periodic perturbations. In macroscopic systems of this type, chaos is directly responsible for easily observable (and often undesirable) effects.

The problem, whether any such effects survive also in quantum mechanics is an important one, especially in connection with studies on microwave ionization of Rydberg atoms. Previous works¹⁻¹¹ have shown that strong ionization and excitation can take place even for frequencies well below the one-photon ionization threshold. There are strong indications that this quantum phenomenon is connected with the appearance of chaotic motion in the corresponding classical system; indeed, in the classical model of a hydrogen atom under an external periodic field, a stochastic transition takes place, leading to unlimited diffusion in phase space and eventually to ionization.

On account of such results, one is led to suspect some quantum process simulating classical chaotic diffusion. On the other hand, previous studies¹²⁻¹⁵ on different models have shown that quantization places severe limitations on classical chaos, that may lead to a complete suppression of chaotic diffusion, even in the semiclassical region. We are then faced with the problem of understanding why in hydrogen atoms this quantum limitation fails to produce its full paralyzing effect, leaving room for "diffusive" excitation and ionization.

Here we present theoretical and numerical results showing that the final state distribution of highly excited hydrogen atoms produced by a monochromatic field is exponentially localized in the number of absorbed photons. These results allow for a theoretical interpretation

of under-threshold ionization and of the characteristic peak structure produced by multiphoton transitions.¹⁶ They also confirm our previous quantum delocalization picture^{4,11} and allow for an estimate of the ionization rate.

In particular we show the existence of a large ionization peak at frequencies much below those required for the conventional one-photon photoelectric effect.⁵ This peak can, for suitable parameter values, be much higher than that of the usual photoelectric effect and its frequency width is jointly determined by two independent effects: the classical chaotic threshold and the quantum delocalization border.

REFERENCES

1. J. E. Bayfield and P. M. Koch, Phys. Rev. Lett. 33, 298 (1974).
2. N. B. Delone, V. P. Krainov, D. L. Shepelyansky, Usp. Fiz. Nauk 140, 355 (1983) (Sov. Phys. Uspeky 26, 551 (1983)).
3. R. V. Jensen, Phys. Rev. A 30, 386 (1984).
4. G. Casati, B. V. Chirikov, D. L. Shepelyansky, Phys. Rev. Lett. 53, 2525 (1984).
5. G. Casati, B. V. Chirikov, I. Guarneri, D. L. Shepelyansky, Phys. Rev. Lett. 57, 823 (1986).
6. R. Blumel and V. Smilansky, "Subthreshold Ionization of Rydberg Atoms in a Radiation Field." Preprint.
7. K. A. H. Van Leeuwen, G. V. Oppen, S. Renwick, J. B. Bowlin, P. M. Koch, R. V. Jensen, O. Rath, D. Richards, J. G. Leopold, Phys. Rev. Lett. 55, 2231 (1985).
8. P. M. Koch, in Fundamental Aspects of Quantum Theory, edited by V. Gorini and A. Frigerio (Plenum, New York, 1987).
9. J. N. Bardsley and M. J. Comella, J. Phys. B 19, L565 (1986).
10. J. E. Bayfield, in Fundamental Aspects of Quantum Theory, edited by V. Gorini and A. Frigerio, (Plenum, New York, 1986).
11. G. Casati, B. V. Chirikov, I. Guarneri, D. L. Shepelyansky "Relevance of Classical Chaos in Quantum Mechanics: The Hydrogen Atom in a Monochromatic Field," Physics Reports (to appear).
12. G. Casati, B. V. Chirikov, J. Ford, F. M. Izrailev, Lectures Notes in Physics 93, 344 (1979).
13. B. V. Chirikov, F. M. Izrailev, D. L. Shepelyansky, Soviet Scientific Review 2C, 209 (1981).
14. D. L. Shepelyansky, Physica 8D, 208 (1983).
15. S. Fishman, D. R. Grempel, R. E. Prange, Phys. Rev. Lett. 49, 509 (1982); Phys. Rev. A 29, 1639 (1984).
16. G. Casati, I. Guarneri, D. L. Shepelyansky, "Exponential Photonic Localization for the Hydrogen Atom in a Monochromatic Field." Preprint.

Invited Paper

QUANTUM MECHANICAL APPROACHES TO MULTIPLE-PHOTON ABSORPTION:
COMPUTING WITH THOUSANDS OF STATES

R. E. Wyatt

University of Texas at Austin
Austin, Texas 78712

Invited Paper

VIBRATIONAL CHAOS IN INFRARED MULTIPHOTON
EXCITATION OF POLYATOMIC MOLECULES

E. A. Ryabov

Institute of Spectroscopy

USSR Academy of Sciences

142092, Moscow region

Troitzk, USSR

The intramolecular vibrational motion for polyatomic molecules subjected to IR multiphoton excitation was studied. It was found that when a molecule is pumped through one of the vibrational modes, during the very process of IR MP excitation (time scale $\leq 10^{-8}$ s), the absorbed energy is statistically redistributed over all other vibrational modes. This redistribution is the result of stochastization of vibrational motion at a sufficient level of vibrational excitation. The existence of a well-pronounced stochastization onset was experimentally found for the investigated molecules. The measured value of this onset for SF_6 , CF_3I , CF_2HCl , CF_3Br , CF_2Cl_2 molecules is in the region of 5000 - 7000 cm^{-1} . Possible mechanisms of stochastization of vibrational motion are discussed.

Invited Paper

COUPLED EQUATIONS APPROACH TO
HALF-COLLISIONS IN INTENSE FIELDS

André D. Bandrauk

Département de chimie, Faculté des Sciences
Université de Sherbrooke
Sherbrooke, Que, Canada J1K 2R1

Bound-bound multiphoton transitions followed by photodissociation can be termed half-collisions. These are generally coherent for small molecules in intense fields. Using techniques of modern quantum scattering theory and the dressed molecule representation, it is possible to deduce half-collision amplitudes from numerical coupled equations approaches. Semiclassical techniques can be used to explain stabilities or instabilities of laser induced resonances. Finally, it will be shown that nonadiabatic interactions between highly excited molecular electronic states compete usually with radiative transitions, thus modifying the power laws usually anticipated at high intensities.

FEMTOSECOND DYNAMICS OF MULTIELECTRON DISSOCIATIVE IONISATION USING A PICOSECOND LASER

L.J. Frasinski, K. Codling and P. Hatherly

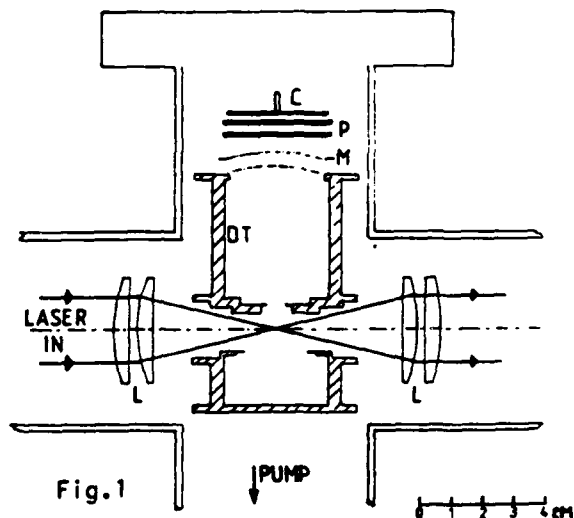
J.J. Thomson Physical Laboratory, University of Reading RG6 2AF, UK.

The question as to whether the mode of multiphoton multiple ionisation of Xe is step-wise or collective has been discussed at length in the literature^{1,2}. We recently suggested that experiments should be performed on the diatomic molecule isoelectronic with Xe (i.e. HI) in an attempt to shed further light on the situation.

The basic idea is straightforward. A diatomic molecule is subjected to a large electric field from a focussed picosecond laser. As the molecule is ionised beyond the single ion stage, the fragment ions mutually repel in the Coulomb field and the energetic ions are detected by a time-of-flight mass spectrometer. If additional electrons are stripped away as the molecule dissociates, the ions are now subjected to an even larger Coulomb repulsion and this will be reflected in the TOF spectrum. Thus the detailed dynamics can be investigated on a time-scale of femtoseconds (the dissociation time-scale) even though the laser pulse is of picosecond duration.

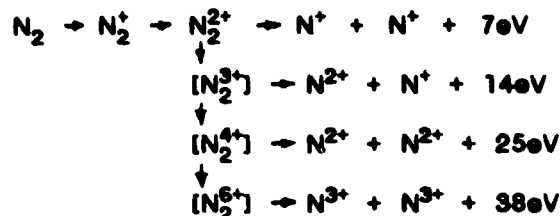
The experimental set-up is shown in fig.1. Light from a 0.6ps laser is focussed by a 1/3 doublet lens (L) to achieve a peak power density of about $3 \times 10^{15} \text{ W/cm}^2$ in the focal spot. Gas is introduced at a pressure of 10^{-6} Torr and the resulting photo-ions subjected to a field of $\sim 10 \text{ kVm}^{-1}$. The ions traverse a drift tube (DT) and are detected by microchannel plates. The ion signal is fed to a transient digitiser and spectra such as those shown here are accumulated in less than 10 minutes.

The TOF spectra obtained when air was introduced into the laser focus region are shown in figs. 2 (a) and



(b) taken with 50v and 100v, respectively, across the 12mm interaction region. The atomic ions can be grouped into two categories. Those that are initially ejected towards the detector have TOF's that decrease almost linearly with initial velocity but those ejected away from the detector, and with the same velocity range, arrive almost simultaneously at the detector producing the sharp peaks N^+ , N^{2+} and N^{3+} . The scales alongside are kinetic energy releases, in eV.

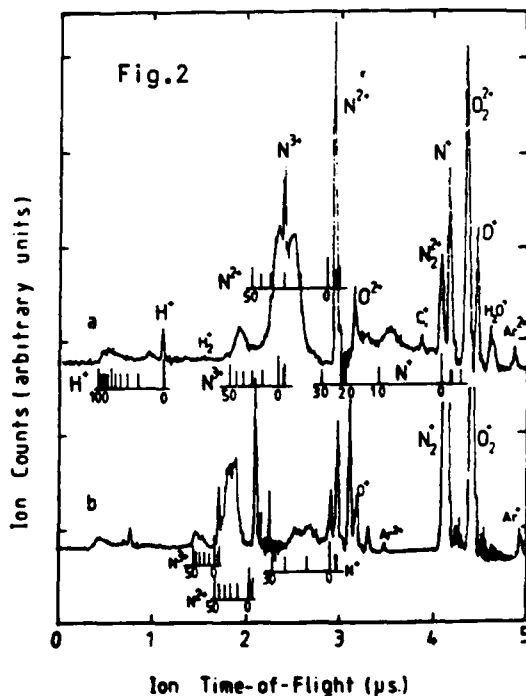
Analysis of the kinetic energy releases of the various N ions leads us to suggest the following sequence of events³.



Taking a simple model of two positively charged ions mutually repelling with a pure Coulomb force, and where the electrons are removed instantaneously, the time-scale of the $N_2^{2+} \rightarrow N_2^{6+}$ process can be estimated.

If all 4 $1\pi_u$ electrons were to be removed from the N_2^{2+} metastable ion (internuclear separation 1.1\AA) at the same time, the resulting N^{3+} ions would share a kinetic energy of 118eV, far in excess of the measured value of 38eV. A truly collective model cannot, therefore, apply. However, if a step-wise process is envisaged where the $[N_2^{3+}]$ ion sheds an electron and then the $[N_2^{3+}]$ ion dissociated before a second electron is ejected from the N^{2+} ion and a further 2 electrons from the N^+ ion, the final N^{3+} ions would share 26eV, the dissociation energy of the original $[N_2^{3+}]$ ion. (In fact 26eV is an overestimate because of the simplicity of the model).

The observed energy release of the N^{3+} ion of 38eV indicates that the

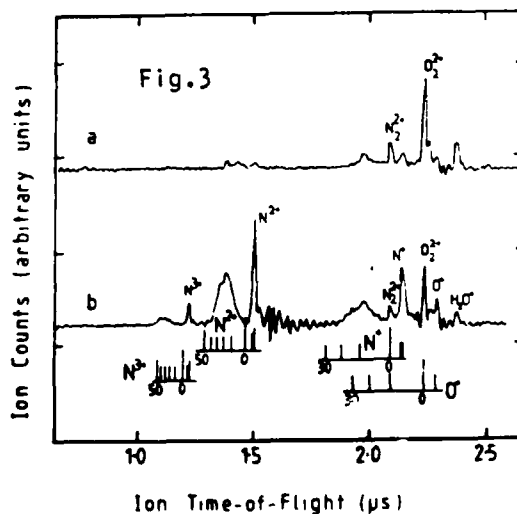


real situation lies somewhere between these extremes and it may be that the relatively large widths of the peaks in the kinetic energy distributions of the ions reflect the finite time of removal of the electrons. This complex process of multielectron dissociative ionisation (MEDI) takes about 20fs, only 10 periods of the laser field. This is 5 times faster than the equivalent process $\text{Xe}^{2+} \rightarrow \text{Xe}^{6+}$ observed using a 0.5ps 193nm laser⁴. A ratio (β/γ) has been suggested as a measure of the importance of sequential ($\beta/\gamma > 1$) or direct ($\beta/\gamma < 1$) processes in terms of experimental conditions². The shorter the laser pulse rise time, the smaller is this ratio but in these experiments the relevant time is the MEDI time-scale of 20fs. This leads to a (β/γ) ratio of less than 1(0.4), which has not been achieved previously. We believe that this increase in ionisation rate and consequent reduction in β/γ is to be associated with the rapid increase in potential difference across the molecule (caused by dissociation) rather than any time development of the envelope of the laser field.

The phenomenon depicted in fig. 3 is consistent with this classical field ionisation model. The figure shows the TOF spectrum with the E-vector of the laser light (a) perpendicular to and (b) parallel with the axis of the drift tube. The molecules are more easily ionised when their axes lie close to the direction of the E-vector, which is to be expected, since the potential difference created by the laser field is larger along the molecular axis than at right angles to it and thus the potential barrier is not so high.

The TOF spectrum of HI is now being analysed but it appears that a step-wise process is adequate to explain the observations

1. P. Lambropoulos *Phy. Rev. Lett.* **55** 2141 (1985)
2. U. Johann et al *Phys. Rev.* **A34** 1084 (1986)
3. L.J. Frasinski et al *Phys. Rev. Lett.* (submitted)
4. A.L. Robinson *Science* **232** 1193 (1986)



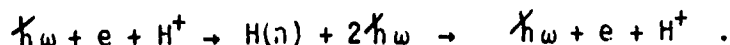
A NEW CLASS OF RESONANCES IN THE $e + H^+$ SCATTERING IN AN EXCIMER LASER FIELD

L. Dimou and F. H. M. Faisal
Fakultät für Physik
Universität Bielefeld
4800 Bielefeld 1
Federal Republic of Germany

In this paper we report on the numerical discovery of a new class of low energy $e + H^+$ scattering resonances which dominate the field modified elastic (Rutherford) and the inelastic (e.g. inverse Bremsstrahlung) scattering cross sections in the presence of a strong excimer laser. Cross sections of these processes are obtained as a function of the incident electron energy at $\hbar\omega = 6.419$ eV. The results are discussed and interpreted physically.

In view of the lack of an exact analytical solution of the fundamental problem of $e + H^+$ scattering in a laser field we are led to attack the problem by exact numerical means. To this end we have extended the powerful close-coupling method of solution of the ordinary electron scattering problems and incorporated the interaction of the radiation field via the Floquet representation of the scattering equations. Our numerical solution of the extended close-coupling equations for the radiative scattering problem reveals a new class of resonances which dominate the cross sections of the elastic (Rutherford) as well as the inelastic (inverse Bremsstrahlung) processes in the presence of the field. These resonances will be referred to below as "capture-escape Rydberg resonances" due to their physical origin which is explained subsequently.

Fig. 1 provides the first numerical evidence of such resonances corresponding to $n = 2$ to 5 principal quantum numbers of the intermediate neutral H-atom. They are due to the "reactions" which can be schematized as



The most prominent features of this result are (a) the existence of a series of very clear resonance structure and (b) away from the resonances the field modified elastic cross sections are rather closely given by the unmodified Rutherford cross section. The resonance structures are indications for the fact that the scattering electrons become captured by the proton in the bound states of the H-atom and then reemitted in the same incident energy channel. This is a resonant induced phenomenon. Thus at a given laser frequency which matches the energy difference between the incident electron energy (positive) and a Rydberg level energy (negative) the laser field can force the electron to emit a photon and cause it to be captured temporarily in the Rydberg-state till the subsequent adsorption of a photon permits the electron to escape from this state into the continuum again. The delay introduced by this capture-escape episode, shows up as a resonance in the scattering signal.

In Fig. 2 we present the corresponding inelastic cross section for the absorption of a photon. This process can be thought of as an inverse Bremsstrahlung process in a strong field at low electron energies. In the absence of the field no such channel is possible and hence the background to this signal is intrinsically zero. Here too we obtain numerical evidence of a very prominent sequence of the "capture-escape-Rydberg resonances".

In Fig. 3 we show the $n=2$ resonance in magnification. It has a width of ~ 5 meV. We note that with increasing field strength this and the other resonances for higher n tend to broaden. In particular the higher Rydberg resonances (which are weak at a given intensity) begin to appear significantly with increasing field strength. We also remark that the width of such a resonance with a given n can be thought of as a measure of the strong field photoionization rate of that particular Rydberg state of the neutral atom.

Finally we note that these resonances can be "tuned" either by varying the photon frequency at a fixed electron energy or by varying the electron energy at a given photon frequency. This flexibility in tuning the resonances combined with the fact that their widths can be manipulated by changing the field intensity may prove to be useful in observing them experimentally.

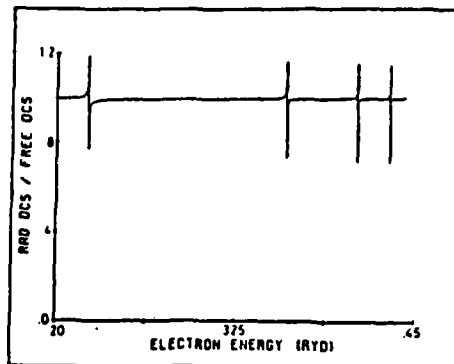


FIGURE 1. The field modified elastic $e + H^+$ scattering in a circularly polarized field at the field strength $F_0 = .005 \text{ au}$ and $\hbar\omega = .472 \text{ Ryd} = 6.419 \text{ eV}$ shown with respect to ordinary Rutherford cross sections, as a function of incident electron energy. The incident momentum is in the direction $\Omega_0 = (\theta=90^\circ, \phi=0^\circ)$ and the final momentum is in the direction $\Omega = (\theta=90^\circ, \phi=90^\circ)$. The field propagation direction is along the z-axis. Note the capture-escape Rydberg resonances for $n=2$ to 5 states of neutral H.

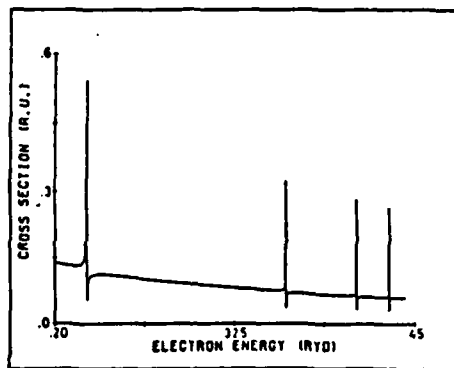


FIGURE 2. The one photon angle integrated absorption cross section as a function of incident electron energy in a circularly polarized field. Field strength $F_0 = .005 \text{ au}$, $\hbar\omega = .472 \text{ Ryd} = 6.419 \text{ eV}$. Incident direction $\Omega_0 = (90^\circ, 0^\circ)$. The field propagation direction is along the z-axis.

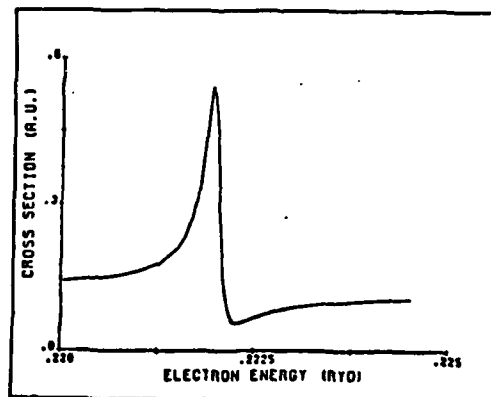


FIGURE 3. Magnification of the one-photon angle integrated absorption cross section for $e + H^+$ scattering in a circularly polarized field in the region of capture-escape Rydberg resonances with $n=2$ state of neutral H. Incident electron momentum along $\Omega_0 = (90^\circ, 0^\circ)$. The laser propagation direction along z-axis. Field strength $F_0 = .005 \text{ au}$, $\hbar\omega = .472 \text{ Ryd} = 6.419 \text{ eV}$.

LASER - ASSISTED POTENTIAL SCATTERING. AN ASSESSMENT
OF RECENT NEW RESULTS

B. Piraux⁺, F. Trombetta⁺⁺, G. Ferrante⁺⁺ and G. Messina⁺⁺

⁺ Imperial College of Science and Technology, Optics Section,
Prince Consort Road, London SW7 2BZ, England

⁺⁺ Istituto di Fisica dell'Università, via Archirafi 36,
90123 Palermo, Italy

A number of new theoretical results has been recently reported on laser-assisted potential scattering [1,2], whose distinctive feature is that the assisting field is strong enough to impart to the electrons an oscillatory velocity v_0 equal or even larger than the initial velocity v_i . In particular, for scattering potentials of relatively long range and parallel geometries (the field polarization parallel to the initial velocity), when the amplitude v_0 of the oscillatory velocity is approximately equal to v_i , strong enhancement of the total cross sections for different number photon channels is found, together with the violation of a known sum rule. The above results and other as well may be given a clear physical interpretation; accordingly, they are believed to be largely independent of the specific approximation used (at least as far as the arising physical picture is concerned). Nevertheless, as the used approximation was the first Born, it is legitimate to ask to which extent both the physical picture and the quantitative results hold beyond that approximation. It is the aim of this communication to try to provide an answer to a number of questions concerning relatively energetic laser-assisted potential scattering, when $v_i \approx v_0$.

In particular: a) we calculate and compare the same quantities (multiphoton total cross sections and sum rule) within three approximations (first Born, eikonal and second Born), and b) we analyze whether or not the inclusion of the laser field modifies the criteria of validity of the first Born approximation, as compared with the field-free case.

A part of our findings are shown in Fig. 1, where we report the ratio of the "eikonal" total cross sections (summed over all the multiphoton channels) to the field-free one vs the ratio v_0/v_i . The numbers on the curves denote the Yukawa potential range used in the calculations.

A complete account will be reported at the Conference.

REFERENCES

- [1] R. Daniele, G. Ferrante, F. Morales and F. Trombetta, J. Phys. B 19, L133 (1986).
- [2] S. Bivona, R. Daniele, G. Ferrante and F. Trombetta, "High Intensity Effects in Multiphoton Free-Free Transitions", in Proceedings of Photons and Continuum States of Atoms and Molecules (Springer-Verlag, 1987), in press.

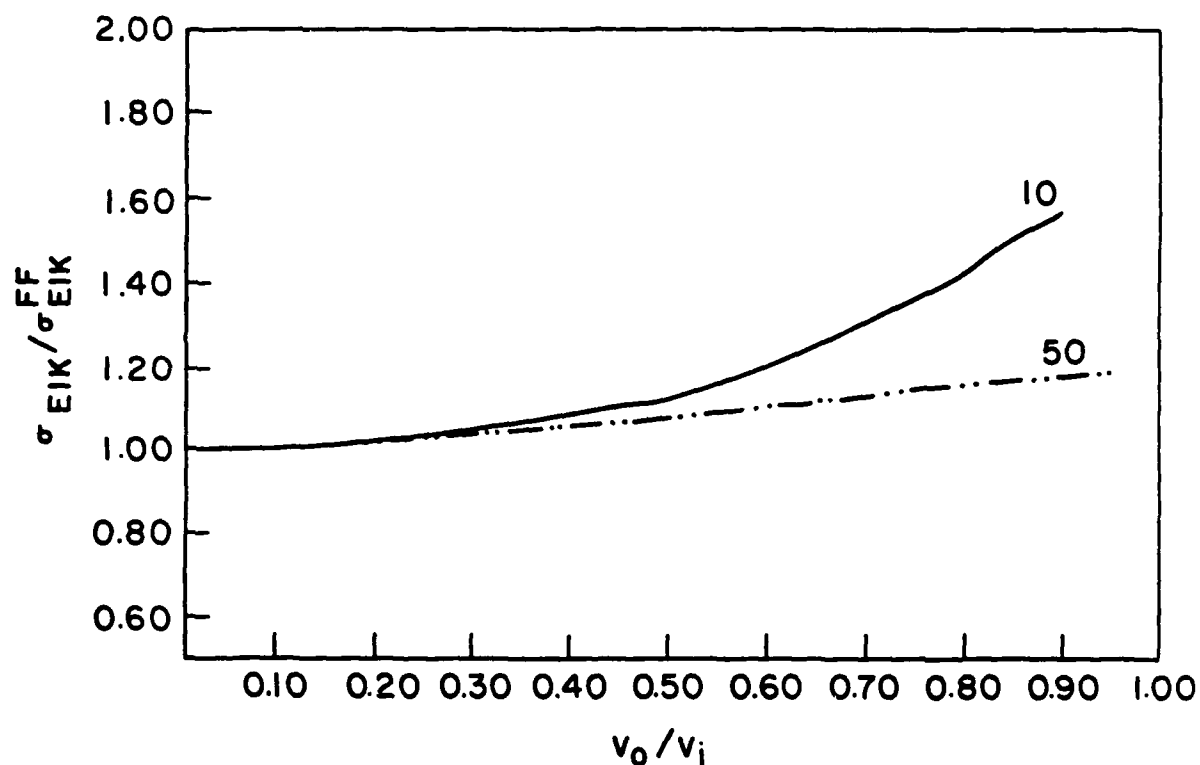


Fig. 1

Invited Paper

ATOMIC PROCESSES IN STRONG LASER FIELDS

H. O. Lutz

Universität Bielefeld
Federal Republic of Germany

ATI POLARIZATION EXPERIMENTS AND CALCULATIONS FOR XENON AND KRYPTON

P. H. Bucksbaum, M. Bashkansky and D. W. Schumacher

AT&T Bell Laboratories

Murray Hill, NJ 07974

We have completed a comprehensive study of the polarization dependence of above-threshold ionization (ATI) in xenon and krypton by 1064 nm focused laser light. The elliptical polarization results show dramatic effects that can be traced directly to the coherent oscillating laser field acting on the photoemitted electrons. Both photoionization rates and angular distributions are affected. We present a calculation based on non-perturbative techniques that predicts most of these effects.

Energy spectra and angular distributions are the principal means of investigating ATI. Previous studies have shown that ATI azimuthal angular distributions for 1064 nm linear polarization are sharply peaked along the polarization direction,¹ whereas circular polarization distributions must be isotropic in the azimuthal plane. Low energy electrons are suppressed in both cases, but the suppression is considerably stronger for circular polarization.²

Our new study shows that the suppression of low energy peaks is both a function of polarization and emission angle (figure 1). For elliptical polarization, the angular distributions develop complicated symmetries with several nodes. Different ATI peaks in the same spectrum often display markedly different angular distribution patterns, with maximum emission along 0°, 90°, or intermediate angles. Figure 2 shows the angular distributions for ATI in krypton for *nearly* circularly polarized light ($I_{LCP}/I_{RCP} \approx 1\%$), for peaks corresponding to absorption of 17 to 31 photons (5.9 to 22.2 eV final energy).

Some qualitative features of these results, such as the fit of the angular distributions to a series in $\cos(2n\phi)$, can be understood from perturbation theory for multiphoton absorption to high angular momentum states. However, A much more complete understanding of the data is obtained by considering the radiation field as a classical time-dependent potential.² Such theories are sometimes called "non-perturbative," since they do not employ time-dependent perturbation theory, nor require quantization of the radiation field. Many

theorists have discussed the close connection between the predictions of these theories, and ATI experimental results.⁴ For example, the resolution of the final state energy spectrum into a series of discrete peaks separated by $h\nu$ is a natural result of the non-perturbative theories.

We have extended these theories for the first time to consider light of arbitrary polarization with spatial and temporal inhomogeneity. We consider the evolution of a ground state atom in the presence of a strong laser field to final Volkov states.⁵ Several similar treatments exist in the literature for circular or linearly polarized plane wave radiation,⁴ but ours represents the first attempt to incorporate all of the controlling factors in a pulsed laser experiment into a single calculation, for arbitrary polarization. The results are in qualitative agreement with the experiments. The complex experimental angular distributions and energy spectra appear in the calculations. In addition, the widths of the electron peaks are generally consistent with ponderomotive surfing of the final state electrons.⁶ Problems persist in matching the intensity scales of the calculations to real experiments.

These new results help to illuminate the most fundamental questions about ATI, concerning the origin and nature of the multiple peaks. In addition, these techniques may be used to explore the effects of the temporal structure of the light field on the electron energy distributions.

References

1. H. Humpert, et al., Phys. Rev. A **32**, 3787 (1985); F. Fabre et al., J. Phys. B **14**, L677 (1981); R. R. Freeman, et al., Phys. Rev. Lett. **57**, 3156 (1986).
2. P. Bucksbaum, et al., Phys. Rev. Lett. **56**, 2590 (1986).
3. L. V. Keldysh, Sov. Phys. JETP **20**, 1307 (1965); H. R. Reiss, Phys. Rev. A **22**, 1786 (1980).
4. H. G. Muller, et al., J. Phys B. **16**, L679 (1983); H. R. Reiss, J. Opt. Soc. Am. B. (to be published May, 1987); W. Becker, *ibid.*: J. Kupersztych, to be published.
5. D. M. Volkov, Z. Phys. **94**, 250 (1935).
6. P. Bucksbaum, et al., Phys. Rev. Lett. **58**, 349 (1987).

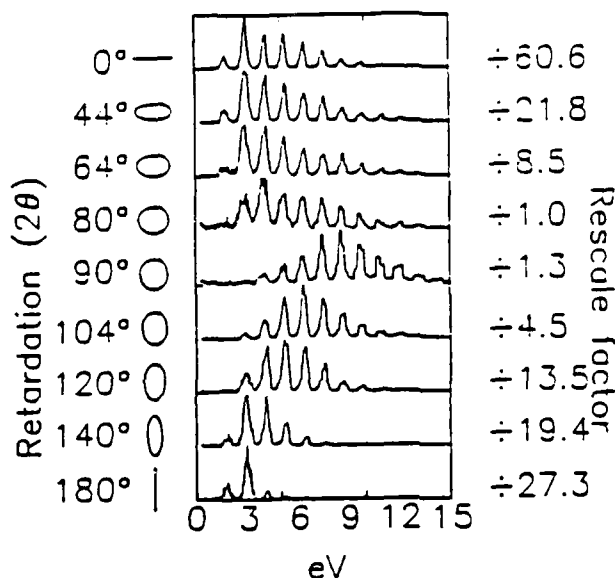


Figure 1. Electron spectra along $\phi=0$ (\hat{x} direction) in Xe. vs. polarization retardation angle 2θ . Here the polarization is $\hat{\epsilon} = \hat{x}\cos(\theta) + \hat{y}\sin(\theta)$.

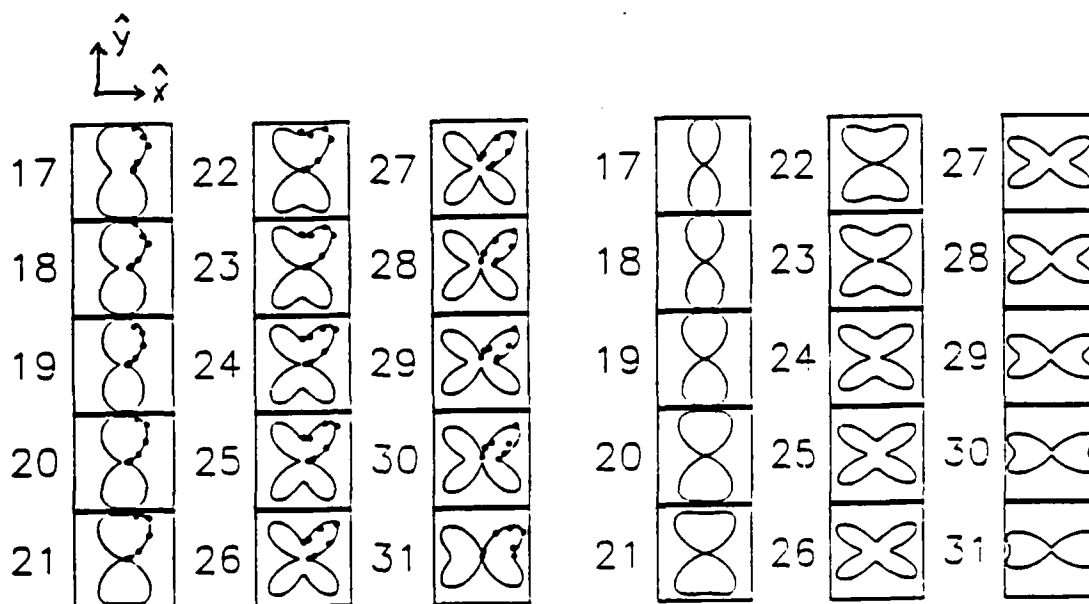


Figure 2. [Left] Azimuthal angular distributions in Kr for 1064 nm 0.12 nsec light pulses with peak intensity $\approx 8 \times 10^{13} \text{ W/cm}^2$, polarization retarded by 80° ($I_{\text{LCP}}/I_{\text{RCP}} \approx 1\%$). The number of photons absorbed for each electron peak is shown. Lines are fits to a series in $\cos(2n\phi)$, $n=0,1,2,3$. [Right] Calculation of azimuthal angular distributions for ($I_{\text{LCP}}/I_{\text{RCP}} = 3\%$), intensity $= 10^{13} \text{ W/cm}^2$.

Theory of Atoms in Strong Electromagnetic Fields

Abraham Szoke
Lawrence Livermore National Laboratory
Livermore, CA 94550

A strong field perturbation theory of atomic multiphoton excitation and ionization has been developed from first principles. It unifies the spirit of the works of Reiss and of Keldysh on the one hand, and of Chu and Reinhardt on the other, but it has a wider range of validity. In the weak field limit it reduces to the known theories of photoionization, electron-atom collisions and the Auger effect - i.e., time dependent perturbation theory. For a one electron atom all the known systematics of multiphoton ionization are obtained correctly: the appropriate power-law dependence at low laser intensity; above threshold ionization, as well as the "closure" of the low energy electron channels at high laser intensity.

The results can be summarized qualitatively in the following statements. There are three different ways an atom can be photoionized. First, the atomic bound states are changed into decaying states (resonances) by the incident electromagnetic field. This is the decay described by Floquet theory. Second, as the amplitude or the frequency of the field varies in time, passages through non-linear resonances occur. These passages, depending on the rate of rise of the field and on the value of the field at which they occur, can cause transitions to excited states and a change in the rate of ionization. Third, the time dependence of the field amplitude and frequency causes direct transitions to unbound states. Each one of these pathways to ionization is described as a transition between "modified" Floquet states. Even high order multiphoton transitions can be treated as first order perturbation; therefore they can be calculated more easily. A clear, qualitative prediction of the theory is that in the "low frequency" regime, ionization is dominated by the dressing of the outgoing electron, while in the presence of atomic

non-linear resonances, or at high laser frequency, ionization proceeds via excited atomic states. Some semi-quantitative calculations will be presented.

The theory uses "modified" Floquet states as basis sets and develops a time dependent perturbation theory using the multiple scale expansion technique. This is always possible for a laser pulse with a narrow spectrum, or in other words, for a single color laser whose pulse contains many optical cycles. The derivation of the equations comes in two versions: in the "naive" one, a time dependent perturbation theory is developed based on the "adiabatic" floquet states of Chu and Reinhardt. A more accurate derivation is based on collision theory. It starts with the recognition that the ionization states of an atom constitute arrangement channels; further, in the presence of an electromagnetic field of constant amplitude and frequency, the modified Floquet states are the stationary states within these arrangement channels. In particular, if an electron is detected with its energy corresponding to the absorption of N photons, the wave function of that electron in the vicinity of the atom can be "dressed" by a large number of photons; this corresponds to continuum-continuum "transitions" in the language of perturbation theory. It is important to realize that the phases within these dressed states are significant, and considering them as real transitions may give wrong results.

The most difficult, unanswered questions in this field are connected with multiple ionization of atoms with many electrons in their valence shell. The following are a representative sample of these questions. Are there any many-electron, coherent excitations - which resemble giant dipole resonances in nuclei - present in these atoms? Is autoionization of these states suppressed by the strong laser field: i.e. do these many-electron excitations decay into states with incoherent electron motions - which may be called a compound atom, in analogy to similar phenomena in nuclei? As the theory presented here can be extended to

many electron atoms, we hope to start answering these questions in the near future.

Work performed under the auspices of the U.S. Department of Energy by the Lawrence Livermore National Laboratory under contract number W-7405-ENG-48.

Multiphoton Ionization of Xenon from 570nm to 600nm

M. D. Perry
Department of Nuclear Engineering
University of California
Berkeley, CA 94704

E.M. Campbell, O.L. Landen, A. Szöke
Lawrence Livermore National Laboratory
Livermore, CA 94550

We have observed up to quadruply charged ions produced by the interaction of intense picosecond laser radiation with xenon under collisionless conditions. The experiments consisted of determining the ionization rate of Xe, Xe^{+1} , Xe^{+2} and Xe^{+3} as a function of both laser intensity in the range $1 \times 10^{12} \leq I \leq 5 \times 10^{14} \text{ W/cm}^2$ and laser frequency from $570\text{nm} \leq \lambda \leq 600\text{nm}$. We present the multiphoton ionization cross-sections for xenon in this range. A comparison with MPI cross-sections obtained at 532nm and 50psec pulsewidths shows some interesting differences.

The laser is an amplified synchronously mode-locked dye system. It starts with a Cw mode-locked Nd:YAG laser synchronously pumping a cavity tuned dye oscillator. The output of the dye oscillator is tunable from 510nm to 620nm and contains typically 2nJ in a 1 psec pulse. This is then amplified up to a maximum of 3mJ in a four stage dye amplifier pumped by the second harmonic output of a Q-switched Nd:YAG laser. The amplified system is capable of working at a maximum repetition rate of 10Hz but is operated at only 2Hz due to rate limitations of our data acquisition system. Spatial filtering and relay imaging is used throughout the dye amplifier both as a means to suppress amplified spontaneous emission and to maintain good beam quality. Saturable absorber jets (DQOC1 in ethylene glycol) are also used for additional ASE suppression and to limit pulsewidth broadening. The amplified output is 3mJ in a transform limited pulse whose width is variable between 1 and 10 picoseconds. Attenuation of the laser intensity on target is obtained by

AD-A202 520

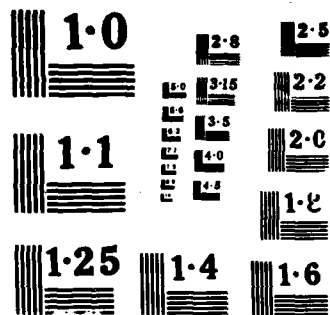
INTERNATIONAL CONFERENCE ON MULTIPHOTON PROCESSES (4TH)
HELD IN BOULDER CO. (U) JOINT INST FOR LAB ASTROPHYSICS
BOULDER CO JUL 88 AFOSR-IR-88-1278 AFOSR-87-0221

2/4

UNCLASSIFIED

F/G 7/5

NL



rotating one of a pair of $\lambda/10$ Glen Thompson polarizers placed in the beam line.

The gaseous target species fills the chamber uniformly via a high precision leak valve. The target density and composition is monitored continuously with a quadrupole mass spectrometer. The ions resulting from the absorption of up to 50 photons are extracted from the focal volume by an electric field of ~ 5000 V/cm and are analysed by a time-of-flight (TOF) spectrometer. The ions are detected with microchannel plates which produce a gain of $\sim 10^6$ electrons/ion. We have clearly demonstrated single ion detection capability with this system. The entire TOF spectrum is recorded by a transient digitizer on each laser shot (see Fig. 1). Also, the laser energy and the time integrated second harmonic intensity, are recorded on each laser shot.

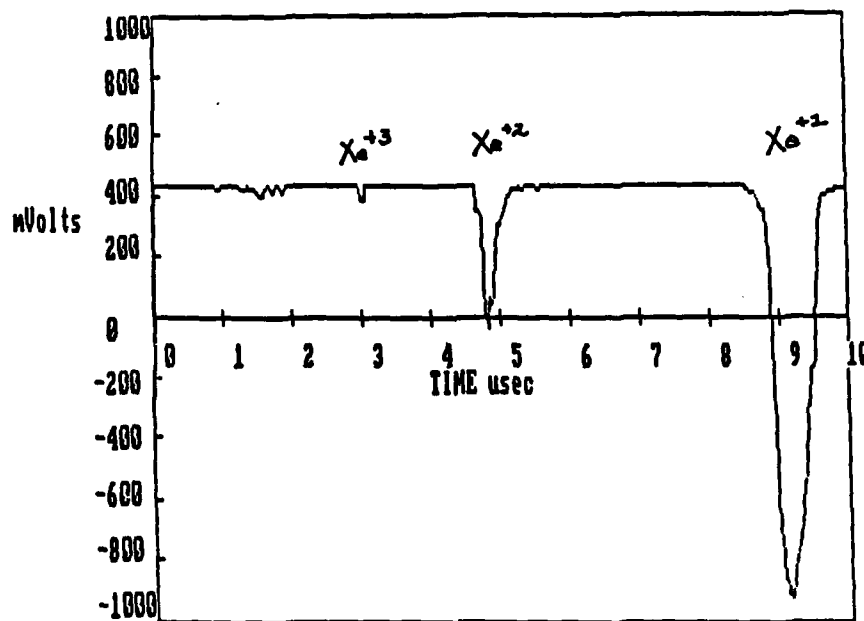


Fig. 1 Time-of-flight spectrum of xenon from a single laser pulse at $I \sim 9 \times 10^{13}$ W/cm² and $\lambda = 5856\text{\AA}$. Xenon target pressure = 7×10^6 torr.

We have measured ion production as a function of laser intensity and frequency. At low intensities we confirm the I^6 power law dependence. At higher intensities we observe saturation for neutral xenon. Saturation intensities are on the order of 10^{13} W/cm^2 throughout the range $570 \text{ nm} \leq \lambda \leq 600 \text{ nm}$ which is in apparent contrast to that measured at longer pulsewidths¹ and $\lambda = 532 \text{ nm}$. These differences may in fact be due to the details of the intermediate states participating in the excitation. We are in the process of doing some calculations in collaboration with others to address these questions.

Work performed under the auspices of the U.S. Department of Energy by the Lawrence Livermore National Laboratory under contract number W-7405-ENG-48.

¹L'Hullier, et al., "Multiply Charged Ions Induced by Multiphoton Absorption in Rare Gases at $0.53 \mu\text{m}$," Phys. Rev A, Vol. 27, No. 5 (1983)

MULTIPHOTON ION PRODUCTION IN INTENSE FIELDS: A QUANTITATIVE APPROACH

G.A. Kyrala, D.E. Casperson, P.H.Y. Lee,
L.A. Jones, A.J. Taylor and G.T. Schappert
Physics Division, Los Alamos National Laboratory
Los Alamos, N.M. 87545

In studying the phenomenon of ion production in intense electromagnetic fields, we are interested in measuring the absolute rates for ion production in order to compare with the various models. We are also interested in the effect of the neighboring atoms on the ionization process. The intense fields are produced by focusing the 1.5ps long, 248nm laser light from a KrF laser with an f/2 on-axis reflecting paraboloid. The focal volume has been mapped out at full laser intensity. The ions are collected in a conventional time-of-flight spectrometer, where the field of view of the spectrometer is limited to 65 microns to maximize the contribution from the Rayleigh focal volume relative to that from outside that volume. The effect of neighboring atoms is studied by varying the pressure, and looking at the modified ion time-of-flight spectra. The effect of charge changing collisions will be presented as well.

GAUSSIAN AND PRE-GAUSSIAN LASER NOISE IN MULTIPHOTON TRANSITIONS

K. Wódkiewicz

Institute of Theoretical Physics, Warsaw University,
Warsaw 00-681, Poland

We present a general theoretical description of Gaussian and Pre-Gaussian laser fluctuations in multiphoton transitions. We review several simple Gaussian models of laser phase and frequency fluctuations based on the Ornstein Uhlenbeck Brownian analogy. We extend our approach to a jumplike and a shotlike description of laser fluctuations [1]. Most simply, the frequency or the phase can be described by a two-state jump process or by independent step-function-like pulses. This allows us to discuss multiphoton transitions without the Gaussian assumption. We establish for each noise a regime when the laser line-shape profile has a Lorentzian power spectrum. This means that just by looking at one-photon processes induced by such a laser, it is impossible to distinguish among these various noise sources. Despite this fact, pronounced differences do appear when such sources of light are used to drive N-photon transitions. All the diffusive and jumplike frequency-fluctuation models predict that the N-photon absorption has a Lorentzian profile with a width that increases as N^2 [2]. From this point of view, there is no difference between diffusive or jumplike fluctuations. The situation is quite different when phase fluctuations are considered. The jumplike phase fluctuations or a shot-noise frequency noise will lead to a N-photon absorption completely different from the diffusive case.

We present next a theory of the multimode laser noise based on a special Markov-chain description of external fluctuations. This chain, composed of n independent

two-state jump processes, forms a Pre-Gaussian stochastic process [3] from which a detailed and exact discussion of the off-resonant N-photon ionization rate can be given [4]. We show that for three jump processes the normalized second-order intensity coherence function is equal to $5/3$ i.e., a value which is very close to the chaotic case of 2! This justifies the Pre-Gaussian character of this Markov chain in the description of chaotic light sources. The Pre-Gaussian noise provides a powerful tool for studying the impact of multimode laser on multiphoton transitions.

References

- [1] K. Wódkiewicz and J. H. Eberly J. Opt. Soc. Am. B3, 628 (1986)
- [2] D. S. Elliot et. al. Phys. Rev. A32, 887 (1985)
- [3] K. Wódkiewicz B. W. Shore and J. H. Eberly J. Opt. Soc. Am. B1, 398 (1984)
- [4] Cao Long Van and K. Wódkiewicz J. Phys. B19, 1925 (1986)

Saturation of an optical transition by a phase-diffusing laser field

M. W. Hamilton,^{} D. S. Elliott,[†] K. Arnett and S. J. Smith*

*Joint Institute for Laboratory Astrophysics, University of Colorado
and National Bureau of Standards, Boulder, Colorado 80309-0440 USA*

The dependence of the optical Autler-Townes spectrum on phase fluctuations of the laser field is a dramatic demonstration of the effect of laser bandwidth on laser-atom interactions.¹⁻³ Through this experiment we have studied the ac Stark splitting of the $3p^2P_{3/2}$ state of atomic sodium when strongly coupled to the atomic ground state by an intense phase-fluctuating laser field. The absorption spectrum of a second (probe) laser, which weakly coupled the 3P level to the $4d^2D_{5/2}$ level has two peaks, each corresponding to one of the ac Stark split components of the 3P level. We have analyzed the relative intensity of these two peaks and the spectral widths of the peaks to determine the influence of the phase fluctuations.^{2,3}

The probe laser and saturating laser were collinear in the interaction region, and perpendicular to the atomic sodium beam. In order to ensure that the field amplitude of the saturating laser was homogeneous over the probed region, the beam diameter of the probe laser was limited to approximately one fifth that of the saturating beam. The intensity of the saturating beam was varied in the range $0.4\text{--}4\text{ Wcm}^{-2}$. The atomic sodium was optically pumped into the $F=2$, $m_F=2$ ground state before entering the interaction region. Both laser beams were circularly polarized using a linear polarizer and Fresnel rhomb, so that only $\Delta m_F=+1$ transitions were induced. Since only transitions to the $F=3$, $m_F=3$ state of the $3p^2P_{3/2}$ level and the $F=4$, $m_F=4$ state of the $4d^2D_{5/2}$ level are allowed, the three state model for this system is quite valid.

The primary data consisted of absorption spectra produced by scanning the probe laser through the $3P\rightarrow 4D$ transition for each of a series of fixed detunings of the saturating laser from resonance with the $3S\rightarrow 3P$ transition. The absorption spectra were measured by monitoring the 330 nm radiation resulting from the decay of the 4D level through the $4P\rightarrow 3S$ transition. The scan of the probe laser was calibrated by directing a portion of the probe laser through a spherical mirror Fabry-Perot interferometer in a near-confocal geometry.

The phase diffusion field was generated by randomly modulating the frequency (and phase) of a cw laser beam using acousto-optic and electro-optic

modulators. This technique has been described elsewhere in detail.⁴ The Gaussian fluctuations were derived from a voltage noise diode, with a voltage controlled oscillator transforming the voltage fluctuations into a constant amplitude, fluctuating frequency r.f. field. The fluctuating frequency was transferred to the optical field in the acousto-optic modulator. The bandwidth of an acousto-optic modulator is limited, however, so that this device was restricted to modulation frequencies of less than 6 MHz. Travelling wave electro-optic modulators were used to modulate the laser beam at frequencies in the range 6 MHz - 1 GHz. The optical field generated in this way is described by

$$E(t) = \frac{1}{2} E_0 e^{i[\omega_0 t + \phi(t)]} + \text{c.c.},$$

where E_0 and ω_0 are the constant amplitude of the field and the mean angular frequency, respectively, and $\phi(t)$ is the stochastically varying phase. The correlation function of the frequency fluctuations $\langle \dot{\phi}(t) \dot{\phi}(t') \rangle = b\beta \exp -\beta |t-t'|$ completely determines the statistical properties of the optical field. The parameters of this exponentially decreasing function are the correlation time of the fluctuations, $1/\beta$, and the spectral density of the fluctuations, b . Control of β and b was attained through the use of active linear shaping networks, and attenuators, respectively, applied to the voltage noise source output. The laser bandshape (ranging from nearly Lorentzian to nearly Gaussian) and the bandwidth (up to 25 MHz full width at half maximum) were completely specified by these two parameters.

The peak height asymmetry of the Autler Townes spectrum, defined as $A = (h_l - h_u)/(h_l + h_u)$, where h_l (h_u) is the height of the lower (upper) probe frequency absorption peak, is a sensitive function of the laser fluctuations. When the saturating laser is tuned to resonance with the 3S-3P transition, the Stark components are symmetrically displaced from the unperturbed transition frequency and are of equal amplitude. As the saturating laser is detuned from resonance, however, the relative peak height changes. In the case of a monochromatic laser, the asymmetry parameter is a monotonic function of the saturating laser detuning, increasing from -1 below resonance to +1 above resonance. In the limit when the saturating laser frequency is far from resonance with the atomic frequency, the two peaks of the probe laser spectrum can be identified with a two-photon process and a two-step process. The former is the direct (albeit nonlinear) excitation of the 4D level, with no excitation of the intermediate 3P level. The latter process involves the off-resonant excitation of the 3P state, and the subsequent promotion to the 4D when the probe is tuned near the unperturbed 3P-4D transition frequency. For a monochromatic saturating laser, the off-resonant excitation of the 3P state is extremely weak,

and the two-photon process dominates the two step process at all frequencies of the saturating laser. We have measured the reversal of this peak height asymmetry under conditions of a broad bandwidth saturating laser whose bandshape is nearly Lorentzian and whose intensity is sufficiently weak. The peak height asymmetry reverts to normal when the laser bandwidth is less than the atomic linewidth, the band shape is nearly Gaussian, the saturating laser is far from resonance with the atomic transition, or the Rabi frequency of the interaction is greater than the inverse of the correlation time of the fluctuations, β .

The frequency widths of the probe laser absorption peaks also show an interesting behavior. The width of the two-photon peak is seen to increase with increasing bandwidth of the saturating laser, as expected. The width of two-step peak, on the other hand, is seen to be independent of the width of the saturating laser, i.e., the excitation to the intermediate 3P state is decoupled from the absorption of the probe laser which induces the 3P-4D transition.

The behavior of the peak height asymmetry and peak widths have been studied theoretically by Zoller and Dziemballa³ following the technique of Dixit, Zoller, and Lambropoulos.¹ Agreement between the experimental observations and the calculations are excellent.

The research was supported by the U.S. Department of Energy, Office of Basic Energy Sciences. M.W.H. wishes to acknowledge the support of the Science and Engineering Research Council, and D.S.E. the support from the National Science Foundation through a Presidential Young Investigator Award.

*Present address: Department of Physics and Applied Physics, University of Strathclyde, 107 Rottenrow, Glasgow G4 ONG Scotland.

† Present address: School of Electrical Engineering, Purdue University, West Lafayette, Indiana 47907.

REFERENCES

1. S. N. Dixit, P. Zoller, and P. Lambropoulos, *Phys. Rev. A* **21**, 1289 (1980).
2. M. W. Hamilton, D. S. Elliott, K. Arnett, and S. J. Smith, *Phys. Rev. A* **33**, 778 (1986).
3. M. W. Hamilton, D. S. Elliott, K. Arnett, S. J. Smith, M. Dziemballa and P. Zoller, to appear in *Phys. Rev. A*.
4. D. S. Elliott, M. W. Hamilton, K. Arnett, and S. J. Smith, *Phys. Rev. A* **32**, 887 (1985).

Theory of Double Optical Resonance: Collisional Broadening and Doppler Effects
on ac Stark Splitting*

Albert M. F. Lau

Sandia National Laboratories, Livermore, California 94550, USA

In an earlier note,¹ it has been shown that application of a theory of ac Stark splitting succeeded in explaining the doublet structure observed² in the multiphoton excitation spectra of hydrogen atoms produced in H₂/air diffusion flames. It was noted that large collisional broadening gave rise to abnormal peak asymmetry in the ac Stark doublet. A theoretical prediction³ of reflection symmetry in the spectra for opposite detunings in the strong pump laser has been confirmed by another experiment.⁴

This paper presents the general results of this theory of a three-level system interacting with two laser fields. Each field may induce single-photon or multiphoton (near-)resonant transition between two levels. The theory includes collisional relaxation and laser bandwidth effects. Under the steady-state and the weak-probe approximations, analytic solutions for the level populations are obtained. Expressions for the resolution of the doublet, resonance peak positions and heights are given in terms of the atomic and laser parameters such as collisional relaxations, laser bandwidths, detunings and intensities.

In the above scheme of H detection in flames, the hydrogen 3p level was excited by absorption of two 243-nm photons and a 656-nm photon via the 2s resonant intermediate level. For a given detuning of the 656-nm laser, the 3p→2s fluorescence was collected as a function of the 243-nm laser detuning from the 1s-2s resonance. Additional calculations using the above theory show that (i) by counter-propagating two 243-nm laser beams so that the Doppler contribution of the 1s→2s two-photon transition is eliminated, the Doppler-averaged three-photon 1s→3p excitation spectra are indistinguishable from the corresponding Doppler-free spectra, thus greatly improving the resolution of the ac Stark doublet, (ii) increase in pressure reduces the ratio of the primary peak to the secondary peak, and (iii) at high enough pressure (> several atm), the ac Stark doublet becomes one broad resonance.

*This work was supported by the U.S. Department of Energy, Office of Basic Energy Sciences, Chemical Sciences Division.

1. A.M.F. Lau, Phys. Rev.A33, 3602 (1986).
2. J.E.M. Goldsmith, Opt.Lett. 10,116 (1985).
3. A.M.F. Lau, Sandia Report No. SAND85-8697, 1985 (unpublished).
4. J.E.M. Goldsmith in Laser Spectroscopy VII, edited by T.W. Hansch and Y.R. Shen, Springer Series in Optical Sciences, Vol.49 (Springer, New York, 1985), p.410.

**MULTISTEP RESONANCE EXCITATION OF AUTOIONIZING
STATES IN THE RARE-EARTH ELEMENTS**

V. N. Fedoseyev

Institute of Spectroscopy

USSR Academy of Sciences

142092, Troitzk, Moscow region, USSR

The laser three-step resonant excitation technique is used to study autoionizing states of the rare-earth elements Eu, Gd, and Tm. Spectra of laser photoionization from a vast collection of two-step excited high-lying states of the atoms have been obtained. A study of intermediate excited states was performed too. Data acquisition was intended to extract optimal ways for photoionization of the atoms by a laser radiation in the spectral range 540-680 nm. The experimentally observed thulium autoionizing Rydberg series has been identified by means of the theoretical calculations based on the relativistic perturbation theory with a zero model potential method.

POPULATION TRAPPING AND A GENERALIZATION OF FERMI'S GOLDEN
RULE FOR THE STRONG BOUND-CONTINUUM TRANSITIONS

Kazimierz Rzązewski, Rafał Kukliński, Institute for Theoretical
Physics,

Jan Mostowski, Institute of Physics,
Polish Academy of Sciences, 02-668 Warsaw, al. Lotników
32/46, Poland.

Most of quantum mechanical decay processes can be described by models in which a bound state is coupled directly to a continuum. If the decay is caused by the external influence, such as laser light, the interaction hamiltonian is a periodic function of time. In the, so called, rotating wave approximation the time dependence of the interaction hamiltonian can be eliminated, leading to a time independent coupling of the bound state to a continuum. Of course decay processes caused by internal static atomic interactions are in a form studied in our talk from the very beginning.

The ionization to the Lorentzian continuum by a monochromatic field in the rotating wave approximation serves as the "canonical" example. Saturation effects, Rabi oscillations and the Autler-Townes type splitting of the long time photoelectron spectrum are the main features of the solution.

An important case of the asymmetric Fano resonance has been intensively studied in early eighties¹. The asymmetric Autler-Townes splitting, the confluence of coherences and the population trapping are the main points. They all occur for a specific value of the laser intensity. This value depends on the parameters of the autoionization resonance. We are perhaps approaching an experimental verification of this predictions.

A novel method of solving the bound-free dynamics will be introduced. It is based on the notion of quantum dynamical maps. The standard harmonic perturbation is replaced by the train of delta-function kicks. Such approach allows for a study of the corrections coming from the counter-rotating part of the interaction hamiltonian.

A drastic dependence of the strong field evolution on the behavior of the wings of the saturated resonance has been discovered this way². For all the resonances that fall off faster than the Lorentzian, the strong field ionization rate tends to zero as the field strength grows. The system exhibits a very weakly damped Rabi oscillations. As a result the long time photoelectron spectrum consists of two very narrow maxima, orders of magnitude narrower than the saturated resonance.

We propose and then verify an estimate of this residual width. The formula is a strong field generalization of the Fermi's Golden Rule³:

$$\Gamma = 2\pi |\Omega(\omega_L + \Omega_0)|^2$$

It relates the residual decay rate Γ to the strength of the bound-free coupling at the point which is shifted from the point determined by the energy conservation of the single photon absorption (usual Fermi's Golden Rule) by the amount proportional to the laser field amplitude known as Rabi frequency (Ω_0).

REFERENCES:

1. K. Rzażewski, J. Eberly: Confluence of bound-free coherences in laser induced autoionization. Phys. Rev. Lett. 47, 408, (1981).
2. K. Rzażewski, J. Mostowski: Soluble quantum map with continuous spectrum. Phys. Rev. A (in press).
3. J. Kukliński, K. Rzażewski: Generalization of Fermi's Golden Rule for the strong field bound-free transitions (submitted).

Application of State-Multipole Heisenberg Equations to Multiphoton Excitation Dynamics *

B. W. Shore and R. Sacks, *Lawrence Livermore National Laboratory*

Coherent atomic or molecular excitation, such as is produced by idealised laser radiation, is essentially a multiphoton process -- one must account for the simultaneous presence of a large number of identical photons. The population histories and temporally varying induced dipole moments produced by such excitation contrast with the behavior predicted for incoherent excitation on the basis of rate equations. These differences remain when the individual transition steps are two-photon (or n -photon) interactions. Whereas incoherent descriptions of such n -photon excitation requires evaluation of rate coefficients by means of generalized golden rule procedures, the description of coherent excitation requires an appropriate time-dependent Schrödinger equation. When the atom undergoing laser-induced excitation is also affected by incoherent processes, such as collisions, this equation no longer suffices. The Heisenberg equations, or equivalent density-matrix equations, permit treatment in which coherence and incoherence play comparable roles in the excitation dynamics. Unlike rate equations, such equations must incorporate complexities that originate in the orientation degeneracy expressed by magnetic quantum numbers. In simple cases of coherent excitation, both for single-photon and multiphoton excitation, the sublevels merely require an average of $2J+1$ independent Schrödinger equations. Relaxation couples the independent equations. It has been known for some time that appropriate state-multipole operators can simplify the description of many phenomena connected with optical pumping. This talk will discuss application of these multipole operators to the description of multiphoton coherent excitation. In some limiting cases the equations simplify, but in general one has a hierarchy of coupled multipole polarizations and coherences in place of the populations and coherences that occur as variables in nondegenerate systems.

* This work was performed under the auspices of the United States Department of Energy by the Lawrence Livermore National Laboratory under contract W-7405-Eng-48.

ABNORMAL PEAK STRUCTURE IN DOUBLY-RESONANT THREE-PHOTON IONIZATION OF A FOUR-LEVEL SYSTEM WITH TWO NEAR-DEGENERATE INTERMEDIATE LEVELS

Mei-Ying Hou, Yong-Bo Shi, Bao-Hua Feng and Yong-Liang Shao
Institute of Physics, Academia Sinica
Beijing, China

Quan-Shen Han
Department of Physics, Central College of Nationalities
Beijing, China

Qing-Shi Zhu
Institute of Chemical Physics, Academia Sinica
Darlian, China

Abnormal peak asymmetry of a Stark splitting in resonant excitation of multilevel systems due to laser bandwidth⁽¹⁾⁽²⁾, laser spatial and temporal distribution⁽³⁾, and collisional effect⁽⁴⁾ has been

experimentally observed. Theoretical investigation of these effects has also been reported recently⁽⁵⁾⁽⁶⁾.

In this paper we report another possible cause for abnormal peak structure in multiphoton excitation (ionization) due to the presence of near-degenerate levels. Here we call level $|i\rangle$ and $|j\rangle$ are near-degenerate if the level difference between level $|i\rangle$ and $|j\rangle$ is comparable with Rabi frequency ω_R in transitions from or to level $|i\rangle$ or $|j\rangle$. Using semi-

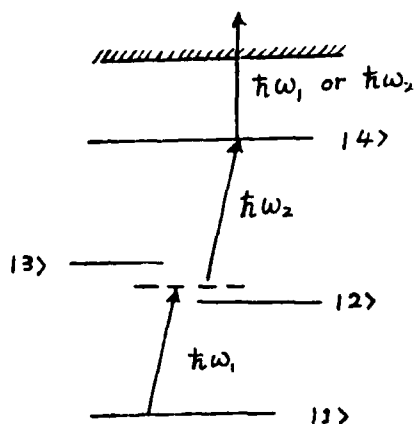


Fig. 1

classical density matrix formalism⁽⁷⁾, we present a numerical calculation on resonant excitation of a four-level system with a pair of near-degenerate intermediate states. As is shown in Fig. 1, level $|2\rangle$ and $|3\rangle$ are radiatively coupled with levels $|1\rangle$ and $|4\rangle$ by near-resonant fields E_1 ($\hbar\omega_1$) and E_2 ($\hbar\omega_2$). In our numerical calculation,

we have neglected the ionization rate because of the much smaller ionization cross-sections. The bandwidth of the laser has been considered by using the phase diffusion model⁽⁵⁾. As is shown in Fig. 2, scanning the weaker beam $\hbar\omega_2$, we obtain an abnormal two-peak

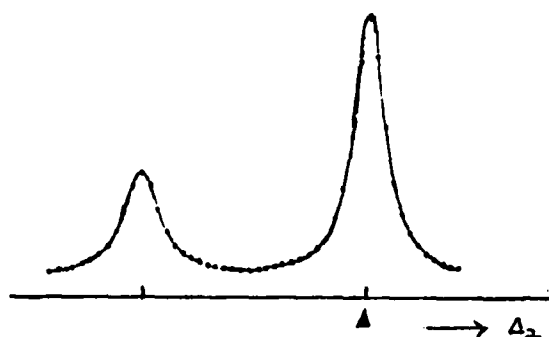


Fig. 2

structure of the ionization profile at the presence of the near-degenerate level. And by scanning the intense beam $\hbar\omega_1$, only one broadened peak will be seen (as is shown in Fig. 3 (a)). The shape of this broadened peak will become asymmetric with the second beam detuned away from on-resonance (shown in Fig. 3 (b)).

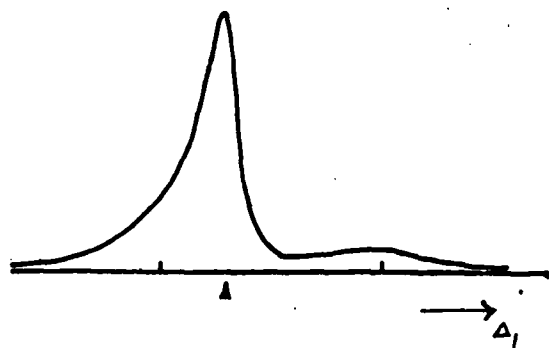
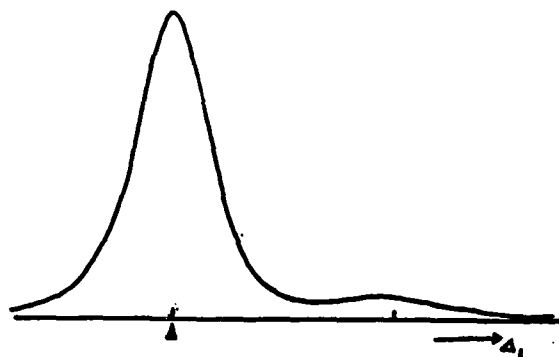


Fig. 3

A preliminary experimental observation of doubly-resonant three-photon ionization in the $\text{Na } 3S \rightarrow 3P_{3/2}, 3P_{1/2} \rightarrow 4D \rightarrow \text{Na}^+ + e^-$ process has been obtained. Comparison between experimental observation and the theoretical predictions are given.

References

1. S.E. Moody and M. Lambropoulos, Phys. Rev. A 15 (1977) 1497.
2. P. Hogan and S.J. Smith, in ICOMP. Rochester, June 1977
3. L. Li, B. Yang, and P.M. Johnson, J. Opt. Soc. Am. B2 (1985) 748.
4. J.E.M. Goldsmith, Opt. Lett. 10 (1985) 116.
5. A.T. Georges and P. Lambropoulos, Phys. Rev. A18 (1978) 587.
6. A.M.F. Lau, Phys. Rev. A33 (1986) 3602.
7. C.Y. Fong and Y.R. Shen, J. Opt. Soc. Am. B3 (1986) 649.

Invited Paper

PRECISE CALCULATIONS OF PROPERTIES OF MULTIPLY-EXCITED STATES

C. F. Bunge

Universidad Nacional Autonoma de Mexico

Mexico

Invited Paper

THE FORMATION AND DECAY OF TRIPLY EXCITED STATES
IN e-He SCATTERING

H.G.M. Heideman

Fysisch Laboratorium, Rijksuniversiteit Utrecht, Princetonplein 5,
3584 CC Utrecht, The Netherlands.

The decay of a doubly excited autoionizing state, which has been excited near its threshold by electron impact, may have a considerable effect on the excitation of the singly excited states. This so-called post-collision interaction (PCI) effect manifests itself as prominent interference structures on the excitation functions of (higher lying) singly excited states. In fact the observation of these PCI structures provides the only possibility to study the electron impact excitation of autoionizing states very close to their thresholds. An extensive experimental study, on e-He scattering, of this kind in our laboratory has revealed the existence of hitherto unknown structures which are interpreted as being caused by a new type of shape resonances lying very close to the thresholds of a particular class of autoionizing states. From the fact that these shape resonances are only observed in the excitation functions of states which can possibly be affected by the PCI effect it is concluded that they almost exclusively decay to their respective parent (autoionizing) states, thereby considerably enhancing the threshold excitation cross sections of these autoionizing states. Using the recently introduced supermultiplet classification for doubly excited states a selection rule for the near-threshold excitation of doubly excited states by electron impact can be deduced from the measurements. Only states with large probabilities in the Wannier region of configuration space (where both electrons in the doubly excited helium atom are at nearly equal distances and on opposite sides of the nucleus) are strongly excited. It is pointed out that these states are precisely the states that can support the above

mentioned shape resonances at their thresholds. From these facts it is concluded that the shape resonances in fact are a new type of triply excited He^- states of the intershell type, in which the three excited electrons move in a highly correlated state with one electron at relatively large distance being weakly bound in the polarization potential of a doubly excited state. The properties of these intershell resonances appear to differ appreciably from those of the triply excited He^- states of the intrashell type, in which all three excited electrons move in the same shell and thus are at nearly equal distances from the nucleus.

Invited Paper

**HYPERSPHERICAL DESCRIPTION OF MULTIPLY-EXCITED STATES
TRIPLY-EXCITED STATES OF He⁻**

S. Watanabe

Equipe de Recherche 261 du CNRS

Observatoire de Paris-Meudon

92190 Meudon, France

Theoretical investigations of two-electron atoms have revealed systematic features in energy levels and lifetimes controlled by correlations. In the recent past, we have seen a unification¹ of the hyperspherical analysis of radial correlations² and the rovibrational description of angular correlations.³ The two-electron correlation patterns are now understood to be isomorphic to the collective modes of a floppy linear triatomic molecule, albeit some subtle differences.

Strong correlations are naturally expected in triply- and multiply-excited states as well. Experimental observations and theoretical studies of these states are scarce so far, but several isolated resonances have been ascribed to temporary formation of triply-excited states.⁴ Recently, it has been recognized that multiply-excited states are produced by multiple charge transfer in the collision of highly charged ions with atoms. This paper extends previous analyses of doubly-excited states to manifolds of triply-excited resonances, thus paving the way for a general treatment of multiply-excited states.

The radial motion of triply-excited electrons is unstable. However, it becomes quasiperiodic when the electrons maintain a certain phase relationship among them. It then becomes meaningful to consider the collective oscillation of the electrons near the equilibrium configuration. There are three fundamental radial modes. One is the symmetric stretching mode (A_1') and the other two are doubly-degenerate radial oscillations (E'). The following coordinates replace the usual independent radial variables,

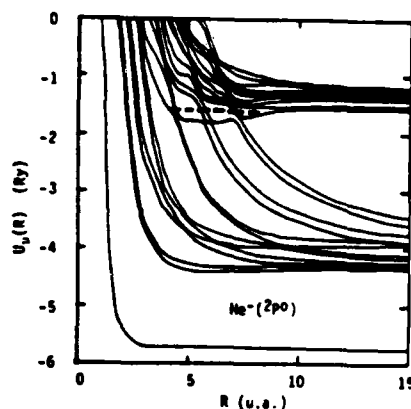
$$R = \left(r_1^2 + r_2^2 + r_3^2 \right)^{1/2},$$

$$\alpha_1 = \tan\left(\frac{r_1}{r_2}\right),$$

$$\alpha_2 = \tan\left(\frac{r_3}{[r_1^2 + r_2^2]^{1/2}}\right).$$

Roughly speaking, R represents the symmetric stretch and α_1 and α_2 represent the doubly-degenerate radial oscillations. The expectation value of the Hamiltonian evaluated at fixed R yields a set of adiabatic potential curves pertaining to the quasi-stable electronic motion in α_1 and α_2 . Figure 1 shows an example of curves for $\text{He}^-(2p^0)$. The well-known triply-excited state at 57.22 eV is marked by a horizontal broken line.

Fig. 1. Hyperspherical adiabatic potential curves for $\text{He}^-(1p^0)$. The lowest curve converges to the ground state energy level of He at $R=\infty$. The group of curves in the intermediate energy range converge to the singly excited states of He; these curves represent doubly excited channels of He^- . Curves in the highest group represent triply-excited channels and converge to the doubly-excited states of He.



There are numerous curves corresponding to triply-excited resonant channels. It is imperative to classify them in accordance with the three-electron collective modes. As a preliminary step, a simple model calculation has been undertaken to analyze the angular correlations. Fig. 2 shows the resultant rotational manifolds of intrashell triply-excited states of $\text{He}^-(N=3)$. Fig. 3 shows, in a very schematic fashion, the three-electron motion corresponding to the first three manifolds. There is an obvious correspondence between the triply-excited states and the rovibrational states of a D_{3h} triatomic molecule such as NH_3 , except for some marginal differences. Further details discussed at the conference.

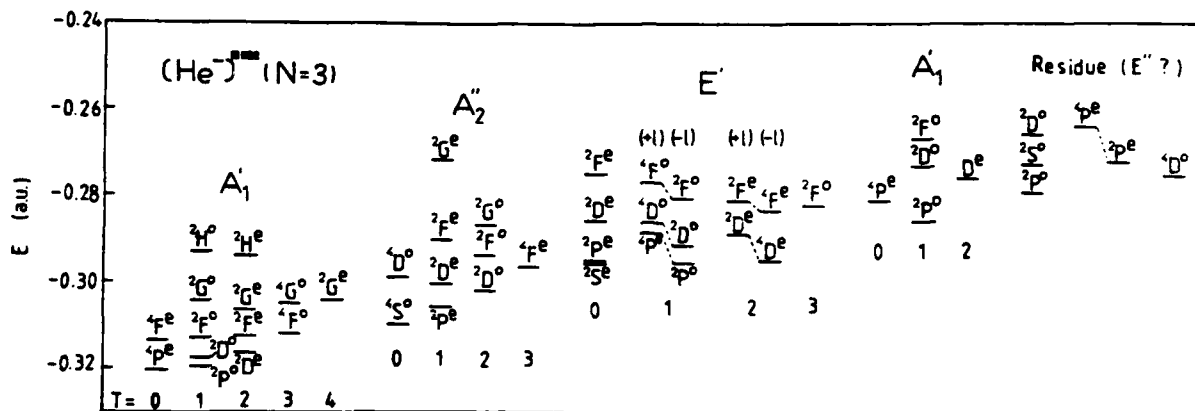


Fig. 2 Rotational manifolds of $(\text{He}^-)^{***}(\text{N}=3)$ by a simple model calculation.

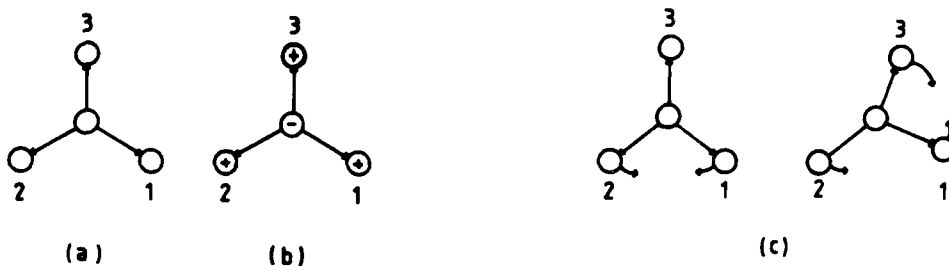


Fig. 3 Schematic representation of electronic motion: (a) corresponds to the first manifold (A_1') of Fig. 2, (b) to the second manifold (A_2''), and (c) to the third one (E').

REFERENCES

1. S. Watanabe and C. D. Lin, Phys. Rev. A 34, 823 (1986).
2. J. H. Macek, J. Phys. B 1, 831 (1968); C. D. Lin, Phys. Rev. A 10, 1986 (1974); U. Fano, Rep. Prog. Phys. 46, 97 (1983) and references therein.
3. D. R. Herrick, K. E. Kellman and R. D. Poliak, Phys. Rev. A 22, 1517 (1980); G. S. Ezra and R. S. berry, Phys. Rev. A 28, 1974 (1983) and references therein.
4. R. K. Nesbet, Phys. Rev. A 14, 1326 (1976).

Invited Paper

THE CONTRIBUTION OF AUTOIONIZING STATES TO MULTIPHOTON
IONIZATION OF ALKALI-EARTH ATOMS

Vladimir I. Lengyel
University of Uzhgorod
Uzhgorod, Ukraine
USSR

Two-Electron Excitation in an Intense Laser Pulse - the
Outer Electron Shell of Magnesium

K Burnett
Blackett Laboratory
Imperial College
London SW7 2BZ

We shall describe how an intense laser pulse (100fs, 10^{12} W/cm peak-power) may be used to drive a coherent oscillation of the pair of electrons in the outer shell of magnesium¹. The oscillation is composed of a coherent superposition of the ground, first excited and doubly excited states². This oscillation can be established in spite of the damping due to photoionisation and auto-ionisation³. We shall discuss to what extent this type of coherent oscillation may be termed collective.

References

1. K. Burnett. "Two Electron - Two photon ionisation in an intense laser field" - to be published.
2. A. Szoke and C.K. Rhodes - Phys. Rev. Lett. 56, 720 (1986).
3. X. Tang and P. Lambropoulos
Physical Review Letters - Volume 58, 2, (1987)
108-111.

PHASE SPACE APPROACH TO TWO ELECTRON IONIZATION

Jan Mostowski

Institute of Physics, Polish Academy of Sciences, Warszawa, Poland

Marek Trippenbach

Warsaw University, Warszawa, Poland

Cao Long Van

Institute for Theoretical Physics, Polish Academy of Sciences, Warszawa, Poland

Multiple ionization of atoms in ultrastrong laser fields is a complicated process which lacks theoretical explanation. First reports of double ionization were published some years ago. Recently Rhodes applied extremely powerful excimer laser, yielding intensities of the order of 10^{17} W/cm^2 and wavelengths of about 200 nm to a systematic study of multielectron ionization in various atoms. It should be stressed that the laser intensities used in these experiments are much larger than in any previous experiment in atomic physics. In fact intensity 10^{17} W/cm^2 corresponds to field strength comparable to the electrostatic field of the nucleus. Therefore experience gained from other theories of atomic radiative processes is of not much help here. No perturbation-like theory nor even "essential states" type of theories can describe processes in such a strong field. In fact no adequate theory of multielectron ionization has been formulated thus far.

In this paper we will study ionization of the two electron (helium) atom in very strong laser field with the help of the so-called phase space averaging method. The method is based on the classical description of the electrons and is particularly well suited for processes in ultrastrong fields. In fact the stronger the field the more accurate the method becomes.

Before discussing the excitations we will present a description of the ground state. The electrons are bounded by the Coulomb potential of the nucleus with charge $2e$. Electrons interact between themselves by electrostatic repulsive forces. No exact wavefunction of this system can be found, good approximations are known.

The phase space averaging method requires the knowledge of the probability distribution in the phase space corresponding to the initial state. The link between the ground state wave function and the probability distribution in the phase space is provided by the coarse grained Wigner function $W(r_1, r_2, p_1, p_2)$. Quantum expectation values can be expressed as moments of the probability distribution. The calcula-

tion of these moments is, however, a nontrivial task due to the high dimensionality of the phase space. Standard Monte-Carlo technique was used to calculate multiple integrals over the phase space.

The validity of the phase space averaging method will be discussed. It will be shown that the errors originating from such a treatment of the electrons may be quite large, of the order of 10%. However, since no adequate quantum theory of multiple ionization exists our approach has the advantage of not being restricted to weak fields. On the contrary, the stronger the external field the better the theory works. This makes our approach an attractive alternative to approximate quantum models.

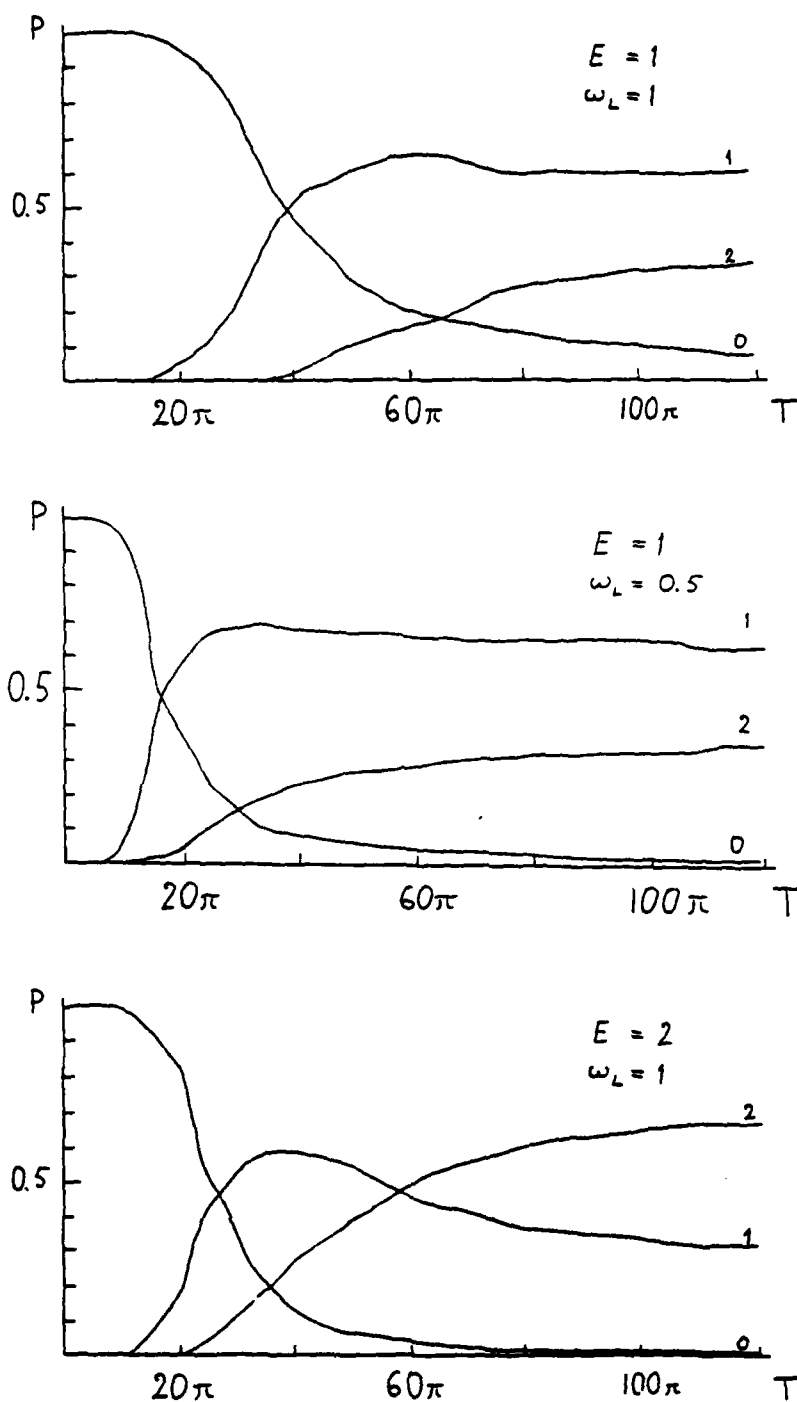
We have solved numerically the evolution of the probability distribution for the two electron atom in a strong electric field by solving Newtons equations of motion. A set of trajectories with different initial conditions was found, the set of initial conditions was chosen in such a way that they formed a representative sample of the initial probability distribution W . The values of the external electric field E_0 were chosen to be 0.5, 1 and 2 in atomic units, the frequencies ω_L of the laser field were taken to be 0.5, 1 and 2 atomic units. These values of the parameters were chosen for computational reasons but they do not differ much from the experimental values, where intensities were of the order of 10^{17} W/cm^2 and the frequency ω_L corresponds to 200 nm, or 0.25 atomic unit.

In order to calculate single and double ionization probabilities we have to determine how many trajectories from the representative sample of the initial probability distribution correspond to two ionized electrons, and how many to one bound and one ionized electron. This is a simple task once the trajectories are found.

Discussion of the results will be presented. The most important results are outlined below. We found that the process of ionization is a very fast one. In fact it takes not more than a couple of optical periods for an atom to (partially) ionize. What is, however, not obvious is that the ionization is not complete in the whole range of times studied. In fact the possibility of finding a neutral atom remains non zero for all times in all the cases. An even more supprizing result is that the ionization probability reaches a "steady state". It means that come of the elements of the initial ensamble representing the ground state get ionized very rapidly while other remain bounded. This does not exclude the possibility that the trajectories, which are bounded for the time range studied will not get ionized at later times by some slow mechanism of the energy uptake.

FIGURE CAPTION

Fig. 1 - 3. Probabilities of finding neutral (0), singly ionized (1) and doubly ionized (2) atom as functions of time for various field strengths and frequencies.



Invited Paper

Unimolecular Decay of Rotational-Selected Polyatomic Molecular
Ions Prepared by Resonance-Enhanced Multiphoton Ionization

H.J. Neusser, H. Kühlewind, A. Kiermeier, E.W. Schlag

Institut für Physikalische und Theoretische Chemie, Technische Universität
München, Lichtenbergstraße 4, D-8046 Garching, West-Germany

During the last decade it has been demonstrated that multiphoton ionization (MPI) can be used as the basis of a novel type of ion sources for mass spectrometry /1/. Since the intermediate spectrum is sharp in many polyatomic molecules resonance-enhanced MPI is extremely selective. In this paper it will be shown that resonance-enhanced two-photon ionization not only leads to the production of vibrational state-selected but also to J rotational quantum number -selected benzene cations. State- and energy-selected ions are of particular interest for the precise investigation of dissociation kinetics. We present the first example of decay time measurements for the unimolecular decay of J-selected molecular ions.

In a one laser two-photon ionization experiment there is generally a certain amount of excess energy above the ionization potential as the laser frequency is determined by the first resonant absorption step to the intermediate state. Excess energy can distribute either to kinetic energy of the electrons or internal energy of the ions. In order to check, whether vibrational state-selected ions are produced, an analysis of photoelectron energy was performed with a home-built time-of-flight photoelectron energy analyzer. Photoelectron spectra of three benzene isotopes $C_6H_6^+$, $C_6D_5H^+$, and $C_6D_6^+$ have been measured. In agreement with recent work /2/ it was shown that for the chosen intermediate states 6^0 and 6^0_{161} more than 90 % of the isotopic benzene ions are produced in a single vibrational state, i.e. the vibrationless ground state or the ν_{16} state of the ion, respectively. In another experiment state-selected ions are produced in a two-laser experiment via the 6^1_0 cold band transition, the second laser frequency tuned close to the ionization potential (Fig.1). J-selection in the ion is achieved by exciting the appropriate J-levels in the intermediate state of the molecule.

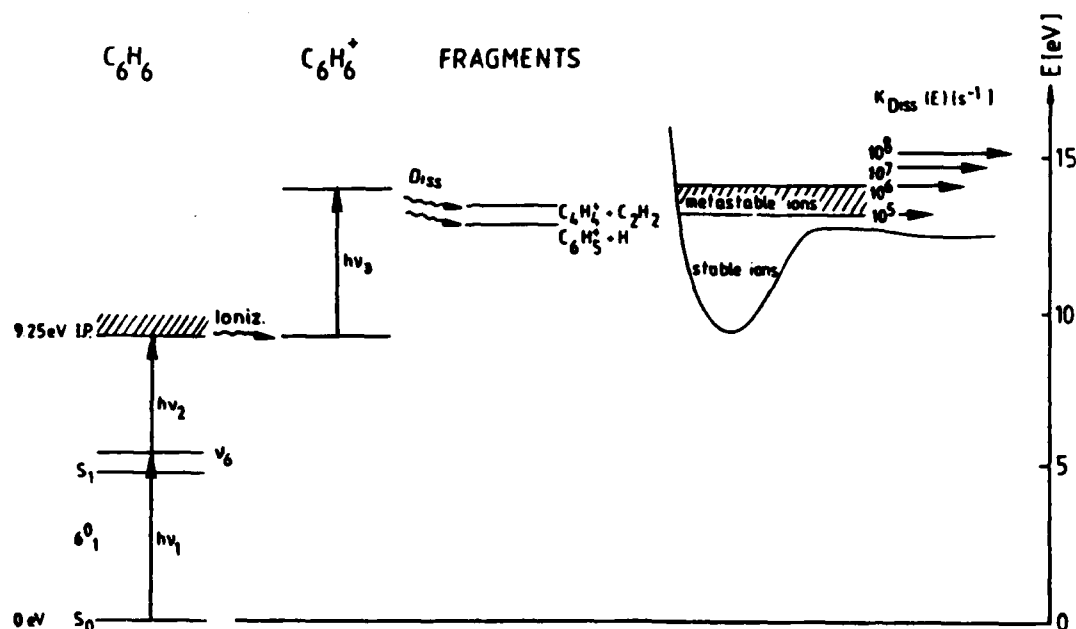


Fig. 1: Three-laser excitation scheme for production of internal energy-selected molecular ions above dissociation threshold

The state-selected benzene ions are produced either in an effusive or in a cooled molecular beam which is located within the acceleration field of a reflectron time-of-flight mass spectrometer /3/. 200 ns later, when the ion cloud has left the molecular beam region, another laser pulse of variable photon energy (4.6 - 5.52 eV) further excites the ions to an energy level slightly above the thresholds for different dissociation channels of low threshold energy (see Fig.1). This leads to the production of $C_6H_5^+$, $C_6H_4^+$, $C_4H_4^+$, and $C_3H_3^+$ ionic fragments and their deuterated analogues, respectively. The energy of the ions is sufficient to induce a metastable decay on a μs timescale, i.e., a decay of the ions on the way from the ion source to the reflecting field. As the reflecting field acts as an energy analyzer, the unimolecular decay rate constants for all isotopic channels could be measured according to the procedure described previously /4/. Since all decay channels of low energy, independent of their H-loss or C-loss character, are competing and originate from one electronic state /4/, the directly measured rate constant is

given by the sum of the individual constants of all competing decay channels. It is found to be governed solely by the total amount of energy deposited in the molecular ion.

No vibrational specificity is found for the three excitation pathways discussed above. This result points to a dissociation which proceeds according to a statistical model of unimolecular dissociation. In addition, we were able to investigate for the first time the influence of J on the decay rate constants for a unimolecular dissociation process. For sharply defined internal energies down to 4.6 eV we found that the decay rate does not change when the rotational quantum number J is varied from 2 to values as large as 60.

To explain our results we performed statistical RRKM calculations of all four competing decay channels. For differently labelled isotopes a good simulation of the experimental results is obtained with one set of vibrational frequencies of the activated complexes correlated by the Redlich-Teller product rule. The measured intramolecular and intermolecular isotope effects yield a microscopic probe of the looseness or tightness of C-H bonds in the activated complexes and provide a direct insight into the character of the reaction coordinate.

In conclusion we have shown that resonantly enhanced two-photon ionization is a versatile method for the production of state-selected polyatomic molecular ions. In a reflectron time-of-flight mass spectrometer the decay rate constants of competing decay channels of internal energy selected ions have been measured for various defined energies and for selected rotational J levels. From our experiment detailed information about the dissociation mechanism and the structure of the activated complexes is obtained.

- /1/ E.W.Schlag and H.J.Neusser, Acc. Chem. Res. 16, 355 (1983)
- /2/ S.R.Long, J.T.Meek, J.P.Reilly, J. Chem. Phys. 79, 3206 (1983)
- /3/ U.Boesl, H.J.Neusser, R.Weinkauff, E.W.Schlag, J. Phys. Chem. 86, 4857 (1982)
- /4/ H.Kühlewind, A.Kiermeier, H.J.Neusser, J. Chem. Phys. 85, 4427 (1986)

Invited Paper

STRUCTURE AND DYNAMICS OF ISOLATED MOLECULES AND CLUSTERS

E. R. Bernstein

Condensed Matter Sciences Laboratory

Chemistry Department

Colorado State University

Fort Collins, Colorado 80523

Multiphoton ionization techniques are employed to determine properties of organic solute/solvent clusters. Discussion will focus on pyridazine, isoquinoline, hydroxyquinolines, allyl- and methoxybenzenes, and cyanoanilines as "solutes" solvated by H_2O , HN_3 and C_nH_{2n+2} . Structure, intramolecular (cluster) vibrational redistribution, vibrational predissociation, and "chemical reactions" will be discussed for these cluster systems.

TWO-PHOTON EXCITATION OF DENSE SODIUM VAPOR NEAR THE $nd^2D_{5/2,3/2}$ ($n=3,4,5,7$)

LEVELS: $Na_2 b^3\Sigma_g^+ \rightarrow X^3\Sigma_u^+$ EXCIMER EMISSION

S. J. Bajic

Department of Chemistry, University of Tennessee,
Knoxville, Tennessee 37916, U.S.A.

R. N. Compton* and J.A.D. Stockdale

Oak Ridge National Laboratory,** P.O. Box X,
Oak Ridge, Tennessee 37831-6125, U.S.A.

Laser excitation and ionization processes in dense (1-10 Torr) sodium vapor have been studied for laser wavelengths near the two-photon-allowed nd^2D states ($n=3,4,5$). In particular, the recently reported (Dinev et al.¹) excimer emission between the lowest triplet states of Na_2 has been studied in greater detail. Significant excimer laser emission is seen only when two-photon pumping occurs near the $4d^2D_{5/2,3/2}$ states. Multiphoton ionization via the nd^2D states was also studied and the ionization was seen to disappear as the pressure was increased from less than 3.5 Torr to 7 Torr, where molecular features began to dominate the spectra. These results, together with the fact that excimer emission actually exhibited a "dip" at the exact position of the two-photon-excited $4d^2D_{5/2,3/2}$ state, suggests a cancellation due to the different pathways to the $4d^2D$ states. Such an interference effect was reported earlier by Malcuit et al.² and more recently by Krasnikov et al.³ The possible suppression of two-photon absorption was first suggested theoretically by Manykin and Afanasev⁴ and treated more recently by Agarwal.⁵

Figure 1 shows the forward-directed emissions when a Nd:YAG pumped dye laser is tuned to near two-photon resonance with the $4d^2D_{5/2,3/2}$ states in sodium. In the region of 790 to 800 nm, directly pumped bound-bound lasing between the two lowest singlet states was observed.

*Also Department of Chemistry, The University of Tennessee, Knoxville, TN 37916, U.S.A.

**Operated by Martin Marietta Energy Systems, Inc. under contract DE-AC0584OR-21400 with the U.S. Department of Energy.

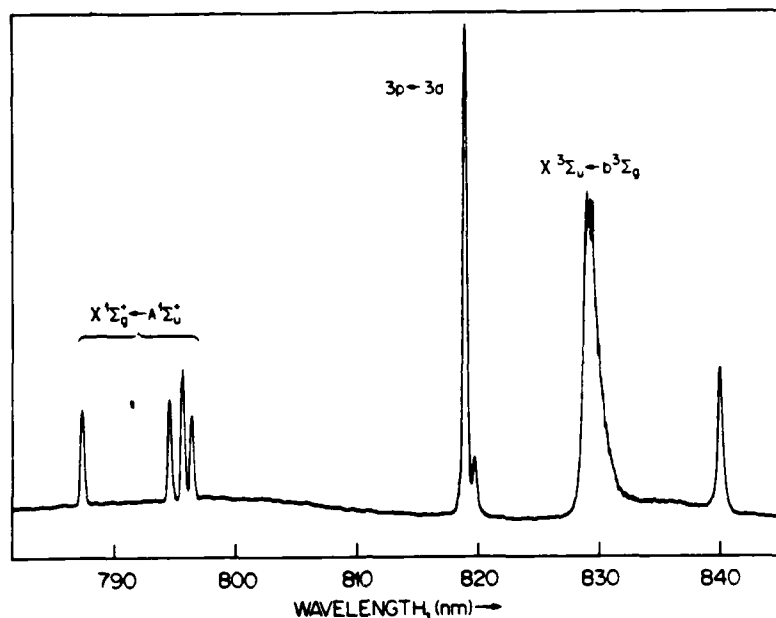


Fig. 1. Forward-stimulated emission in sodium vapor (~1 Torr) produced by two-photon pumping near the $4d^2D_{5/2,3/2}$ level.

The large feature at 818 nm is due to $3d^2D_{5/2,3/2} \rightarrow 3p^2P_{1/2}$ and $3p^2P_{3/2}$ stimulated emission (stimulated emission between $\sim 4d-4p$ and $4p-3d$ completes the cascade stimulated emission).

The breadth and to some extent the position of the excimer emission at ~830 nm is dependent upon the laser intensity, the laser pump frequency, and alkali density (maximum intensity at ~10 Torr). The intensity can be made larger than any other feature in the spectrum and can be made much broader (up to 100 Å) depending upon pump laser frequency and power, and sodium atom density. Figure 2 shows the excimer emission at specific wavelengths versus the laser pumping wavelength. We note a pronounced "dip" at the $3s^2S_{1/2} \xrightarrow{2h\nu} 4d^2D_{5/2,3/2}$ resonance position. If we assume that the excimer emission is somehow related to the population of $4d^2D$ atoms, this result would imply an interference or cancellation effect as discussed earlier.

We have also strongly pumped $4d^2D_{5/2,3/2}$ atoms via a hybrid resonance involving $3p$ atoms. Although intense ionization and stimulated atomic emission was observed, no excimer emission was detected. Possible mechanisms for the two-photon pumping of the excimer

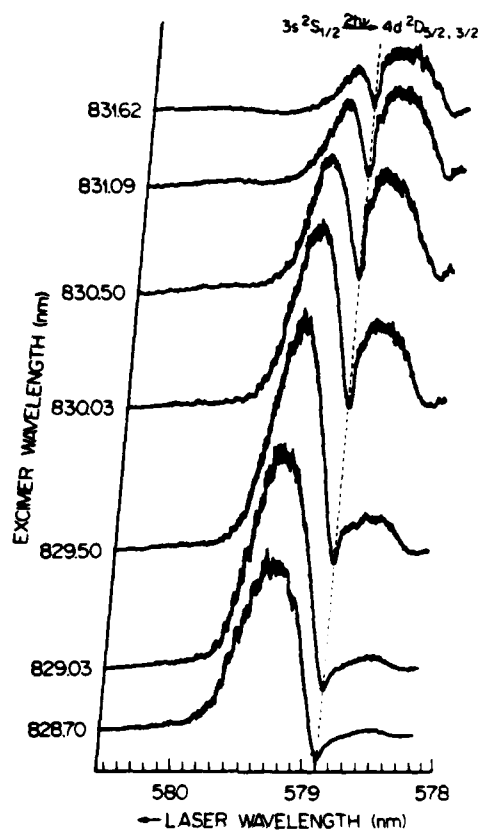


Fig. 2. Excimer emission at various wavelengths versus the laser two-photon pumping wavelength. Note the pronounced "dip" at the $4d^2D$ transition.

laser will be presented. Excimer emission in other alkalis (e.g., lithium at $\sim 1.3 \mu m$ and potassium $\sim 1.1 \mu m$) will be searched for and the results will be presented at the conference.

1. S. G. Dinev, I. G. Koprnikov, and I. L. Stefanov, Opt. Comm. **52**, 199 (1984).
2. M. S. Malcuit, D. J. Gauthier, and R. W. Boyd, Phys. Rev. Lett. **55**, 1086 (1985).
3. V. V. Krasnikov, M. S. Pghenichnikov, and V. S. Solomatin, J.E.T.P. Lett. **43**, 148 (1986).
4. E. A. Manykin and A. M. Afanasev, Zh. Eksp. Theor. Fiz. **52**, 1246 (1967) [Sov. Phys. J.E.T.P. **25**, 828 (1967)].
5. G. S. Agarwal, Phys. Rev. Lett. **57**, 827 (1986).
6. D. D. Konowalow and P. S. Julianne, J. Chem. Phys. **72**, 5815 (1980).

Invited Paper

LINEAR SPECTROSCOPY USING NON-LINEAR OPTICS

J.W. Hepburn, D.J. Hart and I.M. Waller

Centre for Molecular Beams and Laser Chemistry
University of Waterloo, Waterloo, Ontario, N2L 3G1 CANADA

Laser spectroscopy of highly excited states of atoms and small molecules is a rapidly growing field with a great deal of current interest. Up until now essentially all of the experiments in this field have relied on multiphoton excitation to reach these high energy states. While multiphoton excitation has definite advantages, particularly when multiple resonance excitation is used, for a large number of studies it would be far better to excite these high energy states through single photon excitation with a relatively low-powered laser. In order to make this possible, extremely short wavelength lasers must be used. As no broadly tunable, narrowband lasers exist for wavelengths shorter than about 3000Å, non-linear optical methods must be employed to generate tunable coherent light at shorter wavelengths. In the vacuum ultraviolet (VUV) region of the spectrum, below 2000Å, four wave mixing in atomic vapours is currently the best way of generating broadly tunable coherent radiation. In this talk, the use of four wave sum mixing techniques in metal vapours will be illustrated by reference to some recent work from our laboratory in which the dynamics of highly excited molecules was probed with coherent VUV in the 1120Å to 1700Å spectral range.

In recent work in our laboratory, we have used coherent VUV to probe radiative lifetimes of excited states of NO in the 60000 to 70000 cm⁻¹ range under molecular beam conditions¹, and to study the photofragment spectroscopy of various small molecules². In this talk recent results will be presented in which coherent VUV was used to study photofragmentation of triatomic molecules and spin-orbit autoionization in HI. We hope to demonstrate by these two examples that coherent VUV is an exceedingly powerful technique, suitable for a wide variety of experiments in atomic and molecular physics.

In the first study, tunable VUV generated by four wave sum mixing in Mg vapour was used to do Doppler spectroscopy on the S atom products resulting from 1933Å photofragmentation of CS₂ molecules in a supersonic molecular beam. Sample Doppler lineshapes are shown in figure 1. By analyzing these lineshapes, it was possible to obtain information on the energy release and recoil velocity spacial anisotropy in the different CS₂ photofragmentation channels.

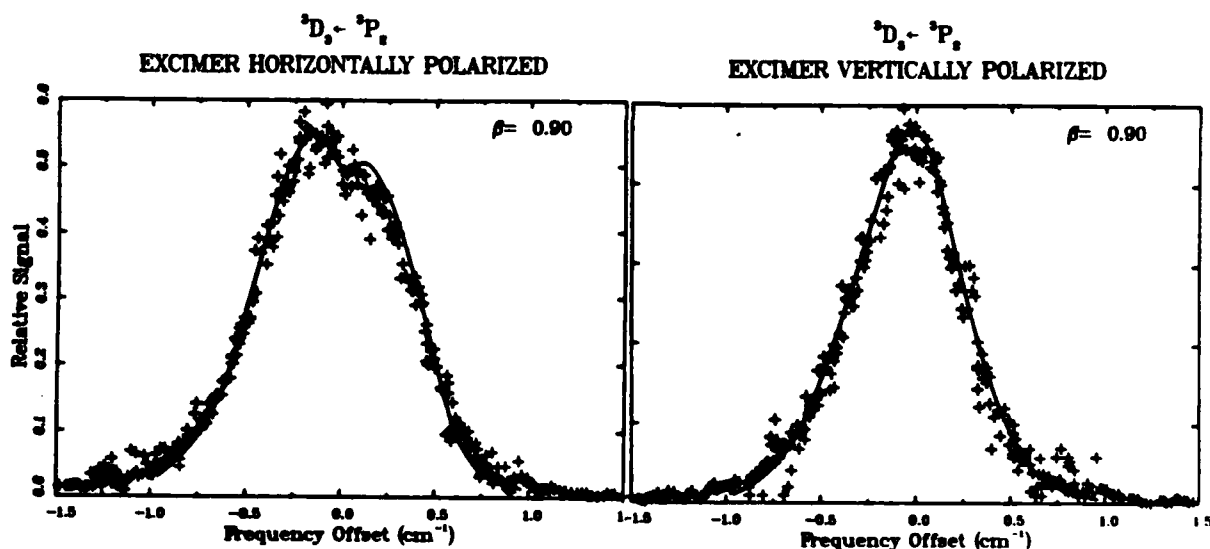


Figure 1: Doppler profiles for the $S(3P_2)$ product from 1933Å photolysis of CS_2 , with the 1933Å laser polarized parallel and perpendicular to the VUV probe laser.

In the second set of experiments, coherent VUV generated by four wave sum mixing in Hg vapour was used to study autoionizing states of HI between the $HI^+ 2\Pi_{3/2}$ and $2\Pi_{1/2}$ ionization limits. These autoionizing states have received recent theoretical attention because of the question of differences in autoionization behaviour between Xe and HI^3 . In a recent multichannel quantum defect theory calculation, sharp resonances were predicted, both in the total cross section and in the anisotropy parameter³. In our experiments, we are taking advantage of the high resolution and high power of our VUV source to study the photoionization of jet-cooled HI, using a low energy electron detector to monitor the photoionization process. These experiments are currently in progress, but some preliminary results are shown in fig. 2, along with the theoretical predictions, for the total photoionization cross-section in the 10.615 to 10.735 eV spectral range. It would appear that there are no sharp resonances in the cross section, as our photon resolution of about 0.1 meV would easily reveal any such resonances. This work, and the possibilities for future work in photoionization spectroscopy using the same experimental setup, will be discussed in this talk.

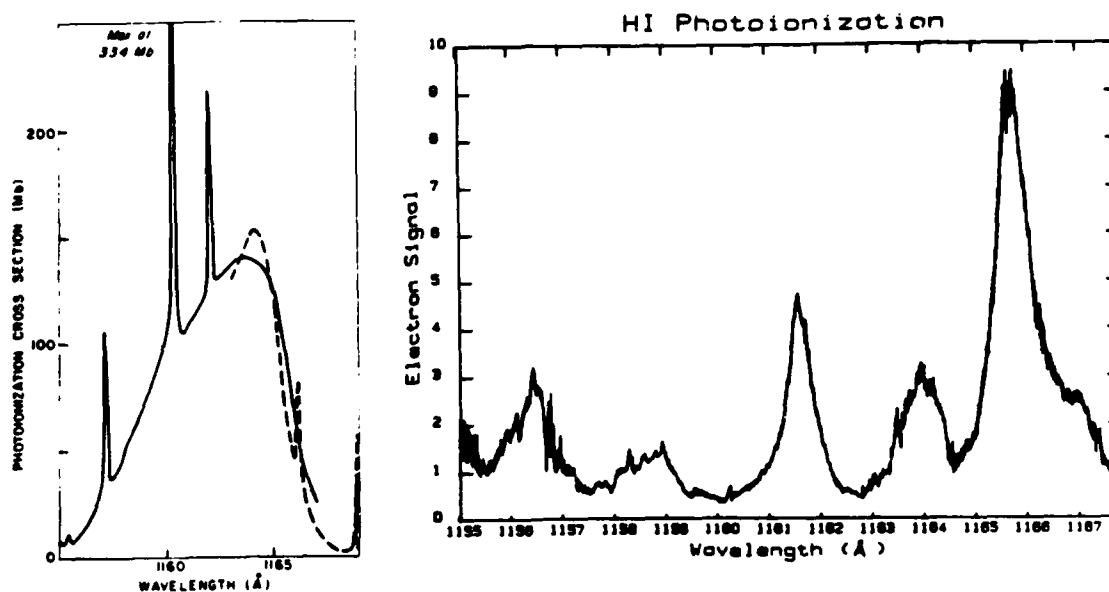


Figure 2: Theoretical and experimental photoionization cross sections for HI. Calculation is from reference 3, data is from our experiment.

REFERENCES

1. D.J. Hart and J.W. Hepburn, J. Chem. Phys. **86**, 1733 (1987).
2. I.M. Waller, H.F. Davis and J.W. Hepburn, J. Phys. Chem. **91**, 506 (1987).
I.M. Waller, H.F. Davis and J.W. Hepburn, "Short Wavelength Coherent Radiation: Generation and Applications", D.T. Atwood and J. Bokor eds. (AIP Conference Proc. #147, New York, 1986), pp. 430-441.
3. H. Lefebvre-Brion, A. Giusti-Suzor, and G. Raseev, J. Chem. Phys. **83**, 1557 (1985).

PROBING OF MOLECULAR ALIGNMENT EFFECTS USING
'SATURATED' PULSED LASER EXCITATION

H. Meyer, R. Dressler, and S. R. Leone*

Joint Institute for Laboratory Astrophysics
University of Colorado and National Bureau of Standards
Boulder, Colorado 80309-0440

The use of laser-induced fluorescence (LIF) to probe rotational alignment of molecules in photodissociation and collision dynamics experiments has attracted great interest recently. Since pulsed lasers are used in many of these experiments, time dependent detection is possible. On the other hand, the poor duty cycle of pulsed lasers may require an LIF probe under 'saturated' rather than linear absorption conditions to obtain more signal. The formulation of the latter process has been investigated extensively.¹ Many measurements, however, may have already embarked on the 'saturated' regime. In this paper we treat theoretically the LIF probing of molecular alignment including 'saturation' effects in the excitation step. Neglecting relaxation, the excitation with a short rectangular pulse of linearly polarized laser light can be described in terms of the optical Bloch equations for an open two level system. Within the rotating wave approximation an analytical solution for the density matrix of the excited state as a function of the laser polarization is found. Using the results of Fano and Macek² the degree of polarization of the fluorescence is calculated from the components of the quadrupole moment of the excited state. Although many different Rabi frequencies are present due to the degeneracy of the angular momentum states involved, in the case of resonant, narrow band excitation the calculated degree of polarization as a function of laser power exhibits strong oscillations. The influence of variations in

*Staff Member, Quantum Physics Division, National Bureau of Standards.

pulse energy and pulse duration is investigated. Since in most experiments the spectral width of the laser pulse is large compared to the natural linewidth, nonresonant interactions lead to strong damping of the Rabi oscillations found for resonant excitation. Additional damping might be caused by variations of the pulse envelope in the case of nonresonant interactions and by phase variations within individual pulses. We show theoretically, and confirm experimentally, that molecular alignment may be measured accurately within the nonlinear absorption regimes.

References

1. C. H. Greene and R. N. Zare, J. Chem. Phys. 78, 6741 (1983).
2. U. Fano and J. H. Macek, Rev. Mod. Phys. 45, 553 (1973).

MPD/MPI OF ORGANOMETALLIC MOLECULES - THE ROLE OF NON-RADIATIVE
PROCESSES IN DETERMINING FREE METAL STATE DISTRIBUTIONS

Joseph Chaiken
Department of Chemistry
Syracuse University
Syracuse, New York 13244-1200

ABSTRACT

We have obtained new MPD/MPI data on a variety of organometallic molecules. We have shown for the first time the correlation between structure of the organometallic and the state distribution of the metal atoms formed by MPD. MPD/MPI spectra of deuterated samples taken at various pressures, laser powers, and electric field (ion collection plates) strengths unequivocally demonstrate that IVR processes are involved in determining the metal atom state distribution. We have also shown that a quantitative correlation exists between IVR rates for uncomplexed ligands and the branching ratios measured for the corresponding complexed ligands. Finally, we have evidence which suggests the effect of electronic relaxation on the MPD product state yields. As an important by-product of these studies, we have observed for the first time, the 7S_3 Rydberg series for all the group VI metals.

RESONANT MULTIPHOTON LASER-SURFACE INTERACTION

J. Reif, H.B. Nielsen, P. Tepper, O. Semmler, and E. Matthias
 Inst. f. Atom- u. Festkörperphysik, Freie Universität Berlin,
 D-1000 Berlin 33, F.R.G.

and

E. Fridell, E. Westin and A. Rosen
 Dept. of Physics, Chalmers University of Technology, and
 University of Göteborg, S-412 96 Göteborg, Sweden

We present proof that resonant multiphoton processes such as multi-photon-photoemission and surface second harmonic generation (SSHG) can be used to probe the electronic structure of crystalline surfaces.

For BaF_2 (111) we find from cluster calculations on the basis of a 10-atom ($\text{Ba}_1\text{Ba}_6\text{F}_3$) planar cluster (cf. Fig. 1) that there exist occupied and excited surface states in the bandgap (Fig. 2). These surface states are mainly due to dangling electrons of the metal ions.

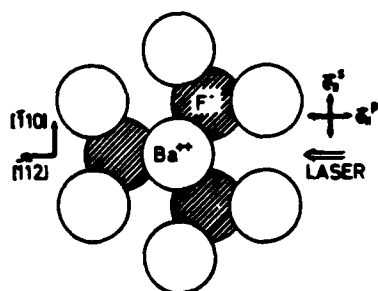


Fig. 1 Schematic representation of the BaF_2 (111) surface, also showing the cluster used in the calculations.

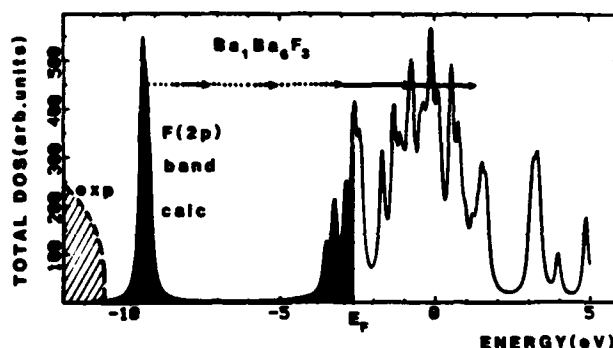


Fig. 2 Density of states at the BaF_2 (111) surface, resulting from the cluster calculations.

Experimentally, we followed two approaches to probe the existence of these states: For clean surfaces under ultra-high vacuum (UHV) conditions we observed the laser-induced emission of electrons and positive ions; for surfaces in realistic environment, i.e. in air we looked for the second harmonic of the incident laser light, generated at the surface. For all experiments, we used a Nd^{3+} -YAG pumped dye laser in the green spectral range (coumarin 152; $500 \text{ nm} \leq \lambda \leq 560 \text{ nm}$).

In the UHV experiments clean surfaces were prepared by cleaving the crystal inside the vacuum chamber. We observed a pronounced spectral

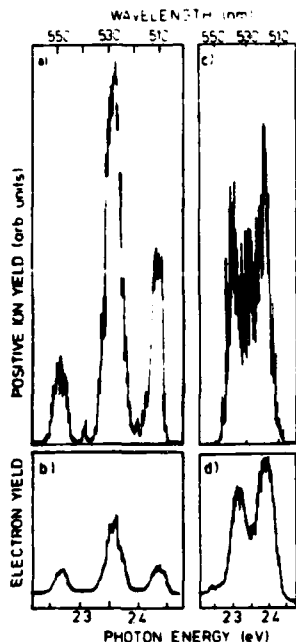


Fig. 3 Yields for electrons and positive ions as a function of laser wavelength; laser polarization parallel to $\langle 11\bar{2} \rangle$ (a,b) resp. $\langle 110 \rangle$ (c,d).

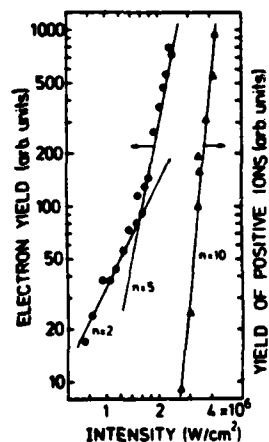


Fig. 4 Electron and ion yield at 518 nm as a function of laser intensity.

dependence for the emission of charged particles which is practically identical for both electrons and positive ions (see Fig. 3). These spectra also depend on the direction of the in-surface component of the linear light polarization, \vec{e}_{\parallel} , with respect to the crystallographic directions (cf. Figs. 1 and 3). Since the single photon energy of less than 2.5 eV is far too small to ionize the surface, even if the occupied states in the middle of the bandgap are taken into account, the emission of charged particles is a multiphoton process. This conclusion is supported by Fig. 4 where in a log-log-plot the electron and ion yields are shown as a function of incident laser intensity. The slopes indicate, that photoemission should be a two-photon process for weak laser intensity, starting from the occupied surface state in the middle of the bandgap (solid arrows in Fig. 2). For higher intensities, a fivephoton process takes over¹, which could originate in the 2p valence band. From the apparent correspondence between ion and electron spectra we deduce that both processes must be highly related. Hence, we conclude from the slope of ten for the ion yield, that two electrons must be emitted to create one positive ion, more likely than a direct 10-photon process. In analogy to a recent model by Itoh and Nakayama² two adjacent holes created by ionization could concentrate on a fluorine atom, thus resulting in electrostatic instability and Coulomb explosion.

Resonant optical second harmonic generation at the surface of centrosymmetric media, in principle, should be an ideal method for probing empty surface states, since firstly it leaves the surface unaltered during the interaction and

secondly it is highly surface sensitive because in dipole approximation the second order polarization vanishes for the centrosymmetric bulk. However, for dielectrics the conversion efficiency ($\sim 10^{-14}$) and hence the signal to noise ratio is extremely poor. Therefore, in order to facilitate the ease of operation, the experiments were conducted in air. Nevertheless, the second harmonic yield reflected the c_{3v} symmetry of the BaF_2 (111) surface when the crystal was rotated around the $\langle 111 \rangle$ direction. Fig. 5 shows the result if both fundamental and second harmonic are s-polarized, i.e. when the signal comes from the dipole contribution only, due to symmetry breaking at the surface. The remaining isotropic part of the signal we attribute to the interface air-adsorbate.

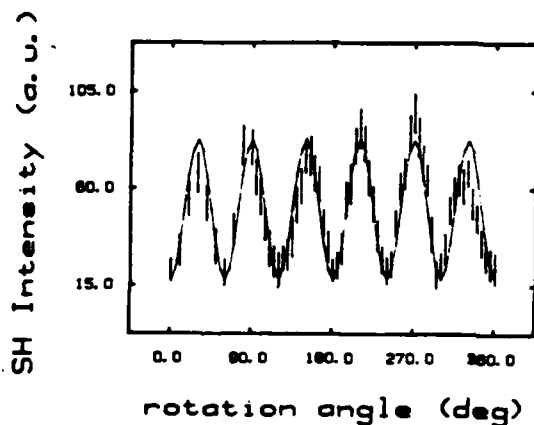


Fig. 5 s-polarized second-harmonic intensity as a function of sample rotation angle for s-polarized excitation.

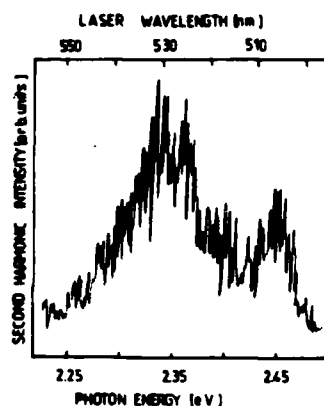


Fig. 6 Wavelength dependence of second harmonic generation (fundamental and second harmonic polarized at $\pm 45^\circ$.)

We found again a pronounced spectral dependence of our signal, similar to the one observed for ionization in UHV (see Fig. 6). Hence we conclude, that even in air the intrinsic surface states exist and can be probed by surface second harmonic generation.

Support from DFG, SNSRC and SBTB is gratefully acknowledged.

¹We favor the 5-photon process over the idea of dynamic resonances as a reason for the slope of 5 since otherwise one should observe a smooth and steady intensity dependence and not a sudden set-in of the steeper slope.

²N. Itoh, T. Nakayama, and T.A. Tombrello, Phys. Lett. **108A**, 480 (1985)

Laser Excitation of Electronic States of Atoms near Surfaces

A. C. GREENFIELD AND K. BURNETT

Spectroscopy Group, Blackett Laboratory
Imperial College, London SW7 2BZ

P. T. GREENLAND

Theoretical Physics, U.K.A.E.A. Harwell
Didcot, Oxon

We shall present a theoretical consideration of a spectroscopy in which an atomic or ion beam in collision with a surface is excited electronically by a laser. The shift and broadening of the atomic energy levels due to the presence of the surface is of great importance to the understanding of surface dynamical processes and we shall describe how information about these two effects can be obtained by monitoring the production of ions or excited atoms in the reflected beam.

The theoretical modelling of this Spectroscopy involves writing down a second quantized Hamiltonian which includes effects of tunnelling into the surface by a two level atom and solving for ion or excited state production rates. Production rates for specific models of the energy-level separation and level widths as an atom approaches a surface will be presented.

References

1. R. Kawai, K.C. Lui, D.M. Newns and K. Burnett - to be published.
2. W. Bloss and D. Hone, Surf. Sci. 72 277 (1978)
3. R. Brako and D.M. Newns, Surf. Sci. 108 253 (1981)

Invited Paper

INFLUENCE OF INTERNALLY GENERATED SUM-FREQUENCY FIELDS ON ODD-PHOTON
EXCITATIONS OF DIPOLE-ALLOWED TRANSITIONS IN ATOMIC GASES

W. R. Garrett

Chemical Physics Section, Oak Ridge National Laboratory *

P. O. Box X, Oak Ridge, TN 37831-6125

* Operated by Martin Marietta Energy Systems, Inc., under contract
DE-AC0584OR-21400 with the U. S. Department of Energy.

NONLINEAR OPTICAL BALANCE

J. J. WYNNE, IBM Thomas J. Watson Research Center,

P. O. Box 218, Yorktown Heights, NY 10598

ABSTRACT: Multiphoton excitation processes are generally expected to show enhancement when the exciting frequencies, or some combination thereof, are tuned toward intermediate resonances. However, contrary to this general expectation, suppression of photoionization, fluorescence, amplified spontaneous emission, and nonlinear optical conversion have all been reported in the presence of resonant multiphoton excitation.¹ At first glance, the nonlinear phenomena manifesting this suppression and the order of the nonlinear processes appear to be quite distinct. In some instances, this suppression has been shown to result from a destructive interference (alternatively, a competition) between alternative excitation pathways to the resonant intermediate state.² For example, three-photon resonance enhancement of five-photon multiphoton ionization is suppressed by coherent third harmonic generation, the polarization induced by the third harmonic wave destructively interfering with the polarization induced by the three photon excitation.

The common mechanism underlying these phenomena is the coherent nonlinear coupling of two or more optical waves via a *dissipative* nonlinear optical medium. As they propagate through the nonlinear medium, the waves develop amplitudes and relative phases that minimize the resonant material excitation, thereby minimizing the dissipative losses. In this way, the excitation pathways come into a nonlinear optical balance. This balance is stabilized by the dissipative processes that increase the losses if the balance is upset in either direction.

Combinations of amplitude and phase that produce greater loss are more rapidly damped out, leaving the minimum loss combination to persist the longest. The nonlinear coupling is mediated by the coherence length of the nonlinear optical mixing process. The case of perfect phase-matching (infinite coherence length) can produce perfect destructive interference, complete suppression, and zero loss. The case of very poor phase matching (nearly zero coherence length) produces no interference, no suppression, and undiminished loss.

Four-wave mixing processes with a single resonant intermediate state, such as third harmonic generation, will be analyzed to show how this nonlinear optical balance is achieved and sustained, yielding predictions for the degree of suppression of the excitation of the resonant intermediate state.

References:

- 1) For example, J. C. Miller, R. N. Compton, M. G. Payne, W. W. Garrett, Phys. Rev. Lett. **45**, 114 (1980).
- 2) H. Kildal and S. R. J. Brueck, IEEE J. Quant. Electronics QE-16, 566 (1980); J. J. Wynne, Phys. Rev. Lett. **52**, 751 (1984); M. S. Malcuit, D. J. Gauthier, R. W. Boyd, Phys. Rev. Lett. **55**, 1086 (1985).

IR AND UV ULTRASHORT PULSE GENERATION BY HYPER-RAMAN SCATTERING AND
FOUR-WAVE MIXING IN METAL VAPORS

Yu P. Malakian
Institute for Physical Research
Armenian Academy of Sciences
378410 Ashtarak-2, USSR

Suppression of N-Photon Absorption by the Four-Wave Mixing Process

Daniel J. Gauthier, Michelle S. Malcuit and Robert W. Boyd

The Institute of Optics
University of Rochester
Rochester, New York 14627

It is often of interest to transfer the maximum amount of population from an atomic ground state to an excited state through use of n-photon resonant absorption of laser light. It is well known that n-photon absorption saturates at high laser intensities due to optical Stark shifts of the atomic levels;¹ however, we have determined that even when the intensity of the laser is sufficiently low so that optical Stark effects can be ignored, other nonlinear optical processes can lead to a decrease of the amount of transferred population. In particular, we have studied the suppression of two-photon resonant excitation of the sodium 3d level by the four-wave mixing process. The nature of the suppression is that new fields generated by the four-wave mixing process create a new excitation pathway connecting the ground and 3d levels, and under quite general conditions this pathway interferes destructively with that due solely to the applied laser field.

The experiment in which we observed competition between two-photon resonant absorption and four-wave mixing was performed in atomic sodium vapor.² An intense laser field of frequency ω_1 is tuned near the 3s-3d two-photon-allowed transition, as shown in Fig. 1. Four-wave mixing³ can then occur, leading to the generation of two new fields, one at frequency ω_2 near the 3d-3p transition and one at frequency $\omega_3 = 2\omega_1 - \omega_2$ which is close to the 3p-3s transition. When the laser is tuned precisely to the two-photon transition, population can be transferred to the 3d level, inverting it with respect to the 3p level, leading to amplified spontaneous emission⁴ at the 3d-3p transition frequency. A measure of the suppression of two-photon

absorption is the decrease of the amount of amplified spontaneous emission, assuming that the fields do not populate the 3p intermediate level.

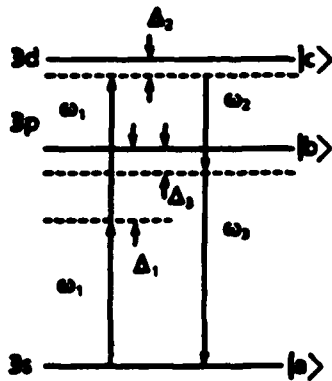


Fig. 1 Energy-level diagram of atomic sodium showing the three levels involved in the four-wave mixing process. A two-photon resonant laser of frequency ω_1 excites the 3d level and four-wave mixing generates two new fields of frequency ω_2 and ω_3 .

We have modeled the suppression of two-photon excitation of the 3d level using the three-level atomic system shown in Fig. 1 in the presence of an applied field with frequencies ω_1 , ω_2 , and ω_3 .⁵ We solve the steady-state density matrix equations of motion appropriate for our model to fourth order in perturbation theory. From this calculation, we obtain the population in the upper level and the nonlinear polarization of the medium which is used to derive coupled amplitude equations for the interacting fields. We find that if the phase mismatch is not too large, the fields evolve spatially to reach steady-state values and that in the presence of this steady-state field the upper level population is at least partially suppressed. For the case of perfect phase matching, complete suppression of the upper level population is predicted. Figure 2 shows the intensity of the three fields, S_i ($i=1,2,3$) and the population in the upper level, $\rho_{cc}^{(4)}$ as a function of the propagation distance for the case of exact two-photon resonant excitation and perfect phase matching, using numbers appropriate to our experimental conditions. It is seen that the fields at frequencies ω_1 and ω_2 grow rapidly from noise and reach a steady-state value. As these fields grow, it is also seen that the population in the excited state begins to decrease and vanishes completely when the fields reach their final value. The vanishing of the upper level population can be traced to a destructive interference between two pathways connecting the ground and excited states.

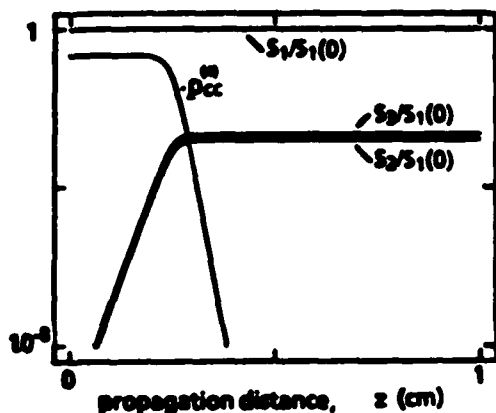


Fig. 2 Spatial evolution of the normalized field intensities S_1 , S_2 and S_3 and the upper-level population $\rho_{cc}^{(4)}$, for the case of perfect phase matching and exact tuning to the two-photon resonance.

In summary, we have shown that under two-photon resonant excitation of an atomic system, the four-wave mixing process generates new fields with the proper phase and amplitude such that the excitation of the upper level is prevented. The nature of the suppression is the destructive interference of the two pathways connecting the ground and excited states. These results can be generalized for any system in which nonlinear wave mixing occurs, such as two-photon resonant third harmonic generation,⁶ three-photon resonant third-harmonic generation⁷ and stokes-anti-stokes generation.⁸

1. L. Allen, R.W. Boyd, J. Krasinski, M.S. Malcuit and C.R. Stroud, Jr., Phys. Rev. Lett., 54, 309 (1985).
2. M.S. Malcuit, D.J. Gauthier, and R.W. Boyd, Phys. Rev. Lett., 55, 1068 (1985).
3. D. Grischkowsky, M.M.T. Loy, and P.F. Liao, Phys. Rev. A, 12, 2514 (1975).
4. L. Allen and G.I. Peters, Phys. Rev. A, 8, 2031 (1973).
5. R.W. Boyd, M.S. Malcuit, D.J. Gauthier and K. Rzazewski, Phys. Rev. A, 35, 1648 (1987).
6. H. Kildal and S.R.J. Brueck, IEEE J. Quantum Electron., QE-16, 566 (1980).
7. W.R. Garrett, S.D. Henderson and M.G. Payne, Phys. Rev. A, 34, 3463 (1987).
8. N. Bloembergen and Y.R. Shen, Phys. Rev., 133, A37 (1964).

MULTIPHOTON IONIZATION INDUCED BY 3rd HARMONIC
INTERNALLY GENERATED IN Kr

P. Lambropoulos and X. Tang

Physics Department, University of Southern California
Los Angeles, California 90089-0484

Recent experimental results by Proctor et al.⁽¹⁾ indicate that 3rd harmonic generation induced in Kr by a pump laser may be more efficient in causing multiphoton ionization than the pump itself, even though the intensity of the 3rd harmonic is several orders of magnitude weaker than the pump. The pump is tunable over the wavelength range 338 to 350 nm. which places the energy $3\hbar\omega$ of three photons above the state $5s'$ where the medium is negatively dispersive. As a consequence, significant 3rd harmonic generation may occur at the appropriate range of pressure.

Four pump photons should cause 4-photon ionization in a region where 4-photon resonant transitions to the Rydberg autoionizing series $nf'[1/2]$ are accessible. The ionization signal should therefore exhibit peaks at such resonances. Experimentally, the peaks were pronounced only at higher pressures which suggests that the generated 3rd harmonic may be responsible for their prominence. This would come about through 2-photon ionization induced by one 3rd harmonic photon plus one pump photon. This conjecture is supported by experimental evidence cited by Proctor et al.⁽¹⁾.

To corroborate the conjecture theoretically, one must demonstrate that the 2-photon process is stronger than the 4-photon even though the source of one of the photons participating in the 2-photon process is much weaker. We present calculations of the relevant quantities based on multichannel quantum defect (MCQD) theory. We have calculated the 4-photon transition to the nf' states using MCQD wavefunctions in truncated summations. Similarly, we calculate the 2-photon transition to the same final state involving one 3rd harmonic photon. Given a

certain pump intensity, we find that the 2-photon process will dominate the 4-photon for an intensity of 3rd harmonic a few orders of magnitude lower as shown in Table 1.

Pump Laser Intensity (W/cm ²)	10 ⁸	5x10 ⁸	10 ⁹	5x10 ⁹
THG Intensity (W/cm ²)	1.0	2x10 ²	4x10 ²	8x10 ⁴

Table 1. 3rd Harmonic intensity for which 2-photon ionization is comparable to 4-photon ionization as a function of pump intensity.

This is compatible with the experimental evidence and provides a measure of the generated harmonic. Thus the role of the pressure is to simply maximize the production of 3rd harmonic through phase matching.

Using our wavefunctions, we can further calculate the non-linear susceptibility from which we obtain an absolute magnitude for the expected amount of 3rd harmonic. We report results of such calculations which can be compared with measurements when they become available.

References

1. M. J. Proctor, J.A.D. Stockdale, T. Efthimiopoulos and C. Fotakis, Chem. Phys. Lett., to be published.

This project was supported by the National Science Foundation, under Grant No. PHY-8306263.

Investigations of Electron Correlations Using
Residual Ion Fluorescence Detection

L.D. Van Woerkom, J.G. Story, and W.E. Cooke
Physics Department
University of Southern California
Los Angeles, CA 90089-0484

We have developed a technique for studying doubly excited states which is particularly sensitive to high energy excitations. This technique, Residual Ion Fluorescence (RIF) detection, does not directly detect the doubly excited atoms, but rather observes them indirectly, through the fluorescence emitted by the ion after the doubly excited state has autoionized. This requires that the excited state have an energy in excess of the atom's ionization limit by at least as much as that necessary to excite the ion to a fluorescing state. Such highly excited states, i.e. those converging on the double ionization limit, are precisely the states where angular correlation between the electrons is expected to be most pronounced.

There exists relatively little information about these states because it has been difficult to excite them or to detect them, selectively. Since these states lie in an energy region where there are as many continua available as there are bound states in a singly excited Rydberg atom, it is imperative that a high degree of specificity be imposed by the excitation and detection processes. The multi-step laser excitation scheme, Isolated Core Excitation (ICE),¹ has made it possible to populate doubly excited states efficiently, and to characterize the state's parent configuration. With RIF detection, it is also possible to directly determine the decay route of a doubly excited state.

Four other detection techniques have previously been used with the

ICE method to excite doubly excited states: (1) total ionization collection,¹ (2) energy and angular analysis of the emitted electrons,² (3) photo-ionization of excited ions,³ and (4) microwave field ionization of the excited ions.⁴ The first two methods become increasingly difficult as the double ionization limit is approached. The high energy requires a multiphoton transition, and single photon photoionization produces a background that makes collection of the total ionization signal impossible. Furthermore, the high, doubly excited states usually autoionize with only a small exchange of energy between the two electrons,⁵ so that the emitted electrons are peaked around zero energy, and difficult to analyze. The third detection technique has been useful for studying states as high as $11sns$ in barium, but it is only crudely selective in its ion state detection. The fourth method has been used to observe the $27d45d$ state of barium, but it is not sensitive to moderate ($n < 20$) ion excitation energies.⁴

Our present system uses a high density atomic beam of barium which passes through an interaction region which is imaged onto the slits of a monochromator. The monochromator allows us the flexibility of selecting any ion fluorescence line to detect, with a resolution of 4nm . Typically, we have monitored the $\text{Ba}^+ 6P_{3/2} \rightarrow 6s$ transition at 455nm . In the interaction region, the atomic beam is crossed by up to four pulsed, tuneable dye lasers. This system is sufficiently efficient that we can observe fluorescent decay of barium Rydberg states such as the $6s40d, ^1D_2$ state. The system also discriminates against scattered laser noise sufficiently well that we observe a noise signal of less than 100 photons from a 1 mJ laser pulse, with the monochromator set at the laser's wavelength.

ACKNOWLEDGEMENTS

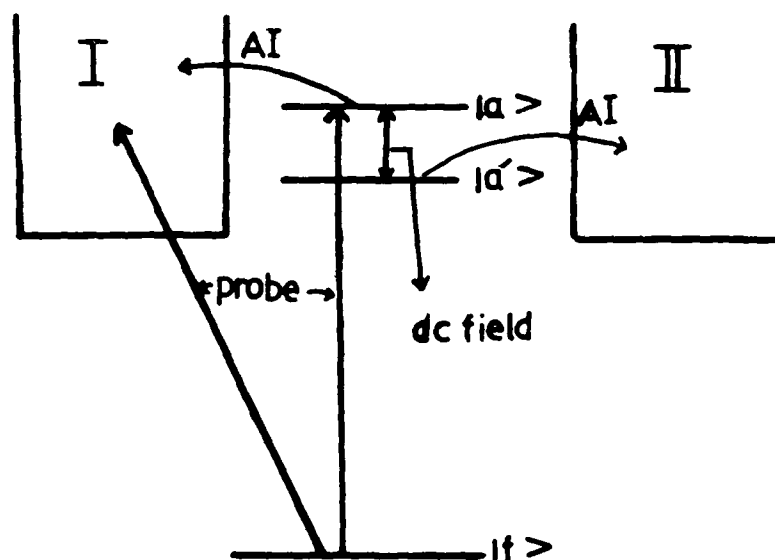
This work was supported by the National Science Foundation, under grant number PHY85-00885. We would like to thank R.R. Freeman for several useful discussions.

REFERENCES

- ¹ W.E. Cooke, T.F. Gallagher, S.A. Edelstein, and R.M. Hill, Phys. Rev. Lett. 40, 178 (1978); S.A. Bhatti and W.E. Cooke, Phys. Rev. A 28, 756 (1983).
- ² R. Kachru, N.H. Tran, P. Pillet, and T.F. Gallagher, Phys. Rev. A 31, 218 (1985).
- ³ L.A. Bloomfield, R.R. Freeman, W.E. Cooke, and J. Bokor, Phys. Rev. Lett., 53, 2234 (1984).
- ⁴ J. Boulmer, P. Camus, and P. Pillet, JOSA B (to be published, May, 1987).
- ⁵ J. Bokor, R.R. Freeman, and W.E. Cooke, Phys. Rev. Lett., 48, 1242 (1982).

INFLUENCE OF DIFFERENT EXIT CHANNELS ON THE INTERFERENCE EFFECTS IN THE AUTOIONIZATION OF TWO STRONGLY COUPLED STATES, S. Ravi and G.S. Agarwal, School of Physics, University of Hyderabad, Hyderabad - 500134, INDIA

We develop a theory of the interference effects¹ in the autoionization of two strongly coupled states, each of which can decay into its own continuum. The system studied is shown schematically in Fig. 1. The two autoionizing states may be either internally coupled or coupled through a dc field. We find that the interference minimum in the absorption spectrum is quite sensitive to the relative magnitudes of the autoionization rates of the uncoupled states. We prove a substitution rule that enables one to get the results for the problem with two exit channels from the results obtained² with a single exit channel. We present the



numerical results for the absorption spectra and the electron yield in each channel. Our theory can be generalized to include several other effects for example radiative decay of the various states can be included. This inclusion enables us to study the dc field induced interference effects in recombination processes. Furthermore a generalization of the present theory enables us to get explicit results for the problem of laser induced autoionization with two exit channels.

1. E.B. Saloman, J.W. Cooper, and D.E. Kelleher, Phys. Rev. Lett. 55, 193 (1985); J.Y. Liu, P. McNicholl, D.A. Harmin, J. Ivri, T. Bergeman and H. J. Metcalf, Phys. Rev. Lett. 55, 189 (1985); J. Neukammer, H. Rinneberg, G. Johnson, W.E. Cook, H. Hieronymus, A. Konig, and H. Springer-Bolk, Phys. Rev. Lett. 55, 1979 (1985); S. Feneuille, S. Liberman, E. Luc-Koenig, J. Pinard, and A. Taleb, J. Phys. B 15, 1205 (1982); J. M. LeComte and E. Luc-Koenig, *ibid.* 18, L357 (1985).
2. G.S. Agarwal, J. Cooper, S.L. Haan and P.L. Knight, Phys. Rev. Lett. 56, 2586 (1986).
3. S. Ravi and G.S. Agarwal, Phys. Rev. A in Press.

INTERFERENCE BETWEEN THE TWO-LEVEL DRESSED ATOM AND THREE-LEVEL FREE INDUCTION DECAY IN CESIUM

H. W. H. Lee and J. E. Wessel
Chemistry and Physics Laboratory
The Aerospace Corporation
El Segundo, California 90254

Whereas coherent excitation of two-level atoms is well understood, currently there is considerable interest in excitation dynamics of three-level systems. Lu, Berman, Yodh, Bai, and Mossberg [1] recently elucidated the important dynamical consequences of dressed atom state preparation on three-level transient spectra. A transmitted weak probe beam (W2) that couples the intermediate and upper levels was shown to undergo complex oscillatory time evolution that is highly dependent on the nature of the coherent superposition of dressed atom states populated in the lower transition (W1).

We will present new results from experimental and theoretical investigation of two-photon free induction decay (FID) in resonantly excited three-level cesium atoms using the dc Stark shifting technique [2]. In contrast to earlier studies [3], we observed the FID of both the lower and upper transitions and found appreciable differences between the two. A phase shift has been observed that arises from an entirely different origin than that observed by Liao et al. [3]. We demonstrate, by rigorous density matrix calculations, that dispersive linear FID accounts for the new phase shift. This represents the first observation of linear FID in a three-level system. Furthermore, we demonstrate that dressed atom effects result in strong amplitude modulation of the FID. A representative measurement is shown in Figure 1a. The new results and interpretations differ markedly from the previously published works. In addition, we present the first clear evidence for simultaneous FID and nutation in the lower transition, induced by a Stark shift of the upper transition.

The FID envelopes are highly nonexponential, with fast and slow decay contributions. The fast and slow decay correspond, respectively, to the linear and nonlinear FID described by Brewer et al. [4] for a two-level inhomogeneously broadened system. The linear FID correlates to the effective inhomogeneous width of the transition, and thus decays rapidly. This contribution is dispersive in nature and accounts for the 180 degree phase shift. This phase shift arises from an entirely different origin than postulated by Marshman et al. [5]. In contrast, the nonlinear FID is absorptive and decays with a slower exponential envelope, with a rate determined by the power broadened width.

The new data were analytically modeled by density matrix calculations. Observed behavior was reproduced well by the model. A simplified dressed atom treatment was used to numerically model the data and derive physical insight. From this we deduce that the complex FID amplitude modulation arises from interference between two separate contributions associated with the two dressed atom states involved in the lower transition. Results from the calculation shown in Figure 1b reproduce the observed FID interference effect where the oscillatory signal vanishes and then reappears, at a time inversely related to W_1 intensity. Dramatic FID curves calculated for larger Stark shifts will be presented.

References

1. N. Lu, P. R. Berman, A. G. Yodh, Y. S. Bai, and T. W. Mossberg, Phys. A33, 3956 (1986); P. R. Berman and R. Salomaa, Phys. Rev. A, 25, 2667 (1982); T. W. Mossberg, A. G. Yodh, and Y. S. Bai, Phys. Rev. (1987).
2. R. G. Brewer and R. L. Shoemaker, Phys. Rev. Lett. 27, 631 (1971); R. G. Brewer and R. L. Shoemaker, Phys. Rev. A6, 2001 (1972); R. G. Brewer in "Frontiers in Laser Spectroscopy", edited by R. Balian, S. Haroche, and S. Liberman, North-Holland, Amsterdam, 1977, page 341.
3. P. F. Liao, J. E. Bjorkholm, and J. P. Gordon, Phys. Rev. Lett. 39, 15 (1977); M. M. T. Loy, Phys. Rev. Lett. 36, 1454 (1976); M. M. T. Loy, ibid, 39, 187 (1977); R. G. Brewer and E. L. Hahn, Phys. Rev. A8, 464 (1973).
4. R. G. DeVoe and R. G. Brewer, Phys. Rev. A20, 2449 (1979); K. L. Foster Stenholm, and R. G. Brewer, Phys. Rev. A10, 2318 (1974).
5. M. F. Marshman, P. M. Farrell, W. R. MacGillivray, and M. C. Standage, Opt. Soc. Am. B3, 607 (1986).

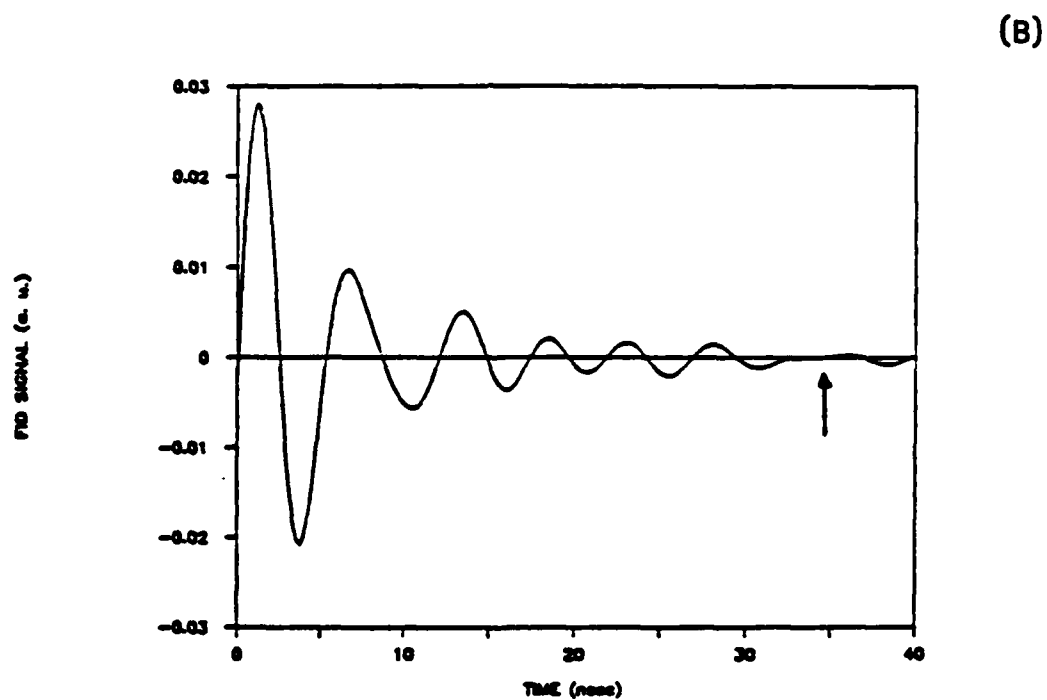
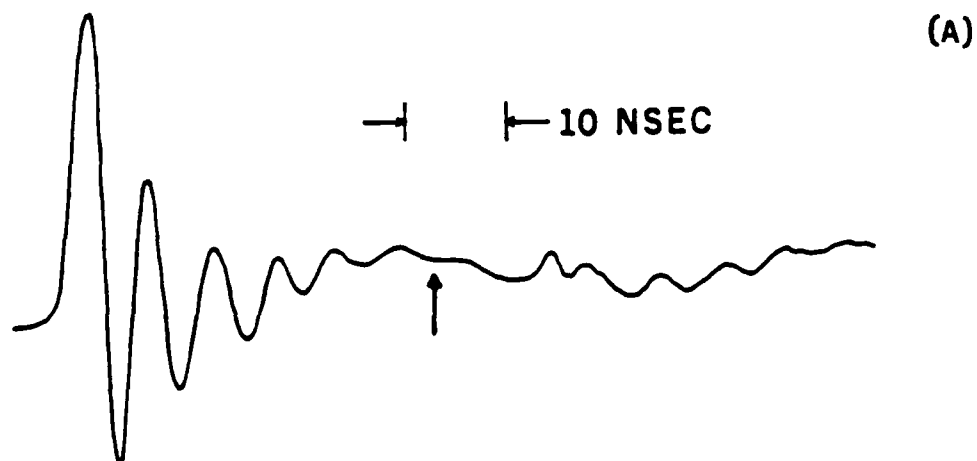


Figure 1. (a) Observed and (b) calculated W2 FID for 140 MHz Stark shifts in the 7d state. The arrows mark the position of destructive interference between the two dressed atom FID channels.

Invited Paper

Vibrational Relaxation of Highly Excited Molecules

Robert J. Gordon, Kenneth M. Beck, and Mitsuo Koshi*

Department of Chemistry, University of Illinois at Chicago, Chicago, IL 60680

The competition between reaction and relaxation of molecules in high vibrational levels plays a central role in unimolecular kinetics. Despite the fundamental importance of such processes, direct measurements of the relaxation rates of highly excited molecules have been reported only in the last few years. Measurement techniques which have been used include IR fluorescence¹ and UV absorption,² which depend critically on spectroscopic properties of the relaxing molecule.

In this study we have used the technique of time-resolved optoacoustics³ to measure the relaxation rates of various polyatomic molecules diluted in an inert gas. With this technique the gas mixture is excited with a pulsed laser in a large acoustic chamber. The resulting acoustic wave is monitored by a fast piezoelectric detector. In this way a single wave is recorded in the absence of any interference effects. From the shape of this wave, and, in particular, from the ratio of the rarefaction and condensation peaks, the relaxation time was determined directly.

Using $\text{SF}_6 + \text{Ar}$ as a prototype system, the initial mean energy of SF_6 was selected by IR multiphoton excitation. Preliminary results indicate that the relaxation time is roughly independent of the initial level of excitation, resulting from an exponential decay of the mean energy. Other molecules which have been studied include ethyl acetate and azulene.

In a second study the vibration-to-vibration transfer rate to an acceptor molecule was measured as a function of mean donor energy. Using SF_6 plus N_2O in argon as a prototype system, we selected the SF_6 donor energy with a pulsed CO_2 laser while monitoring IR fluorescence from the N_2O acceptor molecule.⁴ Using a cold gas filter,⁵ we determined the vibrational temperature

*Present address: Department of Reaction Chemistry, University of Tokyo, Tokyo, Japan

of the ν_2 bending mode of N_2O as a function of time. The vibrational temperature of the ν_3 anti-symmetric stretching mode was also estimated by equating it to the SF_6 vibrational temperature at the fluorescence peak.

The principal findings of this study are (1) that VV transfer to N_2O occurs primarily from high vibrational levels of the donor molecule, while relaxation of N_2O results from back transfer to low levels of SF_6 ; (2) excitation of the ν_2 mode of N_2O is an order of magnitude faster than excitation of the ν_3 mode; and (3) relaxation of ν_2 is an order of magnitude slower than ν_3 relaxation. These results are reconciled by the fact that ν_2 excitation is from the quasi-continuum of SF_6 , while ν_2 de-excitation results from VV transfer to discrete states of SF_6 . A bottleneck in the latter process results in the apparent metastability of the bending mode of N_2O .

1. W. Forst, J. R. Barker, J. Chem. Phys. **83**, 124 (1985)
2. H. Hippler, J. Troe, and H. J. Wendelken, Chem. Phys. Lett. **84**, 257 (1981)
3. K. M. Beck, A. Ringwelski, R. J. Gordon, Chem. Phys. Lett. **121**, 529 (1985)
4. Y. P. Vlahoyannis, M. Koshi, and R. J. Gordon, Chem. Phys. Lett. **118**, 179 (1985)
5. M. Koshi, Y. P. Vlahoyannis, and R. J. Gordon, JCP **86**, 1311 (1987)

Non-thermal intramolecular vibrational energy distribution in isolated infrared multiphoton excited CF_2Cl_2 molecules

Eric Mazur, Kuei-Hsien Chen and Jyhpyng Wang

Department of Physics and Division of Applied Sciences, Harvard University, Cambridge, MA 02138

Anti-Stokes signals from various modes of isolated, infrared multiple photon excited CF_2Cl_2 molecules are measured to determine the intramolecular distribution of vibrational energy. All modes exhibit a collisionless changes in intensity after infrared multiphoton excitation, which shows that the infrared excitation modifies the population of these modes. The distribution of energy among the Raman active modes, which is obtained by comparing the intensities of the anti-Stokes modes, shows a distinct nonequilibrium intramolecular distribution of vibrational excitation energy.

The rather surprising discovery, that isolated polyatomic molecules in the ground electronic state can absorb a large number of photons from a resonant high-power infrared laser,¹ has led to extensive experimental and theoretical studies of this phenomenon during the last decade.² The list of molecules that exhibit this behavior grows continuously,³ and infrared multiphoton excitation evidently is a general property of all but the smallest polyatomic molecules. Clearly, stepwise absorption of infrared laser photons up a single anharmonic vibrational manifold is not possible, and the excitation energy 'dissipates' into an intramolecular 'heat-bath' formed by other nonresonant modes of the molecule. This immediately raises the question how the absorbed energy is distributed among the various modes during this process. The large, and often not even known, number of states renders this problem inherently complicated from a theoretical point of view. Several authors, however, have proposed a statistical description of the ensemble of modes,^{4,5} suggesting an intramolecular equilibrium distribution of vibrational energy among the various modes of an isolated infrared multiphoton excited molecule. The objective of our current research is to directly *measure* the intramolecular distribution of vibrational energy in these isolated infrared multiphoton excited molecules. The general concept of the experiments is as follows. First, an intense infrared laser pulse, resonant with a particular infrared active mode excites an isolated molecule. After the excitation, a pulse from a second laser probes the Raman-active modes. At room temperature the population of the excited states of Raman active modes is only a few percent, so that without infrared excitation only a Stokes signal is observed. If some high lying states of the Raman active modes participate in the distribution of (or directly receive) the excitation energy, the Raman signals may change. Anti-Stokes scattering is a particularly sensitive probe for the population of excited levels in the Raman active mode, because of the absence of signal without excitation.

The experimental setup is discussed in detail in Refs. 6 and 7. Basically, molecules excited by a pulse of either 0.5 or 15 ns duration from a high power tunable CO_2 -laser are probed by a frequency-doubled ruby laser pulse of 20 ns duration. The two laser beams cross in a low pressure cell and scattered light from the interaction region is detected in a direction perpendicular to the two beams. To isolate intramolecular from (collisional) intermolecular effects the signals are measured at pressures low enough to ensure that no significant collisional relaxation of vibrational energy occurs on the time scale of the experiment.

The CF_2Cl_2 molecule has four accessible Raman active modes, three of which, at a shift of 664, 919, and 1082 cm^{-1} respectively, were measured after infrared multiphoton excitation. The C—Cl stretch mode at 919 cm^{-1} is both infrared and Raman active allowing *direct* observation of the energy in the pump mode.

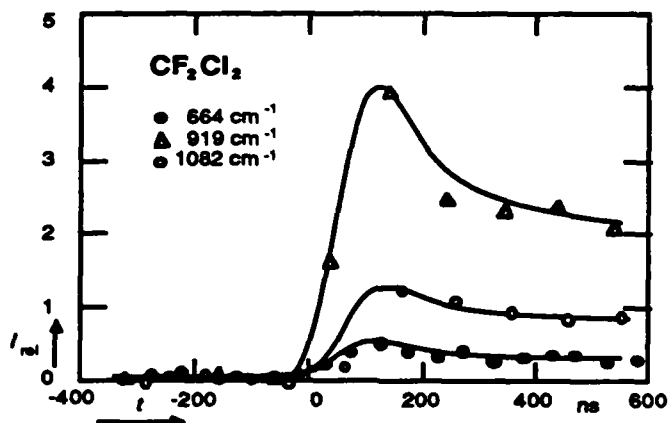


Fig. 1. Intensity of normalized anti-Stokes signals for three modes of CF_2Cl_2 as a function of the time delay between pump and probe pulses at a pressure of 400 Pa. The data points for the mode at 664 cm^{-1} are multiplied by 5. These results were obtained for 15 ns infrared excitation at the $10.6\text{ }\mu\text{m}$ P(32) line, with an average fluence of $1 \times 10^4\text{ J/m}^2$.

In Fig. 1 the anti-Stokes signals of three modes, normalized with the corresponding room temperature Stokes signal, are plotted as a function of the delay time between the two laser pulses. The signals rise within the time resolution of the experiment. The pump mode, at 933 cm^{-1} , clearly contains the largest amount of energy (anti-Stokes—thermal-Stokes intensity ratio). Surprisingly enough, the mode at 664 cm^{-1} remains relatively 'cold'. Changes in energy of the modes with a larger energy step than the energy of the infrared photons (1082 and 1147 vs. 933 cm^{-1}) also occur.

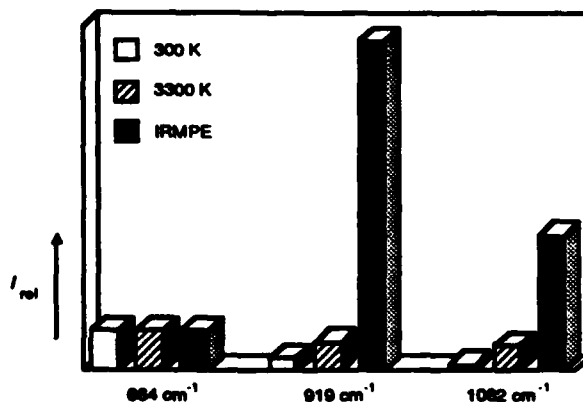


Fig. 2. Comparison of the anti-Stokes to Stokes intensity ratios for 3 modes of CF_2Cl_2 . The grey bars are calculated from the equilibrium intensities at 300 K and 3300 K. The black bars show ratios obtained after infrared multiple photon excitation. For clarity the intensities for 300 K and 3300 K have been multiplied by 6.2 and 0.1, respectively.

The observed collisionless changes in Raman signals provide unambiguous and direct evidence that some of the nonresonant modes do indeed participate in the excitation process. Since the intensity of the signals is proportional to the average energy in the mode, one can obtain the distribution of energy by comparing the ratio of the anti-Stokes intensity to the thermal room temperature value of the Stokes signal, see Fig. 2. The graph clearly shows that the intramolecular distribution of energy of CF_2Cl_2 is highly nonthermal.

- ¹ N.R. Isenor, V. Merchant, R.S. Hallsworth and M.C. Richardson, *Can. J. Phys.* 51, 1281 (1973).
- ² See e.g. the following publications and references therein: V.N. Bagratashvili, V.S. Letokhov, A.A. Makarov, E.A. Ryabov, *Multiple Photon Infrared Laser Photophysics and Photochemistry* (Harwood Academic Publishers, New York, 1985); N. Bloembergen and E. Yablonovitch, *Physics Today* 5, 23 (1978) W. Fuss and K. L. Kompa, *Prog. Quant. Electr.* 7, 117 (1981); D.S. King, *Dynamics of the Excited State*, Ed. K. P. Lawley (Wiley, New York, 1982).
- ³ See almost any issue of *J. Chem. Phys.*
- ⁴ N. Bloembergen and E. Yablonovitch, *Physics Today* 5, 23 (1978).
- ⁵ H.W. Galbraith and J.R. Ackerhalt, in *Laser induced Chemical Processes*, Ed. J.I. Steinfeld (Plenum, New York, 1981).
- ⁶ E. Mazur, I. Burak, and N. Bloembergen, *Chem. Phys. Lett.* 105, 258 (1984).
- ⁷ Jyhpyng Wang, Kuei-Hsien Chen and Eric Mazur, *Phys. Rev. A* 34, 3892 (1986).
- ⁸ Eric Mazur, *Rev. Sci. Instrum.* 57, 2507 (1986).

Invited Paper

CHARACTERIZATION AND EXPLOITATION OF VIBRATIONALLY EXCITED
POPULATIONS PRODUCED BY IRMPA

John R. Barker, T. C. Brown, J.-M. Zellweger, and M. Yerram
Department of Atmospheric and Oceanic Science
Space Physics Research Laboratory, The University of Michigan
Ann Arbor, Michigan 48109-2143

For the past fifteen years, infrared multiphoton absorption (IRMPA) and decomposition have been studied with an eye toward isotope separation and the bond-specific control of chemical reactions.¹ Several important classes of isotope separation methods have been developed, but much of the initial fervor concerning the direct control of chemical reactions cooled, once it became apparent that bond-specific chemistry is not readily achieved. It also became apparent, however, that IRMPA provides a method for producing very large populations of vibrationally excited molecules. Indeed, in many cases, nearly 100% of the molecules in the laser beam can be given large and controlled amounts of vibrational energy. This control of vibrational energy potentially opens another avenue toward the regulation of chemical reactions involving large molecules, similar to that found in small molecules.²

Our approach has been to first characterize the population distributions produced by IRMPA, and then to measure the changes in chemical reactivity induced by vibrational excitation. The first part of this approach has been completed³ and the second part of the work is still under way.

All of the experiments were carried out using 1,1,2-trifluoroethane (TFE), which is easily pumped with a high power CO₂ TEA laser [1079.85 cm⁻¹, 9.6 μ m R(22) line]. Three different experimental measures were used in conjunction with Quack's statistical-dynamical theory⁴ to characterize the population distribution. The absorbed laser energy is a measure of the mean energy of the population distribution (first moment). Collision-free decomposition yields were measured using the Very Low Pressure Photolysis method, in which cell pressures were ≤ 20 mtorr and the fractional decomposition was measured with a modulated molecular beam mass

spectrometer. These results furnished information about the high energy tail of the distribution function.

Time- and wavelength-resolved infrared emission spectra were obtained with a 77K InSb infrared detector and a circular variable filter cooled to 77K. The emission features show that the HF reaction product is produced in vibrational states up to about $v=3$. Emission attributed to FCCH was observed near 3320 cm^{-1} , evidence that the difluoroethylene reaction products undergo secondary photolysis at high intensities. Since the difluoroethylene products at room temperature do not absorb at the laser wavelength, they must be formed with vibrational excitation. Emission from the CH stretch modes of TFE was readily identified near 2980 cm^{-1} and the intensity was determined as a function of laser fluence.

The experimental results from the three techniques were accurately simulated using a Master Equation model that incorporated Quack's statistical-dynamical theory of infrared multiphoton absorption (Cases B and C). Also included in the model were three unimolecular reaction channels (RRKM theory), collisional energy transfer, and the theory of the infrared emission intensity dependence on internal energy. The model included the known TFE molecular properties and only four adjustable parameters, which had to be highly constrained in order to accurately simulate the data.

From the simulations, we conclude that the optical coupling matrix elements at the laser wavelength are dramatically reduced in magnitude for energies near the reaction thresholds. This is due to the vibrational anharmonicity associated with the reaction channels, even in molecules that have not reacted, resulting in vibrational frequency shifts of the absorption lines out of resonance with the laser line. We expect this effect to be quite general and to be observable in other highly vibrationally excited molecules.

The master equation model gave excellent simultaneous agreement with all three sets of experimental data, when parameterized with only four adjustable parameters. The model is not unique and it is under-determined, but the narrow latitude allowed in the parameterization and the excellent agreement with all three experiments give us confidence that the major features of the distributions are accurately described, and they can now be used for quantitative experiments.

For energy transfer measurements, we use infrared emission to monitor the ensemble average energy of vibrationally excited molecules while they are deactivated by collisions.⁵ Experiments were carried out with several mixtures of TFE diluted in argon. By changing the mixture composition, the heat capacity is changed; by changing the laser fluence, the initial level of excitation and the final temperature can be varied. Thus, the effects of both temperature and of initial excitation energy can be explored.

In the experiments, the infrared decay was related to the average amount of energy removed in each deactivating collision through use of the same collisional master equation model used for the photophysical simulations. Thus, the analysis of the experiments exploits the identical model that was used for the characterization of the distribution functions, leading to a fully self-consistent description of the IRMPA process and concurrent collisional deactivation. The results showed that the average amount of energy removed per deactivating collision depends on the initial level of vibrational excitation, but it does not depend significantly on the collider bath gas temperature. These results are in general agreement with other experiments on other molecules.⁶

This quantitative exploitation of population distributions produced by IRMPA demonstrates the general utility of the technique. Currently, we are investigating the effects of vibrational energy on the bimolecular reactions involving TFE. If time permits, recent progress on this effort will be described.

This work is supported by the Army Research Office.

References

1. For recent reviews, see Multiple-Photon Excitation and Dissociation of Polyatomic Molecules, edited by C. D. Cantrell, (Springer, Berlin, 1980).
2. M. Kneba and J. Wolfram, *Ann. Rev. Phys. Chem.* **31**, 47 (1980).
3. J.-M. Zellweger, T. C. Brown, and J. R. Barker, *J. Chem. Phys.* **83**, 6251, 6261 (1985).
4. M. Quack, in Dynamics of the Excited State, edited by K. P. Lawley (Wiley, New York, 1982), 395.
5. J.-M. Zellweger, T. C. Brown, and J. R. Barker, *J. Phys. Chem.* **90**, 461 (1986).
6. J. R. Barker, *J. Phys. Chem.* **88**, 11 (1984).

Multiphoton Absorption and Luminescence of Chromyl Chloride

M. Ivanco, D.K. Evans and Robert D. McAlpine

Atomic Energy of Canada Research Company

Chalk River Nuclear Laboratories

Chalk River, Ontario, Canada

K0J 1P0

ABSTRACT

In this study laser pulse duration (pulse intensity) has been shown to alter the distribution of vibrational states generated by infra-red (IR) multiphoton absorption (MPA). Previous experiments have shown that visible luminescence following IRMPA of chromyl chloride (CrO_2Cl_2) is caused by inverse electronic relaxation (IER) between highly excited vibrational levels of the ground state and an excited electronic state^{1,2} which is radiatively coupled to lower levels of the ground state. We have studied the dependence of MPA and IR induced luminescence of chromyl chloride on laser pulse duration, using single longitudinal mode CO_2 laser pulses of 10 and 60 ns durations. The MPA measurements give information about the mean of the energy distribution and the luminescence measurements about the high energy tail of the distribution above the IER threshold.

Chromyl chloride was studied in the vapour phase under static cell conditions at a pressure of 6.7 Pa (50 mtorr) to ensure collisionless conditions for the duration of both laser pulses. The 10R(32) line of the CO_2 laser (983.25 cm^{-1}) was used and MPA was measured using photoacoustic techniques. The MPA was approximately 2.5 times as great with the short (10 ns) pulse as with the long (60 ns) pulse over the entire laser fluence range covered.

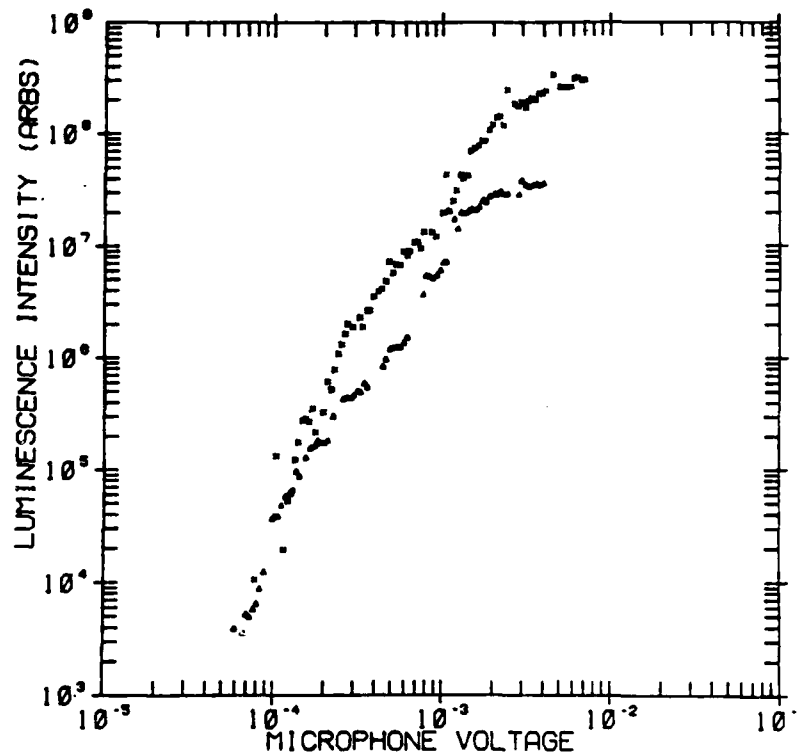


[Figure 1. The luminescence intensity, in arbitrary units, is plotted versus microphone voltage (from the photoacoustic/MPA experiments) for excitation with 10 ns (X) and 60 ns (Δ) CO_2 laser pulses, using the 10R(32) line. This figure is constructed from plots of microphone voltage vs. ϕ (laser energy fluence) and luminescence intensity vs. ϕ .]

Luminescence following excitation by the 10R(32) line was also studied for both laser pulse durations at a pressure of 6.7 Pa. The peak luminescence intensity was measured. A much larger dependence of luminescence intensity on laser pulse duration was noted in these experiments than in the MPA experiments. The data from these two studies can be combined and are shown in Fig. 1. Here luminescence intensity, due to IER, is plotted versus the microphone voltage, or signal amplitude, from the MPA experiments. The microphone voltage is directly proportional to the average number of photons absorbed per

molecule, $\langle n \rangle$. Hence Fig. 1 shows the luminescence intensity observed when the CrO_2Cl_2 molecules are excited to the same average level of excitation with two different pulse durations. As Fig. 1 shows, there is more luminescence with the shorter pulse duration for a given microphone voltage; or mean level of excitation. A reasonable explanation for this observation is that, excitation with the shorter laser pulse affects the competition between further pumping up the vibrational ladder of the ground state and IER in the vicinity of the IER threshold. The rate of IER for intermediate level structure is given by³:

$$\gamma^R(E) = \frac{\rho_s(E)}{\rho_g(E)} \Gamma_s^R(E) \quad (1)$$

where $\Gamma_s^R(E)$ is the radiative width of the excited state for one-photon absorption at an energy E , ρ_s/ρ_g is the vibrational density of states ratio for the excited (s)/ground (g) state and γ^R is the radiative width of the transition resulting from IER. Hence, molecules which are excited further up the vibrational ladder, such as should happen more efficiently with the shorter, more intense, laser pulse will have a more favourable density of states ratio for IER. This accounts for the increased luminescence intensity observed for the shorter laser pulse when the molecules are pumped to the same $\langle n \rangle$.

References

1. Z. Karny, A. Gupta, R.N. Zare, S.T. Lin, J. Nieman and A.M. Ronn, Chem. Phys. 37, 15 (1979).
2. J.Y. Tsao, N. Bloembergen and I. Burak, J. Chem. Phys. 75, 1 (1981).
3. A. Nitzan and J. Jortner, J. Chem. Phys. 71, 3524 (1979).

Invited Paper

MULTIPLE PHOTON ABSORPTION AND SELF-FOCUSING IN CDF_3

S. L. Chin

Laboratoire de Recherches en Optique et Laser

Department de Physique

Université Laval

Québec, Canada G1K 7P4

Invited Paper

IR MULTIPHOTON ABSORPTION WITH A HIGH PRESSURE CO₂ LASER:
ROLE OF THE LASER LINEWIDTH

C. Angelie, R. Capitini and P. Girard

CEA - IRDI/DESICP - Département de Physico Chimie,
CEN Saclay, 91191 GIF sur YVETTE CEDEX, France

The IR multiphoton absorption (MPA) of ¹²CF₃I, ¹³CF₃I, CF₃Br and SF₆ by means of a 10 Atm CO₂ laser has been investigated in a cell, using a double ratiometer method (empty cell and filled cell). The spatial, spectral, and temporal characteristics of the laser emission versus the grating position have been carefully measured separately, showing linewidth broadening and splitting and spatial distortions in the laser gain minima.

The main result of this study is that the peaks observed in the different MPA spectra are clearly correlated to the laser gain curve but not to the fine molecular spectroscopy. After elimination of several possible explanations such as spatial or temporal laser effects, or self focusing or defocusing in the cell, the single possible and most probable explanation lies in a laser bandwidth effect. Assuming this explanation, it is possible in turn to extract from the reported spectra the dependence $\sigma(\gamma_L)$ of the MPA cross section versus the laser bandwidth γ_L .

A semi-quantitative interpretation of the $\sigma(\gamma_L)$ curve is attempted but seems only possible if it is assumed that a background of weak resonances, bearing about 1-2% of the total oscillator strength, and with a typical spacing 0.1 - 0.2 cm⁻¹ plays an important role in the low part of the vibrational ladder.

The data reported are compared with similar published results. It is concluded that only high pressure CO₂ lasers with narrow and well controlled bandwidth are able to put in evidence the MPA molecular pathways toward the quasi continuum.

RATES, RECURRENCES AND POPULATION TRAPPING IN QUASI-CONTINUUM AND STRUCTURED CONTINUUM PHOTOEXCITATION

P. Radmore,⁺ P. Knight^{*} and S. Tarzi^{*}

⁺Department of Electronic and Electrical Engineering, University College, London, WC1E 7JE, U.K.

^{*}Blackett Laboratory, Imperial College, London SW7 2BZ, U.K.

The photoexcitation of a quasi-continuum of atomic or molecular levels by a laser pulse with a fast risetime is considered. We first generalise non-perturbative treatments of quasi-continuum excitation. A second general theoretical method is developed in which resonant states are considered non-perturbatively whereas background non-resonant states are included by a perturbative approximation.

As a simple example we show how our method describes the photoexcitation of a quasi-continuum of equally spaced levels, exhibiting Rabi oscillations periodically perturbed by background states.

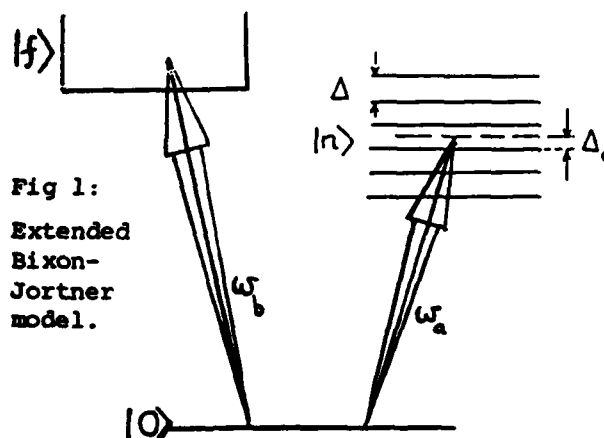


Fig.1: Extended Bixon-Jortner model.

We then examine the case of highly excited atomic states coherently excited from a low-lying initial state. The time-evolution of the coherent superposition of Rydberg levels is shown to be perturbed Rabi oscillation but without the periodic disruption of the

equally-spaced quasi-continuum. Next, we include the effect of further excitation to a second continuum.

The photoexcitation of a structured continuum of states from a single ground state is also considered. We investigate an analytically soluble model in which the dipole matrix elements between the ground state and the continuum vary sinusoidally between zero and a maximum. The time evolution of the ground state population still exhibits the periodic disruption observed in the Bixon-Jortner model, although much reduced. We allow the ground state to be resonant with an arbitrary place in the continuum; population trapping is observed in the case of resonance with a zero in the continuum, as shown in Fig. 2. The final state spectrum exhibits Autler-Townes splitting of the central resonance peak and the approach to a multiple confluence for large excitation strengths. We compare and contrast the results obtained with this model with those of quasi-continuum excitation.

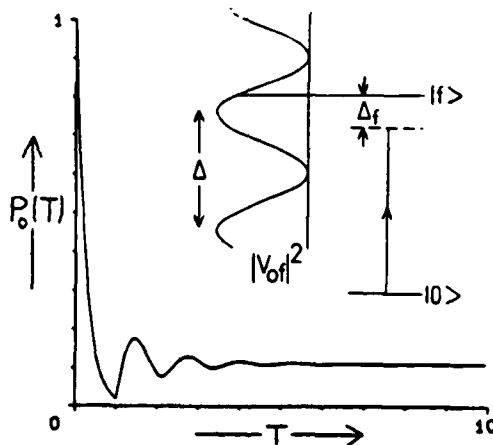


Fig. 2: Structured continuum excitation and ground-state evolution showing population trapping.

References

1. P. M. Radmore, S. Tarzi and P. L. Knight, J. Mod. Opt. (formerly Optica Acta) Vol. 34, (1987).
2. P. M. Radmore and S. Tarzi, J. Mod. Opt., in press (1987).

Invited Paper

FINITE FERMI SYSTEMS METHOD FOR THE MULTIPHOTON PROCESSES IN
MANY-ELECTRON ATOMS

L. P. Rapoport
Voronezh State University
394693 Voronezh, USSR

Invited Paper

Theory of Multiphoton Ionization of Atoms by Strong, Short Pulsed Lasers

Kenneth C. Kulander, Theoretical Atomic and Molecular Physics Group, Lawrence Livermore National Laboratory, Livermore, CA 94550

The theory of short pulse, high intensity laser ionization of multielectron atoms is presently under development. Extensive experimental data on a number of atomic species and for a number of laser wavelengths has spurred interest in finding new theoretical approaches which can transcend the region of validity of perturbation theory. One such approach uses the time dependent Hartree Fock model for the evolution of the atomic wave function in the time varying field. In this model, the wave function is expressed as an antisymmetrized product of electronic orbitals. Each electron moves in response to both the laser field and the mean field of the other electrons in the system. TDHF, unlike its static counterpart does allow some degree of correlation between electrons, but the restriction to a single configuration means the calculated state must be considered to be an average of many configurations for the atom. As the density of states of the atom becomes large, the behavior of the TDHF wave function is expected to be a more accurate approximation to the true state. Also, for very intense fields, such that the interelectronic interactions become small relative to the external field, TDHF is more reliable. Therefore, this is a natural choice for the investigation of high intensity laser effects on atoms.

As a first illustration of the application of this method to multiphoton ionization, results of calculations for helium will be presented. Studies of wavelength and intensity dependence of the excitation and ionization of helium with this model provide insight into the character of the absorption process. The differing preionization dynamics for various photon energies address some of the questions raised in interpretation of recent experiments. Evidence in these results of above threshold ionization, collective excitations and of scattering from pondermotive barriers are found. By projecting the time evolving wave function onto selected bound states, clarification of the excitation dynamics is accomplished. Results from a large number of calculations will be presented.

TWO- AND THREE-PHOTON DOUBLE IONIZATION AND EXCITATION OF XENON

Anne L'Huillier* and Göran Wendin**

* Service de Physique des Atomes et des Surfaces
C.E.N. Saclay, F-91191 Gif-sur-Yvette, France

**Institute of Theoretical Physics, Chalmers University of Technology,
S-412 96 Göteborg, Sweden

We develop a diagrammatic many-body perturbation approach in order to investigate 2- or 3-photon ionization and excitation processes leading to ejection of one or two electrons in xenon (in the weak field limit). The idea is to simulate in a simple way the experimental data obtained in single and double ionization of xenon¹ and in particular to study the "competition" between direct and sequential double ionization processes.^{2,3} The situation discussed in this work is however rather different from the experimental one, since we assume that the photon energy is high enough for only two photons to doubly ionize xenon.

Double ionization of xenon may result from a direct process $\text{Xe} \rightarrow \text{Xe}^{2+}$ or a sequential process, via a singly charged ion in the ground state $\text{Xe} \rightarrow \text{Xe}^+ \rightarrow \text{Xe}^{2+}$ or in an excited state $\text{Xe} \rightarrow \text{Xe}^{+*} \rightarrow \text{Xe}^{2+}$. In order to investigate the efficiency of these processes, we calculate the cross-sections of the elementary transitions involved :

- 1-photon and 2-photon single ionization of Xe
- 1-photon and 2-photon single ionization of Xe^+
- 1-photon single ionization of Xe^+ excited ($5p^4 6s$ and $5p^4 5d$)
- 2-photon double ionization of Xe

2-photon ionization and excitation of Xe (the final state is an excited ion). Our aim is not to derive very accurate and realistic cross-sections, including, for example, the spin-orbit interaction, or for Xe^+ , taking into account open-shell effects, but to obtain reasonably good *average values*. This requires a proper treatment of many-electron polarization effects, which is achieved by means of the random phase approximation with exchange (RPAE). We use *screened dipole interactions* which replace the usual dipole interactions in the one-electron expressions.⁴⁻⁶ We discuss the magnitude of screening effects in the different processes investigated, by comparing the results obtained within the RPAE to the independent-electron (HF) approximation.

In figure 1, we show the distribution of the photoelectrons emitted in a two-photon double ionization process which, from a nearly flat distribution at threshold, becomes more and more peaked as the photon energy increases (one electron taking all the energy, the other one escaping with a zero energy), and finally consists in two (sharp) peaks when sequential two-photon double ionization takes over.

In figure 2, we compare the *branching ratios* between the two-photon ionization processes which, from the same initial state (Xe) lead to different final states (Xe^+ , Xe^{+*} , Xe^{2+}). Ionization and excitation ($\text{Xe} \rightarrow \text{Xe}^{+*} + \epsilon$) seems to be much more important than above-threshold-ionization ($\text{Xe} \rightarrow \text{Xe}^+ + \epsilon$) and direct double ionization ($\text{Xe} \rightarrow \text{Xe}^{2+} + \epsilon_1 + \epsilon_2$).

Finally, we study the efficiency of the different processes leading to ejection of two electrons in Xe : 2-photon direct double ionization and 3-photon sequential double ionization. We develop a simple rate equation model which describes the evolution of the Xe, Xe^+ , Xe^{+*} and Xe^{2+} populations (with a realistic laser intensity temporal distribution). Except for high laser intensities and extremely short pulse durations, double ionization of Xe (using photons whose energy is of the order of 1.3-1.6 Ry) is essentially due to a three-photon sequential double ionization via Xe^+ in its ground state, simply because the Xe population is extremely rapidly depleted due to one-photon ionization ($\text{Xe} \rightarrow \text{Xe}^+$).

This work has been supported by the Swedish Natural Science Research Council.

REFERENCES

1. A. L'Huillier, L.A. Lompré, G. Mainfray, and C. Manus, Phys. Rev. A 27, 2503 (1983); A. L'Huillier, Comments At. Mol. Phys. 18, 289 (1986).
2. M. Crance and M. Aymar, J. Physique 46, 1887 (1985).
3. X.Tang and P.Lambropoulos, Phys.Rev.Lett., 58, 108 (1987)
4. G. Wendin, L. Jönsson, and A. L'Huillier, Phys. Rev. Lett. 56, 1241 (1986).
5. A. L'Huillier, L. Jönsson, and G. Wendin, Phys. Rev. A 33, 3938 (1986).
6. A. L'Huillier and G. Wendin, J. Phys. B 20, L37 (1987) and to be published.

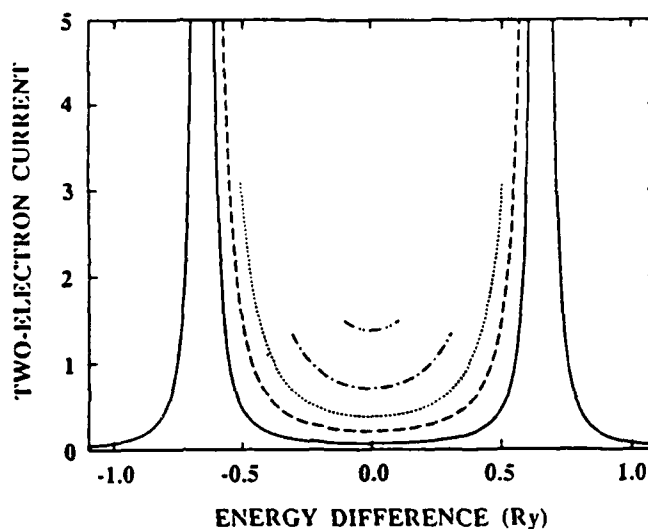


Figure 1: Distributions of the photoelectrons emitted in a two-photon double ionization process as a function of the energy difference (in Ry) for different photon energies : (····) 1.3 Ry ; (---) 1.4 Ry ; (-----) 1.5 Ry (----) 1.6 Ry ; (—) 1.8 Ry.

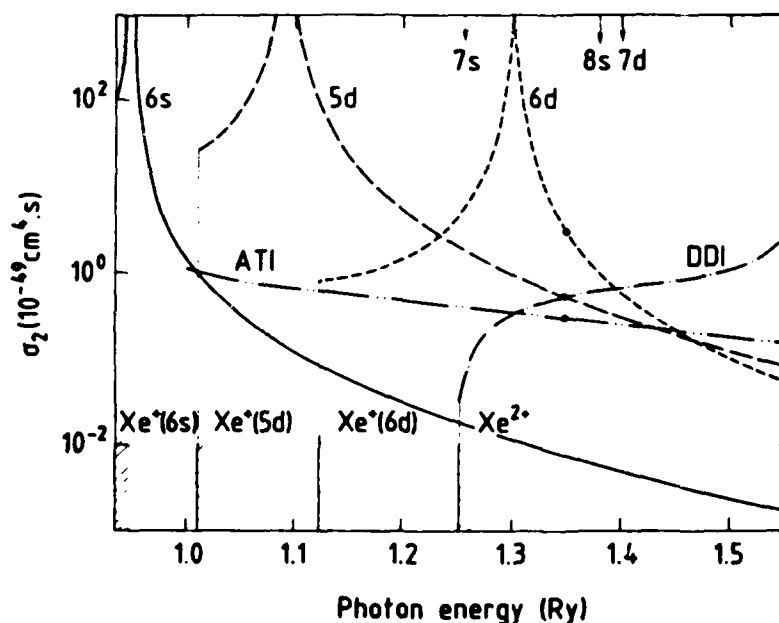


Figure 2: Two-photon one-electron and two-electron Xe ionization cross-sections (cm^4s) as a function of the photon energy (Ry). (---) above-threshold ionization (ATI) ; (---) Direct double ionization (DDI) ; (—), (---), (---) ionization into an excited 6s, 5d, 6d Xe^+ state

**Two-Photon Ionization of Rare Gas Atoms:
A Relativistic Time-Dependent Hartree-Fock Approach.**

Michael G.J. Fink and W.R. Johnson

Department of Physics, University of Notre Dame

Notre Dame, IN 46556

Peter Zoller

Institut für Theoretische Physik, Universität Innsbruck

A-6020 Innsbruck, Austria

Theoretical analysis of multiphoton processes in atoms has so far been based almost exclusively on the single-particle model of the atom; the effects of residual electron-electron interactions have been neglected in most previous studies. An exception is the study by A. L'Huillier, et al. on many-electron effects in multiphoton ionization [1]. Results of recent multiphoton experiments suggest, however, that the electronic structure of the atom does have a substantial effect on the dynamics of multiphoton ionization. Such results have created the need for a more detailed study of electron correlation in multiphoton physics. (For summaries, see. e.g. [2-4].)

The main deficiency of the single-particle picture is that it does not account for core polarization, which is understood to be due to the external field in this context. When core polarization is included, the electrons in nonresonant core orbitals can be virtually photoexcited and generate a time-dependent field that adds to the field seen by the excited or ionized electron. The importance of nonresonant core polarization even in alkali-metal atoms has been demonstrated in a first study of single-photon ionization which was carried out in a theoretical framework essentially identical to the one outlined below [5].

Among the various techniques available for treating electron correlation, an *ab initio* description based on a relativistic time-dependent Hartree-Fock (TDHF) formulation appears attractive for several reasons:

- It is very transparent from a formal point of view, since

perturbed TDHF wavefunctions can be identified with certain terms in many-body perturbation-theory summed up to all orders in the Coulomb interaction. Consequently, we expect that these wavefunctions contain important parts of the electron correlation.

- The relativistic jj-coupling approach accounts naturally for the spin-orbit interaction and so is suitable for describing heavy atoms, which are of particular experimental and theoretical interest.
- The numerical implementation of the TDHF equations requires no approximations other than these imposed by the model itself.

We assume a closed-shell system, such as a rare-gas atom, irradiated by a classical, harmonic, polarized radiation field in the dipole approximation. Our goal is to obtain time-dependent wavefunctions, from which photoionization probabilities and other properties like angular distributions of photoelectrons can be derived.

Given an external perturbation $V(t) = V_0^+ e^{-i\omega t} + V_0^- e^{+i\omega t}$, we set up the atomic wavefunction as a Slater determinant of time-dependent orbitals $u_a(t)$ satisfying the TDHF equation

$$(h_0 - i \partial/\partial t + V_{HF} + V(t)) u_a(t) = 0. \quad (1)$$

Here V_{HF} , the time-dependent Hartree-Fock potential, is defined as

$$V_{HF} u(r) = \sum_b \int d^3r' (u_b(r') 1/|r-r'| u_b(r') u(r) - u_b(r') 1/|r-r'| u(r') u_b(r)) . \quad (2)$$

for any u , and h_0 is the relativistic one-particle Hamiltonian including the nuclear potential. We expand the orbitals in powers and harmonics of the external perturbation

$$u_a = e^{-i\epsilon_a t} (u_a^0 + v_a^+ e^{-i\omega t} + v_a^- e^{+i\omega t} + w_a^+ e^{-2i\omega t} + w_a^- e^{+2i\omega t}) . \quad (3)$$

After sorting terms by order and frequency we obtain the usual

Hartree- Fock equation for the term zeroth order in the radiation field

$$(h_0 - \epsilon_a + V_{HF}^0) u_a^0 = 0 . \quad (4)$$

and RPA-like equations for the first and second order terms

$$(h_0 - (\epsilon_a \pm \omega) + V_{HF}^0) v_a^\pm + (V_{HF}^{1\pm} + V_0^\pm) u_a^0 = 0 \quad (5)$$

$$(h_0 - (\epsilon_a \pm 2\omega) + V_{HF}^0) w_a^\pm + (V_{HF}^{1\pm} + V_0^\pm) v_a^\pm + V_{HF}^{2\pm} w_a^\pm = 0 . \quad (6)$$

where V_{HF}^0 is the frozen-core Hartree-Fock potential of the unperturbed atom and $V_{HF}^{1\pm}$, $V_{HF}^{2\pm}$ are the first and second order positive and negative-frequency parts of the time-dependent Hartree-Fock potential. The angular decomposition of the equations yields a set of coupled nonlocal radial differential equations. This forms the basis for a numerical treatment of the problem and allows a multipole analysis of the angular distribution of photoelectrons, from which ionization amplitudes and angular distributions can be easily calculated. We expect to present preliminary numerical results at the conference.

References

1. Anne L'Huilier, Lars Jönsson, Göran Wendin, Phys. Rev. A **33**, 3938 (1986)
2. Multiphoton Ionization of Atoms, eds. S. L. Chin and P. Lambropoulos (Academic Press, 1984)
3. Multiphoton Processes, Proceedings of the 3rd International Conference Iraklion, Crete, eds. P. Lambropoulos and S. J. Smith (Springer Verlag, 1984)
4. Fundamentals of Laser Interactions, Proceedings of a Seminar held at Obergurgl, Austria, ed. F. Ehlotzky (Springer Verlag, 1985)
5. Michael G.J. Fink and W.R. Johnson, Phys. Rev. A **34**, 3754 (1986)

MULTIPHOTON DETACHMENT IN NEGATIVE IONS OF HALOGENS

Michele Crance

Laboratoire Aimé Cotton, CNRS II

bât 505 91405 Orsay Cedex France

This work is an attempt to calculate multiphoton processes for electronic structures where correlations are known to be important. From this point of view, negative ions are much simpler than complex atoms since they generally have only one bound state and resonances lie well above the detachment threshold. As a consequence, opposite to the situation encountered for multiphoton ionization of neutral atoms, multiphoton detachment occurs towards a structureless continuum and no intermediate resonance is expected. Negative ions of halogens are isoelectronic of noble gases and this work might be a preliminary step in the study of multiphoton ionization of noble gases. Negative ions of halogens have electronic affinities ranging from 3. to 3.6 eV and thus, they can be photodetached by absorption of a small number of photons in visible range. In such conditions, detachment can be achieved with moderate light intensity.^{1,2}

Correlations are important in the building of negative ions ground state, they are also responsible for high lying resonances observed either in one photon detachment or collision experiments. However, correlations should not be very crucial for continuum states just above threshold, in a range of energy of the order of electron affinity. This is precisely the situation corresponding to multiphoton detachment. Starting from these basic considerations, we calculate multiphoton detachment cross sections using a simple description of ions:

- correlations are taken into account in ground state by using Hartree-Fock (HF) wave function,
- correlations are neglected in any other state,
- continuum states are described as a HF core of the atom plus a free electron.

It is well known that HF calculations do not lead to a correct value of electron affinity.³ It has been shown that the representation of

negative ions ground state is greatly improved by multiconfigurational Hartree Fock (MCHF) calculations.⁴ In order to reproduce electron affinity, one has to take into account the admixture, in ground state wave function, of configurations corresponding to core electron excitation such as $p^4 1^2$. The presence of such configurations is crucial in the calculation of electron affinity, however, their weight in the wave function does not exceed a few percent.⁴ Photodetachment for an HF ground state is schematized by

$$np^6 + \hbar\omega \rightarrow np^5 + \epsilon l$$

np^6 and np^5 stand for the ground states of the ion X^- and the atom X respectively. Their energies are $E(X^-)$ and $E(X)$. ϵl is a free electron with energy

$$\epsilon = E(X^-) - (E(X))$$

For extra configurations appearing in MCHF ground state, absorption of n photons is schematized by quantum paths such as

$$p^4 1^2 \rightarrow p^4 1' + \epsilon l$$

followed by

$$p^4 1' \rightarrow p^5$$

that is electronic rearrangement of electrons in final state. It is thus consistent to use HF wave function for negative ion ground state since we neglect correlations in continuum states. When using direct HF wave function instead of MCHF, we omit a multiplicative factor of the order of one, namely, the weight of configuration np^6 in MCHF wave function.

Calculations are performed in the framework of the dressed atom picture for weak intensities. We use the complex dilatation method with finite basis of square integrable wave functions.⁵⁻⁷ The method has been described in Ref. 6. Preliminary results are in agreement with experimental data for one- and two-photon detachment.⁸⁻¹² It is worth noting that, for one-photon detachment, the agreement is the best

for low energy electrons. This is the range of energy which matters the most in calculation of multiphoton processes. Comparison with previous calculations is difficult since simplifying assumptions are quite different.¹³⁻¹⁶ More sophisticated calculations should be carried out to understand discrepancies and agreements.

REFERENCES

1. R. Trainham, G. D. Fletcher, D. J. Larson, Proc. EGAS 1986.
2. C. Blondel, R. J. Champeau, C. Delsart, D. Marinescu, Proc. ICPEAC 1987.
3. H. S. W. Massey, Negative Ions (Cambridge University Press, 1976).
4. C. Froese, The Hartree-Fock Method for Atoms (Wiley, New York, 1977).
5. S. I. Chu, W. P. Reinhardt, Phys. Rev. Lett. 39, 1195 (1977).
6. M. Crance, M. Aymar, J. Phys. B 18, 3529 (1985).
7. M. Crance, M. Aymar, J. Physique (Paris) 46, 1887 (1985).
8. A. Mandl, Phys. Rev. A 3, 251 (1971).
9. D. E. Rothe, Phys. Rev. 177, 93 (1969).
10. R. S. Berry, C. W. Reimann, G. N. Spokes, J. Chem. Phys. 37, 2278 (1962).
11. B. S. Steiner, Phys. Rev. 173, 136 (1968).
12. J. L. Hall, E. J. Robinson, L. M. Branscomb, Phys. Rev. Lett. 14, 1013 (1965).
13. E. J. Robinson, S. Geltman, Phys. Rev. 153, 4 (1967).
14. J. W. Cooper, J. B. Martin, Phys. Rev. 126, 1482 (1962).
15. Yu. V. Moskvina, High Temp. 3, 765 (1965).
16. Yu. V. Moskvina, Opt. Spectr. 17, 270 (1964).

RYDBERG ELECTRONS IN LASER FIELDS :
A FINITE RANGE INTERACTION PROBLEM

A. Giusti* and P. Zoller†

*Laboratoire de Photophysique Moléculaire du CNRS, Bât. 213,
Université Paris-Sud - 91405 Orsay, France

†Institute for Theoretical Physics, University of Innsbruck
A-6020 Innsbruck, Austria

A Theory of Rydberg states in intense laser fields is developed based on the observation that the effect of laser radiation can be described in a scattering formulation as a *finite volume interaction* coupling Coulomb type dissociation channels ¹. Physically speaking, this picture emerges because the long range effect of the laser corresponds to elastic forced oscillations without real absorption or emission of laser photons. The identification of radiative interaction as a short range coupling opens the route for a theoretical approach which treats separately the short and long range processes and connects them in a further step. In particular, laser induced couplings may be incorporated in a multichannel quantum defect (MQDT) treatment, leading us to define a set of dressed channels with intensity dependent quantum defects and mixing coefficients. These quantities may be derived by solving a system of close-coupling equations for the electron wave function (in a frame where the asymptotic electron oscillations have been transformed away ²). This allows us to read off a reaction matrix, which is a smooth function of energy for an energy range small compared with the photon energy.

The outstanding features of the theory are :

(1) It gives a unified description of an entire Rydberg series and adjoining continuum in a laser field ; and more generally of radiative coupling between several Rydberg series and continua in terms of a few energy independent parameters. In particular, this extends and complements the "two-level" theories commonly used to

describe excitations in laser fields.

(ii) Strong field effects in continuum-continuum transitions are taken into account from the outset, limited only by the number of channels included and beyond the validity of (lowest) order perturbation theory. These results are relevant also for low-energy scattering in laser fields and above threshold ionization (ATI) 2,3.

(iii) Electron correlation effects (such as autoionization and perturbation of Rydberg series) and laser interactions can be treated on the same level.

As a first example we have considered a hydrogen atom in circularly polarized laser light at intensities up to approximately $5 \cdot 10^{13} \text{ W/cm}^2$ and frequencies $\omega \approx 0.25 \text{ Ry}$.

Up to nine channels, involving five l-values ($l = 0-4$), were included in the calculations with the reaction matrix read off at typically 35-50 Bohr radii. Fig. 1 shows a theoretical REMPI spectrum obtained by assuming that a first tunable weak

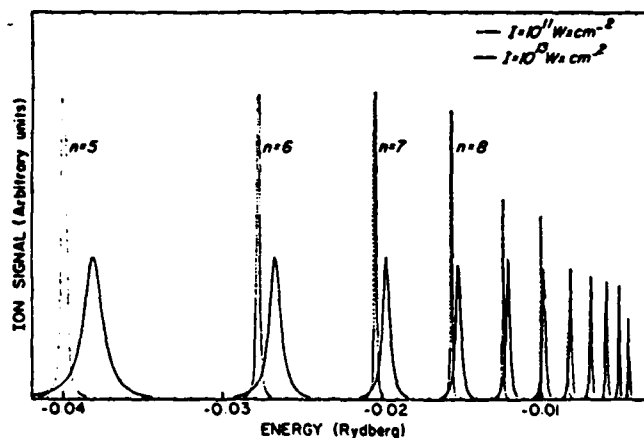


Figure 1 : Theoretical REMPI spectrum scanning the Rydberg region in H, for different intensities of the ionizing radiation field ($\omega = 0.25 \text{ Ry}$).

transition excites selectively the ns Rydberg states which are

then ionized by the strong laser field. Besides the broadening and shift visible on Fig. 1 the smooth reaction matrix yields the partial ionization probabilities P_k corresponding to the absorption of k photons ($k-1$ above thresholds), as they could be measured from an energy analysis of the photoelectrons. Fig. 2 shows the results for the 6s Rydberg state. P is the total ionization probability, and the dashed lines indicate the behavior predicted by

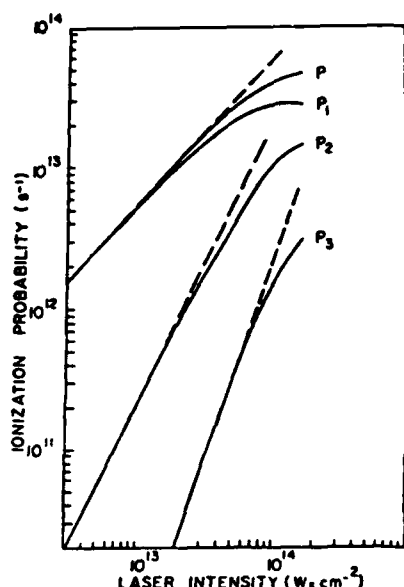


Figure 2 : Partial and total ionization probabilities of the hydrogen 6 state.

perturbation theory ($P_k \propto I^k$). Our weak field values for P_2 agree well with the perturbation results for 2-photon $ATI^{3,4}$.

ACKNOWLEDGMENT

P. Z. acknowledges support by the Fonds zur Förderung der wissenschaftlichen Forschung P6008P and Österreichische Nationalbank 2604.

REFERENCES

1. A. Glustl and P. Zoller, in preparation.
2. W.C. Henneberger, P.R.L. 21, 838 (1968) ; M. Gavrilin, in "Fundamentals of Laser Interactions", lecture notes in Physics, vol. 229, (Ed. F. Ehlotzky, Springer, 1985).
3. S. Klarsfeld and A. Maquet, Phys. Lett., 73A, 100 (1979). M. Aymar and M. Crance, J. Phys. B 13, L287 (1980).

TWO AND THREE-PHOTON IONIZATION OF HELIUM
WITH A RESONANT AUTOIONIZING STATE

H. Bachau

Laboratoire des Collisions Atomiques,
Universite de Bordeaux I, 33400 Talence, France

P. Lambropoulos

University and Research Center of Crete, Iraklion, Crete 71110, Greece
and University of Southern California, Los Angeles, CA 90089-0484

In view of recent experiments^{1,2}, the role of multiply excited states (collective or otherwise) as intermediate resonant states in multiphoton ionization has become very pertinent especially in two-electron atoms. Two additional aspects, namely the importance of correlation and double ionization, are intimately connected with such states. We examine here all three of these aspects in a calculation referring to the helium atom. Our report here presents results on the particular case of 2-photon excitation of the lowest $^1S(1)$ doubly excited state which can then lead to either double ionization or single ionization with the possibility of leaving the ion in an excited state.

We investigate all of the above possibilities quantitatively, examining the dipole coupling between the resonance $^1S(1)$ and continua of the type $n\ell k\ell'$ or $k\ell k'\ell'$ corresponding to 3-photon absorption with one or two electrons, respectively, in the continuum denoted by $k\ell$, while $n\ell$ denotes a bound state of He^+ . It turns out that this particular case is rather unfavorable for direct double ionization which can occur only through correlation. In addition, the transition $1s^2 + 2h\nu \rightarrow ^1S(1)$ can take place only through correlation. Thus the end result will be mainly $\text{He}^+(n\ell)$ with only a small fraction undergoing direct double ionization. Note that the situation will be entirely different if $^1S(1)$ is excited by a 4-photon absorption in which case double ionization requires two additional photons. Then correlation is not necessary which is more favorable for a direct process. Neverthe-

less, the simple case discussed here allows the direct evaluation of correlation which sheds some light on similar situations in alkaline earth atoms.

The approach adopted here has been used in previous work³ (see references herein). Briefly, the autoionizing states are described using the Feshbach formalism⁴. The resonant part of the wave function is solution of the equation:

$$(QH - \xi_s) X_s^{L,S} = 0 \quad (1)$$

H is the total atomic Hamiltonian, L and S are respectively the total angular momentum and the total spin. The projector operator Q ensures that none of the two electrons are in a $1s$ state of He^+ .

$X_s^{L,S}$ is expanded on a basis of hydrogenic functions $U_j^{L,S}$:

$$X_s^{L,S} = \sum_j a_j U_j^{L,S} \quad (2)$$

where $U_j^{L,S}$ is given by:

$$U_j^{L,S} = A [R_{n_1 l_1}^{Z_1}(r_1) R_{n_2 l_2}^{Z_2}(r_2) Y^{L,M}_{(1,2)}] \quad (3)$$

R_{nl}^Z represents the radial part of the hydrogenic function relative to a charge Z . $Y^{L,M}$ is the usual angular part and A is an antisymmetrization operator. $X_s^{L,S}$ is determined through a diagonalization method, Z_1 and Z_2 in Eq. (3) are varied in order to minimize ξ_s . The ground state is determined through the same procedure (with $Q=1$). The continuum of the form nl, kl' is approximated using Coulomb wave functions³. The double continuum $kl_1 k'l'$ is described using an antisymmetrized product of Coulomb functions (calculated for $Z=2$).

If we retain the processes where two photons are involved, it can be shown that the probability of ionization W is given by (in the weak probe approximation):

$$W = \left(\gamma_1 + \gamma_2 \frac{(\delta + Q)^2}{\delta^2 + 1} \right) T . \quad (4)$$

T is the interaction time, γ_1 is a term dominated by the direct ionization process (one photon absorption) and varies as the intensity I of the laser. γ_2 varies as I^2 , δ and Q are two quantities depending, respectively, on the detuning $\Delta(\Delta = 2\hbar\omega - E_{ag})$ and on the path of interference.

The following points are to be emphasized:

- The autoionizing states $^1P(n)$ must be added to the bound (and continuum) states 1P as intermediate states to calculate the dipole matrix elements $D_{ag}^{(2)}$ between the ground state $|g\rangle$ and the doubly excited state $|a\rangle$.

- The evaluation of the dipole coupling between the resonant state $^1S(1)$ and the single continua $n\ell k\ell'$ (or double continua $k\ell k'\ell'$) shows that the ionization to state $n\ell k\ell'$ with $n=2,3$ is favoured. Indeed this effect can be explained simply using correlation considerations. As a result the continuum $1s k\ell$ will be populated by single-photon absorption and configuration interaction. In the case of more complex systems as alkaline earths, production of excited ions will be favoured when the process of photon absorption from a resonance will "compete" with the decay by configuration interaction.

References

1. G. Petite and P. Agostini, J. Phys. Paris 47 (1986) 795.
2. D. Feldman and K. H. Welge, J. Phys. B 15 (1982) 1651.
3. H. Bachau, P. Lambropoulos and R. Shakeshaft, Phys. Rev. A 34 4785.
4. H. Feshbach, Am. Phys. NY. 19, 287 (1962).

This project was supported by the National Science Foundation, under Grant No. PHY-8306263.

AD-A202 520

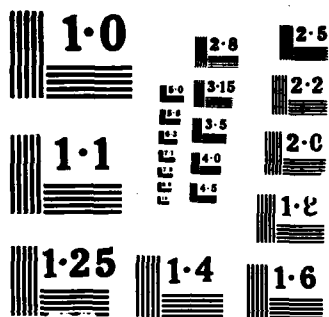
INTERNATIONAL CONFERENCE ON MULTIPHOTON PROCESSES (4TH)
HELD IN BOULDER CO. (U) JOINT INST FOR LAB ASTROPHYSICS
BOULDER CO JUL 88 AFOSR-IR-88-1278 AFOSR-87-0221

3/4

UNCLASSIFIED

F/G 1/3

NL



Invited Paper

STATE-RESOLVED STUDY OF COLLISIONAL ENERGY TRANSFER STUDIED BY LASER
REMPI SPECTROSCOPY

G. Sha, D. Proch, and K. L. Kompa

Max-Planck Institut für Quantenoptik

D-80046 Garching, Federal Republic of Germany

We present a study of the ro-vibronic energy transfer from $N_2(a, v')$ to CO or N_2 , and of the state-to-state rotational transition probabilities at $N_2(a)$ in collisions with rare gas atoms (Ar or He). The experimental scheme involves preparation of electronically excited N_2 via two-photon pumping and relies on resonantly enhanced multiphoton ionization (REMPI) for detection. Cross sections for the overall intermolecular energy transfer are given and the redistribution of energy is mapped out. A mechanism will be suggested which rationalizes the pathways of energy dissipation. The data for the rotational transition probabilities of $N_2(a)$ in collision with a rare gas atom show that transitions occur only between states of like symmetry. Furthermore, our results indicate an additional propensity rule which favors rotational transitions between the "+" or the "-" sublevels of the Λ doublet of the $^1\Pi_g$ state.

Invited Paper

LASER SPECTROSCOPY OF CORE-EXCITED LEVELS OF NEUTRAL RUBIDIUM

S. E. Harris, J. K. Spong and J. F. Young

Edward L. Ginzton Laboratory

Stanford University

Stanford, California 94305

We describe a new technique for obtaining level positions, linewidths, autoionizing times, and oscillator strengths of core-excited levels and transitions. The technique uses a tunable laser to deplete the population of a radiating core-excited level, as other levels within the core-excited manifold are accessed. Level positions and linewidths are ascertained to within about 1.0 cm^{-1} accuracy, and autoionizing times whose Lorentzian linewidths lie beneath the combined Doppler-hyperfine structure are measured.

Invited Paper

NONCLASSICAL RADIATION GENERATORS

H. Walther

Max Planck Institut für Quantenoptik

D-80046 Garching, Federal Republic of Germany

Invited Paper

EN ROUTE TO ONE PETAWATT

G. A. Mourou

Laboratory for Laser Energetics and The Institute of Optics

University of Rochester

Rochester, New York 14627

We will describe the recently developed technique of chirped pulse amplification, which has led to a terawatt Nd:Glass laser system that has a useful pulse repetition frequency and is compact enough to sit on a tabletop. Our technique should permit scaling to output powers several orders of magnitude higher than one terawatt, with almost equally compact size. Output intensities well above 10^{20} W/cm² appear accessible both technically and economically.

Invited Paper

STUDIES OF SOFT X-RAY FLUORESCENCE FROM EXCITED STATES
PRODUCED BY MULTIPHOTON PROCESSES

C. K. Rhodes

Department of Physics
University of Illinois at Chicago
P. O. Box 4348
Chicago, Illinois 60680

Measurements of short wavelength radiation produced by intense ultraviolet (248 nm) irradiation (10^{15} - 10^{16} W/cm²) of the rare gases have revealed the copious presence of both harmonic radiation and fluorescence from excited levels. Strong fluorescence was seen from ions of Ar, Kr, and Xe with the shortest wavelengths observed being below 12 nm. These experimental findings give information on the coupling mechanism governing the nonlinear interaction.

Invited Paper

HIGHLY EXCITED HYDROGEN ATOMS IN STRONG EXTERNAL FIELDS

K. H. Welge

Universität Bielefeld

D-4800 Bielefeld 1

Federal Republic of Germany

Invited Paper

SUMMARY AND OVERVIEW

P. Lambropoulos

Department of Physics
University of Southern California
Los Angeles, California 90089
and
The Research Center of Crete
University of Crete
Iraklion, Crete, Greece

ICOMP IV POSTER SESSION

4:30 PM - July 14, 1987 - Kittredge Residence Hall Complex

Poster No.		Page
1	"Potential Scattering of Electrons in the Presence of Intense Laser Fields Using the Kramers - Henneberger Transformation," R. Bhatt, B. Piraux and K. Burnett (Imperial College, UK)	189
2	"Resonance Collisions in an Intense Laser Field," M. Shah and K. Burnett (Imperial College, UK)	190
3	"Generalized Coherent States for Electrons in External Fields and Application to Multiphoton Free-Free Transitions," S. Varró (Central Research Institute for Physics, Budapest, Hungary), F. Ehlotzky (Institute for Theoretical Physics, Innsbruck, Austria)	192
4	"Modified Coulomb Scattering in Intense, High-Frequency Laser Fields," J. van de Ree (Eindhoven University of Technology, the Netherlands); J. Z. Kaminski (University of Warsaw, Poland); M. Gavrilă (FOM-Institute for Atomic and Molecular Physics, the Netherlands)	194
5	"Two-Photon Free-Free Transitions: Soft-Photon Limit vs. Born Approximation," V. Veniard, A. Maquet (Université Pierre et Marie Curie, Paris); M. Gavrilă (FOM-Institute for Atomic and Molecular Physics, The Netherlands)	196
6	"Dressed States from a Rearrangement of Time-Dependent Perturbation Theory," H. R. Reiss (The American University, Washington, DC)	199
7	"DC-Field-Induced Interferences in Laser-Induced Autoionization," W. Leński, R. Tanaś and S. Kielich (Institute of Physics, A. Michiewicz University, Poznań, Poland)	202
8	"Dispersion-Like Profiles of the Absorptive Response of a Two-Level System Interacting with Two Intense Fields," A. D. Wilson-Gordon and H. Friedmann (Bar-Ilan University, Israel)	205
9	"Autler Townes Splittings for Realistic Pulsed Lasers," P. T. Greenland (AERE Harwell, UK)	208
10	"Photoionization Photodetachment and Pre-Exponential Decay," P. T. Greenland and A. M. Lane (AERE Harwell, UK)	209
11	"Threshold Effects in a Model of Multiphoton Ionization," B. Piraux and P. L. Knight (Imperial College, UK)	211

Poster No.		Page
12	"Threshold Excitation of Rydberg Series by Intense Laser Fields," G. Alber and P. Zoller (University of Innsbruck, Austria)	213
13	"Rydberg Wave Packets in Many Electron Atoms Generated by Short Laser Pulses," G. Alber, W. A. Henle, H. Ritsch and P. Zoller (University of Innsbruck, Austria)	216
14	"A New Aspect of Resonant Multiphoton Processes in Molecules: The Parity Selectivity," D. Gauyacq, S. Fredin, Ch. Jungen and M. Horani (CNRS, Université de Paris-Sud, France)	218
15	"Determination of the Multiphoton Ionization Cross Sections in the Resonant Case," G. Sultan and G. Baravian (CNRS, Université de Paris-Sud, France)	221
16	"Serial and Parallel Multilevel Systems," E. Kyrölä (University of Helsinki, Finland); M. Lindberg (University of Arizona)	224
17	"Comments on Estimating Nonresonant Multiphoton Ionization Rates," B. W. Shore (Lawrence Livermore National Laboratory)	226
18	"Classical vs. Quantum Description of Above-Threshold Ionization," J. Parker and C. R. Stroud Jr. (University of Rochester)	229
19	"Multiphoton Ionization of Hydrogen by a Multimode Field," S. Basile, G. Ferrante and F. Trombetta (Istituto di Fisica dell'Università, Palermo, Italy)	230
20	"Above-Threshold Processes in Intense Fields," M. Edwards, X. Tang and R. Shakeshaft (University of Southern California)	233
21	"Classical Time-Dependent Self-Consistent Field Approach to Intense Field Multiphoton Ionization and Dissociation of Atoms and Molecules," J. Needels, R. Y. Yin and S.-I Chu (University of Kansas)	236
22	"Many-Electron, Complex Eigenvalue Schrödinger Theory for the Treatment of the ac Stark Ionization. I: Negative Ions," T. Mercouris and C. A. Nicolaides (National Hellenic Research Foundation, Athens, Greece)	239
23	"Multiphoton-Electron Interaction Processes in the Continuum," F. F. Körmendi (Institute HTM, Belgrade, Yugoslavia)	240
24	"Multiphoton Ionization of a Model Atom," B. Chen, F. H. M. Faisal, S. Jetzke, H. O. Lutz, P. Scanzano (Universität Bielefeld)	241

Poster No.		Page
25	"A Simple Model for Strong Laser Field Ionization," J. Zakrzewski (University of Southern California); K. Zyczkowski (Jagiellonian University, Krakow, Poland)	244
26	"Ponderomotive Effects in Pulsed Laser Fields," M. Lewenstein (Harvard University)	247
27	"A Comment on the Emission of Radiation During Multiphoton Ionization with Ultra-Intense Laser Pulses," S. L. Chin (Université Laval, Canada)	250
28	"Investigations of Above Threshold Ionization with Sub-Picosecond Pulse Lengths," R. R. Freeman, M. Geusic, S. Darack and H. Milchberg (AT&T Bell Laboratories)	253
29	"Direct Evidence of Ponderomotive Effects via Pulse Duration in Above-Threshold Ionization," P. Agostini, L. A. Lompre, J. Kupersztych, G. Petite and F. Yergeau (CEN/Saclay, France)	256
30	"Multiphoton Transitions to Final Excited Ion States in Strontium: Spectroscopy of Autoionizing States," P. Agostini, A. L'Huillier, G. Petite (CEN/Saclay, France); X. Tang, P. Lambropoulos (University of Southern California and Research Center of Crete, Greece)	257
31	"A New Technique to Study the Rydberg States by MPI Spectroscopy," R. D. Verma and A. Chanda (University of New Brunswick, Canada)	259
32	"Three-Photon Excitation of Autoionizing States of Atomic Krypton and Xenon," S. T. Pratt, J. L. Dehmer and P. M. Dehmer (Argonne National Laboratory)	260
33	"Two-Color Laser Excitation and Ionization of Dense Sodium Vapor," D. Zei (Ripon College); R. N. Compton and J. A. D. Stockdale (Oak Ridge National Laboratory); M. S. Pindzola (Auburn University); P. Lambropoulos and B. Dai (University of Southern California)	263
34	"Laser-Induced Ionization and Stimulated Electronic Raman Scattering in Cesium Vapor Near the $np^2P_{3/2,1/2}(n=6,7,8,9)$ States," J. A. D. Stockdale, R. N. Compton and A. Dodhy (Oak Ridge National Laboratory); W. Christian (Davidson College); P. Lambropoulos and T. Olsen (University of Southern California)	266
35	"Effects of Third-Harmonic Generation on the Multiphoton Ionization Spectra of Noble Gases," C. Fotakis, M. J. Proctor and J. A. D. Stockdale (Research Center of Crete, Greece)	269

Poster No.		Page
36	"Mechanisms for Suppression of Two-Photon Excitation of Na 3d $^2D_{3/2,5/2}$ in Dense Vapor," W. R. Garrett, M. A. Moore, J. P. Judish, M. G. Payne and R. K. Wunderlich (Oak Ridge National Laboratory)	272
37	"Optimizing Resonant Sum-Frequency Mixing," A. V. Smith, W. J. Alford, G. R. Hadley and P. Esherick (Sandia National Laboratories)	275
38	"Resonant Degenerate Four Wave Mixing with Broad-Bandwidth Lasers," A. Charlton, J. Cooper (JILA); G. Alber (University of Innsbruck, Austria); D. Meacher, P. Ewart (Clarendon Laboratory, Oxford, UK)	278
39	"Multiphoton Ionization and Infrared Generation in a Cesium Heat Pipe Oven Near the Two Photon Ionization Limit," W. Christian (Davidson College)	280
40	"Contribution of Multiphoton Absorption to the Nonlinear Refractive Index of SF ₆ ," Y. Beaudoin, I. Golub and S. L. Chin (Université Laval, Canada)	283
41	"Laser-Induced Autoionizing-Like Behavior, Population Trapping and Stimulated Raman Processes in Real Atoms," B. Dai and P. Lambropoulos (Research Center of Crete, Greece and University of Southern California)	286
42	"Multiphoton Double Excitation and Ionization of O ²⁺ ," X. Tang and P. Lambropoulos (University of Southern California)	289
43	"Multiple Ionization and X-Ray Emission Following Inner-Shell Photoionization of Atoms," V. L. Jacobs (Naval Research Laboratory); B. F. Rozsnyai (Lawrence Livermore National Laboratory)	291
44	"Coherent Excitation of Two Electrons in an Intense Laser Field," T. K. Rai Dastidar and K. Rai Dastidar (Indian Association for the Cultivation of Science, Calcutta, India)	292
45	"Resonant Two-Photon Autoionization of H ₂ : Laser Bandwidth and AC Stark Effect on Photoelectron Angular Distribution and Intermediate Lineshape," S. Ganguly and K. Rai Dastidar (Indian Association for the Cultivation of Science, Calcutta, India)	295
46	"Application of Multiphoton Excitation Techniques to Combustion Diagnostics," U. Meier, K. Kohse-Höinghaus, J. Bittner, Th. Just (DFVLR-Institut für Physikalische Chemie der Verbrennung, Stuttgart, West Germany)	297

Poster No.		Page
47	"Doppler-Free Two-Photon Excitation of Molecular Hydrogen," W. L. Glab and J. P. Hessler (Argonne National Laboratory)	300
48	"Photoelectron Spectra from Resonantly Enhanced Multiphoton Excitation of H ₂ via C ¹ Π _u ," M. A. O'Halloran, S. T. Pratt, P. M. Dehmer; and J. L. Dehmer (Argonne National Laboratory)	302
49	"Higher Rydberg and Autoionizing States of CS ₂ ," J. Y. Fan, E. Patsilinaou and C. Fotakis (Research Center of Crete, Greece)	305
50	"Photoelectron Spectroscopic Study of Resonant Multiphoton Ionisation of Chlorine," B. G. Koenders, K. E. Drabe, M. G. Oostwal, D. M. Wieringa, C. A. de Lange (Free University, Amsterdam, The Netherlands)	307
51	"High-Resolution Zero Kinetic Energy Photoelectron Spectroscopy of Nitric Oxide," M. Sander, L. A. Chewter and K. Müller-Dethlefs (TU München, West Germany)	310
52	"Detection of Ionized Hydrogen in Resonant Multiphoton Ionization of Benzene in the Visible," R. Bruzzese, F. Esposito, S. Solimeno, N. Spinelli (FNSMFA, Napoli, Italy)	313
53	"Photodissociation of CH ₃ I Clusters Probed by Multiphoton Ionization," S. Sapers, V. Vaida (University of Colorado); R. Naaman (Weizmann Institute of Science, Israel)	316
54	"REMPI (2+1) in NH ₃ via the \tilde{C} (v ₂ =3) (¹ A ₁ ') State in Vapor and in Discharges," S.-P. Lee, E. W. Rothe, G. P. Reck (Wayne State University)	318
55	"REMPI Spectra of Large Thermally Labile Molecules after IR-Laser Induced Desorption," A. Habekost, H. Ulbrich and H. von Weyssenhoff (Universität Hannover, Germany)	321
56	"Laser-Induced Fluorescence Lifetime of Rubrene by Two Photon Excitation at 1064 nm," F. Bayrakceken (Ankara University, Turkey)	322
57	"Pressure Effects in Organometallic MPD/MPI Experiments," J. M. Hossenlopp and J. Chaiken (Syracuse University)	323
58	"Mechanism of the Infrared Multiphoton Decomposition of Ethanol," D. K. Evans, J. W. Goodale, M. J. Ivanco, R. D. McAlpine (Chalk River Nuclear Laboratories, Canada)	324

Poster No.		Page
59	"UV Laser Multiphoton Ionization Study of Formaldehyde," H. Liu, S. Li, J. Han, C. Wu (Anhui Institute of Optics and Fine Mechanics, Hefei, China)	327
60	"Mechanism of Multiphoton Ionization and Fragmentation of Alkyl Iodides," J. Han, H. Liu, J. Gu, S. Li, C. Wu (Anhui Institute of Optics and Fine Mechanics, Hefei, China)	329
61	"Molecular Model of Multiple-Photon Absorption through Chaotic and Bistable Steady States," J. C. Englund and C. M. Bowden (Redstone Arsenal); F. A. Hopf (University of Arizona)	332
62	"Classical Trajectory Studies of IR Multiphoton Absorption in Diatomic Molecules: Destruction of Coherence by Rotation," R. Parson (JILA)	335
63	"Effects of Strong E. M. Fields in the Continuum of Helium Atom," A. Lami, N. K. Rahman (Università di Pisa, Italy); P. Spizzo (Sezione Chimica-Fisica, Pisa, Italy)	337
64	"Coupled Logistic Map as a Model for Photon Absorption in Multimode Systems," A. Ferretti and N. K. Rahman (Università di Pisa, Italy)	338
65	"Classical Counterparts of Multiphoton Phenomena," Q.-C. Su and J. Javanainen (University of Rochester)	339
66	"Multiphoton Dynamics and Quantum Diffusion in Rydberg Atoms," S.-I Chu and K. Wang (University of Kansas)	341
67	"Ionization of Atoms in a Magnetic Field: The Effect of Closed Classical Orbits on Quantum Spectra," M. L. Du and J. B. Delos (JILA)	344

POTENTIAL SCATTERING OF ELECTRONS IN THE PRESENCE OF INTENSE LASER FIELDS USING THE KRAMERS - HENNEBERGER TRANSFORMATION

R. Bhatt, B. Piraux and K. Burnett

Blackett Laboratory, Imperial College, London SW7 2B2, U.K.

We study potential scattering of electrons in the presence of an intense laser field by using the Kramers - Henneberger (K-H) transformation [1]. As a first step, we consider the one - dimensional scattering of electrons by the polarization potential

$$V(x) = -1/[1+x^2]^2.$$

Within this method, the effective potential becomes periodic and the Schrodinger equation may be transformed into an infinite system of coupled equations, the coupling terms being the Fourier components of the effective potential.

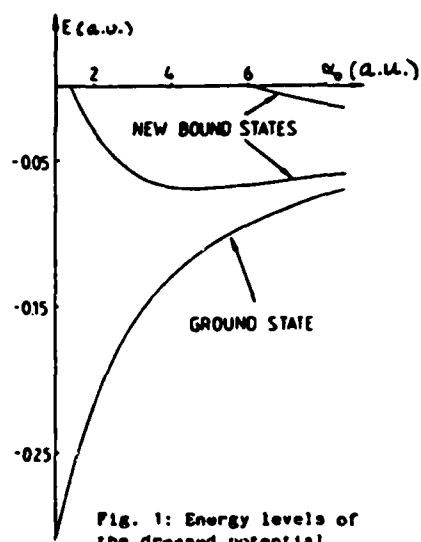


Fig. 1: Energy levels of the dressed potential

We first analyse the dressed potential which is the time average of the effective potential and show that it may support more bound states than the original potential depending on α_0 , the classical oscillation amplitude of the field (see fig. 1).

In order to solve the system of coupled second order differential equations numerically, we consider a finite number of equations; this number strongly depends on the field parameters. This point is discussed in

detail for a wide range of frequencies and laser intensities; in addition, we show that it is only at high frequencies and intensities (yet to be achieved) that the coupling terms may be treated perturbatively, confirming the conditions stated by Gavrilá and Kamiński [2].

Final results for the reflection and transmission coefficients in several open channels are presented and discussed.

References

- 1 W. Henneberger, Phys. Rev. Lett. 21, 838 (1968)
- 2 M. Gavrilá and J. Kamiński, Phys. Rev. Lett. 52, 613 (1984)

RESONANCE COLLISIONS IN AN INTENSE LASER FIELD

M. SHAH AND K. BURNETT

Spectroscopy Group, Blackett Laboratory
Imperial College of Science and Technology
London SW7 2BZ, United Kingdom

The effect of intense laser radiation on atomic collision dynamics has attracted much theoretical^[1] and, more recently, experimental interest^{[2],[3]}. But most of the collisions investigated so far have been of the non-resonant kind.

We are studying resonance collisions in an intense laser field. The analytical form of the resonance interaction is well known which makes it possible to obtain, for example, field dependent collision rates with a much higher degree of certainty than is possible in the non-resonant case^[4]. Following C. Carrington, D. Stacey and J. Cooper^[5], we have included the multiplet structure of the degenerate atomic levels in our model. The atoms follow classical rectilinear paths and the domain of collisions is confined to the binary collision regime. The resonance interaction is limited to the special case of a first order dipole-dipole interaction, and an intense laser field strongly couples the atomic ground and first excited states.

Using Mercury as an example of an atom whose ground state angular momentum $J_g = 0$ and excited state angular momentum $J_e = 1$, the appropriate Schrodinger equations are being numerically integrated to obtain the distribution of final atomic states that result from such light assisted collisions; particular attention is being paid to the effect that the laser intensity has on this distribution. We shall present progress in the theory.

References

1. T. George, The Journal of Physical Chemistry, Volume 86, 1, (1982) 10.
2. P. Kleiber, K. Burnett, J Cooper, Physical Review Letters, Volume 47, 22, (1981) 1595.
3. T. Sizer II and M. Raymer, Physical Review Letters, Volume 56 (1986) 123
4. J. Light and A. Szoke, Physical Review A, Volume 18, 4, (1978) 1363
5. C. Carrington, D. Stacey and J. Cooper, Journal of Physics B: Atomic and Molecular Physics, Volume 6, (1973), 417.

GENERALIZED COHERENT STATES FOR ELECTRONS IN EXTERNAL
FIELDS AND APPLICATION TO MULTIPHOTON FREE-FREE TRANSITIONS

S. Varró

Central Research Institute for Physics
H-1525 Budapest, P.O.Box 49, Hungary

F. Ehlötzky

Institute for Theoretical Physics
University of Innsbruck
A-6020 Innsbruck, Austria

Generalized coherent states are constructed to describe the quasiclassical motion of an electron in a strong low-frequency radiation field and in a constant homogeneous magnetic field in Redmond configuration. These states are shifted Landau states whose centers follow the corresponding classical trajectories. Their shape is determined by the usual azimuthal and main quantum numbers. Since these generalized coherent states form a complete and *orthogonal* set they can be conveniently used as an "in" and "out" basis in Furry picture for the description of scattering processes.

As an example the scattering of an electron by a screened Coulomb potential is considered in the presence of the above two external fields. The scattering potential is treated in the first order Born approximation and the

corresponding cross sections of the induced nonlinear processes are discussed in various limiting cases. Our results are of particular interest for applications in plasma physics (heating of a magnetized plasma by the absorption of radiation). The main advantage of our method is that the treatment of multiphoton scattering problems of charged particles in the two external fields by means of generalized coherent states stresses the quasiclassical features of these processes and elucidates the close interrelation between the quantummechanical boundary value problem and the classical initial value problem.

We should like to emphasize that that our method does not rely upon some quasiclassical approximations, but it gives an exact quantum description of the scattering process. In the same time, however, the results can be directly interpreted almost entirely in terms of classical trajectories.

MODIFIED COULOMB SCATTERING IN INTENSE, HIGH-FREQUENCY LASER FIELDS

J. van de Ree*, J.Z. Kaminski** and M. Gavrilă***,

*Physics Department, Eindhoven Univ. of Technology, Eindhoven, the Netherlands

**Institute of Theoretical Physics, Univ. of Warsaw, Warsaw, Poland

***FOM-Institute for Atomic and Molecular Physics, Amsterdam, the Netherlands

A nonperturbative theory was recently developed to describe electron-atom interactions in high-frequency laser fields^{1,2}. It applies at frequencies already available from excimer lasers in the VUV³, but extends beyond, into the X-ray range. The radiation was assumed monochromatic. By a Floquet analysis, the time-dependent Schrödinger equation was reduced to an infinite set of time-independent coupled equations for the Floquet components of the wave function. It was shown that in the high-frequency limit these reduce to a single equation of the Schrödinger type, containing the "dressed potential" $V_0(\vec{\alpha}_0; \vec{r})$. For linear polarization (polarization vector \vec{e}), V_0 has axial symmetry and even parity. It depends on the intensity I and frequency ω through $\vec{\alpha}_0 = \alpha_0 \vec{e}$, where $\alpha_0 = I^{1/2} \omega^{-2}$ a.u. Consequently, in this limit only elastic scattering can occur (multiphoton free-free transitions are quenched).

We now report on a highly accurate computation of the elastic scattering cross section for a Coulomb potential ($V(r) = -Z/r$). In this case

$$V_0(\alpha_0; \vec{r}) = -(2Z/\pi) (r_+ r_-)^{-1/2} K(2^{-1/2}(1 - \hat{r}_+ \hat{r}_-)^{1/2}), \quad (1)$$

where $\vec{r}_{\pm} = \vec{r} \pm \vec{\alpha}_0$ and K is a complete elliptic integral of the first kind. The corresponding Schrödinger equation was analyzed in a spherical harmonics basis, in which it is equivalent to an infinite set of coupled radial equations. This set was solved by the Sams-Kouri version of the close-coupling method, by adapting a numerical program for radiationless scattering⁴. Detailed convergence tests were carried out.

The cross section depends not only on the scattering angle θ between the initial and final momenta ($\vec{p}_i; \vec{p}_f$) but also on their orientation with respect to $\vec{\alpha}_0$. We define θ_i as the angle between \vec{p}_i and $\vec{\alpha}_0$, and ϕ as the azimuthal angle of \vec{p}_f in a coordinate system having \vec{p}_i as a polar axis, and the x axis in the $(\vec{\alpha}_0, \vec{p}_i)$ plane.

In Fig. 1 we show the scattering angle dependence of the ratio $R = (d\sigma/d\Omega)/(d\sigma_c/d\Omega)$ of the laser-modified elastic cross section to the original Rutherford one, for various values of θ_i and ϕ . We have chosen $Z = 1$, $\alpha_0 = 2$ and electron energy $E = 0.1$ Ry. In all cases $R \rightarrow 1$

as $\theta \rightarrow 0$, since both modified and Rutherford cross sections tend to infinity in the same way. Further, for $\theta \rightarrow 0$, R has infinitely many "Coulomb interference oscillations" due to the departure of V_0 from the Coulomb form close to the nucleus⁵. As seen, large variations occur by changing θ_i and ϕ , particularly at large θ . Further, R is strongly dependent on α_0 . Thus, in the high-intensity, high-frequency regime studied here, large effects on the elastic Coulomb scattering can appear, in a range of parameters now accessible to experiment.

REFERENCES

1. M. Gavrilu and J.Z. Kaminski, *Phys.Rev.Lett.* **52**, 613 (1984), and to be published.
2. M. Gavrilu, in: *Fundamentals of Laser Interactions*, Ed. F. Ehlotzky (Springer Lecture Notes in Physics, vol.229, 1985), p.3.
3. C.K. Rhodes, *Science* **229**, 1345 (1985).
4. J. van de Ree, *J.Phys.B.* **15**, 2245 (1982).
5. M.J. Offerhaus, J.Z. Kaminski and M. Gavrilu, *Phys.Lett.* **112A**, 151 (1985).

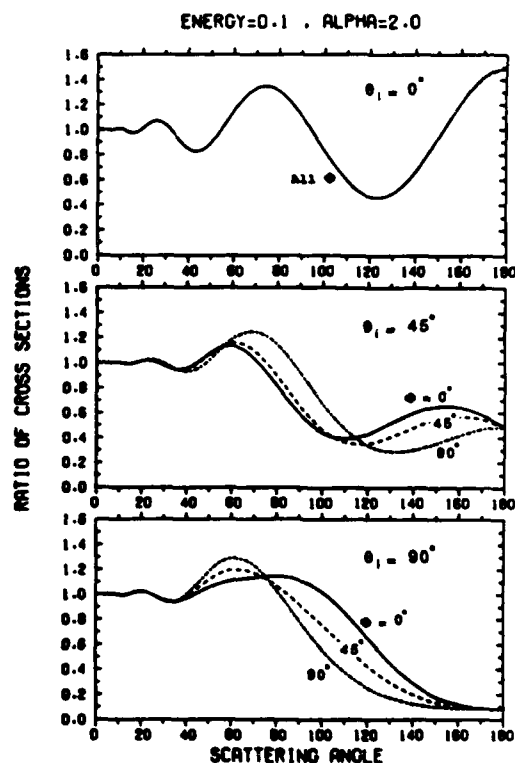


Fig. 1. Ratio of the elastic scattering cross section for the dressed Coulomb potential, to the Rutherford cross section ($z=1$, $\alpha_0=2$, $E=0.1$ Ry).

**Two-photon free-free transitions :
Soft-photon limit vs. Born Approximation.**

V. Veniard*, A. Maquet* and M. Gavrila**

* Laboratoire de Chimie Physique, Université Pierre et Marie Curie
11, Rue Pierre et Marie Curie, F75231 Paris Cedex 05. France.

** FOM-Institute for Atomic and Molecular Physics
Kruislaan 407, 1098 SJ Amsterdam, The Netherlands.

By using Schwinger's representation of the Coulomb Green's function,¹ we have been able to perform an "exact" perturbative calculation of two-photon transition amplitudes, in a Coulomb field, in the nonrelativistic dipole approximation.^{2,3} The analytical, as well as numerical, calculation of such second-order amplitudes in the continuum presents additional difficulties with respect to similar ones related to bound-bound or bound-free transitions, i.e. involving at least one bound state. The origin of these complications is twofold : first the argument of the Green's function is always positive or, more precisely, is located on its cut in the complex energy plane. Though this does not impede to carry on the analytical calculation, it usually makes the computation more difficult.^{4,5} The second additional difficulty arises from the infinite degeneracy of the initial and final scattering states. This typical 1-degeneracy introduces, at least implicitly, one more infinite summation into the calculation, by contrast with similar ones involving one bound state with a given angular momentum. This may explain why, although we have pushed the analytical calculation as far as possible, no simple closed form expression of the amplitudes have been obtained.^{2,3} As a consequence, the dependence of the amplitudes on the parameters governing the dynamics of the process is somewhat hindered by the complexity of the general formulae. These expressions do simplify considerably however in several limiting cases, among which the soft-photon limit and the Born approximation are the most often discussed.

In the (lowest non-vanishing order) Born approximation a direct calculation can be straightforwardly performed and the 2-photon absorption cross section reads (in a.u.):

$$\frac{d\sigma}{d\Omega} = \frac{p_f}{p_i} |f^{(2+)}|^2 = \frac{p_f}{p_i} \left| 4Z \frac{1}{\omega^4} \frac{(e \cdot \Delta)^2}{\Delta^2} \right|^2$$

where Z is the charge of the nucleus, I is the intensity of the laser with frequency ω and polarization e and $\Delta = p_f - p_i$ is the momentum transfer with $p_f^2 = p_i^2 + 2\omega$ (energies expressed in Ry.). We note that the amplitude is real, is proportional to the charge of the nucleus and that no particular assumption is made as regards to the magnitude of ω . This implies that, in general, $p_f \neq p_i$ and accordingly Δ^{-2} is not the usual Rutherford denominator. The calculation can be easily extended to higher order processes, yielding for instance, for n -photon absorption:

$$\frac{d\sigma}{d\Omega} = \frac{p_f}{p_i} Z \frac{2^{n+1}}{n} \left[\frac{\sqrt{I}}{\omega^2} \right]^n \frac{(e \cdot \Delta)^n}{\Delta^2}$$

No similar direct computation is feasible in the soft-photon limit. It is however possible to derive from our exact expressions the lowest order contribution to the amplitudes in terms of the parameter ω/p_i^2 . One obtains in the limit $p_f \sim p_i$:

$$\frac{d\sigma}{d\Omega} = |f^{(2+)}|^2 = \left| 2Z \frac{1}{\omega^4} (e \cdot \Delta)^2 f_c \right|^2$$

where f_c is the Coulomb scattering amplitude for momentum magnitude $p \sim p_i \sim p_f$ and momentum transfer Δ . The corresponding cross section is thus, as expected, proportional to Rutherford's scattering cross section.⁶ We observe that, the expression of the soft-photon cross section is formally similar to the Born approximation one, provided one makes the replacement $p_i \sim p_f$ in the latter.⁷

An interesting particularity of two-photon processes is that, for a given scattering geometry, the cross section is independent on the magnitude of p_i (p_f) provided the condition $\omega/p_i^2 \ll 1$ is met. This remarkable property is specific of two-photon processes, since it is the only case for which the energy

dependence of the numerator $(e.A)^2$ and of the denominator Δ^2 can compensate each other into the expression of the transition amplitude. Note that such a property of independence of the cross section on the energy of the incoming electron could be easily checked, at least in principle. Accordingly, any departure from this simple rule could be unambiguously attributed to higher order effects.

Another nice feature of our exact calculation is that it allows to delineate, in a physically meaningful context, the domains of validity of these approximations. This point will be discussed in more detail in our presentation.

Acknowledgements. This work was jointly sponsored by the CNRS (France) and by the Netherlands Organization for the Advancement of Pure Research (ZWO). The Laboratoire de Chimie Physique is an "Unité associée au CNRS", U.A. 176.

References.

- ¹ J. Schwinger, J. Math. Phys. 5, 1606 (1964).
- ² M. Gavrila, A. Maquet and V. Veniard, Phys. Rev. A, 32, 2537 (1985).
- ³ V. Veniard, M. Gavrila and A. Maquet, Phys. Rev. A, 35, 448 (1987).
- ⁴ W. Zernik and R. W. Klopfenstein, J. Math. Phys. 6, 262 (1965).
- ⁵ S. Klarsfeld and A. Maquet, Phys. Lett. 78A, 40 (1980).
- ⁶ F. E. Low, Phys. Rev. 110, 974 (1958).
- ⁷ H. Kruger and M. Schulz, J. Phys. B, 9, 1899 (1976).

**Dressed States from a
Rearrangement of Time-Dependent Perturbation Theory**

H. R. Reiss

**Department of Physics, The American University
Washington, DC 20016, USA**

Semiclassical time-dependent perturbation theory, as it applies to the wave function of a bound system in a sinusoidally varying electromagnetic field, is rearranged in a form appropriate to a field whose photon energy is very small as compared to the level spacing in the bound system. (Although the rearrangement is correct without restriction.) The procedure adopted is to do the necessary manipulations explicitly in first order and in second order perturbation theory, and then to infer the general N th order term. The correctness of the inference is verified by direct substitution in the Schrödinger equation, which is satisfied to order N . The result is therefore exact as $N \rightarrow \infty$. A very simple approximation emerges from this new series solution in the case of low field frequency under the condition that no near-resonances occur, or that near-resonances can happen only at such very high order that the combination of the introduction of level widths in the denominators with extremely high order suppression in the numerator justifies the neglect of such terms. This approximation then represents a state dressed by a low frequency electromagnetic field. The dressed state is shown to exhibit both energy and angular momentum sidebands. This dressed state is then inserted into a transition amplitude expression for transitions caused by a general interaction Hamiltonian which exists in company with the dressing field, with results that are quite simple in form.

The interaction Hamiltonian for the dressing field is

$$H' = -e\vec{A} \cdot \vec{p}/m + e^2 A^2/2m ,$$

which, upon substitution into matrix elements is converted by the relations

$$\vec{p}/m = -i[\vec{r}, H_0] , \quad A^2 = i[\vec{A} \cdot \vec{p}, \vec{A} \cdot \vec{r}]$$

into matrix elements of $i e \vec{A} \cdot \vec{r}$ between intermediate states as appropriate. Energy factors occur in the terms of the perturbation series expansion that are of the form $\omega_{n_0}/(\omega_{n_0} - k\omega)$, where ω is the frequency of the electromagnetic field and ω_{n_0} is the energy difference $E_n - E_0$ between the two states involved in the matrix element. The rearrangement of the perturbation series is effected by rewriting all such energy factors as

$$\omega_{n_0}/(\omega_{n_0} - k\omega) = 1 + k\omega/(\omega_{n_0} - k\omega) . \quad (1)$$

The unit term on the right hand side in Eq.(1) makes possible closed form summations over intermediate states, and the other term in Eq.(1) leads to expressions in powers of ω (although it is not precisely a pure expansion in powers of ω because it is convenient to leave ω in the denominator). The final wave function for the dressed state is

$$\begin{aligned} \Psi_0^{(N)} = & \left[\sum_{j=0}^N \mathcal{A}^j/j! \right] \Phi_0 + \sum_{k=1}^N \left[\sum_{j=0}^{N-k} \mathcal{A}^j/j! \right] \sum_{n_1} \dots \sum_{n_k} \mathcal{A}_{n_1} \mathcal{A}_{n_2} \dots \mathcal{A}_{n_k} \Phi_0 \\ & \times \omega^k/[\omega_{n_1 0} - k\omega][\omega_{n_2 0} - (k-1)\omega] \dots [\omega_{n_k 0} - \omega] , \quad (2) \end{aligned}$$

where $\mathcal{A} \equiv i e \vec{A} \cdot \vec{r}$ and $\mathcal{A}_{n_i n_j}$ is a matrix element of \mathcal{A} taken between non-interacting intermediate states Φ_{n_i} and Φ_{n_j} . The superscript (N) on Ψ_0 indicates that this is a rearrangement of the Nth order perturbation of the state Φ_0 .

Equation (2) lends itself to a low frequency approximation in a sense described by Mittleman¹, where it is presumed that none of the denominators are resonant (or if

they approach resonance, it is only for very high orders, where finite intermediate state lifetimes avert vanishing denominators²). The hypothesized small magnitude of ω as compared to level spacing then permits one to retain only the leading term in Eq.(2) to give, as $N \rightarrow \infty$,

$$\Psi_0 \approx \Phi_0 \exp(\mathcal{A}). \quad (3)$$

Equation (3) can be expanded as

$$\Psi_0 = \sum_{n=0}^{\infty} i^n J_n(a\vec{A} \cdot \vec{r}) \exp[-i(E_0 - n\omega)t] \Phi_0(\vec{r}), \quad (4)$$

where $\vec{A} = \vec{A} \cos \omega t$ and $\Phi_0 = \Phi_0(\vec{r}) \exp(-iE_0 t)$; or as

$$\Psi_0 = \sum i^n J_n(aar) P_n(\cos \theta) \Phi_0, \quad (5)$$

which exhibit the energy and angular momentum structure of the dressed state in this low frequency case. The Bessel functions in Eq.(4) are suggestive of a connection with the Kroll and Watson result³, but this has not been demonstrated. Friar and Fallieros⁴ have inferred Eq.(3) by essentially extrapolating from the first order expression, but they have shown its gauge invariance.

For transitions caused by a potential $V(\vec{r}, t)$ in the presence of the low frequency field \vec{A} , one can show that the transition amplitude is

$$S_{fi} = -i \int dt \left[\Phi_f, (E_i - E_f + V) \exp(\mathcal{A}) \Phi_i \right], \quad (6)$$

where E_i and E_f are the energies of the bare initial and final states. Equation (6) is an exceptionally simple result.

¹M. H. Mittleman, *Theory of Laser-Atom Interactions* (Plenum, New York, 1982).

²H. B. Babbb and A. Gold, *Phys. Rev.* 143, 1 (1966).

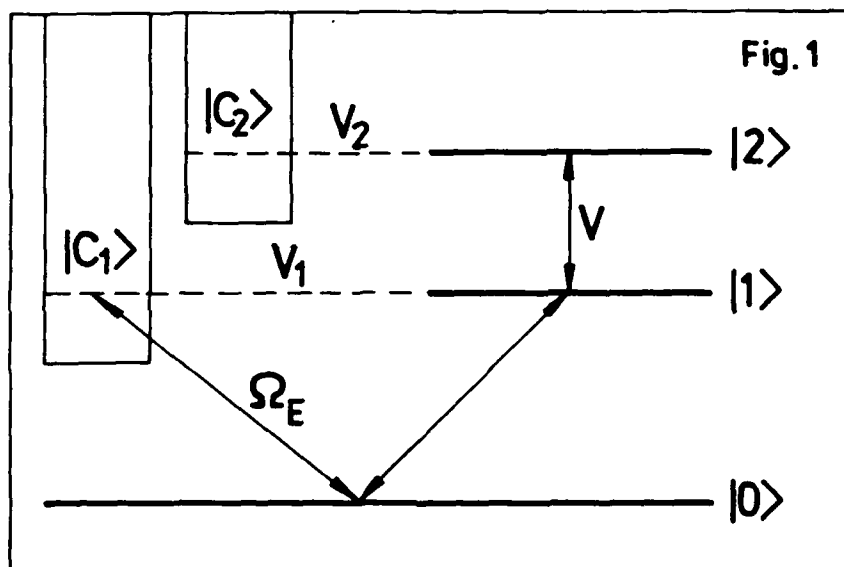
³N. M. Kroll and K. M. Watson, *Phys. Rev. A* 8, 804 (1973).

⁴J. L. Friar and S. Fallieros, *Phys. Rev. C* 34, 2029 (1986).

DC-FIELD INDUCED INTERFERENCES IN LASER-INDUCED AUTOIONIZATION

W. Leoński, R. Tanaś and S. Kielich
Nonlinear Optics Division, Institute of Physics
A. Mickiewicz University
60-780 Poznań, Poland

Recently, DC-field induced resonances in laser-induced autoionization has been the subject of experimental and theoretical research.^{1,2} We have calculated the strong-laser-field photoelectron spectrum for the system displayed in Fig. 1.



Two autoionizing states $|1\rangle$ and $|2\rangle$ are coupled to two orthogonal continua $|c_1\rangle$ and $|c_2\rangle$ and are coupled to each other by a DC electric field. A strong laser field couples the ground state $|0\rangle$ to the state $|1\rangle$ and to the continuum $|c_1\rangle$. We ignore all radiative relaxation effects and concentrate on the influence of the autoionization width of the level $|2\rangle$ on the DC-field induced interferences. The photoelectron spectrum for the system of Fig. 1 is given by

$$\pi W(E) = \gamma_0 \left| \frac{(\delta_2 + i\gamma_2)(\delta_1 + q_1\gamma_1) - V^2 + V\sqrt{\gamma_1\gamma_2}(q_1 - 1)}{(\delta_2 + i\gamma_2)[(\delta_0 + i\gamma_0)(\delta_1 + i\gamma_1) - \gamma_0\gamma_1(q_1 - 1)^2] - V^2(\delta_0 + i\gamma_0)} \right|^2$$

where we have used the notation

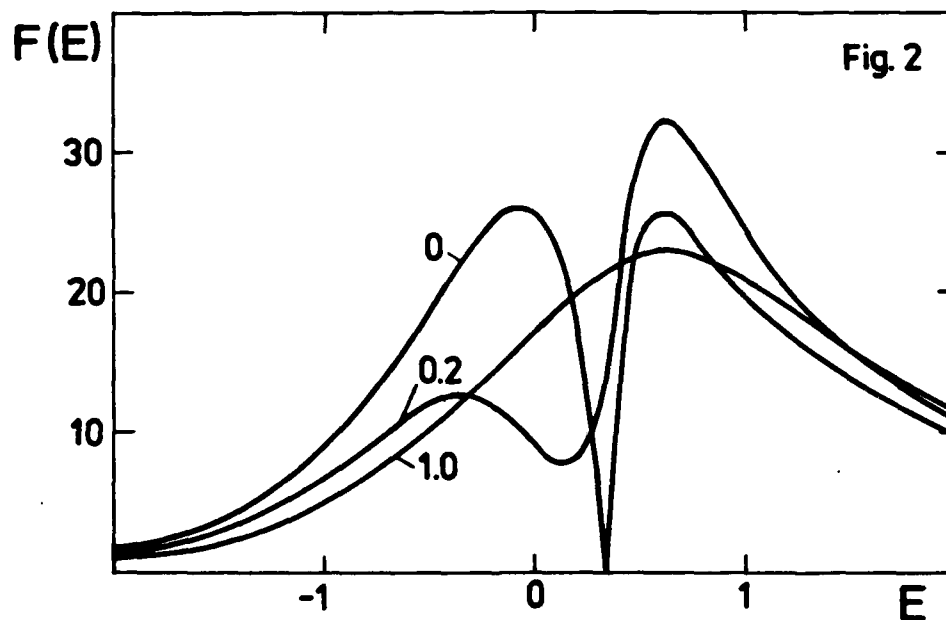
$$\delta_0 = E - E_0 - \omega_L, \quad \delta_1 = E_1 - E_2, \quad \delta_2 = E - E_2$$

with E_i the atomic energies, and

$$\gamma_0 = \pi |\Omega_E|^2 = |\Omega_0|^2 / 4(1+q_1^2) \gamma_1,$$

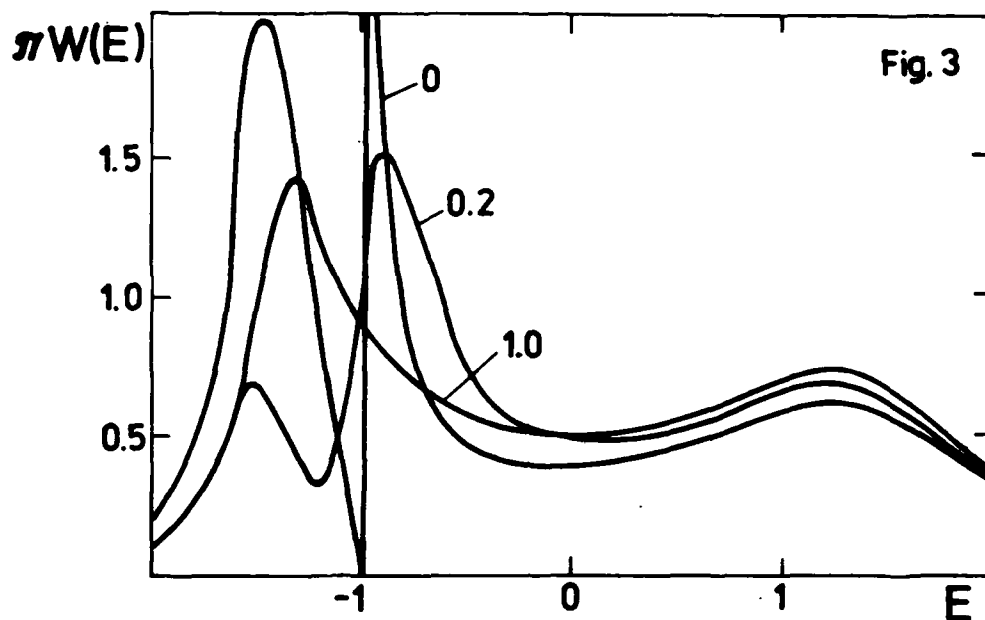
$$\gamma_1 = \pi |V_1|^2, \quad \gamma_2 = \pi |V_2|^2$$

denote the power broadening and autoionizing widths. Ω_0 is the Rabi frequency introduced in Ref. 3, q_1 is the Fano asymmetry parameter, and V describes the DC-field coupling.



In Fig. 2 the weak-field absorption spectrum, the Fano profile, is shown. The parameters, all energies in units of γ_1 , are: $q_1=5$, $V=0.3$, $E_1=E_0+\omega_L=0$, $E_2=0.3$, and the curves are marked with the values of γ_2 . It is seen that the splitting due to the DC field is washed out if the autoionization width γ_2 is large, compare Ref. 1 and 2.

Figure 3 shows the strong field photoelectron spectrum for $\Omega_0=3$ and $E_2=-1$, and other parameters as in Fig. 2. The DC-field induced interference splits one of the Autler-Townes peak, but this splitting too is washed out for large γ_2 .



This research was supported by the Polish Government Grant C.P.B.P. 01.07.

REFERENCES

1. E. B. Saloman, J. W. Cooper, D. E. Kelleher, Phys. Rev. Lett. 55, 193 (1985).
2. G. S. Agarwal, J. Cooper, S. L. Haan, P. L. Knight, Phys. Rev. Lett. 56, 2586 (1986).
3. K. Rzażewski, J. H. Eberly, Phys. Rev. A 27, 2026 (1983).

DISPERSION-LIKE PROFILES OF THE ABSORPTIVE RESPONSE OF
A TWO-LEVEL SYSTEM INTERACTING WITH TWO INTENSE FIELDS

A.D. Wilson-Gordon and H. Friedmann

Department of Chemistry
Bar-Ilan University, Ramat-Gan 52100, Israel

A three-peaked resonance fluorescence spectrum has been predicted by Mollow¹ when a two-level system interacts resonantly ($\omega_1 = \omega_{ba}$) with a saturating pump laser. This behavior has been observed in both the collisionless² and collisional³ regimes. The behavior of a weak probe-wave absorption profile in the presence of a pump wave tuned directly to the resonance frequency has also been studied theoretically by Mollow⁴ and experimentally in an atomic beam by Wu et al.⁵ Here again a three-peaked spectrum is obtained reminiscent of the two-level system resonance fluorescence spectrum. However the two sideband absorption peaks whose detuning $|\Delta_2| = |\omega_{ba} - \omega_2|$ (ω_2 is the probe frequency) from the resonance frequency ω_{ba} is slightly larger than the pump Rabi frequency $2|V_1| = |\mu_{ba} E_1|/\hbar$ are part of the dispersion-like features whose negative absorption (gain) peaks appear on that side of the Rabi frequency which is closer to the resonance frequency.

No intuitive explanation for the appearance of the dispersion-like features has been offered so far. In order to gain some insight into this problem we have generalized the approach of Mollow to the case where the pump and probe lasers are of arbitrary strength. These calculations⁶ are similar to those carried out by Toptygina and Fradkin⁷ and by Agarwal and Nayak⁸ for different purposes. Interaction with a strong probe will of course alter the response of the system to pump radiation. We find in general that whenever the probe absorption increases, the pump absorption decreases and vice versa. Thus the dispersive features of the probe absorption lineshape are also obtained in the pump spectrum but with opposite tendencies (see Fig. 1a). The small peaks (dips) appear in the probe (pump) absorption spectrum of Fig. 1a are "Rabi subharmonics"^{7,8}

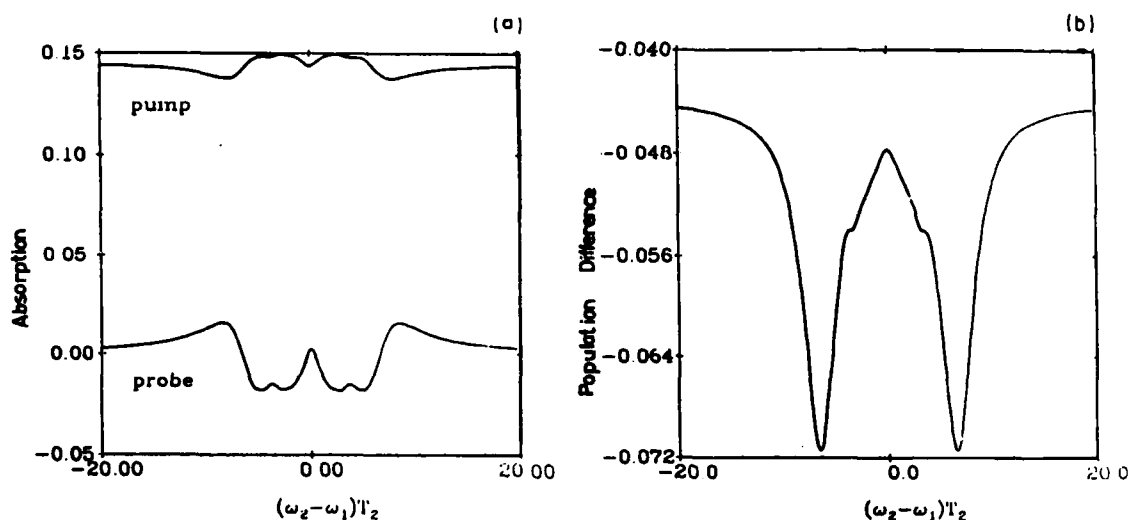


Fig. 1 (a) Pump and probe absorption and (b) population difference for a strong pump and probe of intermediate intensity as a function of $\omega_2 - \omega_1 = \omega_2 - \omega_{ba}$ when $\omega_1 = \omega_{ba}$.

and are due to three-photon processes involving two probe-laser photons and one pump-laser photon. In Fig. 1b, we plot the population difference of the two states as a function of δ for the same intensities as in Fig. 1a. Here we see that when $|\Delta_2| \approx 2|V_1|$, that is, at approximately the center of the dispersion-like features, the population of the ground state is stabilized and population dips are obtained, similar to those found in three-level systems in the presence of two laser fields.⁹

In order to obtain an intuitive understanding of the origin of the dispersive lineshape we have analyzed the probe absorptive response, proportional to $\text{Im}\rho'_{ba}(\omega_2)$, in the limit of low probe intensity¹⁰ and $\omega_1 = \omega_{ba}$. In this limit

$$\text{Im}\rho'_{ba}(\omega_2) = -AV_2[1+B|V_1|^2 - C|V_1|^4] \quad (1)$$

where $2V_2$ is the Rabi frequency of the probe field and

$$A = (1/T_2)(\rho_{bb} - \rho_{aa})^{dc}/(\Delta_2^2 + 1/T_2^2) \quad (2)$$

$$B = [\Delta_2^2(3 + \Delta_2^2 T_2^2) - (T_1 T_2)^{-1}]D^{-1} \quad (3)$$

$$C = 4(1 + \Delta_2^2 T_2^2)D^{-1} \quad (4)$$

$$4D = [4|V_1|^2 + (T_1 T_2)^{-1} - \Delta_2^2]^2 + \Delta_2^2(T_1^{-1} + T_2^{-1})^2. \quad (5)$$

The first term in the steady-state expression Eq. (1) describes one-probe-photon absorption together with spontaneous one-photon emission (determined by the factor A) needed to reach the steady state. The second term describes the absorption of a probe photon and a pump photon together with the spontaneous emission of a photon in a three-photon scattering (TPS) process. The third term corresponds to the stimulated emission of a probe photon and the absorption of two pump photons in a four-photon scattering (FPS) process. The competition between TPS and FPS produces the dispersive behavior of the probe-absorption spectrum at the dressed-atom-states resonances $\omega_2 - \omega_1 = \pm 2|V_1|$ (if $|V_1| \gg 1/T_1, 1/T_2$) determined by the resonance denominator D of Eq. (5). This is confirmed by the transformation of the Bloch equations to the dressed-atom-state representation.

1. B.R. Mollow, Phys. Rev. 188, 1969 (1969).
2. F. Schuda, C.R. Stroud, Jr., and M. Hercher, J. Phys. B 7, L 198 (1974).
3. J.L. Carlsten, A. Szoke, and M.G. Raymer, Phys. Rev. A 15, 1029 (1977).
4. B.R. Mollow, Phys. Rev. A 5, 2217 (1972).
5. F.Y. Wu, S. Ezekiel, M. Ducloy, and B.R. Mollow, Phys. Rev. Lett. 38, 1077 (1977).
6. H. Friedmann and A.D. Wilson-Gordon, in "Methods of Laser Spectroscopy", eds. Y. Prior, A. Ben-Reuven and M. Rosenbluh (Plenum, N.Y., 1986); Phys. Rev. A (submitted).
7. G.I. Toptygina and E.E. Fradkin, Zh. Eksp. Teor. Fiz. 82, 429 (1982) (Sov. Phys. JETP 55, 246 (1982)).
8. G.S. Agarwal and N. Nayak, J. Opt. Soc. Am. B 1, 264 (1984); Phys. Rev. A 33, 391 (1986).
9. B.J. Dalton and P.L. Knight, Opt. Commun. 42, 411 (1982); P.M. Radmore and P.L. Knight, J. Phys. B 15, 561 (1982).
10. R.W. Boyd, M.G. Raymer, P. Narum, and D.J. Harter, Phys. Rev. A 24, 411 (1981).

Autler Townes Splittings for Realistic Pulsed Lasers

P T. Greenland

Theoretical Physics Division, AERE Harwell,
Didcot, Oxon OX11 0RA.

In a series of papers^{1,2,3} the possibility of observing multipeak structures in Double Optical Resonance (DOR) experiments when the pump laser is a transfer-limited pulsed laser was considered. This work extends these results to more realistic situations. In particular both magnetic degeneracy of the atomic levels and Doppler motion of the atoms will be included. The enhancement of the multipeak structure when opposed laser beams are used is important for an experimental test of the predictions, and although many features of the magnetic degeneracy can be seen in the DOR spectrum, they do not alter its fundamental nature.

Other deviations from the ideal experiments envisaged in (1)-(3) will also be considered. These include phase interrupting collisions, lack of reproducibility of pulse shape and laser bandwidth. This enables a more realistic estimate of DOR spectra with pulsed pump lasers to be made.

1. P. T. Greenland, J.Phys.B.At.Mol.Phys. 18 401 (1985).
2. P. T. Greenland Optica Acta 33 723 (1986).
3. M. A. Lauder, P. L. Knight, P. T. Greenland, Optica Acta 33 1231 (1986).

Photoionization Photodetachment and Pre-Exponential Decay

P. T. Greenland and A. M. Lane

Theoretical Physics Division, AERE Harwell,
Didcot, Oxon OX11 0RA, UK.

The decay of a quantum mechanical system has been extensively studied. It is known that if the interaction responsible for the decay of a prepared state is switched on suddenly a certain time elapses before the decay law settles down to its usual exponential form. Since photoionization with a monochromatic laser can be considered as the decay of a dressed state, and since many features of this state are under experimental control, general features of a decaying system may be observed in photoionization experiments.

This work will discuss the possible observation of deviation from exponential decay laws in laser photoionization and photodetachment experiments. The key point is, that the stochastic processes which give rise to the bandwidth of a broad band laser impose a temporal structure on the laser field, and this temporal structure may be used to probe short time-scales in photoionization. Renewal processes, in which the laser phase is randomly incremented at intervals randomly selected from a given distribution will be treated in some detail, and a simple extension in both time and frequency domains will be made, so that arbitrary stochastic processes may be discussed.

The theory will be applied to the photoionization of atoms or positive ions, and the photodetachment of negative ions, with particular emphasis on the experimental observation of the characteristically different pre-exponential decay laws to be expected in these cases. These differences will be related to the threshold behaviour of the photoabsorption cross section.

Extension of the theory to describe the decay law near an autoionizing level will be considered; in particular the time evolution of the decay probability at the Fano minimum will be discussed, and it will be shown that the electron production rate there falls strictly to zero, only for long times. As is well known, this is a quantum mechanical interference phenomenon. The lack of total destructive interference when the photoionizing laser is not completely-coherent leads to electron production at a Fano minimum.

Finally the experimental criteria required to observe these effects will be discussed, in particular the effect of finite laser rise time will be examined. Some comments on the relevance of this work, both to the observation of post exponential decay, and the so called quantum Zeno paradox will be made.

THRESHOLD EFFECTS IN A MODEL OF MULTIPHOTON IONIZATION

B. Piraux and P. L. Knight
 Blackett Laboratory, Imperial College
 London SW7 2BZ
 England

It is well known that a strong radiation field can create a structure in the continuum which is similar to the one produced by configuration interaction when a discrete state is embedded in the continuum.¹ This structure is characterized by a density of states rapidly varying with energy. In our model we assume this density of states to be Lorentzian truncated at $E=0$ and normalized to unity in the energy space. This structured set of continuum states $|E\rangle$ is coupled to a discrete state $|0\rangle$ by a radiation field classically described by $\xi = \xi_0 \cos \omega t$. The modulus squared of the coupling function is given by

$$|V_{0E}|^2 = \frac{V^2 \gamma}{\left[\frac{\pi}{2} + \arctan\left(\frac{\bar{E}}{\gamma}\right) \right]} \cdot \frac{1}{(E-\bar{E})^2 + \gamma^2} \quad (1)$$

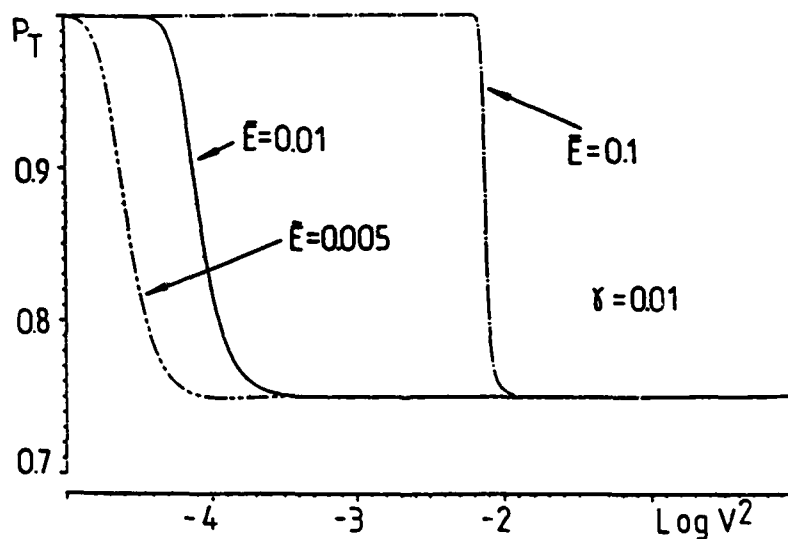
where the constant V characterizes the strength of the interaction; \bar{E} and γ are respectively the center and the half width of the Lorentzian. The wave function of the system is expanded in terms of the states $|0\rangle$ and $|E\rangle$:

$$|\psi(t)\rangle = C_0(t)|0\rangle + \int_0^\infty dE C_E(t)|E\rangle \quad (2)$$

The time dependent probability amplitudes $C_0(t)$ and $C_E(t)$ are obtained by solving the Schrödinger equation by means of the usual Laplace transform method within the Rotating Wave Approximation.

We first analyze the time evolution of the population $|C_0(t)|^2$ of the discrete state at the resonance; for small V , when the threshold effects are negligible, the discrete state population decays exponentially as expected (Weisskopf-Wigner law). This decay becomes incomplete when V increases; in addition $|C_0(t)|^2$ exhibits Rabi

oscillations as a function of time. The physical interpretation is clear: since a Lorentzian structure may be induced by the coupling of a discrete state embedded in a flat continuum, we might expect for large V a strong coupling between this state and the ground state $|0\rangle$ giving rise to Rabi oscillation in the probability of occupation of the unperturbed states; in that case, it is more convenient to use the concept of dressed states² and see the problem as a decay of a superposition of two dressed states coupled to a flat continuum. This decay will lead to quantum beats and two peaks in the electron spectrum separated by the Rabi frequency (Autler-Townes effect). However, for increasing V , one of the dressed states moves down and may lie below the edge of the flat continuum: in that case, there is no decay of this dressed state and the second peak in the spectrum disappears. This point is confirmed by our calculations and results about the spectrum will be presented. This analysis is also confirmed by the fact the total probability $P_T = |C_0|^2 + \int_0^\infty dE |C_E|^2$ at $t \rightarrow \infty$ may be less than 1 for large V as shown in the figure.



REFERENCES

1. L. Armstrong, Jr., B. L. Beers and S. Feneuille, Phys. Rev. A **12**, 1903 (1975).
2. P. L. Knight, J. Phys. B **12**, 3297 (1979).

Threshold Excitation of Rydberg Series by Intense Laser Fields

G. Alber and P. Zoller

Institute for Theoretical Physics

University of Innsbruck, A-6020 Innsbruck, Austria

Excitation of a neutral atom by a laser pulse close to the photoionization threshold is an interesting dynamical problem due to the presence of the infinite number of Rydberg states, which are involved in the excitation process. This represents therefore the extreme opposite limit to the excitation of isolated atomic states, which is well understood on the basis of a "two"-...level approximation and assumes that the Rabi-frequency, which determines the strength of the laser induced coupling between the resonantly coupled states, is much smaller than the energy separation between adjacent excited states.

We have developed a theory of excitation of atoms close to the photoionization threshold. It is based on the observation that the effect of laser radiation on atoms can be described as a finite volume interaction coupling Coulombic dissociation channels¹. This offers the possibility to treat laser- and electron correlation induced channel couplings on the same footing within the framework of a multichannel quantum defect theory (MQDT)² with intensity dependent MQDT-parameters. Therefore this approach extends the well known "two"-...level theories as it is able to deal with the coupling of a Rydbergseries and the adjoining continuum as a whole (=excitation channel) to a bound state and to characterize it in terms of a few energy independent MQDT-parameters. Electron correlation effects like autoionization are also easily included. Within this theory we obtain simple analytical (asymptotic) expressions for the observables, such as ground state- or ionization probability, describing the excitation process close to threshold.

As an example Figs.1a,b,c show the ground state probability P as a function of the laser pulse duration τ for three values of the mean excited energy $\bar{\epsilon} = \epsilon_g + \omega = -1/2\bar{\nu}^2$ (a.u.) representing three characteristic dynamical situations. Whereas for laser excitation far below threshold the

atom exhibits a "few"-level dynamics, which manifests itself in slightly modified Rabi-oscillations of the ground state probability (see Fig. 1a), the excitation dynamics close to threshold is quite different (see Figs. 1b,c). In particular, the following physical picture emerges from our theory:

(1) The threshold excitation regime is characterized by the fact that many Rydberg states are excited, i.e. $\Delta\nu \approx \tau \cdot \bar{\nu}^3 \gg 1$ (a.u.), which is a combined condition on the laser intensity and the mean excited energy $\bar{\epsilon}$. Thereby the spectral energy width, which is associated with the excitation process, is determined by the ionization rate τ (extrapolated below threshold). This implies that the excitation is localized in time to a time interval of order $1/\tau$, which is much smaller than the classical orbiting times $T_e = 2\pi \bar{\nu}^3$ (a.u.) of the excited Rydberg states.

(2) As the ground state of the atom is localized to a volume of the order of a few Bohr radii only the radial dependence of the excited state wavefunctions in this spatial region is important for the excitation process, which is much smaller than the extension of typical Rydberg states. So the excitation process is localized in space.

This localization of the excitation process in space and time implies that the laser pulse creates a radial electronic wavepacket.

The time scale associated with the motion of this wave packet is the classical orbiting time of an electron in the Coulomb field of the atomic core T_e . Figs 1b,c show that for short laser pulses, i.e. $\tau \ll T_e$, the ground state amplitude exhibits an exponential decay governed by the ionization rate τ , which we would expect for the decay of a bound state into a continuum. For long laser pulses, i.e. $\tau > T_e$, the excited electronic wavepacket is deexcited by stimulated transitions back to the ground state as soon as it approaches the atomic core. Figs 1b,c also indicate the spreading of the excited radial wavepacket, which manifests itself in the broadening of the stimulated emission peaks (revivals) ³.

References:

- /1/ A.Giusti and P.Zoller (in preparation)

/2/ M.J.Seaton, Rep.Prog.Phys. 46, 167 (83)

/3/ G.Alber and P.Zoller (in preparation)

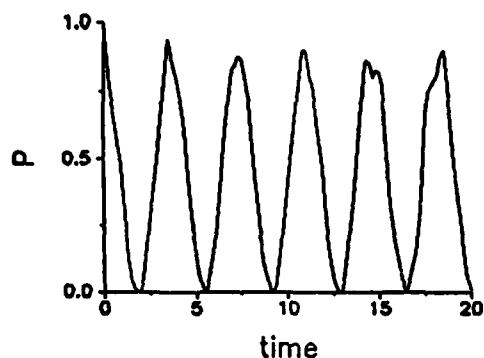


Fig.1a: Ground state probability as a function of the laser pulse duration τ in units of the mean classical orbiting time T_E with $\bar{\nu} = 50$, $\gamma = 10^{-6}$, $\alpha = 0$ (quantum defect of excited Rydberg series).

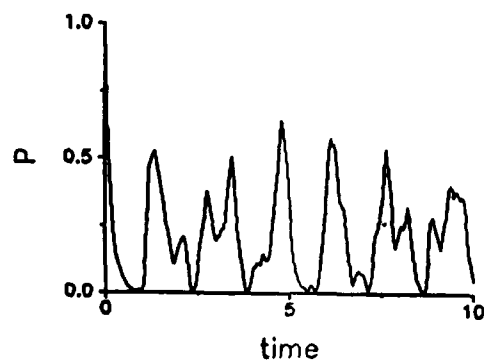


Fig.1b: Same as Fig.1a with $\bar{\nu} = 100$, $\gamma = 10^{-6}$, $\alpha = 0$.

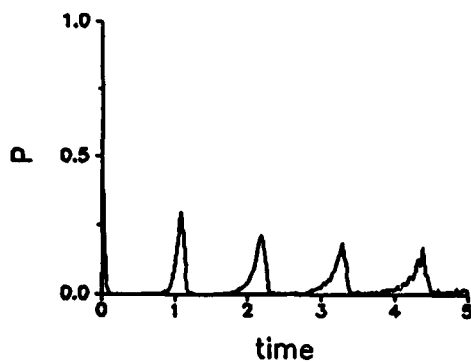


Fig.1c: Same as Fig.1a with $\bar{\nu} = 200$, $\gamma = 10^{-6}$, $\alpha = 0$.

Rydberg wave packets in many electron atoms generated by short laser pulses

G. Alber, W. A. Henle, H. Ritsch and P. Zoller

Institute for Theoretical Physics,

University of Innsbruck, 6020 Innsbruck, Austria

An atomic electron excited by a short laser pulse from a low lying bound state to a superposition of many Rydberg states corresponds to a (radial) wave packet moving on a Kepler orbit [1]. Wave packets are generated in this case because (i) the photon absorption from the initial bound state is localized in space in a volume small compared to a Rydberg orbit; and (ii) the laser pulse duration τ is assumed to be short so that its spectral width \hbar/τ simultaneously excites many Rydberg states around some mean principal quantum number \bar{n} : $\hbar/\tau \gg dE_n/dn|_{\bar{n}}/2\pi \approx \hbar/T_{E_{\bar{n}}}$ with E_n the Rydberg energies and $T_{E_{\bar{n}}}$ the classical orbit time corresponding to the mean excited energy $E_{\bar{n}}$.

The dynamics of the motion of the wave packet can be observed in a two-photon experiment where a first short pulse excites the wave packet, which at a later time is probed by a second short pulse. The transition probability of this two-photon process as a function of the time delay will show peaks whenever the time between the two laser pulses is a multiple of the classical orbit time (quantum beats between n -states). This allows us to study quantum and classical aspects of the electron motion in a truly time-dependent way.

In a many electron atom a (single) valence electron excited to a Rydberg wave packet can exchange energy with the ion core (electron correlation), whenever the wave packet passes through the atomic core region. Since the spatial extent of the Kepler orbit is much larger than the size of the atomic core we can view this orbiting of the electron as a succession of below-threshold (in)elastic scattering events from the ion core. The study of wave packets in the many electron atom will thus measure a "below threshold" scattering matrix reflecting the electron core interaction.

We have developed a theory of two-photon processes with short time delayed pulses based on a "smooth" multichannel quantum defect theory (MQDT) Green function. The theory allows us to derive simple analytical expressions for the transition probabilities which have a straightforward physical interpretation and are directly related to the MQDT parameters obtained in the conventional MQDT analysis of spectroscopic data.

As an example, Fig. 1 shows a plot of a two-photon transition probability as a function of the time delay between two laser pulses in an atom with two interacting Rydberg series (with ionization thresholds $I_1 < I_2$). The first two peaks labeled by (0,1) and (1,0) correspond to a single revolution of the wave packet in the first ($\Delta\tau \approx T_1$) and second ($\Delta\tau \approx T_2$) channel, respectively. The peak denoted by (1,1) is associated with a wave packet having made one revolution on the first (second) orbit, being scattered inelastically by electron ion-core interaction into the second (first) orbit ($\Delta\tau \approx T_1 + T_2$); the height of this peak is thus a measure of the electron correlation between channel 1 and 2.

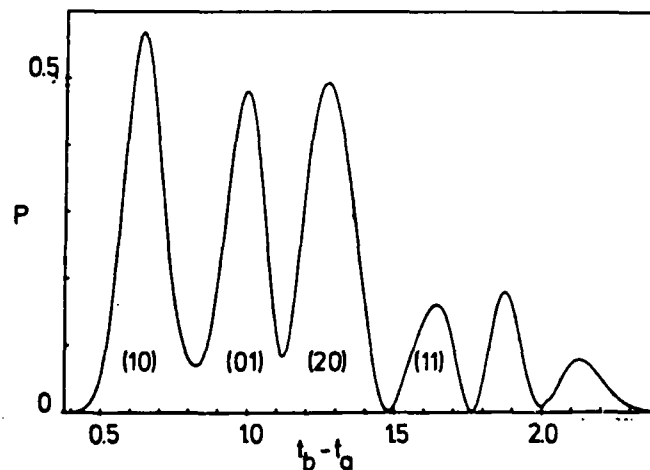


Fig.1 Two-photon transition probability as function of time delay.

References:

1. G. Alber, H. Ritsch and P. Zoller, Phys. Rev. A 34, 1058 (1986)
2. W. A. Henle, H. Ritsch and P. Zoller, submitted for publication.
3. D. Parker and C. R. Stroud jr., Phys. Rev. Lett. 56, 716 (1986)

A NEW ASPECT OF RESONANT MULTIPHOTON PROCESSES IN MOLECULES : THE PARITY SELECTIVITY

D. GAUYACQ, S. FREDIN, Ch. JUNGEN and M. HORANI

Laboratoire de Photophysique Moléculaire du CNRS

Bâtiment 213 - Université de Paris-Sud,

91405 - ORSAY Cedex France

The role of near-resonant intermediate states in multiphoton processes has been demonstrated in a number of previous works on optical multiphoton absorption (1,2), multiphoton photoelectron spectroscopy (3) and multiphoton dissociation (4). A different and new aspect concerning the influence of the near-resonant intermediate states on the parity selectivity is presented. The parity selectivity does not act as a selection rule but rather as a propensity rule on molecular symmetry.

The symmetry propensity rules are established for a 3-photon transition between two Π states, in the case of a dominant contribution to the 3-photon transition probability from a near-resonant Σ state. Selective population of only one Λ -doublet component in the upper Π state can be achieved regardless of the experimental resolution.

As an illustration the three-photon line strengths of the NO, $C^2\Pi-X^2\Pi$ (0,0) band have been calculated by considering the dominant near-resonant pathways via the $A^2\Sigma^+$ state. The parity selection in the upper $C^2\Pi$ state is confirmed by experimental observations as shown in Figure 1 in which part of the N_{12} branch of the NO, C-X 3-photon band is displayed. Figures 1a and 1b show the calculated 3-photon line strengths when only the symmetry selection rules are considered (the tensor formalism of Dixon et al (5) has been used with the corresponding ratio between the tensor components : $[T_{+2}^3(B) + T_{-2}^3(B)] / T_0^3(B) = (a)0 ; (b)1$). Figure 1c displays the calculated 3-photon line strengths when the symmetry propensity rules are considered.

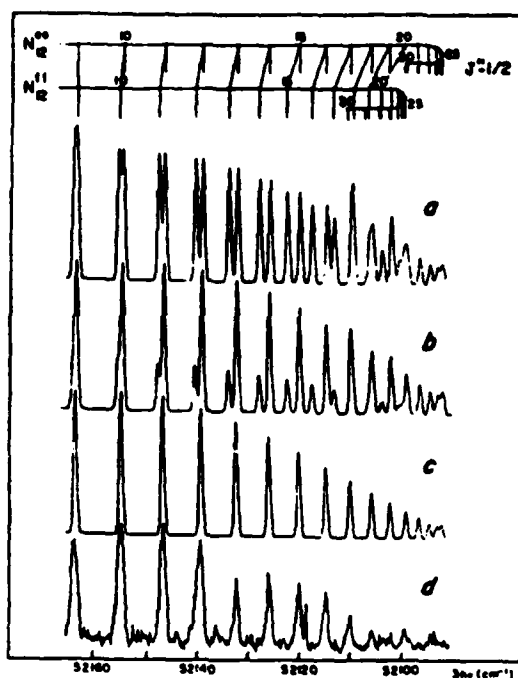


Figure 1

Figure 1d shows the experimental (3+2) MPI spectrum. As shown by the complete agreement between the calculated (1c) and experimental (1d) spectra, a selective population of the Π^+ Λ -doublet component is obtained via the N_{12} absorption line. This example corresponds to the most dramatic case of parity selection via multiphoton excitation. However, in most cases the parity selection is only partially achieved, hence appearing as a propensity rule rather than a selection rule.

In photodynamic studies of excited molecular states, the MPI technique is often used as a sensitive and selective probe of the reaction products. The parity selection (total or partial) introduced by the multiphoton probe has to be taken into account, especially in the case where the geometry of the photon-induced reaction is studied by measuring the relative population of the photo-fragment Λ -doublets. The multiphoton symmetry propensity rules provide substantial simplification in many other applications especially when the multiphoton technique is combined with double resonance, as has been shown in a recent study of Rydberg states of NO (6).

- (1) - Ph. A. Freedman, Can. J. Phys., 55 (1977) 1387.
- (2) - R.S. Tapper, R.L. Whelen, G.S. Ezra and E.R. Grant, J. Chem. Phys., 88 (1984) 1273.
- (3) - J.C. Miller and R.C. Compton, J. Chem. Phys., 75 (1981) 22.

- (4) - L. Biglo, R. S. Tapper and E. R. Grant, J. Chem. Phys., 88 (1984) 1271.
- (5) - R. N. Dixon, J. M. Bayley and M. N. R. Ashfold, Chem. Phys., 84, (1984) 21.
- (6) - S. Fredin, D. Gauyacq, M. Horani, Ch. Jungen, G. Lefevre and F. Masnou-Seeuws, Mol. Phys. (1987).

Determination of the multiphoton ionization cross sections in the resonant case

G. Sultan and G. Baravian

Laboratoire de Physique des Gaz et des Plasmas - Associé au CNRS -
Université de Paris-Sud 91405 ORSAY FRANCE

The multiphoton ionization (MPI) cross-section is determined in the case where the ionization of neutral particles takes place via an intermediary resonant state. A preliminary simplified model using a square laser pulse is presented and it gives general informations about the evolution of the different species versus the time and the flux value afterwards a more realistic model is used to determine the RMPI cross section for the carbon monoxide.

The diagram in figure 1 shows the levels and the processes taken into account. The equations governing the evolution of the different species are the following

$$dn_1/dt = -w_1 n_1 + \beta n_2 - w^+ n_1 \quad (1)$$

$$dn_2/dt = w_1 n_1 - w_2 n_2 - \beta n_2 \quad (2)$$

$$dn^+/dt = w_2 n_2 + w^+ n_1 \quad (3)$$

where n_1 , n_2 , and n^+ represent respectively the populations of the ground state, the resonant state and the continuum with probabilities designed by w_1 for the transition $1 \rightarrow 2$, w_2 for $2 \rightarrow c$, and w^+ for $1 \rightarrow c$, β represents all the terms for depopulation of n_2 other than $2 \rightarrow 3$ as for example the deexcitation towards a lower level or the dissociation in molecules. In the case where w^+ is weak as compared to w_1 and w_2 , w_1 , w_2 and β are supposed to be constant during the time of interaction, the evolution of the

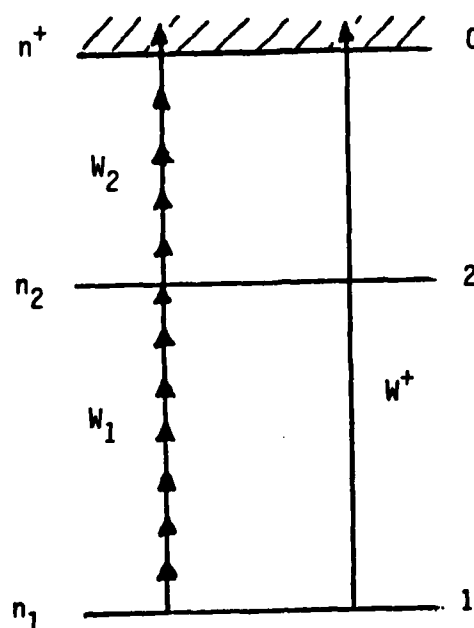


Figure 1

of the populations may be written

$$n^+(t) = n_1(0) \{1 + (a/b) \text{shbt.exp}at - \text{chbt.exp}at \} \quad (4)$$

$$n_1(t) = n_1(0) \text{exp}at \{(-w_1 + w_2 + \beta)/(2b) \text{shbt} + \text{chbt} \} \quad (5)$$

$$n_2(t) = n_1(0) (w_1/b) \text{shbt.exp}at \quad (6)$$

where $n_1(0)$ is the population of the ground state at the time $t=0$,

$$a = (w_1 + w_2 + \beta)/2 \text{ and } b = (1/2) \sqrt{(w_1 + w_2 + \beta)^2 - 4 w_1 w_2}$$

In the case where β is negligible, the solution for n^+ can be written

$$n^+(t) = n_1(0)/(w_1 - w_2) \{w_1 (1 - \exp(-w_2 t)) - w_2 (1 - \exp(-w_1 t))\} \quad (7)$$

Let $w_1 = \sigma_m \phi^m$ and $w_2 = \sigma_n \phi^n$ where σ_m and σ_n are respectively the cross-sections for interactions with m and n photons for the transitions $1 \rightarrow 2$ and $2 \rightarrow c$. The analysis of the expression (7) gives the following results

(i) for weak values of the laser flux ϕ we have $w_1 \tau \ll 1$ and $w_2 \tau \ll 1$

where τ is the pulse duration, then $n^+(t)$ takes the form $n^+(t) = n_1(0) w_1 w_2 \tau^2 / 2 = \phi^{m+n}$, the slope of the curve $\ln n^+$ vs $\ln \phi$ is equal to $m+n$ with the obvious condition that it is possible to create at least one ion with these flux values

(ii) for intermediate values of ϕ , if $n < m$, it happens that only the transition $2 \rightarrow c$ is saturated ($w_1 \tau \ll 1$ and $w_2 \tau \approx 1$), this leads to $n^+(t) = n_1(0) w_1 \tau / e = \phi^m$, the slope is equal to m

(iii) for high values of ϕ , $w_1 \tau \approx w_2 \tau \approx 1$, n^+ does not depend on ϕ and the slope is equal to 0.

Application to CO

When the laser flux is not constant but varies both versus time and space it is possible to obtain only numerical results.

For a Gaussian spatio-temporal distribution of the power density within the focal region the flux takes the form

$$\phi(r, z, t) = \phi_0 S_0 / S_z \cdot \exp\{-(r/r_0)^2 - (t-t_0)^2\} \quad (8)$$

where ϕ is the maximum flux reached at time $t=t_0$ for $r=0$ and $z=0$ (see figure 2), $S_0 = \pi b^2$ and $S_z = \pi r_0^2$.

The eq.(8) allows us to determine, at any time, isophote surfaces [1]. The surface corresponding to a flux ϕ_α is related to the flux ϕ by the relation

$$\phi_\alpha(r, z, t) = \phi(t)/\alpha \quad (9)$$

where α is an arbitrary attenuation factor and

$$\phi(t) = \phi \exp\{-[t-t_0]/\tau\}^2\}$$

The equation of the isophote surfaces can be written as

$$r^2/b^2 = (z^2/a^2 + 1) \ln(\alpha a^2/z^2 + a^2)$$

and are quasi-ellipsoidal.

In order to evaluate the number of particles we define an elementary volume dV bounded by 2 isophotes corresponding to 2 factors $\alpha=A^i$ and A^{i+1} . The number of ions created in the shell during the time dt is calculated by using the eq.(1) (2) and (3). The cross sections for CO σ_7 and σ_5 for interactions with 7 and 5 $h\nu$ are determined by adjusting the experimental data [2] and the calculated ones by using the preceding model, the results are (fig. 3)

$$\sigma_7 = 3 \times 10^{-84} \text{ s}^{-1} (\text{W}/\text{cm}^2)^{-7} \text{ and}$$

$$\sigma_5 = 3.2 \times 10^{-55} \text{ s}^{-1} (\text{W}/\text{cm}^2)^{-5} .$$

[1] G. Baravian and G. Sultan Physica 128C, 343 (1985)

[2] G. Sultan and G. Baravian Chemical Physics 103,417(1986)

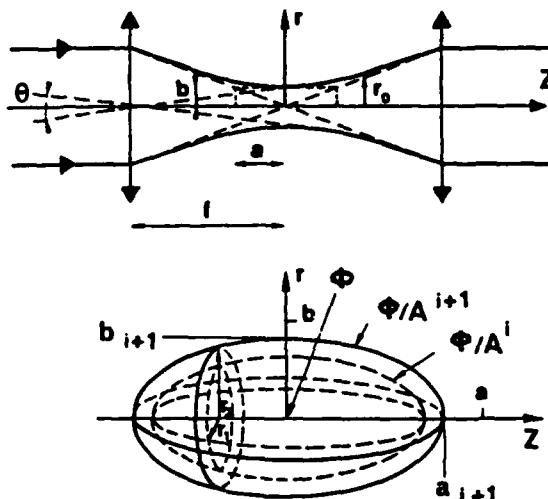


Figure 2

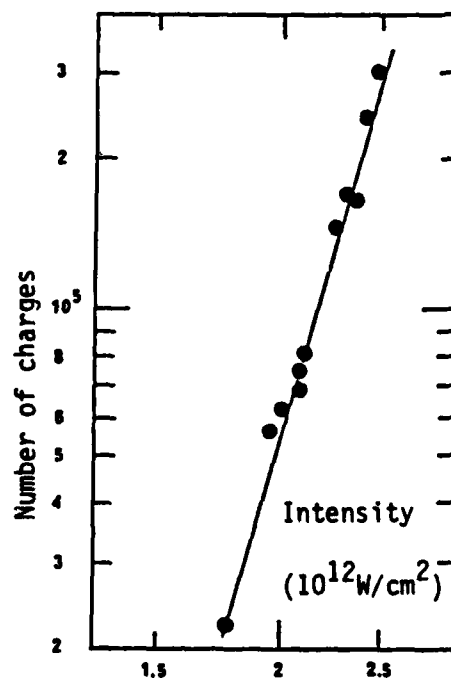


Figure 3

SERIAL AND PARALLEL MULTILEVEL SYSTEMS

E. Kyrölä

Department of Physics, University of Helsinki
Siltavuorenpenger 20 D, 00170 Helsinki 17, Finland
and

M. Lindberg

Optical Sciences Center, University of Arizona
Tucson, Arizona 85721, USA

Multiphoton processes in atoms and molecules are traditionally analyzed by using perturbation theory (see e.g., Ref. [1]). In cases where the driving field is strong or nearly resonant the perturbation approach cannot be trusted and more accurate solutions are needed. For two- and three-level systems exact solutions are in many cases straightforward to obtain and the related non-perturbative phenomena like Rabi oscillations, saturation and dynamic Stark-splitting are well-known. If genuine multilevel systems are considered exact solutions are usually impossible to find and numerical calculations must be used. We will consider here a method which can be used to facilitate the analysis of such complicated multilevel problems.

We consider an N -level system where various levels are coupled together by external field. We describe the dynamics by the Schrödinger equation ignoring all incoherent processes. We assume further that the time-dependence can be removed from the Hamiltonian. The problem is then solved if the eigenvalues and eigenvectors of the time-independent Hamiltonian can be found. However, it is clear that an arbitrary N -level Hamiltonian is complicated enough to prevent a general solution. On the other hand, if we consider different N -level configurations from topological point of view we can find two special forms for which several exact solutions have been found (see e.g., Ref. [2]). These are so-called serial and parallel configurations (see Fig. 1). Both systems have been found to display periodical behaviour different from familiar Rabi oscillations in few-level systems. In the serial system the population moves in the form of a wave from one end of the ladder to another whereas in the parallel system the ground state population periodically decays and recurs.

The known dynamics is not the only feature which distinguishes the serial and parallel systems from other multilevel configurations. They both also share the property being structurally the simplest N -level systems i.e., they have only the minimal $N - 1$ couplings whereas a general N -level system may have $N(N - 1)/2$ couplings. It seems therefore worthwhile to seek connections between these spe-

cial systems and arbitrarily coupled multilevel systems. The connections can be established by finding unitary transformations which change the representation of a given Hamiltonian matrix into the desired serial or parallel form. If such transformations are found we can investigate the dynamics of a given multilevel system in the equivalent serial or parallel setting.

We have shown [3] that for three- and four-level systems the transformations to serial and parallel form can be easily found. These transformations can be used to investigate conditions for coherent population trapping. For higher dimensional systems transformations are possible to find only for some specialized coupling schemes. We have succeeded in finding the transformations between the serial and parallel systems themselves. This has made it possible to consider how the recurrence dynamics and the population wave dynamics are related to each other.

[1] P. Lambropoulos, in *Advances in Atomic and Molecular Physics*, Vol. 12, edited by D.R. Bates and B. Bederson (Academic Press, New York, 1976).

[2] C.D. Cantrell, V.S. Letokhov and A.A. Makarov, in *Coherent Nonlinear Optics, Recent Advances*, edited by M.S. Feld and V.S. Letokhov (Springer, Heidelberg, 1980).

[3] E. Kyrölä and M. Lindberg, *Phys. Rev. A* (in press).

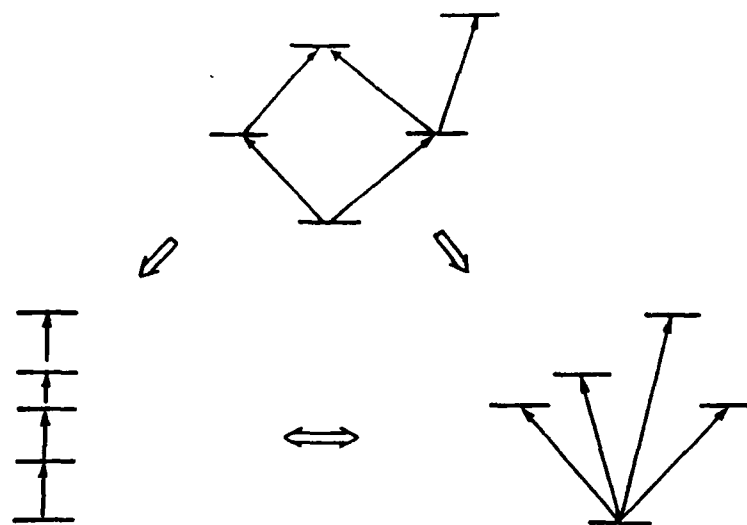


Fig.1 By unitary transformations an arbitrary multilevel system (top) can be brought into serial (left) or parallel (right) form. These special forms are also related by unitary transformations.

Comments on Estimating Nonresonant Multiphoton Ionization Rates*

Bruce W. Shore, *Lawrence Livermore National Laboratory*

Time dependent perturbation theory provides the following expression for the rate at which a single atom absorbs n photons via multiphoton transitions between initial field-atom state $|i\rangle$ and final field-atom state $|f\rangle$:

$$Rate_n = \frac{2\pi}{\hbar} |\langle f | T_n(E_i) | i \rangle|^2 \delta(E_i - E_f).$$

$T_n(E)$, the transition operator responsible for this process, is the product of n dipole-interaction operators, interspersed with $n-1$ operators $(E-H^0)^{-1}$, with summations over intermediate-state energies. In general this product will be sensitive to photon frequency ω and will exhibit resonance properties. If the frequency ω is not near any resonant frequency, we can approximate the products by an average energy $\hbar\Delta_n$ raised to the power $n-1$. This traditional approximation enables us to write the n -photon transition rate as

$$Rate_n = \frac{2\pi}{\hbar} \tilde{\omega}_n(b) \left| \hbar\Delta_n \langle b | \left(\frac{d \cdot \epsilon}{\hbar\Delta_n} \right)^n | a \rangle \right|^2 \left(\frac{2\pi I}{c} \right)^n.$$

where ϵ is the polarization unit vector and I is the intensity, and the atomic states (as contrasted with the field-atom states) are $|a\rangle$ and $|b\rangle$. The density of states $\tilde{\omega}_n(b)$ expresses, amongst other factors, the n th order correlation function for the electric field, and so it parameterizes the statistical properties of the radiation.

Work by Lambropoulos (1985) suggests that photon flux F (photons per unit area per unit time) rather than photon intensity $I = \hbar\omega F$ is the significant quantitative measure of the field-atom interaction in the rate-equation regime. It is useful to express formulas by means of dimensionless ratios involving atomic units. For that purpose we introduce the atomic unit of length a_0 , of energy, e^2/a_0 , of time τ_{AU} , and of flux \mathcal{F}_{AU}

$$\tau_{AU} = \frac{a_0 \hbar}{e^2} = 2.42 \times 10^{-17} \text{ sec}, \quad \mathcal{F}_{AU} = \frac{1}{a_0^2 \tau_{AU}} = 1.496 \times 10^{33} \text{ cm}^{-2} \text{ sec}^{-1}.$$

It is useful to parameterize the rate coefficient by introducing a dimensionless *flux utilization factor* ζ_n such that the rate coefficient takes the form

$$Rate_n = \frac{1}{\tau_{AU}} \left(\frac{\zeta_n F}{\mathcal{F}_{AU}} \right)^n.$$

That is, the rate coefficient is the atomic unit of rate, times the dimensionless ratio $(F/\mathcal{F}_{AU})^n$, times the dimensionless factor

$$(\zeta_n)^n = \tilde{\omega}_n(b) (\hbar \Delta_n)^2 \left| \langle b | M^n | a \rangle \right|^2.$$

The operator M that appears here is

$$M = \sqrt{\frac{2\pi\hbar\omega}{c}} \mathcal{F}_{AU} \frac{d.\epsilon}{\hbar\Delta_n} = \sqrt{2\pi\alpha} \sqrt{\frac{\hbar\omega}{e^2/a_0}} \frac{(e^2/a_0)}{\hbar\Delta_n} \frac{d.\epsilon}{ea_0}.$$

The work by Lambropoulos (1985) can be interpreted as providing the following values for ζ_n for multiphoton ionization of a wide variety of atoms:

$$\zeta_2 = \zeta_3 = 1, \quad \zeta_4 = 2, \quad \zeta_n = 3 \text{ for } n > 4.$$

Multiphoton rates may therefore be expected to become increasingly important for photon fluxes approaching the value of $10^{33} \text{ cm}^{-2} \text{ sec}^{-1}$.

It is customary to parameterize the single-photon rate coefficient by means of a cross section. This cross section $\sigma_1(a \rightarrow b)$ is usually defined as the ratio of the rate per atom to the photon flux F . It is

$$\sigma_1(a \rightarrow b) = \frac{Rate_1}{F} = a_0^2 \zeta_1 = (2\pi a_0)^2 \left(\frac{\omega a_0}{c} \right) \left(\frac{e^2}{a_0} \right) \tilde{\omega}_1(b) \left| \langle b | \frac{d.\epsilon}{ea_0} | a \rangle \right|^2.$$

There are several ways to extend this definition to n -photon processes and thereby parameterize the dependence of the rate coefficient $Rate_n$ upon the n th power of light intensity I or photon flux F . One traditional way introduces a "generalized cross section" as the ratio of $Rate_n$ to $(F)^n$. An alternative definition as the ratio of $Rate_n$ to $(I)^n$ is also used. In either case the "generalized cross section" has unusual n -dependent units, and takes a wide range of values. A more satisfactory definition maintains area as the units for cross section, and defines an n -photon cross-section $\sigma_n(a \rightarrow b)$ by the formula

$$\frac{Rate_n}{F} = \sigma_n(a \rightarrow b) \left(\frac{F}{\mathcal{F}_{AU}} \right)^{n-1}.$$

This expression differs from the definition of the single-photon cross section only by the dimensionless ratio of photon flux to atomic unit of flux. This n -photon cross section has the expression

$$\sigma_n(a \rightarrow b) = (a_0)^2 (\zeta_n)^n \left(\frac{F}{\mathcal{F}_{AU}} \right)^{n-1} = \sigma_1(a \rightarrow b) \frac{(\zeta_n)^n}{\zeta_1}$$

This expression provides a simple scaling relationship involving only the single-photon cross section and the flux utilization factor. The present parameterization is, according to the published expressions of Lambropoulos (1985), only very weakly dependent on n for $n > 4$, and a value of $\zeta_n = 3$ would appear to be suitable for most cases. The simplicity of this result suggests that the flux utilization factor may offer a more useful descriptor of multiphoton rates than does a generalized cross section.

References: P. Lambropoulos, Phys. Rev. Lett. 55, 2141 (1985); P. Lambropoulos and X. Tang, JOSA B (May, 1987) *in press*.

* This work was performed under the auspices of the United States Department of Energy by the Lawrence Livermore National Laboratory under contract W-7405-Eng-48.

Classical vs. Quantum Description of Above-Threshold Ionization

Jonathan Parker and C. R. Stroud, Jr.

Institute of Optics

University of Rochester

Rochester, NY 14627

We present the results of two calculations of above-threshold ionization of hydrogen. The applied field is taken to have a gaussian pulse shape, and a duration of several optical cycles.

The first calculation is completely classical. We integrated Newton's equations for an ensemble of classical electrons which initially are distributed in a way that approximates the probability distribution for a quantum mechanical bound state.

The second calculation is semiclassical using a classical field identical to that used in the previous calculation, and a quantum mechanical atom. We numerically solve Schrödinger's equation for a complete set of discrete states which are the eigenstates of a hydrogen atom in a spherical cavity of large radius.

The excitation of an ensemble of classical electrons is found to have a characteristic intensity dependence not found in general in the quantum mechanical case. For example, classically in a one-photon transition from a bound state to the continuum, the atom absorbs energy approximately at the Fermi Golden Rule rate. However, the excited-state electron energy distribution may be strikingly different in the two cases. The highest energy of the classical electrons will be intensity dependent rather than $\hbar\omega$ above the ground state as in the quantum mechanical case. As the field becomes intense, and as many photons are absorbed, the energy spectrum of the quantum mechanical atom begins to acquire the characteristic intensity dependence of classical electrodynamics. We will describe the similarities and differences between the two formalisms in more detail, and show that many of the features observed in above-threshold ionization are simply understood in terms of a classical theory.

MULTIPHOTON IONIZATION OF HYDROGEN BY A MULTIMODE FIELD

S. Basile, G. Ferrante and F. Trombetta

Istituto di Fisica dell'Università, via Archirafi 36,
90123 Palermo, Italy

We report a theoretical treatment of multiphoton ionization of hydrogen atoms by a strong laser field, when the ejected electrons absorb more photons than the minimum required to go into the continuum. The treatment is based on the S-matrix; thus, to some extent, it follows the same line of thought of the old Keldish's treatment,¹ which in a slightly revised version recently has been reconsidered also by Reiss² and Becker *et al.*³

Compared to the previous similar use of the S-matrix method the following points are considered distinctive features of our treatment. (i) We treat the case of a real atom, without model assumptions of whatsoever kind as to the atomic characteristics. (ii) The effort is made to construct an accurate wave function for the ejected electrons moving under the joint action of the laser field and of the potential of the residual ion; it is achieved by an extension to the continuum case of the quasi-energy formalism. (iii) As it is generally recognized that actual experiments are performed at many laser intensities simultaneously, a multimode model for the laser is used; at the moment, it is taken that the laser spectrum has a vanishing bandwidth; bandwidth effects are delayed to a next investigation. (iv) All the integrals and summations entering the theoretical treatment are performed exactly (analytically or numerically), without resorting to the saddle point method, or to ad hoc ansatz concerning the behavior of the pertinent matrix elements.

Using the leading term of a general wave function of the ejected electrons in the presence of two fields, we have performed a selected set of calculations, which are partly shown in Fig. 1-3. Altogether the numerical results show a rewarding, general agreement with experimental observations.

The physical meaning of the theoretical treatment on which the results reported in Fig. 1-3 are based amounts to a direct population

of the various continuum states through one-step multiphoton absorption from the ground state of the hydrogen atom. Neither intermediate discrete transitions nor continuum-continuum ones are included. An analysis of the influence of the latter is left for a further investigation. Anyway, in strong field situations the nonresonant one-step multiphoton bound-free transitions are expected to give the leading contributions to the overall process.

Figure 1 shows the angular distribution of the electrons ejected into the first continuum state above threshold. Qualitatively it reproduces well the experimental measurements in cesium at these intensities.⁴ In Fig. 2 we show the ionization rates for the various continuum states as functions of the mean field intensity; they exhibit a perturbative behavior for weak fields, while increasing the field intensity one finds the inversion of the ionization rates, i.e. the ionization towards higher energy continuum states becomes more probable. It is evident that such a peak inversion is due to a non-perturbative saturation of the ionization rates and that the higher the continuum state reached by the electron the higher the intensity at which saturation occurs. This behavior, which is observed experimentally, is obtained here within an ab initio treatment, without using ad hoc assumptions on the continuum-continuum transitions,⁵ not taken into account. Fig. 3 shows photoelectron energy spectra for several mean field intensities. Of course, the same features as in Fig. 2 are recovered; let us also remark the broadening and shift towards high energy of the peak envelope, well-known experimentally.

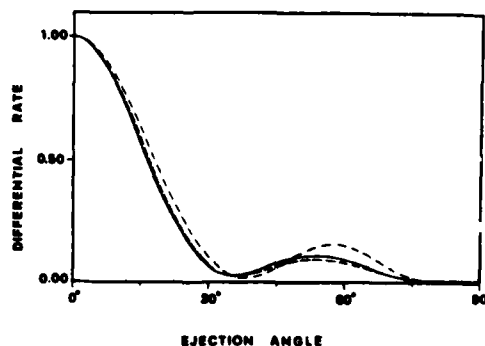


Fig. 1 Angular distributions for absorption of the minimum number of photons to reach the continuum for three field intensities (in W/cm^2):
 10^{11} ; — 10^{12} ; - - - 10^{14} .

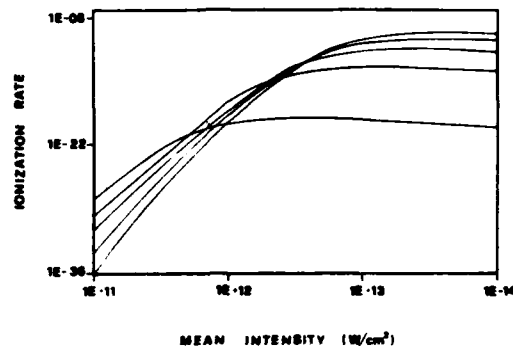


Fig. 2 Ionization rates (in atomic units) vs the mean field intensity (in W/cm^2), for the five continuum states of lower energy.

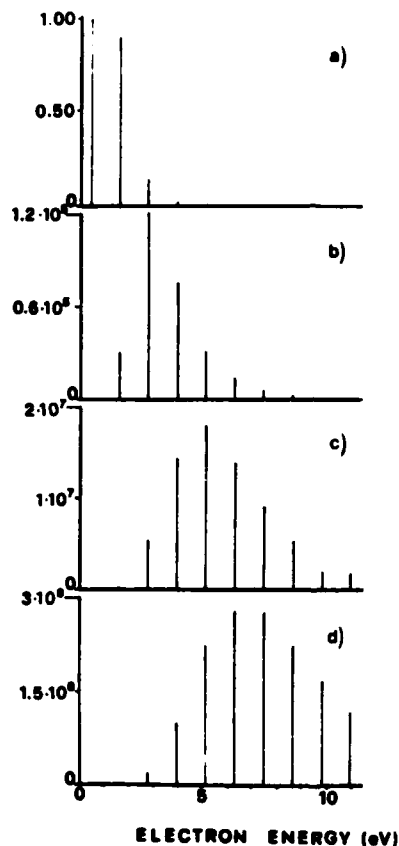


Fig. 3 Photoelectron energy spectra (normalized to the first peak) for various mean field intensities (in W/cm^2): a) $5 \cdot 10^{11}$; b) $2.5 \cdot 10^{12}$; c) $5 \cdot 10^{12}$; d) $7.5 \cdot 10^{12}$.

We plan to report at the conference on other points as well, such as improvement of the present treatment, comparison with alternative models, calculation of other relevant quantities and so on.

REFERENCES

1. L. V. Keldysh, Zh. Eksp. Teor. Fiz. **47**, 1945 (1964).
2. H. R. Reiss, Phys. Rev. A **22**, 1786 (1980).
3. W. Becker, R. R. Schlicher and M. O. Scully, J. Phys. B **19**, L785 (1986).
4. G. Petite, F. Fabre, P. Agostini, M. Crance and M. Aymar, Phys. Rev. A **29**, 2677 (1984).
5. Z. Deng and J. H. Eberly, J. Phys. B **18**, L287 (1985).

ABOVE-THRESHOLD PROCESSES IN INTENSE FIELDS

M. Edwards, X. Tang, and R. Shakeshaft

Physics Department, University of Southern California
Los Angeles, California 90089-0484

In the treatment of above-threshold processes one encounters continuum-continuum matrix elements, whose evaluation presents a numerical problem far more challenging than the evaluation of bound-bound and bound-continuum matrix elements. This extra complexity is, however, somewhat artificial in the sense that nonnormalizable functions appear only as an artifact of the particular theoretical approach; the emergent electron is, after all, initially bound and can in principle be described by a normalizable wavefunction throughout the ionization process, even if the electron continues to absorb photons after it has sufficient energy to escape. As elaborated upon elsewhere¹, the root of the difficulty lies in the (unphysical) requirement that the electron depart with a definite energy - wavepacket spreading is neglected - so the electron is represented by a nonnormalizable (continuum) wavefunction. Furthermore, the (physical) requirement that this wavefunction be regular at the origin implies that it has the character of a standing wave, comprised of outgoing and ingoing parts. The ingoing part, as it stands, is unphysical; only when standing waves of different energies, spread over a narrow bandwidth inversely proportional to the lifetime of the atom, are superposed does the wavefunction acquire the correct asymptotic character of an outgoing wave, which describes the electron leaving the atom. The key to obviating this difficulty is to split the standing wavefunction of the emergent electron into its outgoing (+) and ingoing (-) parts. This decomposition results in a decomposition of the multiphoton matrix element, $M^{(N)}$, into two parts, $M^{+(N)}$ and $M^{-(N)}$. The matrix element

$M^{+(N)}$, which contains only the outgoing part of the final wavefunction, can be easily handled by rotating the integration contour into the upper right quadrant of the complex plane. This rotation transforms the outgoing part of the final wavefunction into a normalizable function, and the evaluation of $M^{+(N)}$ becomes equivalent to the evaluation of a bound-bound matrix element. A similar trick - rotating the integration contour into the lower right quadrant - is not helpful in evaluating $M^{-(N)}$ since its integrand contains outgoing Green's functions which, under this transformation, increase exponentially at large distances. However, within perturbation theory a simple recurrence relation² connects $M^{-(N)}$ to $M^{+(N)}$, so that it is unnecessary to calculate $M^{-(N)}$ directly. We have used this technique³ to calculate cross sections and angular distributions, within perturbation theory, for 3- and 4-photon ionization of Rb and Cs at wavelengths where two photons are sufficient to ionize. We will present comparison with experimental data⁴.

Beyond perturbation theory the neglect of wavepacket spreading gives rise to a negative imaginary part, $-\Gamma/2$, in the energy of the electron. This imaginary part must be neglected in the ionization matrix element, for otherwise this matrix element would be infinite. This results in a violation of gauge invariance¹. In fact, the matrix element for ionization to a specific channel is infinite in the length gauge. In the velocity gauge, diagrams of higher order than lowest (nonvanishing) order are infinite, but the divergences cancel. We have performed nonperturbative calculations of ionization rates to specific channels for the hydrogen atom. Results will be presented. We have also performed calculations of widths and shifts in the ground-state energy of hydrogen using an integral equation approach⁵, and we obtain good agreement with Chu and Cooper⁶.

REFERENCES

1. R. Shakeshaft, J. Opt. Soc. B. to be published May 1987.
2. R. Shakeshaft, Phys. Rev. A 34, 244 (1986); A 34, 5119 (1986).
3. M. Edwards, X. Tang, P. Lambropoulos, and R. Shakeshaft, Phys. Rev. A 33, 4444 (1986); M. Edwards, X. Tang, and R. Shakeshaft, Phys. Rev. A, to be published.
4. A. Dodhy, R. Compton, J. Stockdale, Phys. Rev. Lett. 54, 422 (1985); G. Petite, F. Fabre, P. Agostini, M. Grance, and M. Aymar, Phys. Rev. A 29, 2677 (1984).
5. X. Tang and R. Shakeshaft, Z. Phys. D, to be published.
6. S.-I. Chu and J. Cooper, Phys. Rev. A 32, 2769 (1985).

Classical Time-Dependent Self-Consistent Field Approach
to Intense Field Multiphoton Ionization and Dissociation
of Atoms and Molecules**

J. Needels, R.Y. Yin, and Shih-I Chu
Department of Chemistry, University of Kansas
Lawrence, Kansas 66045

A classical version of the time-dependent self-consistent field (TDSCF) method is presented for general nonperturbative treatment of multiphoton excitation (MPE), ionization (MPI), and dissociation (MPD). A bundle of trajectories for each mode (particle) is integrated along a time-dependent single-mode (or single particle) potential function which contains an averaged interaction with the other modes (particles). The method has been applied successfully to MPE/MPD of SO_2 molecule.¹ It is found that the (computationally much more efficient) TDSCF calculations are capable of reproducing quantitatively the essential dynamics obtained from the fully classical trajectory results (Fig. 1). In addition to providing detailed MPE dynamics (Fig. 2), the TDSCF averaged quantities (such as the intensity-dependent average number of photons absorbed per molecule \bar{n}) are in good agreement with the experimental data of Simpson and Bloembergen² (Fig. 3). This establishes the usefulness of the classical TDSCF method as a potential practical technique for exploring detailed mechanisms in multiphoton dynamics. We are currently extending the method to the study of detailed mechanisms in multiphoton and above-threshold ionization of complex atoms³ in the presence of ultraintense laser fields ($I = 10^{16} \sim 10^{18} \text{ W/cm}^2$). The results will be presented at the conference.

** Supported by ACS-PRF and DOE.

1. J. Needels and S.I. Chu, Chem. Phys. Lett. (in press).
2. T.B. Simpson and N. Bloembergen, Chem. Phys. Lett. **100**, 325 (1983).
3. R.Y. Yin and S.I. Chu, (to be published).

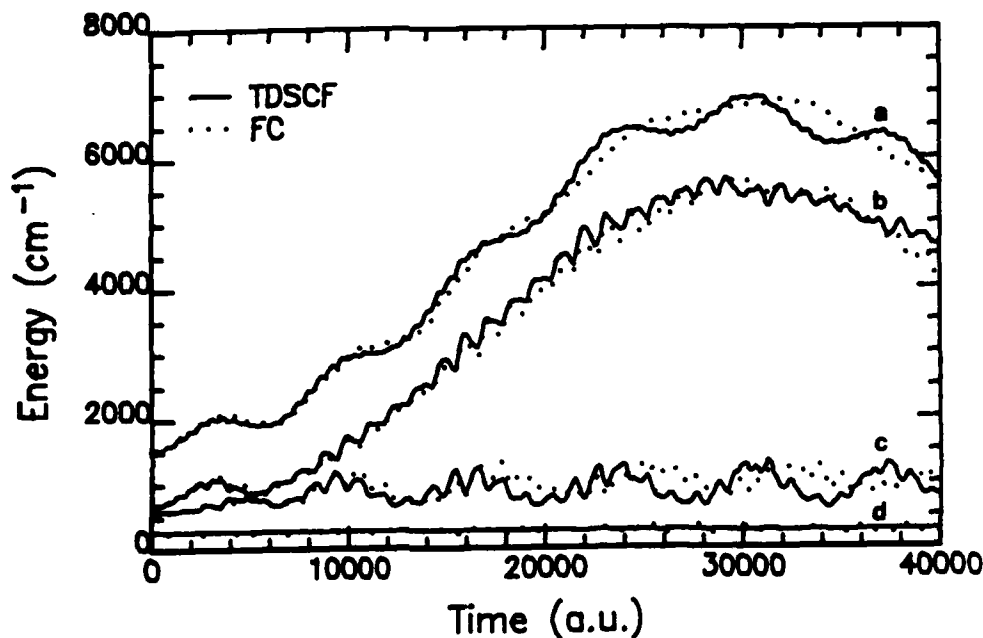


Fig.1 Comparison of the classical TDSCF and fully classical (FC) trajectory calculations for the average energy of SO_2 subjected to a laser frequency of 1150 cm^{-1} and laser intensity of 1 TW/cm^2 . Curve a: total energy of SO_2 , curve b: mode 1 (sym. stretch vib.) energy, curve c: mode 3 (anti-sym. stretch vib.) energy, and curve d: mode 2 (bending vib.) energy. Note the mode selective excitation of mode 1 at this frequency.

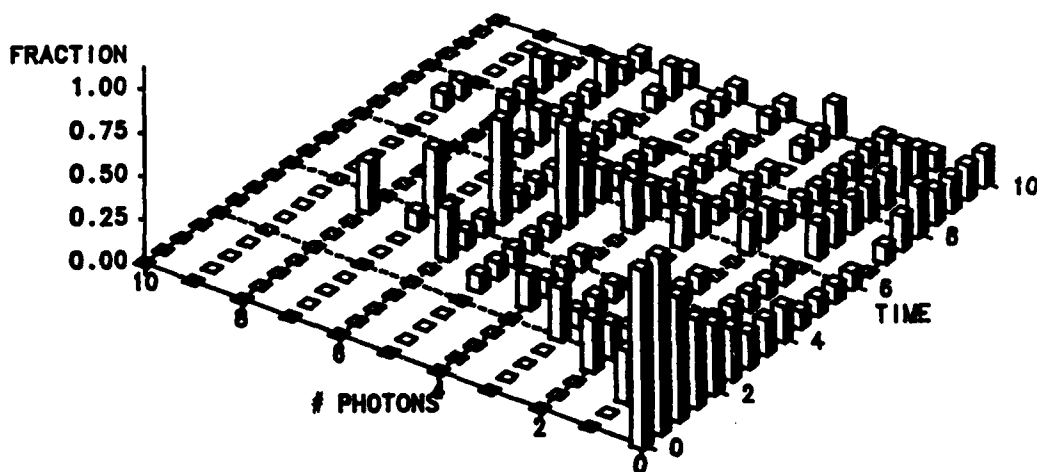


Fig.2. Time-dependent multiphoton excitation dynamics of SO_2 driven by a laser field with frequency at 1140 cm^{-1} and intensity at 1 TW/cm^2 . (Time values are given in atomic units multiplied by 10^{-4}). The excitation is measured by the fraction of classical trajectories in the pump mode (mode 1) categorized by the number of photons absorbed.

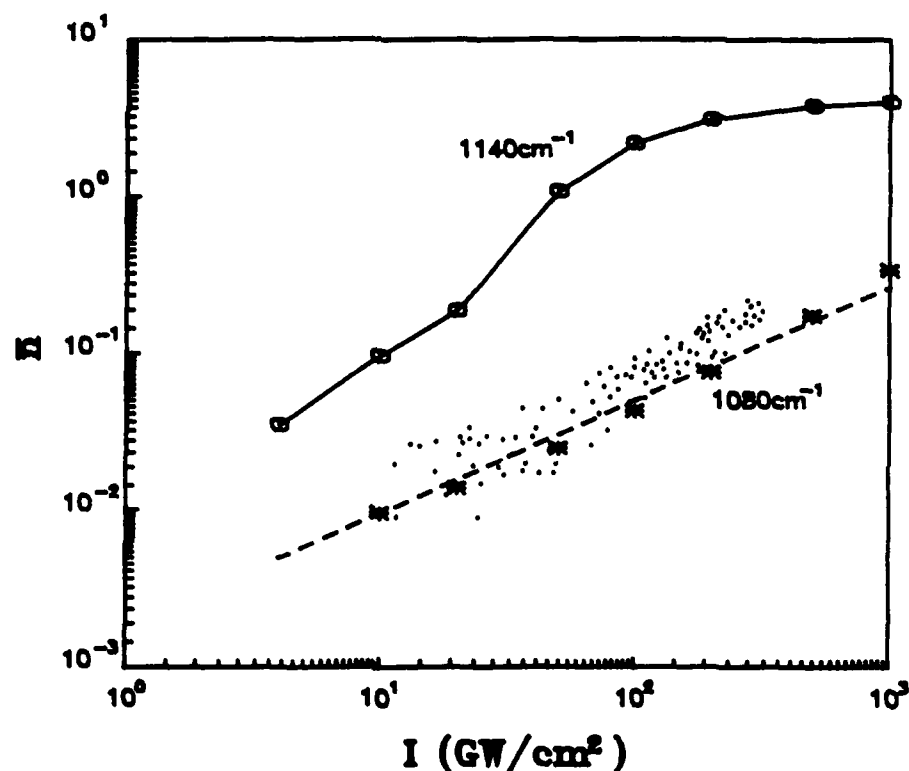


Fig.3 Average number of photons absorbed (\bar{n}) per molecule versus laser intensity. TDSCF results: solid line with circles for laser frequency at 1140 cm^{-1} , * * * line for frequency at 1080 cm^{-1} . The 1080 cm^{-1} results show a linear rising with intensity (the ---- line is a linear least square fitting) whereas the 1140 cm^{-1} (close to sym. stretch mode frequency) results show a saturation of multiphoton absorption at high intensity. The 1080 cm^{-1} TDSCF data agree well with the experimental results shown as dots in the figure.

MANY-ELECTRON, COMPLEX EIGENVALUE SCHRÖDINGER THEORY FOR
THE TREATMENT OF THE AC STARK IONIZATION. I: NEGATIVE IONS

Theodoros Mercouris and Cleanthes A. Nicolaides
Theoretical and Physical Chemistry Institute
National Hellenic Research Foundation
48, Vas. Constantinou Ave., 116/35, Athens
Greece

We present a many-electron theory which aims at the quantitative understanding of polyelectronic atoms or molecules in ac Stark fields ($V=Fz\cos\omega t$). It is based on the theory and concepts related to the calculation of resonances from the complex eigenvalue Schrödinger equation.³⁻⁵ The complex eigenvalues in the present problem are related to the time evolution of the system and are obtained by an iterative technique which optimizes the square integrable functions (and their mixing coefficients) representing the continuous spectrum by looking for the stability of the complex eigenvalues for each frequency ω and strength F of the external field. Our first application involves the Li negative ion, which has three bound states.⁶

REFERENCES

1. J. H. Shirley, Phys. Rev. 138, B979 (1965).
2. A. Maquet, S. Chu, and W. P. Reinhardt, Phys. Rev. A 27, 2946 (1983).
3. C. A. Nicolaides and D. R. Beck, Int. J. Qu. Chem. 14, 457 (1978).
4. C. A. Nicolaides and Th. Mercouris, Phys. Rev. A 32, 3247 (1985).
5. Th. Mercouris and C. A. Nicolaides, Z. Phys. D 5, 1 (1987).
6. C. F. Bunge, Phys. Rev. Lett. 44, 1450 (1980); D. R. Beck and C. A. Nicolaides, Phys. Rev. A 28, 3112 (1983).

MULTIPHOTON - ELECTRON INTERACTION PROCESSES IN THE CONTINUUM

F. F. Körmendi
Institute HTM
Belgrade, Yugoslavia

A theoretical analysis is given of the multiphoton-free electron interaction processes at ultrapowerful laser intensities on the basis of previously obtained results in Ref. 1, 2 and 3. It is shown that the photon ensemble, interacting with electrons, behaves as a photon gas undergoing "phase transitions" at different beam intensities, where the photon density plays an analogous role to the role of temperature in statistical physics, manifesting itself in self-paralleling, in the appearance of solitons etc. The critical beam intensities are evaluated above which the various phenomena become possible.

The obtained results are applied to cosmophysics, particle acceleration and to the generation of short wavelength radiation.

REFERENCES

1. F. Körmendi, Optica. Acta. 28, 1559 (1981).
2. F. Körmendi, Optica. Acta. 31, 301 (1984).
3. F. Körmendi, III Intern. Conf. on Multiphoton Proc. Abstract book, P. 32. Univ. of Crete (1984).

MULTIPHOTON IONIZATION OF A MODEL ATOM

B. Chen*, F. H. M. Faisal, S. Jetzke, H. O. Lutz, and P. Scanzano

Fakultät für Physik, Universität Bielefeld

Postfach 8640, D-4800 Bielefeld, Federal Republic of Germany

*Low Energy Nuclear Physics Institute, Beijing Normal University
Beijing, China

Recent experiments in multiphoton ionization of noble gas atoms in intense laser fields show photoelectron spectra, in which the peaks are spaced by the photon energy $\hbar\omega$. These peaks are due to the absorption of more than the minimum number of photons required to ionize the atom. The experimental data reveal new aspects which cannot be well understood in terms of the usual picture involving the lowest non-vanishing order perturbation theory. Many experimental factors, e.g., the often poorly controlled space and time structure of the laser pulse make quantitative comparison between theory and experiment extremely difficult. In this paper we investigate within a solvable model the influence of the angular momentum of the initial state, small changes of the laser intensity as well as the type of polarization on the angle integrated electron ejection rates. The T-matrix in this model^{1,2} for electron ejection by net absorption of N photons is simply given by

$$T_L^{(N)} = (E_i - E_f) \phi_i(\vec{k}_N) \sum_{n=-\infty}^{\infty} J_n\left(\frac{\delta_e}{2\omega}\right) J_{N+2n}(\vec{k}_N * \alpha_0) \quad (1)$$

(linear polarization)

$$T_C^{(N)} = (E_i - E_f) \phi_i(\vec{k}_N) J_N(k_N \alpha_0 \sin \theta_{K_N}) * e^{iN\phi_{K_N}} \quad (2)$$

(circular polarization)

$\phi_i(\vec{k}_N)$ is the Fourier transform of the initial state wave function.
 $\delta_e = E_0^2/2$ with the maximum field strength E_0 and the photon energy $\hbar\omega$.
 E_i and E_f are the initial and final energies of the electron. The calculation of the rates is straight forward and will be presented.

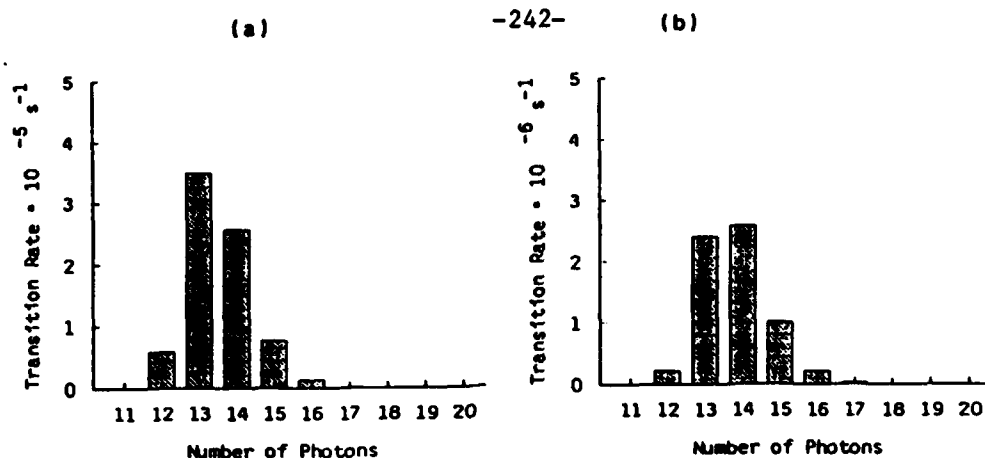


Figure 1. Electron ejection spectra obtained with circularly polarized light with $h\nu=1.17$ eV and a laser intensity of $4 \times 10^{12} \text{ W/cm}^2$ for $l_i=0$ (a) and $l_i=1$ (b).

Figure 1 shows the energy spectra of ejected electrons at a fixed intensity of the incident laser for two different angular momenta l_i of the initial state. The significant influence of the angular momentum on the ejection rates can be easily seen. The second figure shows two spectra at a fixed intensity, for $l_i=1$ and $h\nu=1.17$ eV calculated for linearly and circularly polarized light. This example demonstrates dramatically how much the data alter if the type of polarization is changed. Studying a whole class of examples besides those shown here, we come to the conclusion that great care should be taken in drawing firm conclusions from comparison of currently available experimental data and theoretical calculations.

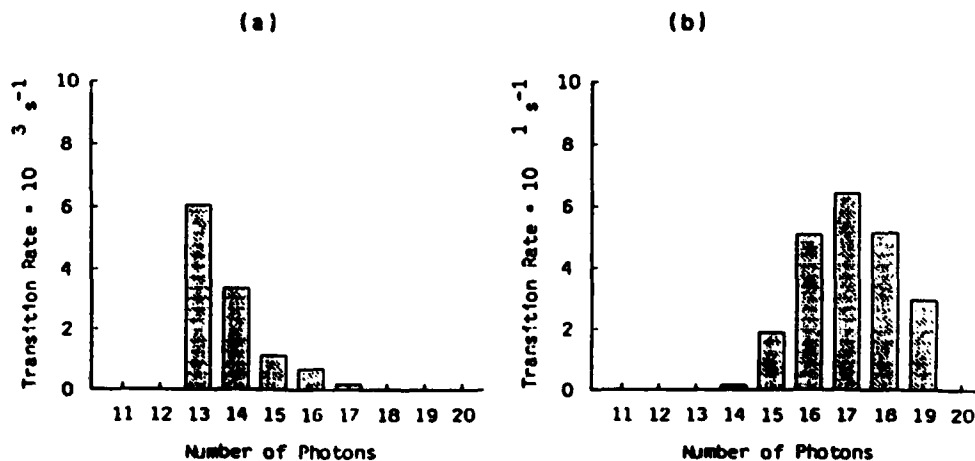


Figure 2. Comparison of electron spectra for (a) linearly and (b) circularly polarized light. The laser intensity is $1.9 \times 10^{12} \text{ W/cm}^2$, $h\nu=1.17$ eV and $l_i=1$.

Besides these model calculations we also plan to present first results for the multiphoton ionization of atomic hydrogen by a Nd-YAG laser and compare them with recently obtained experimental data.³.

REFERENCES

1. F. H. M. Faisal, J. Phys. B 6, L81 (1983).
2. B. Chen, F. H. M. Faisal, S. Jetzke, H. O. Lutz, P. Scanzano, Phys. Rev. A, submitted (1986).
3. D. Feldmann, B. Wolff, H. Rottke, M. Wemhöner, K. H. Welge, Abstract ICOMP IV (1987).

A SIMPLE MODEL FOR STRONG LASER FIELD IONIZATION

Jakub Zakrzewski*

Department of Chemistry, University of Southern California

Los Angeles, Ca 90089-0482

Karol Zyczkowski

Institute of Physics, Jagiellonian University

ul. Reymonta 4, 30-059 Krakow, Poland

We discuss the ionization of a model one-dimensional atom. Our "atom" is described by a finite rectangular potential well of width A and depth V_0 . The sinusoidal perturbation (laser field) is approximated by a train of δ -kicks that are alternating in sign. The one dimensional models of ionisation have been studied before with both sinusoidal^{1,2} and δ -perturbations³; they concentrated, however, on the ionization rate only. We study both the ionization rate and the photoelectron spectra trying to get some insight into the different mechanisms which affect the "Above Threshold Ionization" electron spectra⁴ in strong laser fields. We ignore the influence of the ponderomotive force⁵ restricting ourselves to investigations of the role played by continuum - continuum (c-c) transitions. Although the potential discussed is short ranged, by changing the width of the well A we are able to see the influence of the potential range on the ionization (which was not possible before^{1,3}).

The one-dimensional model discussed is defined by the Hamiltonian:

$$H = p^2/2m + V(x) - eEx \sum_k (-1)^k \delta(t - kT/2) \quad (1)$$

where E is the amplitude of the field. The hamiltonian (1) is periodic with period T , however, as

*on leave from Institute of Physics, Jagiellonian University, Krakow, Poland

$$\sum_k (-1)^k \delta(t - kT/2) = \frac{2}{T} \sum_{n=-\infty}^{+\infty} \exp[2\pi i(2n+1)t/T] \quad (2)$$

the perturbation contains all odd harmonics of the basic frequency ω_L . We construct a quantum map which gives the wave function after the $n+1$ pair of kicks in terms of the wave function after the n -th pair:

$$\psi_{n+1} = \exp(-igx) \exp(-\frac{iT}{2\hbar} H_0) \exp(igx) \exp(-\frac{iT}{2\hbar} H_0) \psi_n \quad (3)$$

where $g = eET/2\hbar$ and ψ_0 corresponds to the initial atomic state at $t=0$ which we choose to be the ground state.

We evaluate the map (3) within the basis of field free hamiltonian eigenfunctions. To follow the evolution of the system on computer we discretize the continuum (putting the system in a large box of size L) and introduce carefully chosen high energy "cut-off".

Our findings may be summarized as follows:

- * The continuum-continuum interaction may be safely ignored as far as the ionization rate is concerned. Thus we confirm the results of Ref.3 (obtained for an extremely short ranged δ -potential).
- * The behaviour of the ionization rate as a function of the intensity is well described by the perturbative theory power law even for very strong laser field - in contadiction to Keldysh⁶-like analysis.
- * The photoelectron spectra are strongly influenced by c-c transitions.
- * Both the singular (sometimes called diagonal⁴) part and the regular part of the c-c matrix elements play very important role in the spectral shape obtained. We have tried to separate the effect of say the singular part by neglecting the regular part of the c-c matrix elements and vice versa. However, in such cases the normalization of the wave vector was not preserved as soon as the field was intense enough to induce significant ionization. This implies that both parts strongly interfere with each other and should be both taken into account simultaneously in any more realistic treatment of strong field ionization. To our surprise neglecting c-c transitions altogether was less "devastating" to the norm of the wave vector than any "separation" attempt.

* We were not able to observe "peak switching" in the photoelectron spectra. That may be due to the persisting short ranged character of the potential studied as well as to the fact that the form of our perturbation implied one - photon ionization processes to be dominant no matter what was the value of the basic perturbation frequency ω_L (note the presence of higher harmonics in (2)). This limitation of the model seems to be its main drawback.

We acknowledge illuminating discussions with K.Rzazewski, J.Mostowski, M.Lewenstein and H.S. Taylor. This work was supported in part by Polish Government grant CPBP0107. J.Z. acknowledges support from NSF grant CHE-8511496.

REFERENCES:

1. S. Geltman J.Phys. B 10, 831 (1977).
2. E. J. Austin J.Phys. B 12 4045 (1979).
3. R. Blumel and R. Meir J.Phys. B 18, 2835 (1985).
4. Due to lack of space we are not able to give all due references here. For a recent list of references see for example J. Grochmalicki, J.R.Kuklinski and M.Lewenstein J.Phys. B 19, 3649 (1986).
5. H. G. Muller and A. Tip Phys. Rev. A 30, 3039 (1984).
6. L. V. Keldysh Sov.Phys.-JETP 20, 1307 (1965).

PONDEROMOTIVE EFFECTS IN PULSED LASER FIELDS

Maciej Lewenstein*

Lyman Laboratory, Harvard University, 02138 Mass.

One of the most intriguing phenomena observed in the above threshold ionization (ATI) is the vanishing of low energy peaks in the photoelectron spectrum [1,2]. Explanations of the apparent threshold shift based on the concept of ponderomotive force do not seem to fit to all the experimental data [3]. This criticism may be summarized as follows:

- i) there are data which show disappearance of slow electrons in the spectrum over much greater energy range than predicted by ponderomotive potential theory (PPT);
- ii) there are data which do not show disappearance of slow electrons as predicted by PPT.

Lambropoulos pointed out that in fact ionization may take place during the rising time of the laser pulse [4]. This explains the statement ii), since the electrons "feel" weaker ponderomotive effect at the time when they are born. It is a purpose of this note to show how these ideas can be described quantitatively in the framework of essential states approach [5]. It is obvious that temporal pulse shape effects may be described in such a framework by including time dependent coupling, proportional to the slowly varying pulse shape function $f(t)$. Simplified (but reasonable) description of ponderomotive effect can be formulated using appropriate form of bound-free and free-free matrix elements. For example a bound-free matrix element should be

$$D(\omega, t) \sim d[\omega - a^2 f^2(t)] \theta[\omega - a^2 f^2(t)] \quad (1)$$

where θ is a step function, a^2 -measures the intensity of the laser field in appropriate units. The form $D(\omega, t)$ assures that a bound state couples only to the accessible states in the continuum (i.e. the ones having energy larger than ponderomotive barrier). For the simplest version of essential states model [4] one obtains Schroedinger equations:

*on leave from Institute for Theoretical Physics, PAS, 02668 Warsaw, Poland

$$\dot{\alpha} = -i\epsilon a^N f^N(t) \int_0^\infty d(\omega - a^2 f^2(t)) \theta(\omega - a^2 f^2(t)) \beta_1(\omega, t), \quad (2a)$$

$$\begin{aligned} \dot{\beta}_n(\omega, t) = & -i(\omega - \Delta_n) \beta_n(\omega, t) - i\epsilon a^N f^N(t) d(\omega - a^2 f^2(t)) \theta(\omega - a^2 f^2(t)) \alpha(t) \delta_{n1} \\ & - i g a f(t) d(\omega - a^2 f^2(t)) \theta(\omega - a^2 f^2(t)) \int_0^\infty d(\omega', t) (\beta_{n+1}(\omega', t) + \beta_{n-1}(\omega', t)) d\omega' \end{aligned} \quad (2b)$$

where ϵ -measures the effective N-photon transition element, g -measures a relative strength of free-free transitions and $\Delta_n = \omega_0 - (N+n-1)\omega_L$ determines the position of the peak in the photoelectron spectrum. α is a bound state amplitude, while β_n describe the amplitudes of the successive continua. By direct inspection (for particular pulse shapes such as $\exp(\gamma t)$, $1/\cosh(\gamma t)$) one can show that in fact generalized Wigner-Weisskopf approximation holds for the system of eqs. (2). This can be expressed as the Markov property of the continuum response functions:

$$\begin{aligned} \int_0^\infty d(\omega - I(t)) d(\omega - I(t')) e^{-i(\omega - \Delta)(t - t')} \theta(\omega - I(t)) \theta(\omega - I(t')) = \\ = S(\Delta, t) \delta_+(t - t') + S^*(\Delta, t) \delta_-(t - t') \end{aligned} \quad (3)$$

where

$$S(\Delta, t) = \lim_{\epsilon \rightarrow 0} \int_0^\infty |d(\omega - I(t))|^2 \theta(\omega - I(t)) \frac{1}{\epsilon + i(\omega - \Delta)} \quad (4)$$

while $\delta_\pm(t - t') = \lim_{\epsilon \rightarrow 0} \delta(t - t' \pm \epsilon)$. Note that $S(\Delta, t)$ includes both Stark shift and decay rate. The decay is connected to the real part of $S(\Delta, t)$ and is switched off for $\Delta < a^2 f^2(t)$. Such generalized W-W approximation (3) reduces the solution of the eqs. (2) to matrix inversion and solution of the first order linear differential equation for $\alpha(t)$. It leads to time dependent saturation of free-free transitions. The following comments should be made, concerning the results obtained from (2):

- i) the results fit well and explain some of the experimental data (i.e. ionization of Ne and He for $\alpha = 1064$ nm, see Lompre et al.);
- ii) the Stark shift effects (usually neglected) play essential role. For example they enable for the transitions to the second peak, after the decay rate to the first one has been switched off;

iii) the W-W approximation brakes down, when the effective bound-free ionization rate ($\epsilon^2 a^{2N}$) becomes comparable to the laser frequency. Unfortunately this condition may hold in fact in experiments with NdYag lasers in the range of intensities 10^{14} - 10^{15} W/cm².

This work has been supported by U.S. Office of Naval Research (N00014-850-K-0724).

REFERENCES

1. P. Kruit et al., Phys. Rev. A 28, 248 (1983), L. A. Lompre et al., JOSA B 2, 1906 (1985).
2. H. G. Muller et al., J. Phys. B 16, L679 (1983).
3. Pan Liwen et al., JOSA B 3, 1319 (1986).
4. P. Lambropoulos, Phys. Rev. Lett. 55, 2141 (1985).
5. Z. Deng, and J. H. Eberly, Phys. Rev. Lett. 53, 1810 (1984).

A COMMENT ON THE EMISSION OF RADIATION DURING MULTIPHOTON
IONIZATION WITH ULTRA-INTENSE LASER PULSES

S. L. Chin

Laboratoire de Recherches en Optique et Laser (LROL)
Département de Physique
Université Laval, Ste-Foy (Québec) G1K 7P4
Canada

It is pointed out that broadband radiation will be emitted during a multiphoton ionization experiment using an ultra-intense laser pulse. This would be due to the collapse of the excited electron in the continuum lower than the ponderomotive potential back into the atom. A recent experimental observation of supercontinuum generation in gases by Corkum et al. seems to confirm this.

Introduction: In recent years, experimentalists have measured extensively electron spectra in studying very intense laser interaction with atoms (Agostinetti et al.,¹ Kruit et al.,² Lompré et al.,³ Bucksbaum et al.⁴). It is recently observed that the ponderomotive potential played a significant role in modifying the electron spectra during above threshold ionization (ATI) of atoms (Freeman et al.,⁵ Bucksbaum et al.⁶). A consensus among active researchers in this field is that further understanding of the interaction process might require the measurement of electromagnetic radiation emitted during the ionization process. The purpose of this paper is to point out that the ponderomotive potential might still play a role in influencing the measurement of electromagnetic radiation when a very intense laser pulse interacts with atoms.

Model: Figure 1 shows a schematic energy diagram of an atom in an intense laser field. Level 1 is the ground state. Level 2 is the unperturbed ionization limit. In the laser field, it is raised to Level 3 by an amount of $e^2 E^2 / 4m\omega^2$, the ponderomotive potential. Discrete levels of the atom are not shown. Through multiphoton absorption, an electron can be excited into the continuum above "Level 2".

However, only those electrons whose energy can overcome the ponderomotive potential

$$U_p = \frac{e^2 E^2}{4m\omega^2}$$

will be able to leave the atom.^{5,6,7} Here, E is the laser electric field, ω is the laser frequency and e and m are the charge and mass of an electron. Electrons excited into the continuum between limits 2 and 3 will be "trapped" momentarily and collapse (or be scattered) back into the atom. These "trapped" electrons would first collapse through the continuum below "3" onto a discrete level of the atom which has a finite lifetime. From here, it would make its quantum jumps through the intermediate discrete levels back to the ground state.

Now the collapse of an electron through the continuum below "3" onto a discrete level is similar to the capture of an orbital electron by a nucleus of charge Ze (see Ref. 8). In the latter case, radiation is emitted whose distribution $F(\omega)$ is of the form

$$F(\omega) \propto Z^2 \frac{1}{\hbar\omega} \left[\frac{\omega^2 (\omega^2 + \omega_0^2)}{(\omega^2 - \omega_0^2)^2} \right]$$

where ω_0 is the orbital frequency or the transitional dipole frequency of the electron around the nuclear charge Ze . Figure 2 shows a sketch of such a distribution. In the present case, the nucleus is replaced by the singly charged parent ion (of charge $+e$; hence, $Z=1$). The "orbital" frequency of the electron can be considered as the oscillating frequency of the quasi-free (hence quasi-classical) electron in the laser field (in the continuum below the limit 3) which is the laser frequency. Hence, during the interaction of an intense laser field with atoms, one should expect to observe electromagnetic radiation whose distribution is similar to the one shown in Fig. 2, with ω_0 identical to the laser frequency. Also, since this broadband radiation is emitted by the quasi-free electron through the region bounded by the ponderomotive potential, it is expected that the frequency distribution of the radiation emitted by the collapse of electrons into different singly charged atomic or molecular ionic species would be almost identical so long as a comparable number of quasi-free electrons had been excited into the continuum between "3" and "2" (Fig. 1) and the ponderomotive potentials were the same (i.e. under the same laser intensity). A recent experimental observation by Corkum, Rolland and

Srinivasan-Rao,⁹ (here referred to as CRS) seemed to have provided evidence to the above prediction.

Indeed, they have observed almost identical broadband emissions from different gases using ps and fs pulses. The spectral shape of these emissions is similar to that of Fig. 2. More detail comparison with the experiment will be discussed at the meeting.

References

1. P. Agostini, F. Fabre, G. Mainfray, G. Petite, N. K. Rahman, Phys. Rev. Lett. 42, 1127 (1979).
2. P. Kruit, J. Kimman and J. Vanderziel, J. Phys. B 14, L597 (1981).
3. L. A. Lompré, A. L'Huillier, G. Mainfray, C. Manus, JOSA-B 12, 1906 (1985).
4. P. H. Bucksbaum, M. Bashkansky, R. R. Freeman, T. J. McIlrath and L. F. Di Mauro, Phys. Rev. Lett. 56, 2590 (1986).
5. R. R. Freeman, T. J. McIlrath, P. H. Bucksbaum and M. Bashkansky, 1986, "Ponderomotive effects on angular distributions of photoelectrons." The author acknowledge the receipt of a preprint of this paper.
6. P. H. Bucksbaum, M. Bashkansky, and T. J. McIlrath, "Scattering of electrons by intense coherent light," Technical Digest, Topical Meeting on Multiple Excitations of Atoms, Oct. 20-22, 1986, Seattle, WA (published by The Optical Society of America).
7. A. Szöke, J. Phys. B: At. Mol. Phys. 18, L427 (1985).
8. J. D. Jackson, Classical Electrodynamics, 2nd edition, John-Wiley and Sons, New York (1975).
9. P. B. Corkum, C. Rolland, and T. Srinivasan-Rao, Phys. Rev. Lett. 18, 2268 (1986).

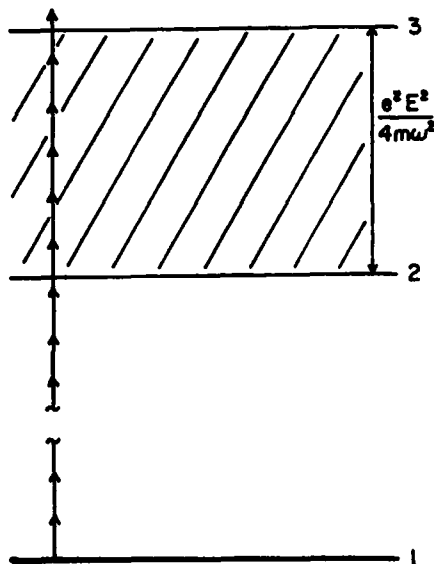


Figure 1.

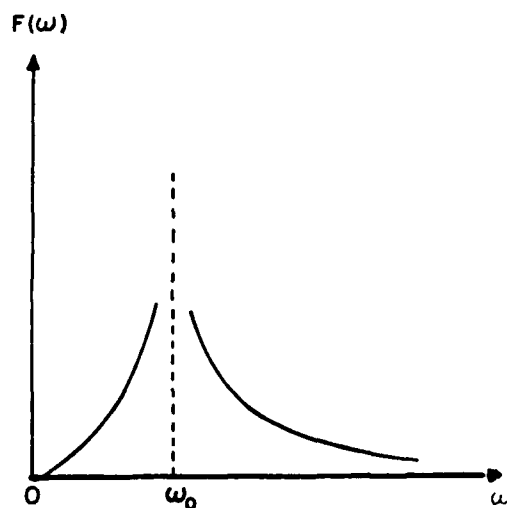


Figure 2.

**Investigations of Above Threshold Ionization with
Sub-Picosecond Pulse Lengths**

R.R. Freeman, M. Geusic, S. Darack, and H. Milchberg

AT&T Bell Laboratories
Murray Hill, NJ, 07974

We have investigated Above Threshold Ionization in Xenon using high intensity pulses of light at 616nm with pulse widths ranging from approximately 13 psec down to shorter than 500 fsec. This is by far the shortest pulse lengths ever used to investigate ATI, and this range is sufficiently short that dramatic changes in the shape and position of the low energy ATI peaks are readily observed. Further, a wholly new phenomena occurs for the shortest pulse widths and the lowest energy electron peak: the peak is observed to break up into an apparently random series of extremely narrow (instrument-resolution limited) peaks.

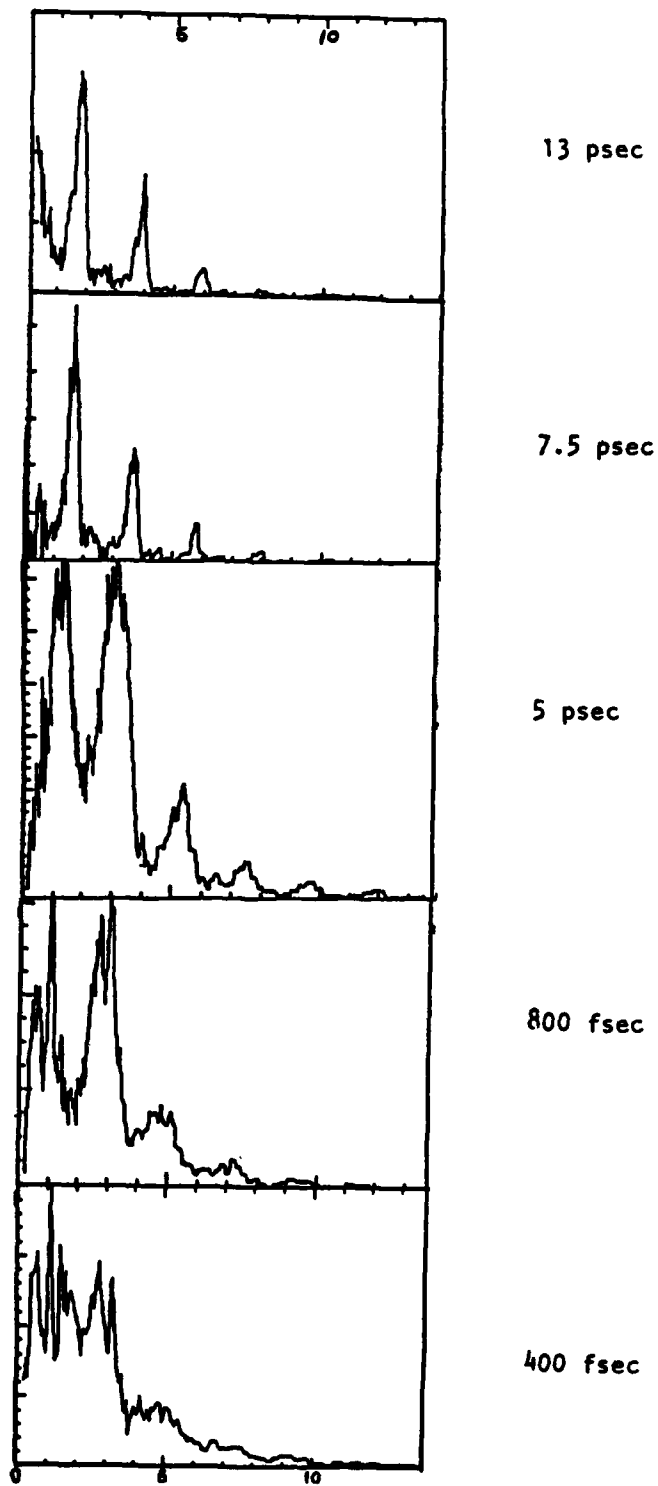
The apparatus consists of an oscillator sync-pumped by a cw-mode-locked YAG laser. The output pulse width of this oscillator is adjusted from 5 to 13 psec by detuning the cavity length. Short pulses down to less than 500 fsec are obtained by standard grating compression techniques. The output from the oscillator is amplified in a 4 stage linear amplifier that preserves the pulse width while achieving gains of nearly 10^6 . The laser is directed into a vacuum vessel with base pressure of less than 10^{-7} Torr. The xenon is introduced by means of a leak valve, and the ionized electrons are recored by a time of flight instrument with a measured resolution of better than 100 mV at 5 Volts. Extreme care was taken

to operate the experiment so that space-charge effects remained negligible.

The behavior of the electron spectrometer was first checked using 2ns, 532nm light. Under these conditions the instrument was found to record ATI peaks at the expected energy, with the expected resolution. The attached figure shows the results of using the short pulse 616nm light. This preliminary data clearly shows some remarkable phenomenolgy: 1) Even at 13 psec, where the approximate intensity is 10^{13}Wcm^{-2} , the lowest energy peaks show largely "red-wing" broadening, while the higher peaks *are not shifted or broadened*; 2) As the pulse width shortens, the low energy peaks actually begin to shift, and the higher energy peaks show signs of broadening; 3) At the shortest pulse length there is very significant shifting, and *the lowest energy peak breaks up into apparently random, extremely narrow peaks*. Although the data shown on the figure is preliminary, with the peak intensity of the pulses increasing approximately a factor of 4 from the top trace to the bottom, the major trends, including the break-up of the lowest energy electron peak, are found to reproduce reliably.

The energy broadening and shifting recorded here is in approximate agreement with time dependent ponderomotive potential trajectory simulations we have developed previously, yet these results will play a very significant role in determining the nature of the ATI process itself. This is because all models of the role of the ponderomotive potential ultimately require detailed knowledge of the mechanics of the ionization process itself, e.g., just where in the pulse does ionization take place.

Dependence of ATI at 616nm on
Pulse Length



DIRECT EVIDENCE OF PONDEROMOTIVE EFFECTS VIA PULSE
DURATION IN ABOVE-THRESHOLD IONIZATION

P. Agostini, L. A. Lompre, J. Kupersztych, G. Petite and F. Yergeau
Service de Physique des Atomes et des Surfaces
CEN/SACLAY
91191 Gif-Sur-Yvette Cedex
France

The energy spectra of electrons produced in strong field above-threshold ionization of Xenon by a YAG laser are shown to be shifted and broadened when pulse shorter than 50 ps are used. The shifts crucially depend on the ratio of the pulse duration to the lapse of time taken by the electron to escape from the focal spot. Red shifts up to 0.9 eV with 30 ps pulse were measured and found to vary linearly with the light intensity. A theoretical model, based on a classical description of the electron behavior in strong fields accounts for most of the experimental data.

MULTIPHOTON TRANSITIONS TO FINAL EXCITED ION STATES
IN STRONTIUM: SPECTROSCOPY OF AUTOIONIZING STATES

P. Agostini, A. L'Huillier, G. Petite
Service de Physique des Atomes et des Surfaces
CEN/SACLAY - 91191 Gif-Sur-Yvette Cedex, France

X. Tang, P. Lambropoulos
University of Southern California, Los Angeles CA 90089-0484
and Research Center of Crete, Iraklion, Crete 71110, Greece

We report experimental and theoretical investigations of multiphoton ionization of Strontium atoms to final ion states $5s\ S_{1/2}$, $4d\ D_{3/2,5/2}$, $5p\ F_{1/2,3/2}$.

Experimentally, a strontium atomic beam is ionized by absorption of 3 or 4 photons from a picosecond dye laser pumped by the second harmonic of a Nd-YAG mode locked laser. The ion signal or the energy-resolved electron signals are recorded as a function of the laser wavelength and intensity. The various ionization channels are identified, according to the photo-electron energies as

$$5s^2\ ^1S_0 + 3\ h\nu \rightarrow 5s\ S_{1/2} + e^- \quad (1)$$

$$5s^2\ ^1S_0 + 4\ h\nu \rightarrow 5s\ S_{1/2} + e^- \quad (2)$$

$$5s^2\ ^1S_0 + 4\ h\nu \rightarrow 4d\ D_{3/2,5/2} + e^- \quad (3)$$

$$5s^2\ ^1S_0 + 4\ h\nu \rightarrow 5p\ F_{1/2,3/2} + e^- \quad (4)$$

In the range of Rhodamine 6G (560-580 nm) several two and three-photon resonances are met.³

Theoretically, we have used a combination of Multiconfiguration Hartree-Fock (MCHF) with strong field techniques which allow the inclusion of the effect of the field on the atomic structure. The formalism is also extended to include intercombination transitions (singlet-triplet mixing) which are quite strong in Strontium.

We first analyze the two-photon resonances on states $5p^2\ ^3P_0$ and $5s\ 5d\ ^3D_2$ and their AC-Stark shifts. The coefficients of configuration mixing are tested by comparing the theoretically predicted shifts to the observed values. The singlet-triplet mixing coefficients are obtained from angular distribution experimental data.² The good agreement between theory and experiments gives confidence in the results of the MCHF calculations.³ We then calculate the various line shapes corresponding to transitions (1) to (4) with no other experimental input than the laser intensity. The result compares reasonably well with the experimental lineshapes.

Spectroscopic information about autoionizing states like $5p\ 6s\ ^3P_1$, $5p\ 6s\ ^1P_1$, $5p\ 5d\ ^3D$, $5p\ 5d\ ^1D$, $4d\ 4f\ ^3D$, $4d\ 4f\ ^1D$ is obtained either directly from three-photon resonances or indirectly through the influence of these states on the two-photon resonances AC-Stark shifts.⁴

REFERENCES

1. G. Petite and P. Agostini, J. de Phys. 47, 795 (1986).
2. D. Feldmann (unpublished).
3. P. Agostini, A. L'Huillier, G. Petite, X. Tang and P. Lambropoulos; Proceedings of Third International Symposium on Resonance Ionization Spectroscopy, Swansea Sept. 1986 (to be published).
4. P. Agostini, A. L'Huillier, G. Petite, X. Tang and P. Lambropoulos (to be published).

A NEW TECHNIQUE TO STUDY THE RYDBERG STATES
BY MPI SPECTROSCOPY

R. D. Verma and Alak Chanda

Department of Physics, University of New Brunswick
Fredericton, New Brunswick, Canada

A new technique to study the Rydberg state of Ba-atom has been developed. In this technique Multiphoton Ionization signal is detected by selectively exciting the ground state ion (6s) to an excited state (6p) which results in a collimated ASE signal at 6p→5d transition of Ba⁺. Discrete Rydberg states, 6snl (l=0,2), as well as autoionizing Rydberg states, 5dnl (l=0,2) and 6pnl (l=0,2), are observed by this novel but very simple method.

THREE PHOTON EXCITATION OF AUTOIONIZING STATES OF ATOMIC KRYPTON AND XENON*

S. T. Pratt, J. L. Dehmer, and P. M. Dehmer
Argonne National Laboratory, Argonne, Illinois 60439

Recently, Gangopahyay et al.¹ reported calculations of the three photon ionization spectra of Xe in the energy region between the $\text{Xe}^+ 2p_{3/2}^o$ and $2p_{1/2}^o$ fine-structure thresholds. These calculations show distinct resonant structures corresponding to $J = 1$ and $J = 3$ autoionizing Rydberg series of xenon converging to the $\text{Xe}^+ 2p_{1/2}^o$ threshold. For this reason, we have recorded the experimental three photon ionization spectrum of Xe in the same spectral region. Using linearly polarized light, four different Rydberg series are allowed by the selection rules for three photon transitions, and all four of these series are observed. These correspond to the $ns'[1/2]_1^o$, $nd'[3/2]_1^o$, $nd'[5/2]_3^o$, and $ng'[7/2]_3^o$ Rydberg series. All four series have $\text{Xe}^+ 2p_{1/2}^o$ ion cores, and the notation $n\ell'[K]_j^o$ corresponds to $j_c\ell$ coupling, in which the angular momentum of the ion core, j_c , is coupled to the orbital angular momentum of the Rydberg electron, ℓ , to give K , which is then coupled to the Rydberg electron's spin to give J .

Figure 1 shows the three photon ionization spectrum of Xe obtained using linearly polarized light between 2791.00 Å and 2800.75 Å. Two members of three different Rydberg series are clearly discernible; these correspond to the sharp $ns'[1/2]_1^o$ and $nd'[5/2]_3^o$ series, and the broad $nd'[3/2]_1^o$ series. In this spectral range, the intense $ns'[1/2]_1^o$ peaks obscure the members of the $ng'[7/2]_3^o$ series. At lower n , these two series are resolved, as is shown in Figure 2. Figure 2 also shows that with circularly polarized light the $J = 1$ series becomes forbidden, and only the $J = 3$ series are observed. In this manner, the higher $ng'[7/2]_3^o$ series members are also observed.

The three photon ionization spectrum of atomic Kr has also been recorded in the region just above the $\text{Kr}^+ 2p_{3/2}^o$ threshold, and it displays structure analogous to that observed in Xe. However, the low

lying members of only three series are present in the spectrum, and the members of the $nd'[5/2]_3^0$ series are not observed.

Photoelectron spectra and photoelectron angular distributions have been determined for a number of resonances in the xenon and krypton

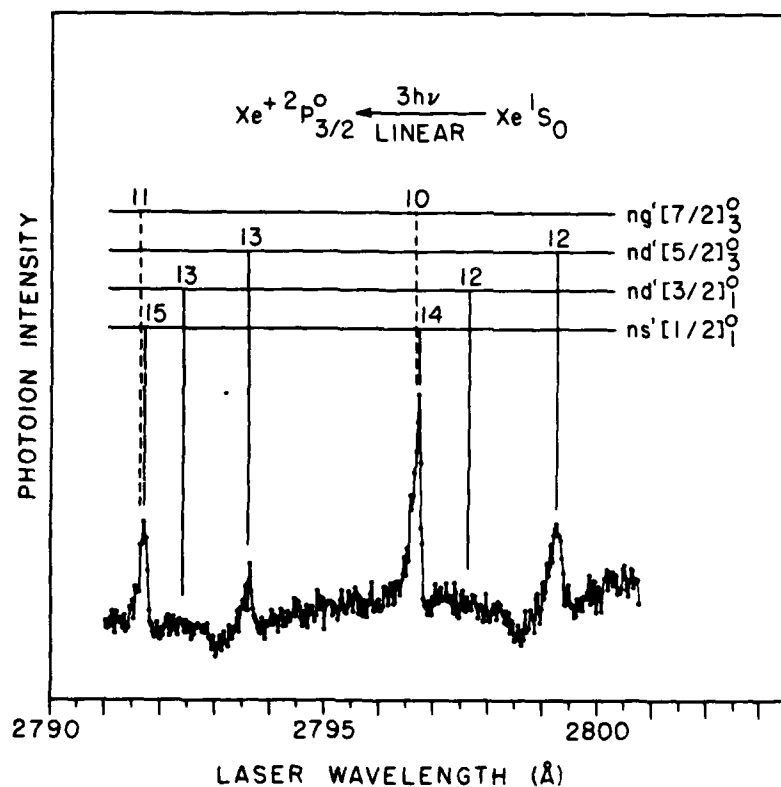


Fig. 1. Three three photon ionization spectrum of atomic Xe between 2800.75 Å and 2791.00 Å obtained using circularly polarized light.

spectra. The photoelectron spectra all show a single peak corresponding to the production of Xe^+ or $\text{Kr}^+ 2P_{3/2}^0$. No evidence for above-threshold ionization is observed in any of these spectra. The photoelectron angular distributions will be compared with the theoretical results.¹

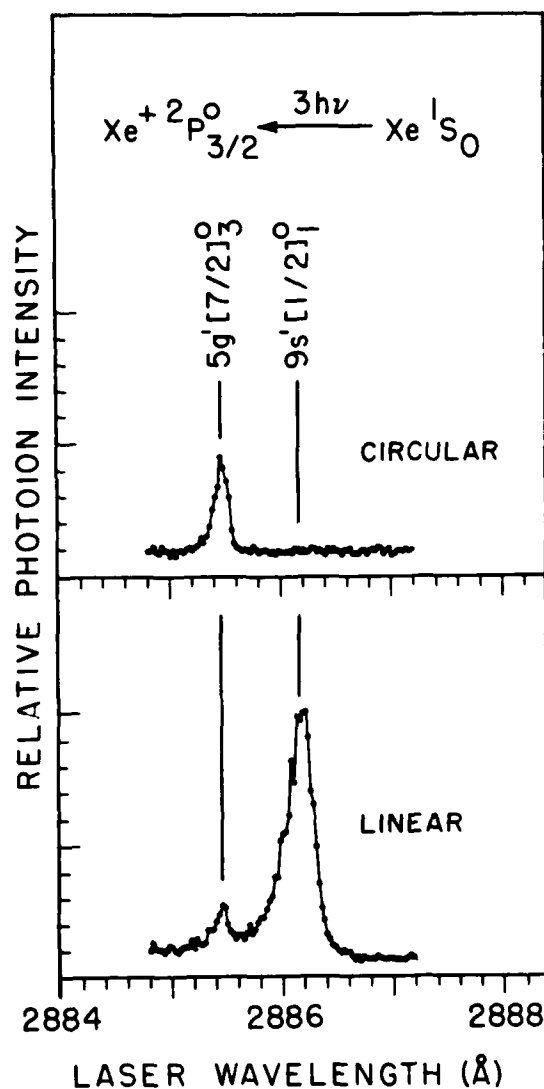


Fig. 2. The three photon ionization spectra of atomic Xe near the $9s'[1/2]_1^0$ autoionizing resonance obtained using linearly and circularly polarized light. The spectra are plotted so that the relative peak heights reflect the approximate relative intensities of the peaks in the two spectra.

Reference

1. P. Gangopadhyay, X. Tang, P. Lambropoulos, and R. Shakeshaft, Phys. Rev. A 34, 2998 (1986).

*This work was supported by the U.S. Department of Energy, Office of Health and Environmental Research, under Contract W-31-109-Eng-38 and by the Office of Naval Research.

TWO-COLOR LASER EXCITATION AND IONIZATION OF DENSE SODIUM VAPOR

Dino Zei

Department of Physics, Ripon College
Ripon, Wisconsin 54971

R. N. Compton* and J. A. D. Stockdale

Oak Ridge National Laboratory,**
P.O. Box X, Oak Ridge, Tennessee 37831-6125

M. S. Pindzola

Department of Physics, Auburn University
Auburn, Alabama 36830

P. Lambropoulos† and Bonian Dai

Department of Physics, University of Southern California
Los Angeles, California 90089-1341

Two independently tunable, linearly polarized dye laser beams have been counterpropagated through a heat pipe containing sodium vapor at densities from 0.1 to 10 Torr. The frequency of the first laser ω_1 is incremented through both $3p^2P_{1/2,3/2}$ fine structure levels while the second laser ω_2 is tuned to reach the $ns^2S_{1/2}$ and $nd^2D_{3/2,5/2}$ levels ($n=5$ to 35). When ω_1 is off-resonance, strong ionization signals are observed corresponding to two-photon excitation of ns and nd states. These signals are shown as peaks C and F in Fig. 1. Note that the maxima in these peaks change position as the wavelength of each laser is varied in accordance with $\hbar\omega_1 + \hbar\omega_2 = E(ns^2S)$ or $E(nd^2D)$. An interference effect has been discovered in the polarization properties of two-photon excitation of the $ns^2S_{1/2}$ states. The polarization [defined as the intensity measured when the two planes of polarization of the laser beams are parallel minus the intensity when perpendicular divided by the sum of the intensities, i.e., $P = (I_{\parallel} - I_{\perp}) / (I_{\parallel} + I_{\perp})$] goes from +1 to -1 as ω_1 is tuned between the $3p^2P_{1/2,3/2}$ fine structure levels (see Fig. 2).

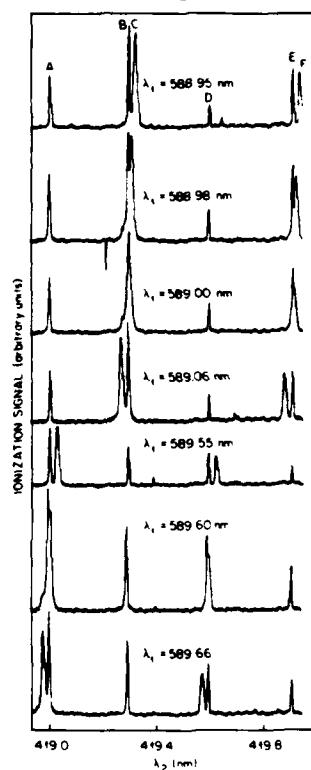


Fig. 1. Two-color ionization signal observed when tuning the probe laser and incrementing the pump laser near the $3p^2P_{3/2,1/2}$ states. See text for assignments.

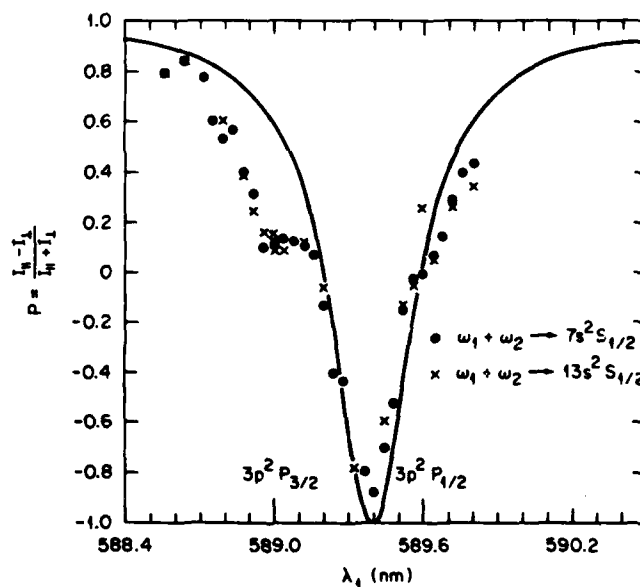


Fig. 2. Comparison of theory and experiment for the polarization properties of two-color laser excitation of 7s and 13s excited states when tuning near the 3p fine structure levels.

A much weaker (less than 10%) change is observed for the unresolved $nd^2D_{5/2,3/2}$ fine structure levels. The fact that the J-levels are unresolved washes out the polarization dependence. The polarization effect shown in Fig. 2 is due to an interference between the two pathways to the $ns^2S_{1/2}$ level. A straightforward theoretical calculation accurately accounts for the data (solid line in Fig. 2) except for the case when the first laser is in resonance with the $3p^2P_{3/2}$ or $3p^2P_{1/2}$ state. This has a trivial explanation due to another process to be discussed next.

When ω_1 is either on- or off-resonance strong ionization signals are observed corresponding to transitions between $3p^2P_{3/2}$ or $3p^2P_{1/2}$ states and higher $ns^2S_{1/2}$ and $3p\text{-}nd^2D_{3/2,1/2}$ states (peaks A,B,D and E in Fig. 1). Both experiment and theory show that these signals are due to dissociation of quasi-molecules followed by resonant $3p\text{-}ns$ and nd transitions. Such spectral features have been termed "hybrid resonances" in earlier one-color studies. The use of two colors allows us to study "hybrid resonances" in greater detail.

In the particular cases where ω_1 is on-resonance with the $3p$ states, very strong dipole forbidden $3p \rightarrow np$ transitions are seen for high values of n . Theoretical analysis shows these features to be due to l -mixing collisions in the laser field. This phenomenon was seen much more weakly in the earlier beam experiments of Burkhardt *et al.*¹

The dual dye lasers were pumped by a 1 MW nitrogen laser (see Ref. 2 for details). The heat pipe has also been described earlier.³ In all cases ionization signals are due to collisions.

REFERENCES

- * Also Department of Chemistry, The University of Tennessee, Knoxville, TN 37916.
- ** Operated by Martin Marietta Energy Systems, Inc. under contract DE-AC0584OR-21400 with the U.S. Department of Energy.
- † Also Department of Physics, University of Crete, Greece
- 1. C. E. Burkhardt, M. Ciocca, W. P. Garver, J. J. Leventhal, and J. D. Kelly, *Phys. Rev. Lett.* **57**, 1562 (1986).
- 2. R. N. Compton and J. C. Miller, *J. Opt. Soc. B* **2**, 355 (1985).
- 3. S. Hamadani, J. A. D. Stockdale, R. N. Compton, and M. S. Pindzola, *Phys. Rev. A* **34**, 1938 (1986).

LASER-INDUCED IONIZATION AND STIMULATED ELECTRONIC RAMAN SCATTERING
IN CESIUM VAPOR NEAR THE $np^2P_{3/2,1/2}$ ($n=6,7,8,9$) STATES

J. A. D. Stockdale, R. N. Compton,* and Adila Dodhy**
Oak Ridge National Laboratory,*** P.O. Box X,
Oak Ridge, Tennessee 37831-6125

W. Christian
Physics Department, Davidson College
Davidson, North Carolina 28036

P. Lambropoulos† and T. Olsen†
Physics Department, The University of Southern California
Los Angeles, California 90089-1341 and University of Crete, Greece

A tunable ND:YAG pulsed dye laser has been used to study simultaneous ionization and stimulated electronic Raman scattering (SERS) in cesium vapor from room temperature ($\approx 10^{-6}$ Torr) up to $\sim 500^\circ\text{K}$ ($p \approx 10$ Torr) for cases in which the laser frequency is tuned at or near the $np^2P_{3/2,1/2}$ ($n=6,7,8,9$) levels. At low atom number densities ionization occurs as a result of resonantly-enhanced multiphoton ionization (MPI). When the laser is tuned in resonance with the $6p^2P_{3/2,1/2}$ states, the second photon is in accidental near resonance with both of the $6d^2D_{5/2,3/2}$ states which enhances the three-photon ionization rate. The measured ratio of the ionization signal for the two fine-structure levels is a strong function of the laser power as predicted earlier.¹ At high cesium densities (~ 1 -10 Torr), ionization is dominated by chemi-ionizing collisions between two fast, excited $6p^2P_{3/2,1/2}$ atoms. At cesium atom number densities and laser powers where strong SERS emission is observed² originating from near the $7p^2P$ and $8p^2P$ levels, ionization occurs over a broad range of laser wavelengths (10-20 Å) and follows the SERS signal including a pronounced "dip" at the line center. A major contribution to the "dip" corresponding to the position of the $7P_{1/2,3/2}$ levels is due to an interference between the one-photon pathway and a three-photon coherent process which is doubly near resonance. The cancellation of a one-

photon resonance would then be analogous to (but more complicated than) the interference between three-photon excitation and third-harmonic generation discussed earlier.^{3,4} Figure 1 shows the ionization signal in the vicinity of the $7p^2P_{3/2}$ level at high and low pressures.

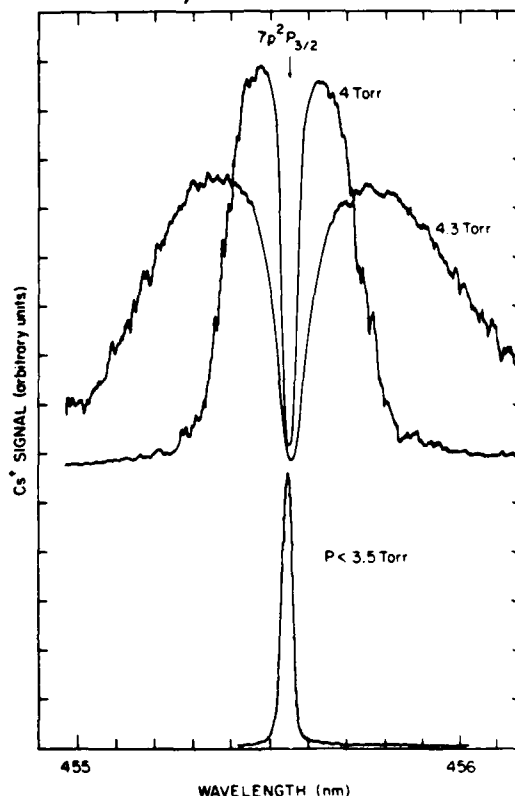


Fig. 1. Ionization spectra in the vicinity of the one-photon allowed $7p^2P_{3/2}$ state of cesium at high (top) and low (bottom) cesium atom number densities.

At these densities and laser powers ($\sim 10^6$ W/cm²), we attribute most of the ionization signal to photoionization of real $(n-1)p^2P$ atoms produced by sequential SERS and stimulated $ns^2S \rightarrow (n-1)p^2P$ emission. For the case of initial one-photon excitation to the vicinity of the $7p^2P_{3/2,1/2}$ states we have detected this emission in both forward and backward directions. Figure 2 illustrates the ionization pathway. In a separate high atom number density beam experiment ($\sim 10^{13}$ atoms/cm³) employing electrostatic energy analysis of the ionization products we detect intense signals of low-energy electrons in addition to the normal two-photon ionization signal. We believe this low energy

electron signal to be due to photoionization of real 6P excited atoms produced when the laser is tuned near to the 7P excited levels. We take this as further evidence for an important relationship between SERS and MPI at high densities.

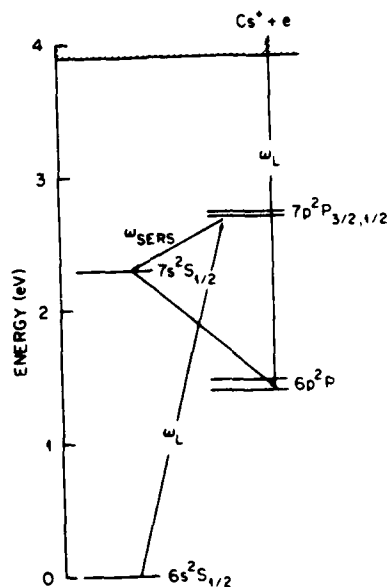


Fig. 2. SERS dominated ionization pathway for one-photon excitation of cesium in the vicinity of the $7p^2P_{3/2,1/2}$ levels.

REFERENCES

- * Also Department of Chemistry, The University of Tennessee, Knoxville, Tennessee 37916.
- ** Present Address: Max-Planck-Institut fur Quantenoptik, Garching, Federal Republic of Germany.
- *** Operated by Martin Marietta Energy Systems, Inc. under contract DE-AC05-84OR-21400 with the U. S. Department of Energy.
- † Also Department of Physics, University of Crete, Greece.
- ‡ Permanent Address: Physics Department, Lewis and Clarke College, Portland, Oregon 97219.
- 1. W. Christian, R. N. Compton, J. A. D. Stockdale, J. C. Miller, C. D. Cooper, X. Tang, and P. Lambropoulos, Phys. Rev. A **30**, 1775 (1984).
- 2. Nonlinear Optics of Free Atoms and Molecules, by D. C. Hanna, M. A. Yuratich, and D. Cotter, (Springer-Verlag, Berlin 1979) p. 187 et seq.
- 3. J. C. Miller and R. N. Compton, Phys. Rev. A **25**, 2056 (1982).
- 4. D. L. Jackson and J. J. Wynne, Phys. Rev. Lett. **49**, 543 (1982).

**Effects of Third-Harmonic Generation on
the Multiphoton Ionization Spectra of Noble Gases**

C. Fotakis, M.J. Proctor⁺ and J.A.D. Stockdale⁺⁺

Research Center of Crete
Institute of Electronic Structure and Laser
P.O. Box 1527, Iraklion, Crete, Greece

There is a renewed theoretical and experimental interest on multiphoton ionization (MPI) studies of noble gases in spectral regions near 3-photon resonances, which may give rise to third-harmonic generation (THG) [1]. In this work we report simultaneous measurements of THG and MPI in Kr over the ultraviolet region between the 3-photon $5s'(J=1)$ resonance and the 4-photon ionization regime. The principle MPI features observed include the p' and f' autoionizing Rydberg series leading to the 2P_2 ionization threshold [2]. With increasing pressure, the f' spectral lines exhibit a profound line narrowing, increase in intensity and lineshape asymmetry reversal, as shown in Figure 1. These findings are compatible with the presence of the third-harmonic field, whose intensity and spectral

⁺ Current address : AERE, Harwell, Oxon, U.K.

⁺⁺ Permanent address : Oak Ridge National Lab., Chemical
Physics Section, Tennessee, U.S.A.

profile are strongly pressure dependent. As the Kr pressure increases, the THG intensity increases leading to a 2-colour, 2-photon ionization mechanism (involving 1-THG and 1-UV photon), which dominates the direct 4-photon excitation process. This conclusion is strengthened further by the results of recent theoretical work [3].

References

- [1] W.R. Garret, W.R. Ferrell, M.G. Payne and J.C. Miller, Phys. Rev. A34 (1986) 1165 and references therein.
- [2] P.R. Blazewicz, J.A.D. Stockdale, J.C. Miller, T. Efthimiopoulos and C. Fotakis, Phys. Rev. A35 (1987) 1092.
- [3] X. Tang and P. Lambropoulos (to be published).

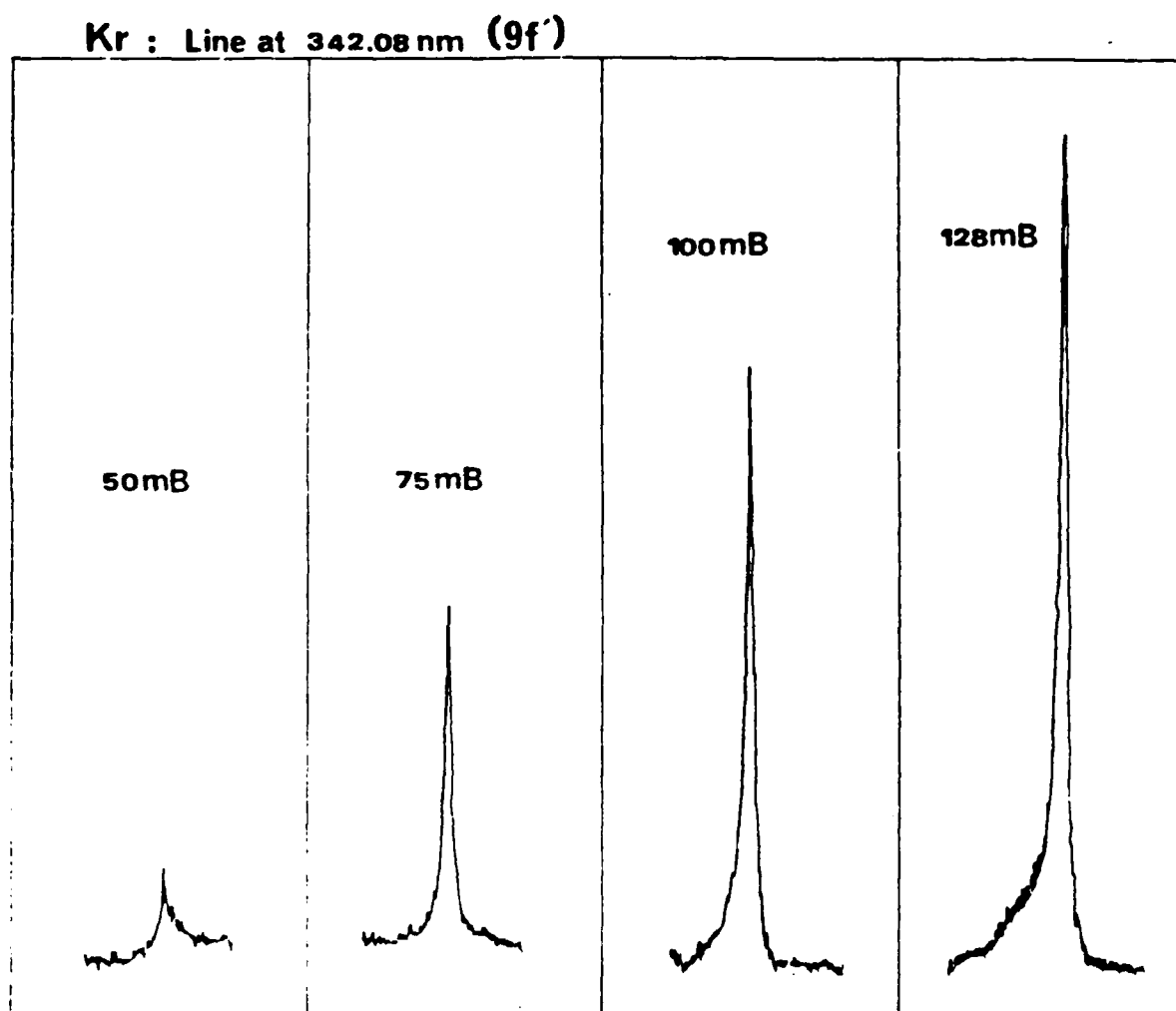


Figure 1 : Pressure dependence of the f' autoionizing Rydberg series of Kr.

AD-A202 520

INTERNATIONAL CONFERENCE ON MULTIPHOTON PROCESSES (4TH)
HELD IN BOULDER CO. (U) JOINT INST. FOR LAB. ASTROPHYSICS
BOULDER CO JUL 88 AFOSR-IR-88-1278 AFOSR-87-0221

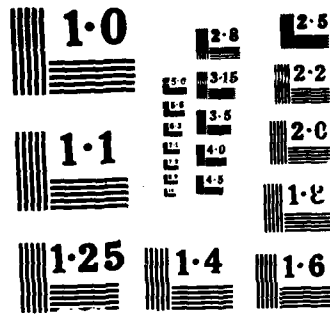
4/4

UNCLASSIFIED

F/G 7/5

NL

END
100
88



MECHANISMS FOR SUPPRESSION OF TWO-PHOTON EXCITATION OF
Na 3d $^2D_{3/2,5/2}$ IN DENSE VAPOR*

W. R. Garrett, Mary Ann Moore**, J. P. Judish,
M. G. Payne, and R. K. Wunderlich***

Chemical Physics Section, Oak Ridge National Laboratory,
P.O. Box X, Oak Ridge, Tennessee, USA, 37821-6125

In two recent experiments Malcuit, Gauthier, and Boyd¹ and Krasnikov, Pshenichnikov, and Solomatin² investigated the suppression of a two-photon excitation process in Na vapor when two simultaneous excitation pathways were provided within phase-matching constraints originally predicted by Manykin and Afanas'ev.³ In the first instance, the behavior of ASE from Na 3d states populated by two-photon laser excitation was monitored in the presence of parametric four-wave mixing from the same state.¹ In the other experiment reduced resonant two-photon absorption involving Na 3S \rightarrow 4S was observed in the presence of FWM driven by a third laser beam², as originally analyzed in Ref. 3.

In a separate study of parametric processes associated with excitation of Na 4d we have observed strong suppression of the two-photon Rabi frequency connecting the 3S and 4d states of Na, leading to decreases in resonantly enhanced degenerate four-wave mixing and resonance ionization associated with pumping of this state.^{4,5} We found that all the results could be explained by the strong broadening and a.c. Stark splitting of the 4d state produced by ASE and stimulated hyper-Raman-parametric four wave mixing from this level. The broadening and splitting of the level resulted in strong suppression of the two-photon pumping rate (and of ionization out of the state) except for the

*Research sponsored by the Office of Health and Environmental Research, U.S. Department of Energy under contract DE-AC05-84OR21400 with the Martin Marietta Energy Systems, Inc.

**Graduate Student, University of Tennessee, Knoxville, Tennessee.

***Present address: Max-Planck-Institut fur Kernphysik, D6900 Heidelberg 1, FRG.

"The submitted manuscript has been authored by a contractor of the U.S. Government under contract No. DE-AC05-84OR21400. Accordingly, the U.S. Government retains a nonexclusive, royalty-free license to publish or reproduce the published form of this contribution, or allow others to do so, for U.S. Government purposes."

short region at the entrance of the laser beam into the metal vapor. No interference effect was needed to explain the data. A similar mechanism can be invoked to explain the results of Malcuit *et al*¹ involving two-photon pumping of the 3d state. The parametric process would also produce the strong suppression of resonant ionization through this level as observed by us⁵ and by Bajic, Compton, and Stockdale.⁶

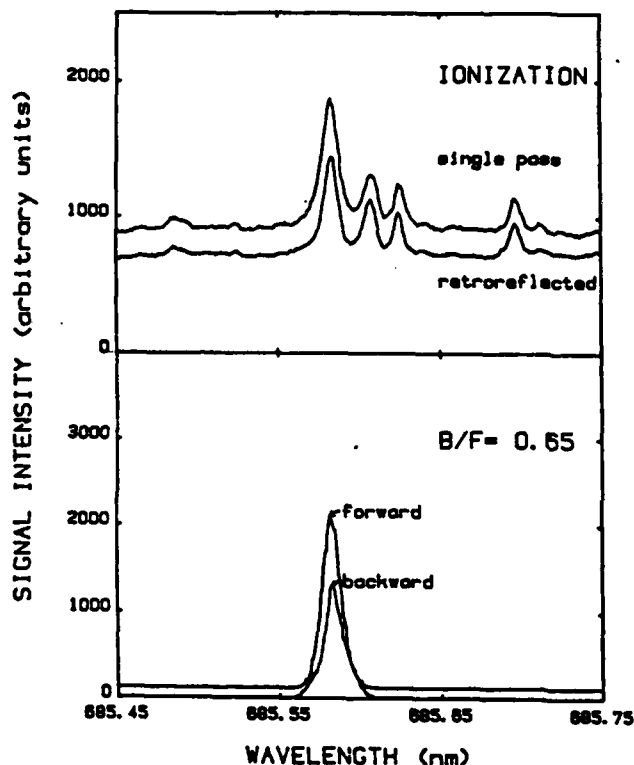


Fig. 1. (a) Ionization signals versus laser wavelength in unidirectional (top) and counter-propagating (bottom) geometries. Peaks on either side of the atomic resonance are due to Na dimers. (b) Backward and forward infrared intensities at the two-photon atomic resonance. $P_{Na} = 0.15$ Torr; Laser Energy = 0.65 mJ/pulse; 35 cm f.l. lens.

We have conducted an experiment which can distinguish between a suppression mechanism based on an interference effect and one based on the proposed broadening and shifting effects. We operate a Na heat pipe with an internal charge collecting wire with which ionization can be monitored in a simple low gain mode. Our earlier studies and those of Bajic *et al*⁶ have already established that resonant ionization is strongly suppressed at 3d and 4d resonances. However, if the interference mechanism is responsible for the suppression, then the use of counterpropagating

beams will restore the two-photon pumping of the 3d state in that part of the total excitation process where one photon from each beam is absorbed. We have conducted such experiments in the same regime of pressure and laser intensity as that of Ref. 3. Results of one set of such measurements are shown in Fig. 1.

Shown in the top trace of the figure is the ionization signal as a function of laser wavelength as the laser in an unidirectional beam, is tuned through two-photon resonance with the $4D_{3/2,5/2}$ level. Indeed the atomic resonance is severely suppressed - to the extent that the atomic line at 685.56 nm is comparable to the signal produced by Na dimers (other peaks) which are fortuitously present at a low concentration. The second trace shows the ionization signal (at the same total intensity) in a counterpropagating beam geometry. Note that the atomic resonance signal is not enhanced as it would be if the suppression were due to an interference effect.⁷⁻⁹ The bottom traces show the rates of backward to forward infrared emission (and the position of the atomic resonance), to indicate that the conditions are similar to those in Ref. 1.

These and other data on suppression of two-photon excitation in dense vapor will be described.

REFERENCES

1. M. S. Malcuit, D. J. Gauthier, and R. W. Boyd, Phys. Rev. Lett., 1086 (1985).
2. V. V. Drasnikov, M. S. Pshenichnikov, and V. S. Solomatin, JETP Lett. 43, 148 (1986).
3. E. A. Manykin and A. M. Afanas'ev, Sov. Phys. JETP 21, 619 (1965); 25, 828 (1967).
4. R. K. Wunderlich, W. R. Garrett, and M. G. Payne, Bull. Am. Phys. Soc. 32, 280 (1987).
5. R. K. Wunderlich, W. R. Garrett, and M. G. Payne, "Saturation Effects in Parametric Four-Wave Mixing in Na Vapor" (unpublished).
6. S. J. Bajic, R. N. Compton, and J. A. Stockdale (private communication).
7. W. R. Garrett, W. R. Ferrell, M. G. Payne, and J. C. Miller, Phys. Rev. A 34, 1165 (1986).
8. D. J. Jackson and J. J. Wynne, Phys. Rev. Lett. 49, 543 (1982).
9. G. S. Agarwal, Phys. Rev. Lett. 57, 827 (1986).

Optimizing Resonant Sum-Frequency Mixing

A. V. Smith, W. J. Alford, G. R. Hadley, and P. Esherick

Sandia National Laboratories

Albuquerque, NM 87185

Obtaining the greatest possible conversion efficiency in a nonlinear mixing process in an atomic vapor requires a careful choice of input frequencies and input intensities. These choices are critical because they determine the refractive index mismatch and the nonlinear susceptibility. Furthermore, for a two-photon resonant process, they can be used to tailor the ratios of various nonlinear processes such as two-photon absorption, Raman loss or gain, and intensity-dependent refractive indices which are critical in achieving high efficiencies. If efficiency is to be maximized, it is also essential to identify the efficiency limiting processes in order to minimize their importance and to decide what to include in a realistic mathematical modeling of the mixing process. We have been studying these issues for two-photon resonant sum-frequency mixing in general and more specifically for generation of 130.2 nm light by mixing in Hg.

In this report we wish to emphasize three aspects of mixing. The first is how one chooses the best set of input frequencies and intensities based on atomic characteristics. The others are the efficiency limiting roles of quantum mechanical interference and of amplified spontaneous emission (ASE) from the resonant level.

For a discussion of two-photon resonant four wave mixing, it is convenient to separate the third order nonlinear susceptibility as usually defined into three parts as follows:

$$\chi^{(3)}(-\omega_4; \omega_1, \omega_2, \omega_3) = \frac{(ea_0)^4}{6(hc)^3} S(\omega_1 + \omega_2) \chi_p(\omega_1) \chi_p(\omega_4) \quad (1)$$

$$\chi_p(\omega) = \sum_f \left[\frac{\langle i | \vec{d} \cdot \vec{e}_\omega | f \rangle \langle f | \vec{d} \cdot \vec{e}_\omega | g \rangle}{\omega_f - \omega} + \frac{\langle i | \vec{d} \cdot \vec{e}_\omega | f \rangle \langle f | \vec{d} \cdot \vec{e}_{\omega'} | g \rangle}{\omega_f - \omega'} \right] \quad (2)$$

where $\omega + \omega' = E_i$ with i designating the two-photon resonant intermediate level. The \hat{e}_ω 's are unit vectors defining the polarization of light at frequencies ω , and d is the dipole moment operator. Thus $\chi_p(\omega_1)$ describes the part of $\chi^{(3)}$ involving waves 1 and 2 while $\chi_p(\omega_4)$ describes the part involving waves 3 and 4. The S factor is the appropriately Doppler broadened two-photon resonant denominator.

Using these definitions, the four coupled equations describing the growth of the four waves have similar form with the derivative of the electric field of wave 1, A_1 , given by

$$\frac{dA_1}{dz} = iC\omega_1 S(\omega_1 + \omega_2) \left[\chi_p(\omega_1) \chi_p(\omega_4) A_4 A_2^* A_3^* \exp(i\Delta kz) + \chi_p(\omega_1)^2 A_1 |A_2|^2 \right] \quad (3)$$

When S is imaginary, i.e. for exact two-photon resonance, the first term in brackets is associated with mixing of waves 2, 3, and 4 to produce polarization at the frequency ω_1 , while the second term is associated with two-photon absorption of photons from beams 1 and 2 leading to population of the resonant state. The other three equations are similar in form but with the two-photon absorption term replaced by a term describing the Raman process of absorption of ω_4 and emission of ω_3 .

To determine the limits of mixing efficiency and to reach an understanding of the limiting factors, we have numerically integrated these equations for the plane wave case. We find that on resonance with $\Delta k = 0$, the conversion process saturates when the two terms inside brackets in Eq. (3) become equal. This occurs when ω_4 builds up to a level such that

$$\chi_p(\omega_1) A_1 A_2 = \chi_p(\omega_4) A_3^* A_4 \quad (4)$$

At this point no further mixing nor two-photon absorption occurs. We interpret this as being due to a destructive interference between two channels from the ground state to the two-photon resonant state. The two channels are two-photon absorption of waves 1 and 2 on one hand and the Raman process of absorption of wave 4 and emission into wave 3. As a result of this effect, we find that the best conversion efficiency occurs when $\chi_p(\omega_1) \approx \chi_p(\omega_4)$ and the photon fluxes of the three input waves

are approximately equal. Energy conversion efficiencies under these conditions range from 20% to as high as 40%. The ratio of χ 's can generally be altered for a fixed output frequency ω_4 by changing the frequencies ω_1 and ω_2 . Thus for maximum efficiency, this can be an important consideration in selection of the input frequencies. Of course refractive index matching is also of critical importance in this selection.

In frequency mixing in Hg we have identified another process which can have a profound effect on mixing efficiency. When tuned to the two-photon resonance, population built up in the resonant level leads to ASE to a lower lying level. This radiation power broadens the two-photon transition leading to a reduced value for $S(\omega_1+\omega_2)$. We have shown experimentally that replacing the Doppler broadened line shape by a Gaussian line shape with a width given by $[(\Delta\omega_D)^2+(\Delta\omega_P)^2]^{1/2}$ is a good approximation in the presence of ASE. Here $\Delta\omega_D$ is the Doppler width and $\Delta\omega_P$ is the Rabi width associated with the observed ASE intensity. In fact, for Hg the line shape function is also complicated by isotope shifts of about the size of the Doppler width, but detailed modeling of the observed shapes shows that the replacement above is a good approximation. Although ASE does not alter the effect of the interference discussed above, it does lead to greatly increased interaction lengths before saturation is reached thereby reducing practical efficiencies.

ASE can be avoided by tuning slightly off the two-photon resonance. However, this leads to reduced value of $S(\omega_1+\omega_2)$ and also to an intensity-dependent refractive index that introduces an intensity-dependent value of Δk . We are presently examining this case for mixing in Hg. Preliminary indications are that efficiencies can be quite high but at the expense of increased interaction lengths. It remains to be determined whether best mixing efficiencies can be achieved by tuning to the two-photon resonance with ASE broadening or by tuning slightly off resonance with a nonlinear refractive index and reduced S value.

This work was performed at Sandia National Laboratories, supported by the U.S. Department of Energy under contract number DE-AC04-76DP00789.

Resonant Degenerate Four Wave Mixing with Broad-bandwidth Lasers

A. Charlton[†], J. Cooper[†], G. Alber^{*}, D. Meacher^{**} and P. Ewart^{**}

[†] Joint Institute for Laboratory Astrophysics, University of Colorado and National Bureau of Standards, Boulder, Colorado, USA

^{*} Institute for Theoretical Physics, Innsbruck, Austria

^{**} Clarendon Laboratory, University of Oxford, Oxford, UK

Many nonlinear optical or multiphoton processes involve pulsed lasers which provide a radiation field with a finite bandwidth. The associated field fluctuations can lead to significant modification of the interactions. Such effects have been studied extensively in the cases of laser induced fluorescence and multiphoton absorption and ionization^[1-4]. Much less work has been done on parametric processes such as four-wave mixing. We present the results of a theoretical and experimental study of laser-bandwidth effects on the practically important process of resonant degenerate four-wave mixing, DFWM.

Our theoretical model treats the case of two intense counter propagating pump fields of finite bandwidth, which are characterised by a chaotic field, and a weak, monochromatic probe beam interacting with a medium consisting of a gas of two-level atoms. Such a model was previously treated in an earlier publication^[5]. The present theory revises this earlier work which omitted two seemingly lower order terms involving population differences, one of which can not actually be neglected when the medium is driven into saturation by strong fields. The density matrix equations describing the time evolution of the atomic polarization coupled to fluctuating fields are solved by integration in the time domain using an appropriate decorrelation approximation. The problem is complicated in the case of DFWM using counterpropagating beams. The polarization responsible for the generated signal must be correctly spatially averaged over

the interaction volume. This procedure requires that both spatial and temporal correlations be correctly taken into account. In the general case this is a very difficult problem especially when effects of atomic motion are to be included. We present a steady state solution in the case where the laser bandwidth exceeds all other relaxation rates in the problem and where the Doppler width of the atomic transition is greater than the natural width but still less than the laser bandwidth. This is a situation often encountered experimentally.

The experimental problem centres on the production of an intense source of variable bandwidth, tunable radiation which approximates to a chaotic field. Such a source, a mode-less laser, has recently been developed^[6]. The output consists of a spectrally narrowed, and tunable, continuum which may be considered as a very large number of closely spaced, uncorrelated modes. We have used this laser to study resonant DFWM in atomic vapours. The DFWM reflectivity has been measured as a function of pump intensity for different laser bandwidths. Direct comparison of experimental results with theoretical predictions is complicated by several factors. These include the effects of opacity near the atomic resonance, the transient nature of the interaction using pulsed lasers and the spatial variation of laser intensity across the beam. We present the results of experiments using sodium and barium vapour where taking into account these factors, the main theoretical predictions have been confirmed.

References

1. B.R. Mollow, Phys. Rev. 175, 1555 (1968)
2. G.S. Agarwal, Phys. Rev. A1, 1445 (1970)
3. H.J. Kimble and L. Mandel, Phys. Rev. A15, 689 (1977)
4. P. Zoller and P. Lambropoulos, J. Phys. B13, 69 (1980)
5. G. Alber, J. Cooper and P. Ewart, Phys. Rev. A31, 2344 (1985)
6. P. Ewart, Optics Commun. 55, 124 (1985).

MULTIPHOTON IONIZATION AND INFRARED GENERATION IN A CESIUM HEAT
PIPE OVEN NEAR THE TWO-PHOTON IONIZATION LIMIT*

W. Christian
Davidson College

Infrared generation and multiphoton ionization were observed in a heat pipe oven following excitation using a high power Nd:YAG pumped dye laser tuned near the two-photon resonances of the high D and S states. The ionization signal shown in figure 1 was primarily three-photon ionization with an enhancement at the two-photon resonances while the infrared emission spectrum had two distinctly different characteristics depending on the pressure within the oven. At pressures above 3 Torr, the IR emission shown in figure 2 was coincident with the MPI peaks and was due primarily to fluorescence or OPSE from the high Rydberg states pumped by the laser to low lying unpopulated states. At pressure below 2 Torr, however, IR emission was detected when the laser was tuned between the two-photon S and D state resonances.

The shape of the IR emission shown in figure 3 suggests hyper-stimulated electronic Raman scattering.¹ In this process, two photons are absorbed into a virtual state which emits an IR Raman photon into one of the neighboring P or F states. Since hyper-stimulated electronic Raman scattering did not occur when the laser was coincident with a two-photon resonance and since the density was not high enough for OPSE, a dip in the total IR emission was observed coincident with the MPI peak.

References

1. D. Cotter, D. C. Hanna, W. H. W. Tuttlebee, M. A. Yuratich, Optics Comm. 22, 190 (1977).

*Research supported by National Science Foundation grant No. CHE-856912.

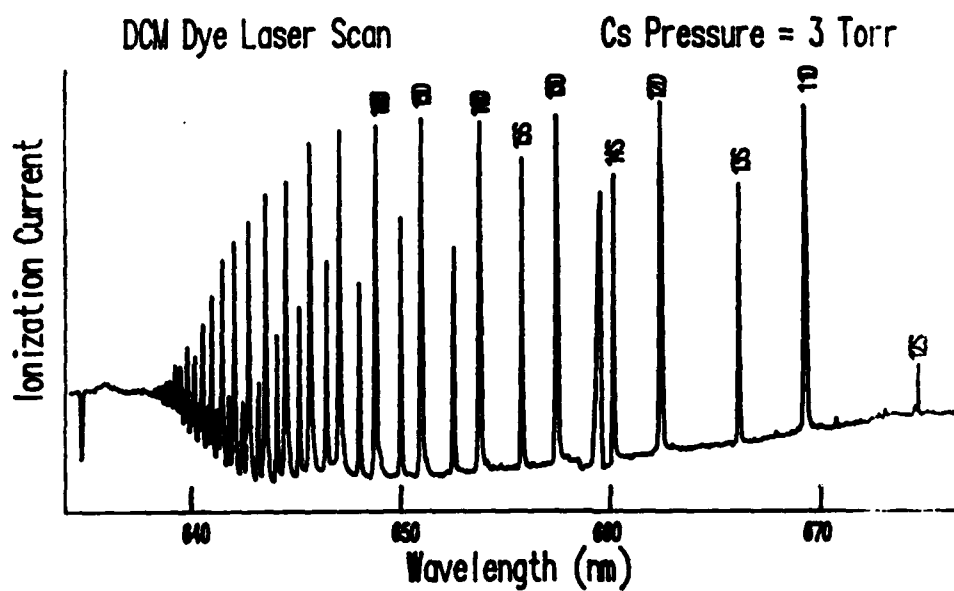


Figure 1.

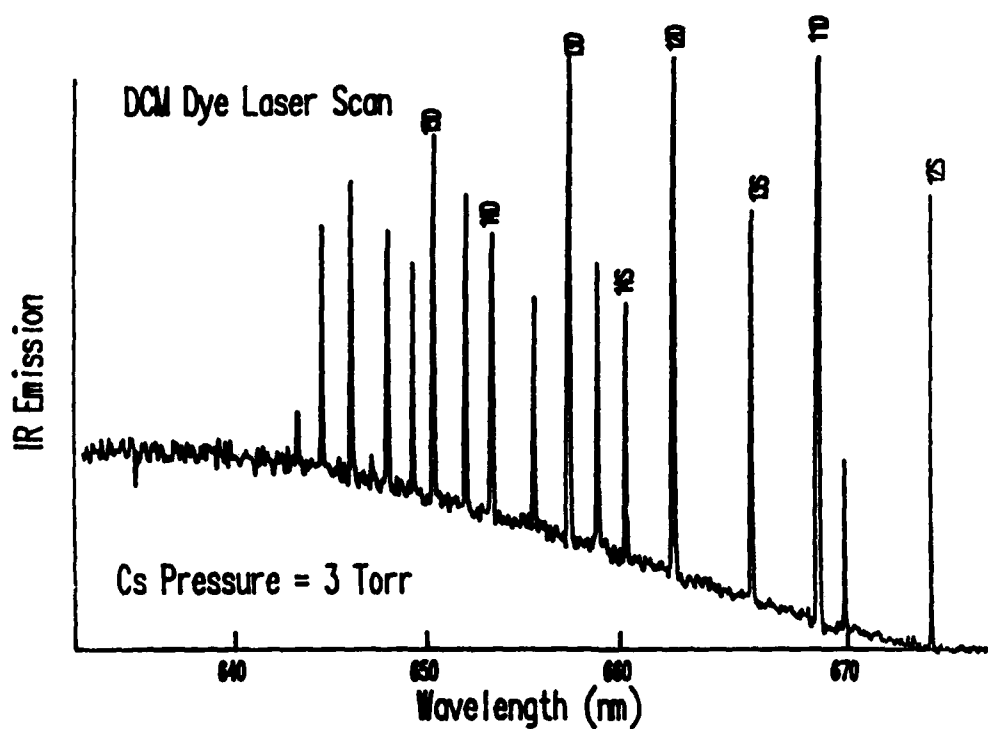


Figure 2.

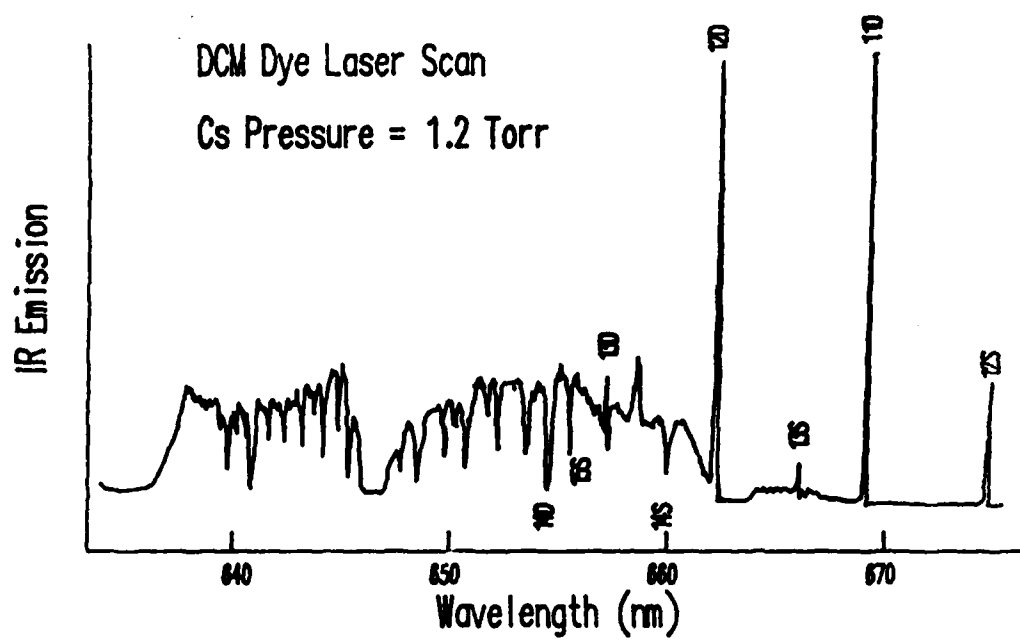


Figure 3.

CONTRIBUTION OF MULTIPHOTON ABSORPTION TO THE NONLINEAR
REFRACTIVE INDEX OF SF₆

Y. Beaudoin, I. Golub and S. L. Chin
Laboratoire de Recherches en Optique et Laser
Département de Physique, Université Laval
Québec, Canada G1K 7P4

Laser beam propagation effects play an important role in experiments on multiphoton excitation and dissociation of molecules. In order to evaluate quantitatively these effects data is needed on the nonlinear refractive index of a multilevel system. We present here a simple technique for direct measurement of the nonlinear dispersion of a molecular gas in the IR. The dependence of the refractive index n of SF₆ on laser fluence exhibits novel features which are attributed to the contribution of the quasi-continuum.

The nonlinear refractive index n_2 and the related nonlinear susceptibility $\chi^{(3)}$ of SF₆ were derived from indirect experiments by measuring the reflectivity of phase-conjugated signal¹ or from the self-focused beam diameter dependence on laser intensity.² In particular the latter technique has also the disadvantage of being influenced by the intensity dependent absorption.³ The susceptibility was also calculated theoretically by simulating the vibration-rotation structure of SF₆ molecule^{4,5} without taking into account the quasi-continuum (QC).

The experimental apparatus consists of a single longitudinal mode CO₂ pulsed laser irradiating, after amplification and spatial filtering, a 1.5 cm long prismatic cell containing the SF₆ gas. The laser pulse is 200 nsec long and has a diameter of 5 mm. The spatial deviation of the gaussian laser beam is measured by a detector array as a function of SF₆ gas pressure p in the range 0-2 torr at different CO₂ laser lines and for different laser fluences.

Dispersion curves at various laser fluences are shown in Fig. 1. At high laser fluence the dispersion curve undergoes a red shift and broadening as compared to that at low laser fluence indicating that the molecules have climbed the anharmonic vibrational ladder. This

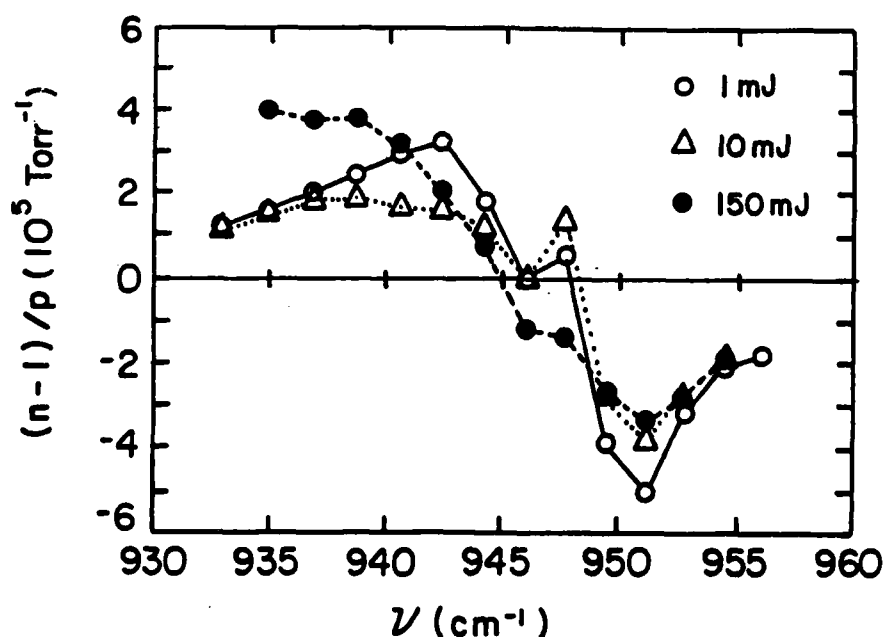


Fig. 1. Dispersion of the refractive index of SF₆ for three different CO₂ laser energies.

correlates well with the similar behavior of the absorption curve.⁶ We also obtain the well-known effects of self-focusing (S.F.), self-defocusing (S.D.) and the transition from S.D. to S.F. with increasing the laser fluence.⁷ Figure 2 shows the dependence of the refractive index as a function of the energy E of the laser pulse at the P(28) CO₂ laser line. The index goes through a minimum and then increases rapidly at high E . This dependence agrees qualitatively with the indirect measurement of Bertsev et al.² in the sense that n went through a minimum although they did not obtain a significant increase of n at high laser fluence, while contradicting the theoretical calculation of Ackerhalt et al.⁴

To explain our results, we invoke that in our experiments the average number of photons absorbed by one molecule is up to 10, and around 50% of the molecules are excited to the QC.⁸ At low laser fluences, the transitions $V=0 \rightarrow V=1$ is saturated leading to a decrease in the refractive index (Fig. 2). With increasing fluence, higher vibrational transitions become quasi-resonant (due to the "red shift"),

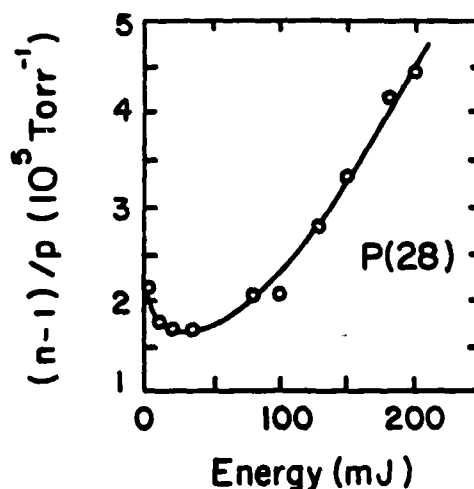


Fig. 2. Variation of the refractive index $(n-1)/p$ with energy at a frequency of 936.8 cm^{-1} .

leading to an increase in n . For still larger fluences, the polarizability of the "hot" molecules in the QC starts to contribute to the n . The density of states in the QC is very high.⁸ Thus the polarizability of "hot" molecules integrated over the states⁹ in the QC, may be quite large, explaining the observed high value of n (Fig. 2).

Future experiments with shorter CO_2 laser pulses and increased intensity will allow to go further in the QC and to study in more detail its influence on the nonlinear refractive index.

REFERENCES

1. L. T. Bolotskikh, V. G. Popkov, A. K. Popkov and V. M. Shalaev, *Sov. J. Quantum Electron.* **16**, 616 (1986).
2. V. V. Bertsev, M. O. Bulanin and I. A. Popov, *Opt. Spectrosc.* **51**, 178 (1981).
3. P. Bernard, P. Galarneau, and S. L. Chin, *Opt. Lett.* **6**, 139 (1981).
4. J. R. Ackerhalt, H. W. Galbraith and J. C. Goldstein, *Opt. Lett.* **6**, 377 (1981).
5. J. R. Ackerhalt, D. O. Ham, A. V. Novak, C. R. Phipps, Jr., and S. J. Thomas, *IEEE J. Quantum Electron.* **QE-19**, 1120 (1983).
6. A. V. Novak and J. L. Lyman, *J. Quant. Spectrosc. Radiat. Transfer* **15**, 945 (1975).
7. A. V. Novak and D. O. Ham, *Opt. Lett.* **6**, 185 (1981).
8. V. S. Letokhov and A. A. Makarov, *Sov. Phys. Usp.* **24**, 366 (1981).
9. Y. Beaudoin, P. Galarneau, A. Normandin, and S. L. Chin, *Appl. Phys. B* **42**, (1987), to be published.

Laser-induced Autoionizing-like Behavior, Population
Trapping and Stimulated Raman Processes in Real Atoms

Bo-nian Dai and P. Lambropoulos

University and Research Center of Crete, Iraklion, Crete 71110, Greece

and

Physics Department, University of Southern California
Los Angeles, California 90089-0484

The last ten years have seen a number of papers¹⁻⁷ devoted to what is referred to as autoionizing-like (AL) behavior, when two bound atomic states of a one-electron atom are coupled to the same continuum state by two independent lasers. Let $|g\rangle$ be a ground and $|a\rangle$ an excited state below threshold, with respective energies E_g and E_a . One laser of frequency ω_1 is chosen so that $E_g + \hbar\omega_1$ is above the ionization threshold, while the frequency ω_2 of a second laser is such that $E_a + \hbar\omega_2 \approx E_g + \hbar\omega_1$. The atom, being initially in state $|g\rangle$, will simply ionize if only laser ω_1 is turned on. With both lasers on, a number of interference effects may be manifested as the frequencies and intensities of the two sources are varied. One much discussed^{3,4} such effect, for example, may lead to trapping atomic population in the excited state $|a\rangle$. A related quantity is the line-shape of ionization⁷ (or equivalently absorption² of the radiation at ω_1) as ω_1 is tuned around the resonance value $\hbar\omega_1 = E_a - E_g + \hbar\omega_2$ with ω_2 held fixed. As asymmetric line-shape has been predicted^{1,2} (hence the characterization AL) and its implication on other processes, such as harmonic generation has been contemplated.^{5,6} In recent experiments, however, Feldmann et al.⁷ found no such asymmetry and pointed out that Raman processes made the dominant contribution.

We present a theory and the results of realistic calculations that:
(a) Demonstrate that certain important aspects overlooked in previous theories introduce qualitative changes and drastically modify expectations on population trapping; (b) Unify apparently different

processes; (c) Interpret existing experimental results; (d) Demonstrate that theoretical modelling of these processes with free parameters not derived from atomic calculations can lead to quite misleading conclusions and expectations.

For the experiment of Feldmann et al.⁷, we show that because of the dominance of the Raman processes the q parameter is 2.4×10^3 which explains why no asymmetry was observed.

The results of our analysis of the data of ref. 2 are summarized in Fig. 1a through c. Fig. 1a demonstrates the importance of the Raman

coupling $D_{ga}^{(2)}$ without which the line-shape is qualitatively different from what was observed.

Fig. 1b demonstrates that population trapping to the excited state $|a\rangle$ is only short term and is limited by ionization of $|a\rangle$ due to laser I_1 ; an effect that has been overlooked in previous work.^{3,4} Because of this additional ionization channel, any population trapping will be significant only for times such that $\gamma_a^{(1)} t < 1$ where $\gamma_a^{(1)}$ is the ionization width of $|a\rangle$ due to laser I_1 .

Fig. 1c shows the time evolution of the ground state.

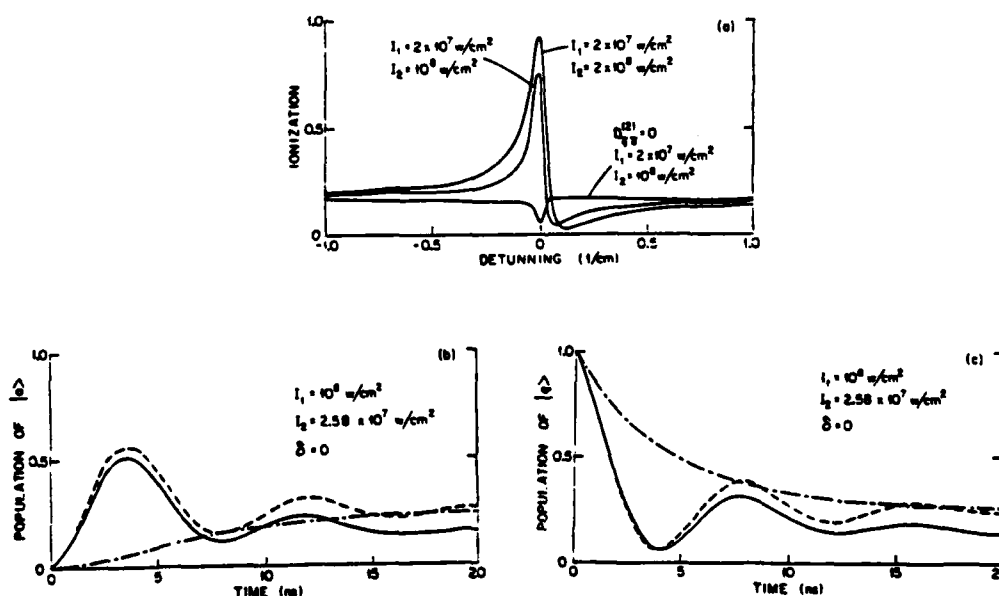


Fig. 1a. Ionization line shape for various combinations of laser intensities with and without the Raman process indicated. The states 6s and 8s of Cs are coupled to the p continuum by two lasers of intensities I_1 and I_2 and frequencies $\omega_1=33,715 \text{ cm}^{-1}$ $\omega_2=9,397.83 \text{ cm}^{-1}$ as in the experiment of ref. 2. The pulse duration is 5 ns.

Fig. 1b. Population of state $|a\rangle = 8s$ as a function of pulse duration, for $\delta=0$ and the indicated intensities.

———— Calculation includes all decays for $|a\rangle$ and $|g\rangle$.

i.e. $\gamma_a^{(1)} = 0$, $\gamma_a^{(2)} = 0$, $D_{ga}^{(2)} = 0$.

- - - - Calculation with $\gamma_a^{(1)}=0$ but with the Raman included.

— · — Calculation with $\gamma_a^{(1)}$ and $D_{ga}^{(2)}$ set equal to zero.

Fig. 1c. Population of state $|g\rangle=6s$ as a function of pulse duration for $\delta=0$ and the indicated intensities. The various lines correspond to the conditions of Fig. (1b) above.

References

1. Yu. I. Heller and A. K. Popov, Opt. Commun. 18, 449 (1976); also Sov. Phys. JETP 51, 255 (1980).
2. Yu. I. Heller, V. F. Lukinykh, A. K. Popov and V. V. Slabko, Phys. Lett. 82A, 4 (1981).
3. P. E. Coleman and P. L. Knight, J. Phys. B 15, L235 (1982).
4. P. E. Coleman, P. L. Knight and K. Burnett, Opt. Commun. 42, 171 (1982); P. L. Knight, M. A. Lauder, P. M. Radmore and B. J. Dalton, Acta Physica Austriaca 56, 103 (1984) and references therein.
5. S. S. Dimov, L. I. Pavlov, K. V. Stamenov and G. B. Altshuller, Opt. Quantum Electron. 15, 305 (1983).
6. S. S. Dimov, L. I. Pavlov, K. V. Stamenov, Yu. I. Heller and A. K. Popov, Appl. Phys. B 30, 35 (1983).
7. D. Feldmann, G. Otto, D. Petring and K. H. Weige, J. Phys. B 19, 269 (1986).

This project was supported by the National Science Foundation, under Grant No. PHY-8306263.

MULTIPHOTON DOUBLE EXCITATION AND IONIZATION OF O^{2+}

X. Tang and P. Lambropoulos

Physics Department, University of Southern California
Los Angeles, California 90089-0484

Continuing our studies⁽¹⁾ of multiphoton excitation and ionization of multielectron atoms and ions, we have considered excitation and ionization processes of carbon-like O^{2+} under strong pulsed lasers of intensity up to 10^{14} W/cm². We report results on double ionization induced by processes of up to fourth order. Our calculations address questions pertaining to the role of doubly excited states, the relative importance of direct and sequential double ionization and the possibility of inverted ionic populations.

The absorption of two photons each of which has frequency $\omega=365338$ cm⁻¹ lead from the ground state $1s^2 2s^2 2p^2(3P_0)$ to the doubly excited state $3d^2(3P_0)$ which lies at about 287485 cm⁻¹ above the first ionization threshold. One more photon leads directly to O^{4+} through single-photon double-electron ejection from the $3d^2$ state. Single-photon absorption from the $3d^2$ state can also lead to excited states of O^{3+} . We present calculations for the branching ratios of such processes.

In a different process, two photons each of frequency $\omega=330526$ cm⁻¹ lead to the excitation of $3p^2(3P_0)$ from where it takes two more photons to obtain O^{4+} . Again O^{3+} can be obtained by single-photon absorption from $3p^2(3P_0)$ with branching ratios leading to various excited states.

The double ionization through the $3d^2$ requires correlation in the transition from $3d^2$ to the double continuum $k\bar{k}l'l'$, but does not require correlation for the two-photon transition $2p^2 \rightarrow 3d^2$. On the contrary, double ionization through the $3p^2$ requires correlation for the two-photon transition $2p^2 \rightarrow 3p^2$ but not for the transition $3p^2 \rightarrow k\bar{k}l'l'$. We evaluate and discuss the relative magnitudes of the

two schemes and the implications for the role of correlation in multiphoton transitions.

The wave-functions are generated by a multiconfiguration Hartree-Fock⁽²⁾ calculation. The transition probabilities and the behavior of the system as a function of the laser intensity are calculated through R-matrix techniques obtained through the resolvent operator as employed in previous work⁽¹⁾.

References

1. X. Tang and P. Lambropoulos, Phys. Rev. Lett. 58, 108 (1987).
2. C. F. Fisher, Comput. Phys. Commun. 4, 107 (1972).

This project was supported by the National Science Foundation, under Grant No. PHY-8306263.

MULTIPLE IONIZATION AND X-RAY EMISSION FOLLOWING
INNER-SHELL PHOTOIONIZATION OF ATOMS*

V. L. Jacobs

E. O. Hulburt Center for Space Research
Naval Research Laboratory
Washington, D.C. 20375-5000

B. F. Rozsnyai

Lawrence Livermore National Laboratory
Livermore, California 94550

We have developed a model for determining the probabilities of emitting a given number of Auger electrons and the probabilities of the various radiative transitions during the cascade decay process which follows the creation of a distribution of vacancies among the nl-subshells of an atomic system. It has been assumed that the elementary radiative and Auger processes occur sequentially and independently of the initial ionization process. Particular emphasis has been given to the decay products resulting from single inner-shell vacancies. Results of calculations have been obtained for single inner-shell ionization of neutral iron and iron ions, taking into account all of the Auger, Coster-Kronig, and electric-dipole radiative transitions which can occur during the inner-shell vacancy cascade process.

*This work has been supported by the U. S. Office of Naval Research.

COHERENT EXCITATION OF TWO ELECTRONS IN AN INTENSE LASER FIELD

T. K. Rai Dastidar and K. Rai Dastidar

Indian Association for the Cultivation of Science

Calcutta 700032, India

Correlated excitation of two electrons in intense laser fields has long been a subject of speculation¹ as a possible clue to the phenomenon of above-threshold double ionization.² Depending on laser wavelength, intensity and pulse duration, either stepwise double ionization (SDI) or direct double ionization (DDI) or both can occur.

As a background to the work described below, a few salient features observed experimentally in double ionization are outlined:

i) Double ionization almost invariably requires higher intensity than single ionization does.

ii) Sr and Xe undergo DDI at 1064 nm laser wavelength but SDI at 532 nm.^{3,4}

iii) The index of non-linearity observed⁵ for production of doubly ionized Sr and Ba is in each case much less than the number of photons required to raise the atoms from their ground state to the doubly ionized state.

iv) Double ionization occurs for short pulses only; Ca irradiated with nanosecond pulses does not yield doubly charged ions, whereas with picosecond pulses at 1064 nm, the yield of Ca^{++} exceeds that of Ca^+ .⁶

We demonstrate below that under certain conditions for intensity, wavelength and pulse duration, two (or more) electrons in an atom can collectively respond to a laser field and be coherently excited, and that this coherent excitation can maintain the degree or 'tightness' of their radial correlation initially present. As Wannier⁷ showed in a different context, tight radial correlation leads to double electron escape from the nucleus (or the ionic core).

We can add the matrix elements $\langle f | \vec{r}_1 \cdot \vec{E} e^{-i\omega t_1} | i \rangle$ and $\langle f | \vec{r}_2 \cdot \vec{E} e^{-i\omega t_2} | i \rangle$ for photon absorption by the electrons coherently

if the two operators match in phase. For this we require that $|t_1 - t_2| \ll 1/\omega$. The physical consequence of this coherent addition of these two elements is that the system passes from the state $|i\rangle$ to $|f\rangle$ with $E_f = E_i + 2\hbar\omega$ in one direct double-excitation step, and that the resultant matrix element depends linearly on the field strength E , whereas conventional perturbation theory leads to a quadratic power dependence for a two-photon excitation.

We use hyperspherical coordinates (e.g. Ref. 8) to describe a two-electron atom:

$$\begin{aligned}\psi &= R^{-5/2} \sum_{\mu} F_{\mu}(R) \phi_{\mu}(\alpha_1 \hat{r}_1, \alpha_2 \hat{r}_2) \\ \phi_{\mu} &= A_{\mu} (\cos \alpha_1)^{l_1} (\sin \alpha_2)^{l_2} P_{n_r}^{(l_2 + 1/2, l_1 + 1/2)}(\cos 2\alpha) \\ &\quad \sum_{m_1 m_2} (l_1 l_2 m_1 m_2 | l_1 l_2 LM) Y_{l_1 m_1}(\hat{r}_1) Y_{l_2 m_2}(\hat{r}_2).\end{aligned}$$

The subscript n_r of the Jacobi polynomial is the radial correlation quantum number (n_{rc} of Fano⁸). It equals the number of nodes in the Jacobi polynomial along

$$\cos 2\alpha \left(- \frac{r_1^2 - r_2^2}{R^2} \right)$$

and can be visualized to provide a measure of the 'tightness' of radial correlation.

Putting $r_1 = R \cos \alpha$ and $r_2 = R \sin \alpha$, we evaluate the matrix element $T = \langle f | \vec{r}_1 \cdot \vec{E} + \vec{r}_2 \cdot \vec{E} | i \rangle$. It turns out that if $\Delta l = +1$ for both the electrons, T imposes a selection rule $\Delta n_r = 0$; if $\Delta l = -1$ for both electrons, $\Delta n_r = 0$ or $+1$. Thus coherent excitation either maintains or increases the degree of radial correlation, and hence provides a direct pathway to DDI.

The coherence condition $|t_1 - t_2| \ll 1/\omega$ mentioned earlier implies that for visible light, $|t_1 - t_2|$ should be $\sim 1-2$ a.u. of time. An atom presents a cross-sectional area of order $n^4 a_0^2$ to a laser beam, n being the principle quantum number of the outer-shell electrons. Thus for this condition to be satisfied, the photon flux should be at least of

order $1/n^4$ photon a_0^{-2} (a.u. of time) $^{-1}$. Since the photon flux equals $I/\hbar\omega$, it is obvious that the larger the wavelength, the smaller the intensity required to satisfy the coherent excitation condition; whereas for smaller wavelengths, single-ionization signal would be likely to have saturated by the time intensities are raised high enough to meet the said condition. Thus we would generally expect SDI at shorter wavelengths and DDI at larger wavelengths. Furthermore, for a given power, narrow pulses provide higher peak intensity and thus larger photon flux.

We see therefore that all the features (i)-(iv) mentioned at the outset are qualitatively explained by this proposed coherent double excitation mechanism. More detailed work-out of the model is in progress.

REFERENCES

1. See e.g. L. A. Lompre and G. Mainfray in 'Multiphoton Processes,' ed. P. Lambropoulos and S. J. Smith (Springer, 1984) p. 23.
2. See M. Grance, Phys. Rev. 144, 117 (1987) for a review.
3. P. Agostini and G. Petite, Phys. Rev. A 32, 3800 (1985).
4. A. L'Huillier, L. A. Lompre, G. Mainfray, C. Manus, J. Phys. B 16, 1363 (1983).
5. I. S. Alelsakhin, N. D. Delone, I. P. Zapesochny and V. V. Suran, Sov. Phys. JETP 49, 447 (1979).
6. P. Agostini and G. Petite, J. Phys. B 17, L281 L811 (1985).
7. G. Wannier, Phys. Rev. 90, 817 (1953).
8. U. Fano. Rep. Prog. Phys. 46, 97 (1983).

RESONANT TWO-PHOTON AUTOIONIZATION OF H_2 : LASER BANDWIDTH AND
AC STARK EFFECT ON PHOTOELECTRON ANGULAR DISTRIBUTION
AND INTERMEDIATE LINESHAPE

S. Ganguly and K. Rai Dastidar

Indian Association for the Cultivation of Science,
Calcutta 700032, India

We have earlier¹⁻³ reported on work on the resonant two-photon autoionization of H_2 in a single-mode laser field. In the present work we incorporate two factors not considered earlier, viz. laser bandwidth effect and ac Stark effect, and determine their influence on the photoelectron angular distribution (PEAD) and the intermediate lineshape.

Figure 1 shows the PEAD at a laser intensity of 10^6 W/cm² at three different values of laser bandwidth γ_L obtained using the phase diffusion model. Figure 2 shows the effect of the ac Stark shift of the intermediate level on the PEAD at two different intensities: the narrowing down of the waist at the higher intensity is significant.

Finally, the effect of the variation of laser bandwidth γ_L on the resonant lineshape of the intermediate state is shown in Figure 3 at an intensity of 10^{11} W/cm², where the ac Stark shift of the level is important. The spectacular effect of the Stark shift, namely the broadening and left-shifting of the peak is clearly marked at the lowest bandwidth. As the bandwidth is increased this effect vanishes, leading to a narrow lineshape symmetrical around zero detuning.

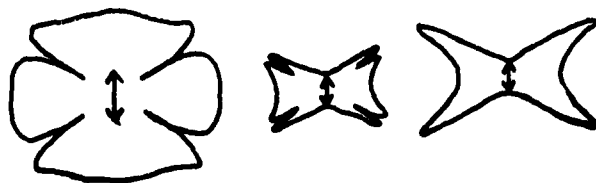


Fig. 1. PEAD at $\gamma_L = 10\gamma_s, 100\gamma_s$ (left to right) where γ_s , the spontaneous decay width of the intermediate $B^1\Sigma_u(v_1=0, j_1=1)$ level = 1.25×10^{-3} cm⁻¹. The final H_2^+ ion level is $X^2\Sigma_g(v_1=1, j_1=0)$.



Fig. 2. Effect of the ac Stark shift on the PEAD at $I = 10^8 \text{ W/cm}^2$ (left) and 10^{12} W/cm^2 (right), with a laser bandwidth $\gamma_L = 1.36 \times 10^{-2} \text{ cm}^{-1}$. The intermediate and ionic levels are $B^1\Sigma_u(v_i=1, j_i=1)$ and $X^2\Sigma_g(v_i=0, j_i=0)$ respectively.

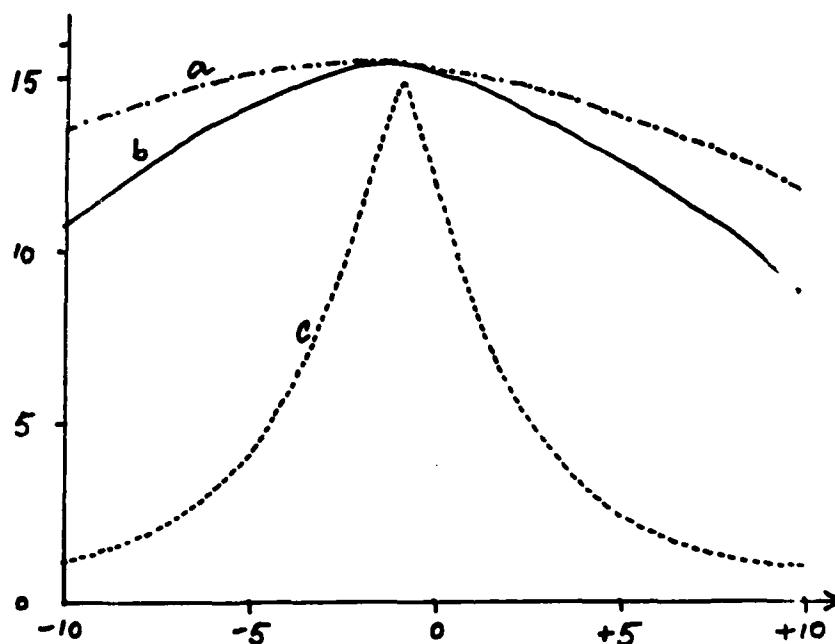


Fig. 3. Intermediate lineshape vs detuning (of Ref. 2) in units of $\gamma_L + \gamma_s$ (γ_s equal to $1.36 \times 10^{-3} \text{ cm}^{-1}$) at different laser bandwidths. γ_L for curve a, $1.36 \times 10^{-3} \text{ cm}^{-1}$ curve b, $1.36 \times 10^{-2} \text{ cm}^{-1}$; curve, $1.36 \times 10^{-1} \text{ cm}^{-1}$. Intermediate and ionic levels same as in Fig. 2.

REFERENCES

1. K. Rai Dastidar, S. Ganguly and T. K. Rai Dastidar, XIV ICPEAC (1985) Book of Abstracts, p. 98.
2. S. Ganguly, K. Rai Dastidar and T. K. Rai Dastidar, Phys. Rev. A 33, 337 (1986).
3. K. Rai Dastidar, S. Ganguly and T. K. Rai Dastidar, Phys. Rev. A 33, 2106 (1986).

Application of Multiphoton Excitation Techniques to Combustion Diagnostics

U. Meier, K. Kohse-Höinghaus, J. Bittner, Th. Just
DFVLR-Institut für Physikalische Chemie der Verbrennung,
Stuttgart, W. Germany

Multiphoton techniques have been developed rapidly from a subject of fundamental research to applications in various fields. Here we present results of experiments on combustion diagnostics.

For a detailed understanding of combustion processes, particularly with respect to pollutant formation, measured absolute concentrations of atoms and molecular radicals are of considerable importance for the development and critical examination of chemical-kinetic flame models. Methods based on multiphoton excitation have been proved useful for the detection of these species in several respects. They provide sensitive spatially resolved detection of atoms like H and O with high-lying excited states which are not accessible to single-photon excitation due to the opacity of flames in the VUV region. Moreover, species which do not exhibit fluorescence like CH_3 can be detected by multiphoton ionization.

We describe here measurements of absolute H atom concentrations in low-pressure flames. Hydrogen atoms are detected by two-photon excitation of the $(n=3)$ - state at about 205 nm followed by fluorescence observation of the Balmer- α radiation at 656 nm. The derivation of absolute concentrations from measured fluorescence signals is accomplished by a calibration method: Fluorescence intensities in the flame are compared with those resulting from known atom concentrations generated in a discharge flow reactor¹.

Since pressure and chemical composition are different for

the flame and the reference system, the measured fluorescence signal in the flame has to be corrected for the loss of intensity due to the considerably higher quenching rate compared with flow reactor conditions. We do this by solving the rate equations for the populations of the atomic levels involved with the appropriate values for the quenching rates in the flame and in the flow reactor, respectively. We then relate the resulting fluorescence intensities.

The quenching rates are determined from measured individual quenching rate constants for different collision partners and their respective concentrations in both systems. The quenching rate constants are, in turn, determined from measurements of radiative lifetimes in the flow reactor. Such experiments have been performed for quenching of $H(n=3)$ by flame-relevant gases such as H_2 , O_2 , H_2O , CH_4 , C_2H_2 and N_2 . Part of the measurements has been extended to elevated temperatures. In addition, we measured quenching rate constants for a series of noble gases since these data can provide useful information for the understanding of the dynamics of the collision process.

The calibration described above can under unfavourable conditions be affected by saturation or successive ionization. Furthermore, it has been reported² that photolytic atom production from flame gases like vibrationally excited water can be a significant source of additional H atoms. Therefore, these effects have been considered in the rate equation system. It turns out that at sufficiently low power densities they are generally negligible under our flame conditions.

As a result, figure 1 shows concentration profiles of H atoms in H_2 - O_2 -Ar flames at 95 mbar for three different stoichiometries, together with the results of a chemical-kinetic model³.

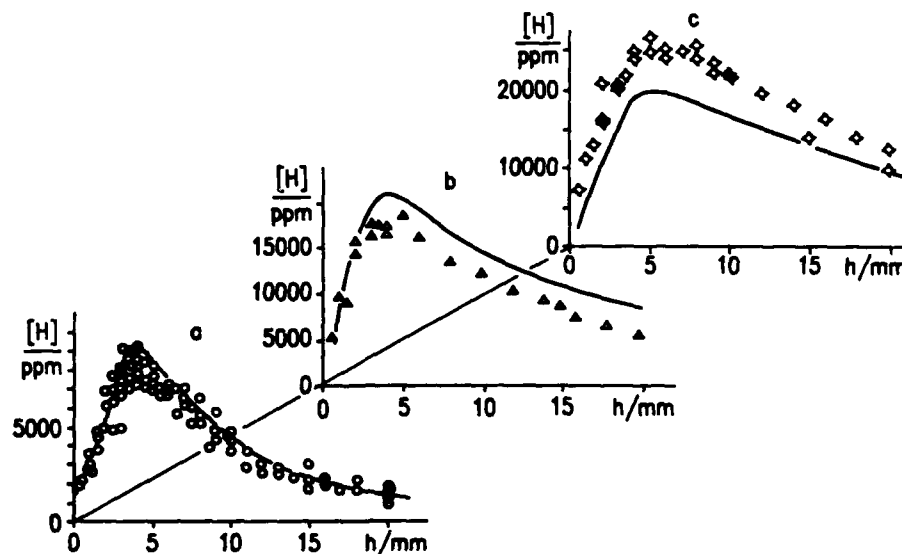


Fig.1: H atom concentrations in $\text{H}_2\text{-O}_2\text{-Ar}$ flames at 95 mbar; a: $\phi=0.6$, b: $\phi=1.0$, c: $\phi=1.4$. The symbols represent experimental values, the lines the results of flame model calculations³

In addition, we are presently developing a detection scheme for CH_3 for application in hydrocarbon flames. First results have been obtained in a flow reactor and in a low pressure $\text{CH}_4\text{-O}_2$ flame.

References

- 1 U. Meier, K. Kohse-Höinghaus, Th. Just
Chem. Phys. Lett. 126, 567 (1986)
- 2 J.E.M. Goldsmith
Opt. Lett. 11, 1419 (1986)
- 3 J. Warnatz
Ber. Bunsenges. Phys. Chem. 82, 834 (1978)

Doppler-free Two-photon Excitation of Molecular Hydrogen

Wallace L. Glab and Jan P. Hessler

Chemistry Division

Argonne National Laboratory

Argonne Illinois 60439 USA

We have observed two-photon allowed transitions from the $X^1\Sigma_g^+(1s\sigma)$ ground state to the $E^1\Sigma_g^+(2s\sigma)$ excited state of molecular hydrogen under Doppler-free conditions in a static cell by using counter-propagating beams of narrow-band light at 201.7 nm. This ultraviolet light was produced by mixing in beta-barium borate¹ the amplified output of a tunable, single-mode dye oscillator² at 606 nm with its second harmonic at 303 nm. We obtained Doppler-free excitation spectra by monitoring the two-photon resonant, three-photon ionization signal as a function of the wavelength of the dye oscillator. This wavelength was measured by simultaneously acquiring the fluorescent spectrum from molecular iodine³ and the transmission of a Fabry-Perot interferometer. The energy of the two-photon transitions and their widths were determined by fitting the observed line profiles to a Lorentzian line profile. The widths of all transitions were determined by the time-averaged spectral width of the light source. An example of the $Q_2(0,0)$ two-photon transition is shown below.

These results provide the most precise measurements of the energies of the lowest components of the $E^1\Sigma_g^+(2s\sigma)$ electronic state and, thereby, may be used to test the effective adiabatic potential and nonadiabatic eigenvalue corrections used to calculate the energy of the levels in this state. In addition, these results may be combined with high-resolution measurements of the $E^1\Sigma_g^+(2s\sigma)$ to $B^1\Sigma_u^+(2p\sigma)$ fluorescent transitions to deduce the precise energies of levels in the B-state. When combined with the results of our recent study of high singlet np Rydberg states⁴, they also yield the most precise results for the first two ionization limits of the hydrogen molecule. We also report preliminary measurements of the two-photon excitation cross section for this transition.

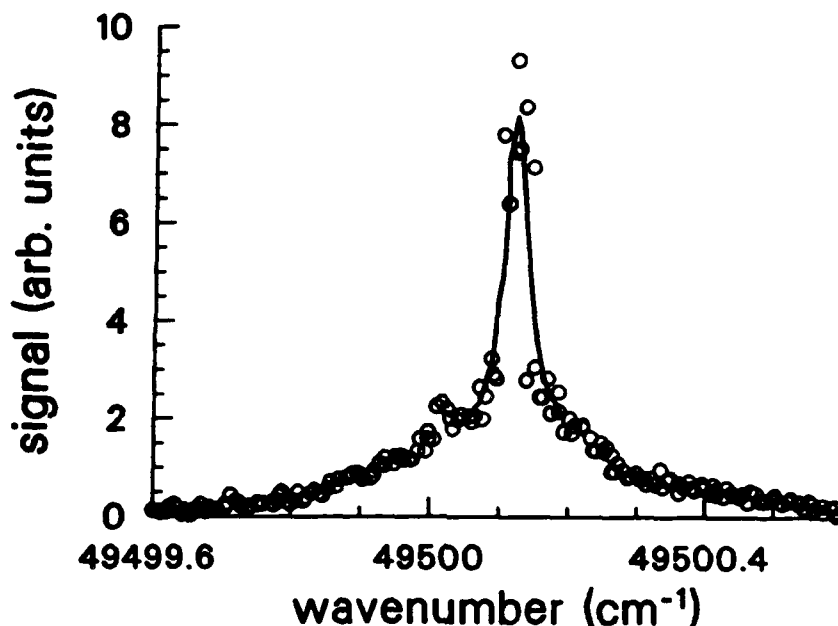


Figure 1. The two-photon transition from the $X^1\Sigma_g^+(1s\sigma, v = 0, J = 2)$ state to the $E^1\Sigma_g^+(2s\sigma, v = 0, J = 2)$ state of molecular hydrogen. The solid line represents the Lorentzian line profile which is centered at $49500.125 \text{ cm}^{-1}$ with a fwhm of 0.040 cm^{-1} .

This work was supported by the United States Department of Energy, Office of International Security Affairs, under Contract GC-01-01-06-1.

References

- ¹W. L. Glab and J. P. Hessler, submitted to Letters to the Editor of Applied Optics.
- ²M. G. Littman, Applied Optics 23, 4465 (1984).
- ³S. Gerstenkorn and P. Luc, "Atlas du Spectre d'Adsorption de la Mole'cule d'Iode", Centra National de la Recherche Scientific, Paris, 1978.
- ⁴W. L. Glab and J. P. Hessler, Phys. Rev. A, March issue, 1987.

**Photoelectron Spectra from Resonantly Enhanced
Multiphoton Excitation of H_2 via $C\ ^1\Pi_u^*$**

M. A. O'Halloran, S. T. Pratt, P. M. Dehmer, and J. L. Dehmer
Argonne National Laboratory, Argonne, Illinois 60439

Photoelectron spectra have been obtained following three photon resonant, four photon ($3 + 1$) ionization of H_2 via the $C\ ^1\Pi_u$, $v'=0-4$, states. These spectra were determined using a magnetic bottle electron spectrometer,¹ which measures angle-integrated photoelectron intensities with 50% collection efficiency for electrons with kinetic energies up to 10 eV. The present experiment confirms and extends our previously reported results,² which were obtained with a hemispherical electron energy analyzer.

The $C\ ^1\Pi_u$ state is the lowest Rydberg state converging to $H_2^+ X\ ^2\Sigma_g^+$. In the ($3 + 1$) multiphoton ionization process discussed here, the production of the ionic vibrational state with $v^+=v'$ is the dominant channel, but there is significantly greater population observed in the off-diagonal channels ($v^+ \neq v'$) than is predicted either by Franck-Condon overlap or by ab initio, Hartree-Fock level calculations.³ This is illustrated in Fig. 1, which compares the vibrational branching ratios obtained in the present experiment, for ($3+1$) excitation via $C\ ^1\Pi_u$ [$Q(1)$ transition], with those calculated by Dixit, Lynch, and McKoy.³ The vibrational branching ratios obtained for excitation of all observed intermediate levels were qualitatively the same as those shown for excitation via $Q(1)$ transitions, indicating that neither perturbations of the intermediate state by the $B\ ^1\Sigma_u^+$ state, nor accidental resonances at the four photon energy with sharp autoionizing structure in the continuum can explain the significant disagreement between experiment and calculation.

As the vibrational quantum number of the resonant intermediate state is increased, a pattern of increasing change of both the vibrational and rotational state of the ion relative to that of the resonant intermediate state is observed (Figs. 2 and 3). If the ion and photoelectron are considered in Hund's case (d) coupling, and only s- and d- partial waves are considered, then parity selection rules determine that the allowed

values of change of rotational quantum number, $\Delta N = [N^+(H_2^+) - J'(C^1\Pi_u)]$, are $\Delta N = 0, \pm 2$, for Q-branch excitation and $\Delta N = \pm 1, \pm 3$, for R-branch excitation. For (3+1) ionization via $C^1\Pi_u$, $v'=0$, no evidence of photoelectron peaks corresponding to the larger values of change of rotational quantum number is observed (Fig. 2). As the vibrational quantum number of the intermediate level is increased, the intensity of the the photoelectron peaks corresponding to larger changes of rotational angular momentum increases (Fig. 3). These peaks tend to be significantly larger for the off-diagonal vibrational bands ($v^+ \neq v'$), indicating that the photoionization dynamics that produce changes of vibrational energy in the ion relative to the intermediate state also involve larger exchanges of angular momentum between the ion and the departing photoelectron.

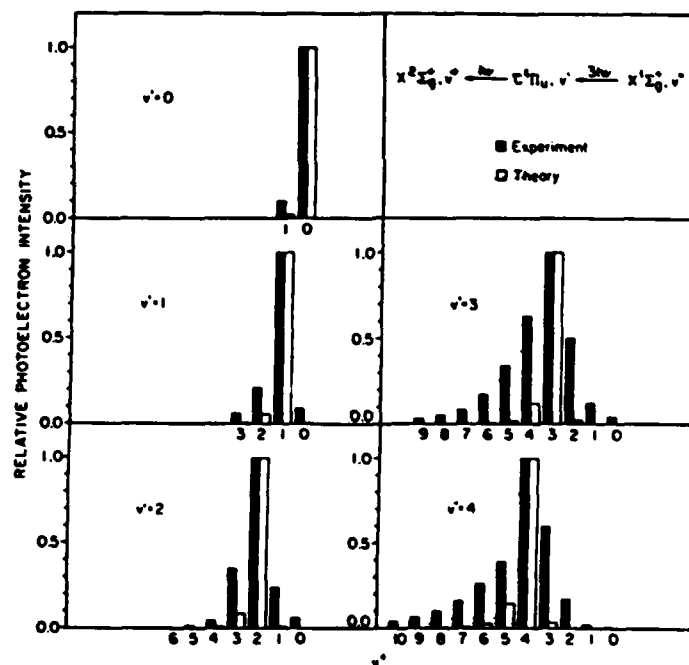


Fig. 1. Vibrational branching ratios determined for three photon resonant, four photon ionisation of H_2 via $C^1\Pi_u$, v' , [Q(1) transitions]. Calculation is that of Dixit, Lynch and McKoy, Ref. [3].

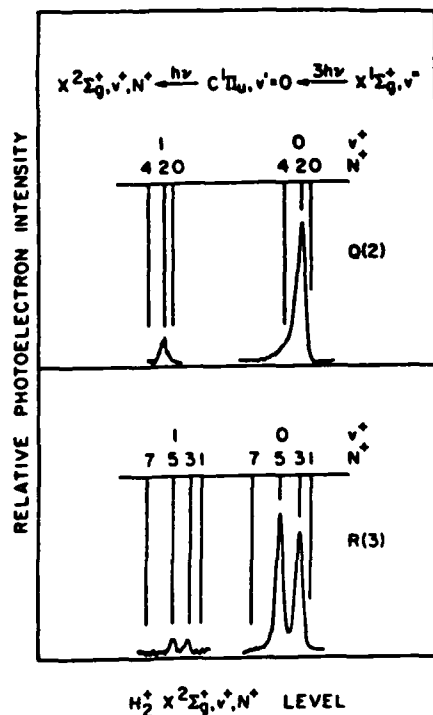


Fig. 2. Photoelectron spectra determined at the wavelengths of three photon resonant $H_2 C^1\Pi_u, v'=0 + X^1\Sigma_g^+, v''=0$, Q(2) and R(3) transitions. Spectra of individual vibrational bands were recorded separately. Relative areas of vibrational bands are set equal to the vibrational branching ratios.

References

1. P. Kruit and F. H. Read, J. Phys. E **16**, 313 (1983).
2. (a) S. T. Pratt, P. M. Dehmer, and J. L. Dehmer, Chem. Phys. Lett. **105**, 28 (1984); (b) S. T. Pratt, P. M. Dehmer, and J. L. Dehmer, J. Chem. Phys. **85**, 3379, (1986).
3. S. N. Dixit, D. L. Lynch, and V. McKoy, Phys. Rev. A, **30**, 3332, (1984).

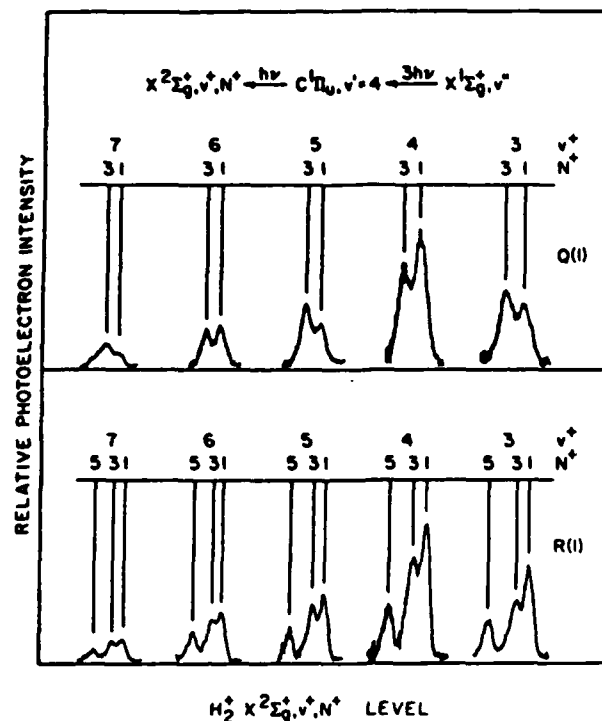


Fig. 3. Photoelectron spectra determined at the wavelengths of three photon resonant $H_2 C^1\Pi_u, v'=4 + X^1\Sigma_g^+, v''=0$, Q(1) and R(1) transitions.

*Work supported by the U.S. Department of Energy, Office of Health and Environmental Research, under Contract W-31-109-Eng-38 and by the Office of Naval Research.

HIGHER RYDBERG AND AUTOIONIZING STATES OF CS₂J. Y. Fan^{*}, E. Patsilinacou and C. Fotakis

Research Center of Crete

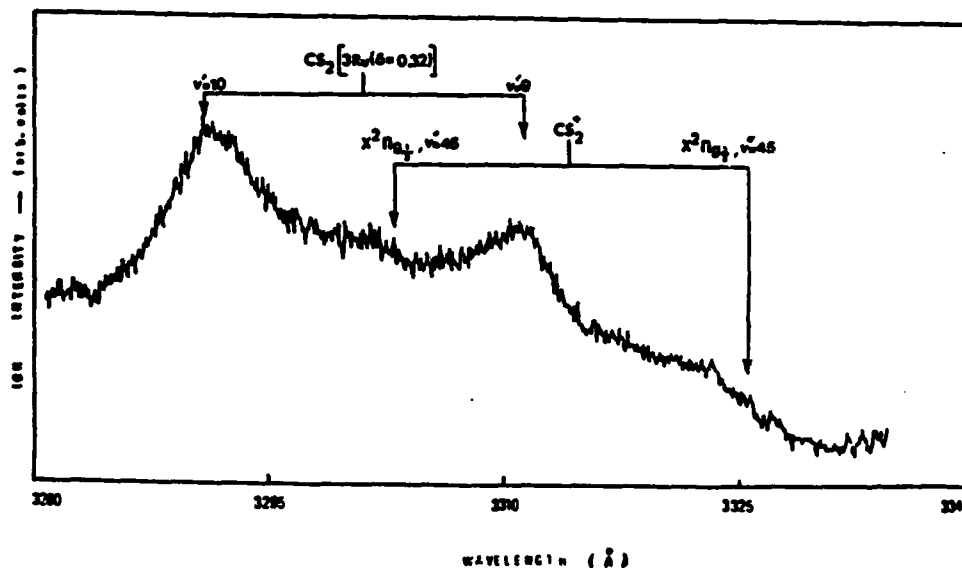
Institute of Electronic Structure and Laser

P. O. Box 1527, Iraklion, Crete

Greece

Highly excited states of CS₂ in the region of ~11 eV, i.e. ~1 eV above the first ionization threshold, have been studied by employing multiphoton ionization techniques combined with mass, electron energy and fluorescence analysis. Several interesting features have been observed and attributed to autoionizing states of CS₂, as e.g. the broad peaks at 3316 and 3296 Å shown in Figure 1. These peaks have also been observed in single photon excitation by using synchrotron radiation¹ and may be assigned to the 3R_u ($\delta = 0.32$) Rydberg series of CS₂, converging to the 12.56 eV limit.² Furthermore, the stepwise continuum background shown in Fig. 1 may be interpreted in terms of the existence of higher vibrational levels of CS₂⁺. The two steps which appear at ~3329 and 3309 Å are tentatively assigned to the ²Π_{g3/2} (0,45,0) and ²Π_{g1/2} (0,45,0) of CS₂, resulting in a spin-orbit splitting of ca. 480 cm⁻¹. Two-color experiments investigating highly excited states of CS₂⁺ in the same energy region are currently in progress and will be reported.

FIG. 1

Fig. 1 : 3-photon ionization spectra of CS₂.

REFERENCES

*Permanent address: Shanghai Institute of Optics and Fine Mechanics,
P.O.B. 8211, Shanghai, China.

1. C. Fotakis, D. Solgadi, C. Lardeux, A. Zehnacker and F. Lahmani (to be published).
2. M. Ogawa and M. C. Chang, Can. J. Phys. 48, 2455 (1970).

Photoelectron spectroscopic study of resonant multiphoton ionisation of chlorine .

B.G. Koenders, Karel.E. Drabe, M.G. Oostwal, D.M. Wieringa, C.A. de Lange

Department of Physical Chemistry, Free University

De Boelelaan 1083, 1081 HV Amsterdam, The Netherlands.

New spectroscopic information on molecules and atoms can be obtained by resonance enhanced multiphoton ionisation (REMPI) using many of the advantages of the mpi scheme. For example, more-photon selection rules allow a study of one-photon forbidden intermediate states. The generally stepwise nature of the REMPI process then provides information on the resonant intermediate state. Detailed information on intermediate and ionic states can be obtained by analysing the kinetic energies of the electrons ejected upon ionisation.

We report photoelectron spectra of molecular chlorine obtained by (3+1) ionisation.

Recently in our laboratory a differentially pumped 2π electron spectrometer for the detection of reactive and short-lived chemical species was constructed. Electrons produced in multiphoton processes are time-of-flight analysed and the results are presented in two forms:

- (i) the total electron signal integrated over all electron kinetic energies measured as a function of wavelength (similar to total ion current detection)
- (ii) energy resolved photoelectron spectra obtained at constant excitation wavelength by converting time-of-flight results to an energy scale.

We report preliminary results on (3+1) photoionisation of chlorine in the one-photon wavelength region of 379 nm to 409 nm. The three photons access intermediate Rydberg states in the same VUV region as studied by Moeller et al.[2] in one-photon absorption. Armed with the ab initio calculations of Peyerimhoff et al. [1], who calculated that various Rydberg states are heavily perturbed by Rydberg-valence interactions, Moeller et al. obtained an assignment of various complicated spectral features.

In fig.1 we show the total electron signal as a function of wavelength. The attractive and powerful information obtained by photoelectron spectroscopy (PES) of the Rydberg states mentioned can be illustrated by the $2^1\Pi_u(v'=0)$ Rydberg state (see fig.2a). The PE spectrum is very simple and is easily identified (using known data of the Cl^+_{2} ion [3]) as arising from ionisation to the $2^1\Pi_{g,1/2}$ ionic state. We can therefore immediately conclude a) from the simple PE Franck-Condon progression and ionic state reached that this low-lying vibrational level is not perturbed by valence interactions, b) from the fact that

ionisation is mainly to the $v=0$ of the ion that the intermediate Rydberg state has $v'=0$ and should have a vibrational frequency close to the $2\Pi_{g,1/2}$ ion vibrational frequency (about 645 cm^{-1}). Similarly, simple PE spectra are obtained for $2^1\Pi_u$ $v'=0$ to $v'=4$, $2^3\Pi(1_u)$ $v'=0$ to $v'=2$ and $2^3\Pi(0^+_u)$ $v'=0$ to $v'=1$. The results obtained for the $2\Pi_u$ states prove the vibrational assignment of Moeller et al.[2] to be correct. In addition, the ionic states observed in the PE spectra support the singlet and triplet assignments of Moeller et al.[2]. Finally, the PE spectra of these $2\Pi_u$ states show no perturbation by valence interactions, in excellent agreement with the calculations of Peyerimhoff et al.[1]. In contrast to the simple PE spectra of the $2\Pi_u$ states we show in fig.2b the PE spectrum of the $2^1\Sigma_u^+ v'=0$ state. We observe a long progression arising from ionisation leading to $2\Pi_{g,1/2}$ and/or $2\Pi_{g,3/2}$ ionic states. In addition, we also observe vibrational structure associated with the $2^1\Sigma_g^+$ ionic state. The results show the intermediate state to have mixed electronic character, and therefore fully support the assignment of Moeller et al.[2]. The mixed electronic character is easily understood from the computations of Peyerimhoff et al.[1], who calculated this state as a composition of the $1^1\Sigma_u^+$ Rydberg state (ionising mainly to the $2\Pi_g$ ionic states) and a valence state (ionising mainly to the $2^1\Sigma_g^+$ state).

In summary we conclude that photoelectron spectra of Rydberg like states populated by multi-photon absorption provide detailed information on electronic perturbations, and are of considerable help in untangling complicated spectra.

References

- [1] S.D. Peyerimhoff and R.J. Buenker, *Chemical Physics* **57** (1981) 279-296
- [2] T. Moeller, B. Jordan, P. Gürtler, G. Zimmerer, D. Haaks, J. Le Calvé, M. Castex, *Chemical Physics* **76** (1983) 295-30
- [3] H. van Lonkhuyzen and C.A. de Lange, *Chemical Physics* **89**(1984) 313-322

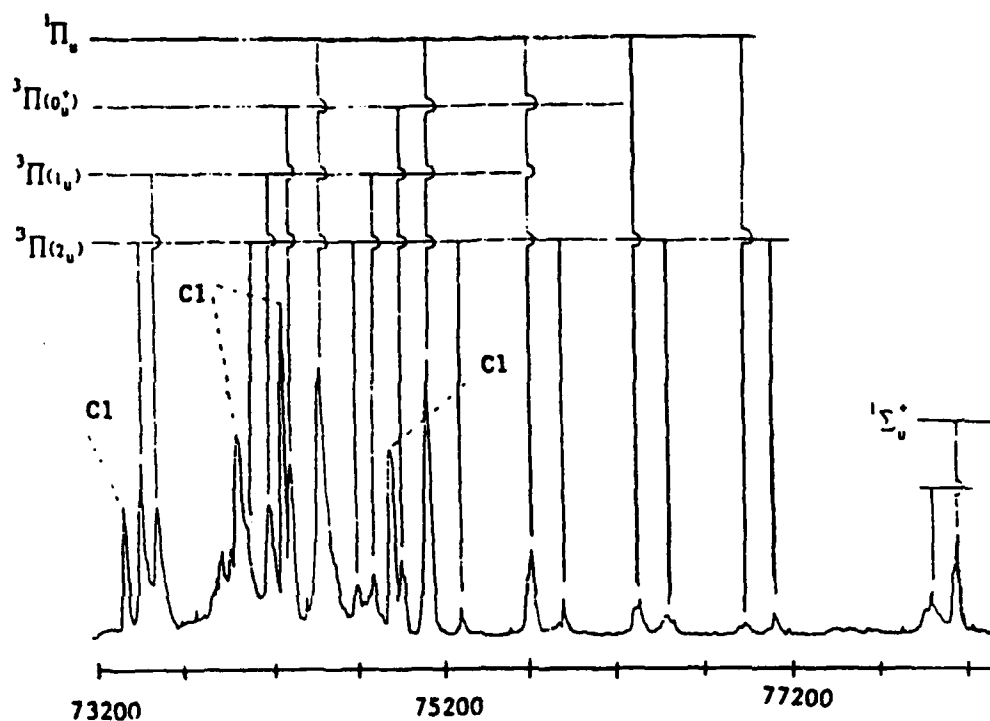


Fig.1 Total electron signal as a function of three photon energy. The range shown is similar to that of the one-photon spectra of Moeller et al.[2].

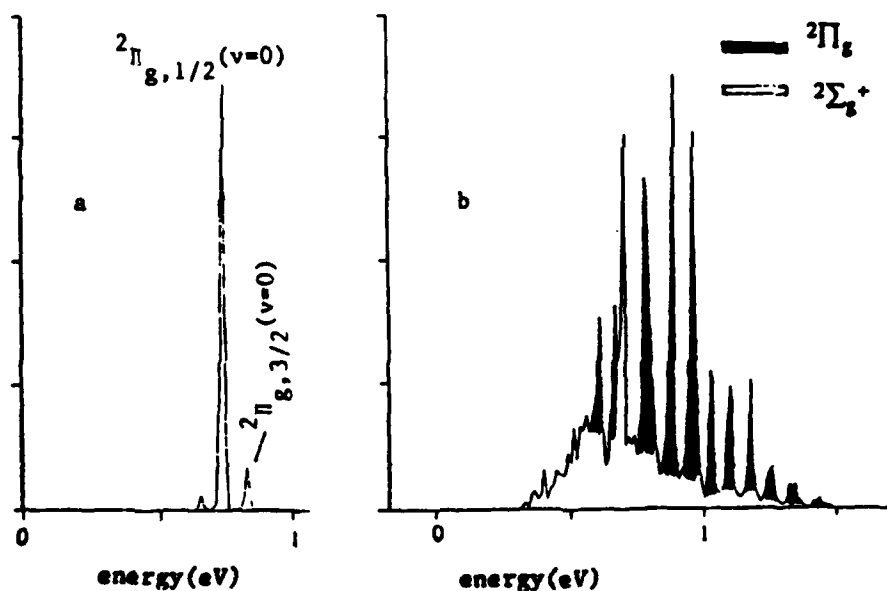


Fig.2 a) Energy resolved photoelectron signal arising from (3+1) ionisation via the $2^1\Pi_u^+(v'=0)$ intermediate Rydberg state. b) Energy resolved photoelectron signal arising from (3+1) ionisation via the $2^1\Sigma_u^+(v'=0)$ intermediate Rydberg state.

HIGH-RESOLUTION ZERO KINETIC ENERGY PHOTOELECTRON SPECTROSCOPY OF NITRIC OXIDE

M. Sander, L. A. Chewter and K. Müller-Dethlefs
Institut für Physikalische und Theoretische Chemie
TU München Lichtenbergstr. 4,
D-8046 Garching, West Germany

Conventional photoelectron spectroscopy (PES), despite some effort, offers typical energy resolution of around 10 meV (80 cm^{-1}). In all but a few cases, such as H_2^+ and D_2^+ or high J states of NO^+ , where the rotational states are widely spaced, this lack of resolution prevents the observation of rotational structure in the ion. To this end our novel method of zero kinetic energy photoelectron spectroscopy (ZEKE-PES) has been developed. This method employs two-color photoionization via a resonant intermediate state under field free conditions. Detection of ZEKE electrons only is facilitated in a steradiancy analyzer with a small delayed pulse field. A photoelectron energy resolution of 1 cm^{-1} was obtained. Full details of the method and results for NO and benzene have already been reported.¹

Here we present results obtained from two-color laser ZEKE-PES of nitric oxide via different rovibronic levels of the vibrationless ($v=0$) $\text{A}^2\Sigma^+$ state. We use the $(\text{P}_1)\text{A} \leftarrow \text{X}^2\pi$ transition to populate the F_1 rotational levels of the $\text{A}^2\Sigma^+$ state with definite N_A , $J_A = N_A + 1/2$ and parity $(-1)^{N_A}$. The second laser is scanned around the $\text{X}^1\Sigma^+$ ($v^+=0$) ground state of the ion to measure the ionizing transitions into rotational states with $J^+=N^+$.

Figures 1 to 4 show the ZEKE-PES spectra for ionization from $J_A=1/2$ ($N_A=0$), $J_A=3/2$ ($N_A=1$), $J_A=5/2$ ($N_A=2$) and $J_A=7/2$ ($N_A=3$), respectively. Each spectrum displays a number of discrete well separated peaks corresponding to the rotational levels of the vibrationless $\text{X}^1\Sigma^+$ ground state of the NO^+ ion (the rotational quantum numbers $N^+=J^+$ of the ion are indicated). In all spectra the photoionizing transitions for no change in rotation (i.e. $\Delta N=N^+-N_A=0$) are strongest. However, there are also important contributions for $\Delta N \neq 0$ ionizing transitions. For $N_A=0$ (Fig. 1) we observe transitions into $N^+=2$, $N^+=1$ and $N^+=3$. The approximate intensities of these $\Delta N \neq 0$ transitions are, compared to the $N^+=0 \leftarrow N_A=0$ transition, 0.5 for $\Delta N=2$,

0.2 for $\Delta N=1$ and 0.1 for $\Delta N=3$. For $N_A=1$ (Fig. 2) we also find $\Delta N \neq 0$ transitions, but the intensities relative to the $N^+=1-N_A=1$ transition are smaller than for $N_A=0$. The intensities of the $\Delta N \neq 0$ transitions (relative to $N^+=2-N_A=2$) become even smaller for $N_A=2$ (Fig. 3). For $N_A=3$ (Fig. 4) the $\Delta N \neq 0$ transitions are barely above the noise level and the spectrum is dominated by the $N^+=3-N_A=3$ transition.

The rather strong angular momentum transfer observed in the photoionization process and, in particular, the drastic decrease of the probabilities for $\Delta N \neq 0$ transitions with increasing initial rotational quantum number N_A can be explained by a simple model. To this end we consider the terms in the continuum state Hamiltonian which scatter a particular partial wave of the outgoing electron into other partial wave channels thereby changing the rotation of the core. These terms come from the interaction with the core's dipole and quadrupole moment as well as its polarizability, leading to the interaction operator $V = H_{\text{quad}} + H_{\text{dipol}} + H_{\text{pol}}$. We also take into account l-mixing in the A state which corresponds to mixing of the mechanical rotation (quantum number R_A). If one ignores interference effects, a simple picture involving two steps may be drawn: in a first step a $\Delta(N^+-R_A)=0$ Rydberg or continuum state is excited (probability p_1); in the second step this $\Delta(N^+-R_A)=0$ state interacts isoenergetically with a $\Delta(N^+-R_A) \neq 0$ ionic state (probability p_2). The probability p for observing a $\Delta(N^+-R_A) \neq 0$ transition is then $p=p_1 \cdot p_2$.

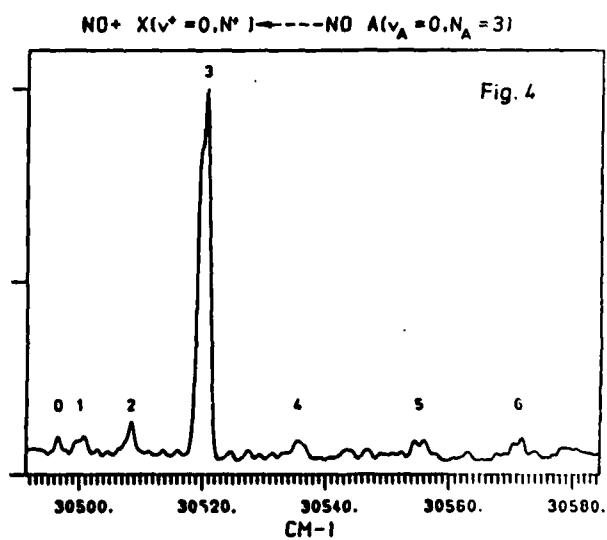
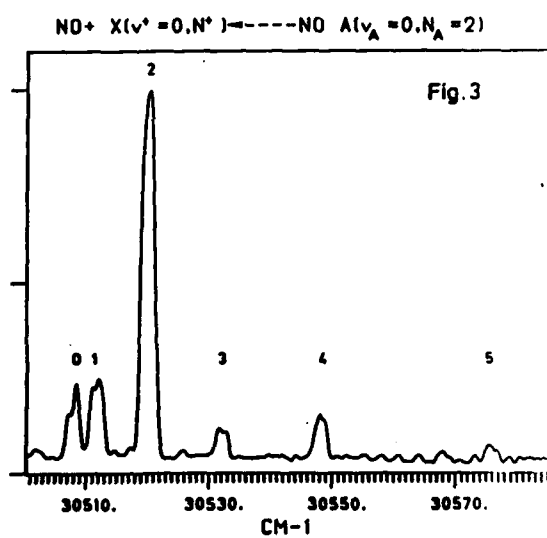
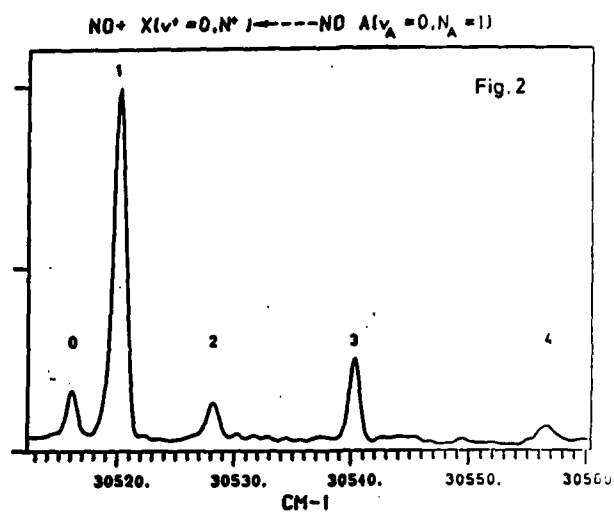
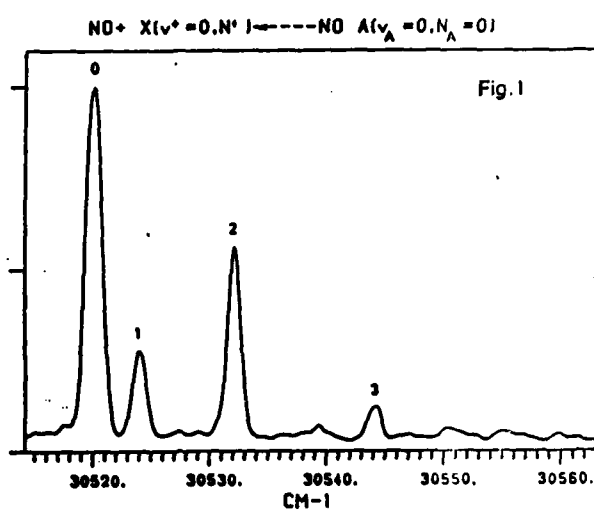
$$p_1 \propto |\langle R_A, 1 \pm 1 | \mu | R_A, 1 \rangle|^2 \rho(E_{N^+} - E_R)$$

$$p_2 \propto \frac{|\langle N^+, 1^+ | V | R_A, 1 \pm 1 \rangle|^2}{[B^+ N^+(N^++1) - B^+ R_A(R_A+1)]^2}$$

The strong dependence of the $\Delta N \neq 0$ photoionizing transitions arises from the energy denominator in p_2 .

B^+ is the rotational constant of the ion, μ is the electric dipole operator and $\rho(E_{N^+} - E_R)$ corresponds to the density of $\Delta(N^+-R_A)=0$ Rydberg or continuum states.

1. K. Müller-Dethlefs, M. Sander and E. W. Schlag, Z. Naturforsch. **39a**, 1089 (1984); L. A. Chewter, M. Sander, K. Müller-Dethlefs and E. W. Schlag to appear in J. Chem. Phys.; K. Müller-Dethlefs, M. Sander and E. W. Schlag, Chem. Phys. Lett. **112**, 291 (1984).



DETECTION OF IONIZED HYDROGEN IN RESONANT MULTIPHOTON
IONIZATION OF BENZENE IN THE VISIBLE.

R. Bruzzese, F. Esposito, S. Solimeno, N. Spinelli

Dipartimento F.N.S.M.F.A.

Pad. 20 Mostra d'Oltremare, 80125 Napoli (Italy).

A common feature of all recently reported laser-ionization mass-spectrometry experiments on polyatomic molecules is the extensive fragmentation of the molecules into smaller and energetically more costly ions. For example, in the case of benzene, which has been studied extensively as a test molecule, ionic fragments requiring a minimum energy equivalent to nine UV photons have been observed¹. In most of these experiments on benzene use was made of UV, near UV, or UV plus visible laser radiation^{1,2,3,4}. The results obtained in this multiphoton ionization-dissociation (MPID) experiments have been successfully interpreted within the framework of statistical theories⁵.

We report in this paper resonance-enhanced MPI studies of benzene (in gas phase) in the visible, carried out by using a time-of-flight (TOF) mass spectrometer for analyzing the ionic photofragments. The new, remarkable feature of our results is the appearance in the MPI mass spectra of a peak corresponding to ionized atomic hydrogen. This feature has never been reported in the case of MPID of benzene in the UV or UV+visible.

The experimental apparatus is very similar to the one described in ref. 6. A grating-tuned oscillator-amplifier dye laser pumped by a N_2 laser generates tunable radiation having a linewidth of 1 cm^{-1} . The beam is focused to a waist size of about $12 \mu\text{m}$, with a power density of $\sim 10^{10} \text{ W/cm}^2$. The laser pulse duration is about 7 ns (FWHM). A stainless-steel vacuum chamber, kept at a working pressure of 10^{-6} - 10^{-4} mbar, contains the glass-needle injector, the ion source, the drift tube and the ion detector. The ion detector was built by assembling a focused-dynode detector and a venetian-blind first dynode in order to obtain both the high-quality signal of a focused multiplier and the

narrow spread of ion trajectories ensured by the venetian-blind shaped dynode. Ions are detected and their time measured at the rate of one single ion per laser pulse. The detector response throughout the entire spectrum of parent and fragment ions is mass independent and proportional to the relative abundances.

A MPI scheme similar to that of ref.6 was used to ionize benzene molecules with visible photons: a two-photon resonant (excitation to the $1B_{2u}$ intermediate state), four-photon ionization process.

In Fig.1 we report the mass spectra of benzene obtained at one resonant (4948 Å), case A, and one nonresonant (4972 Å), case B, laser wavelength. The two mass spectra were obtained in the same experimental conditions, namely, at a pressure of 2.6×10^{-5} mbar (room temperature), and using a laser intensity of about 1.3×10^{10} W/cm². It must be

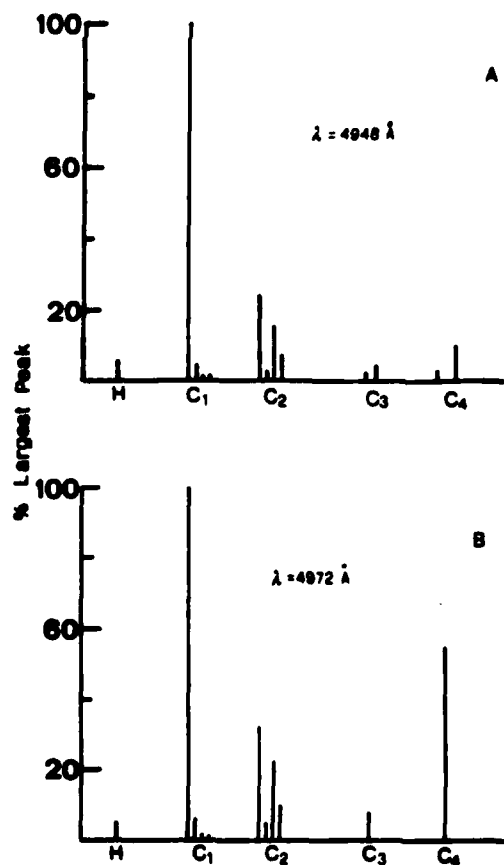


Figure 1.

noted that there is a factor of about 10 between the number of ions obtained in resonance and off-resonance, though this is not evident from Fig.1 where the height corresponding to a given ion photofragment is reported as percentage of the largest peak (C^+ in both cases). As easily seen, there is clear evidence of ionized atomic hydrogen. The identification of the peak corresponding to hydrogen was obtained by checking their arrival time against the time corresponding to C^+ ions, well known because of the previous calibration of the TOF spectrometer. Moreover, by using a Montecarlo program we also checked simulated arrival times against

the experimental times of flight. We have found a very good agreement between the experimental and numerical values of the time difference between the arrival of C^+ and H^+ atoms. The dependences on the laser power at 4948 Å for the total ion yield and for H^+ ions gave slopes of about 4 and 5.1, respectively.

We have also carried out a number of tests which enable us to exclude the possibility that the hydrogen ions are caused by electron impact processes with photoelectrons produced by stray laser-light striking the walls of the vacuum vessel. Moreover, comparison between experimental and Montecarlo-computed times of flight confirms that the hydrogen ions are produced within the laser-molecules interaction volume. Finally, the laser intensities used in our experiment are two or three orders of magnitude smaller than the ones needed to promote direct nonresonant six-photon ionization of neutral hydrogen produced in the dissociation of benzene.

In conclusion, our experimental findings clearly seem to indicate that the ionized hydrogen observed in the laser mass spectra of benzene is the result of the MPI, and consequent photodissociation, of the molecules. In other words, it is produced as a consequence of the laser induced photodissociation process in our specific experimental conditions, whatever the dissociation mechanism.

We think that our experimental results, besides their novelty, can also be of great interest for testing the statistical theories thus far developed for explaining the fragmentation dynamics and its mechanisms.

References.

- 1) L.Zandee, R.B.Bernestein, J.Chem.Phys., 71, 1359 (1979).
- 2) V.S.Antonov, V.S.Letokhov, Appl.Phys., B24, 89 (1981).
- 3) J.T.Meek, S.R.Long, J.P.Reilly, J.Chem.Phys., 86, 2809 (1982).
- 4) H.Kuhlewind, A.Kiermeier, H.J.Neusser, J.Chem.Phys., 85, 4427 (1986), and references cited therein.
- 5) W.J.Chesnavich, M.T.Bowers, in "Gas Phase Ion Chemistry", (M.T. Bowers, ed.) vol.1, pp.119 ff, Academic Press (N.Y.-1979).
- 6) M.Armenante, R.Bruzzese, N.Spinelli, S.Solimano, F.Vanoli, Jour. Opt.Soc.Am., B2, 1088 (1985).

PHOTODISSOCIATION OF CH_3I CLUSTERS PROBED BY MULTIPHOTON IONIZATION

S. Sapers, V. Vaida

Department of Chemistry and Biochemistry

University of Colorado

Boulder, CO 80309-0215

and

R. Naaman*

Department of Isotopes Research

Weizmann Institute of Science

Rehovot, Israel 76100

The dissociation of neutral and charged clusters has recently been the object of considerable effort motivated by an interest in understanding the spectroscopy and dynamics of the "caging" of a chromophore by "solvent" molecules. Multiphoton ionization (MPI) and resonantly enhanced multiphoton ionization (REMPI) are ideally suited spectroscopic techniques for the study of "caged" chromophores.

Our lab is currently studying methyl iodide in "caged" environments where the "solvent" molecules are either CH_3I or rare gases. Methyl iodide clusters involve strong chromophore-solvent cage interactions. REMPI into a system of Rydberg states occurring in the vicinity of 170 - 220 nm produces ionized clusters (dimers, trimers, etc.) which undergo photofragmentation to form the cluster minus a methyl or iodine group (e.g. $\text{CH}_3\text{I}-\text{CH}_3^+$, $\text{CH}_3\text{I}-\text{I}^+$, $(\text{CH}_3\text{I})_2\text{CH}_3^+$, etc.). Excitation into repulsive valence band (230-300 nm) followed by MPI of the photofragments produces cluster size dependent results (dynamic effects). Dimers readily dissociate to form I_2^+ , resulting from initial single photon dissociation followed by I_2 recombination and MPI. Larger clusters "trap" the chromophore, which slows down or prevents dissociation from occurring. In the large cluster limit trapping is complete and REMPI through the valence state occurs, culminating in photoproducts which resemble those from excitation through the Rydberg

state. Similar studies using Ar, Kr and Xe are underway. These results show that clustering effects the photodissociation process with respect to the lifetime of the photoreactive state, as probed by REMPI, and the subsequent dynamics of photofragmentation.

MPI and REMPI wavelength resolved spectroscopic studies of these "caged" systems are in progress. A two-color REMPI study of "caged" dissociative systems, where one laser is scanned over the region of the repulsive surface and a specific parent and/or fragment ion is observed (e.g. CH_3I^+ , $(\text{CH}_3\text{I})_2^+$), gives lifetime information of the trapped chromophore. Furthermore REMPI of non-dissociative systems in clusters would enable us to map out the electronic structure of a caged system, and therefore probe the effect of neighbor-neighbor interactions.

The studies of CH_3I clusters demonstrates the utility of MPI and REMPI to (a) probe systems that are in the one photon UV and VUV regions with tunable light, and (b) selectively access photochemically "slow" systems in a zero background experiment (ion counting).

*1986-87 JILA Visiting Fellow.

REMPI (2+1) IN NH_3 VIA THE $\tilde{\text{C}}(\text{v}_2=2)$ ($^1\text{A}_1'$) STATE IN VAPOR
AND IN DISCHARGES

Seong-Poong Lee and Erhard W. Rothe
Department of Chemical Engineering and Research Institute
for Engineering Sciences, Wayne State University
Detroit, MI 48202

and

Gene P. Reck
Department of Chemistry
Wayne State University
Detroit, MI 48202

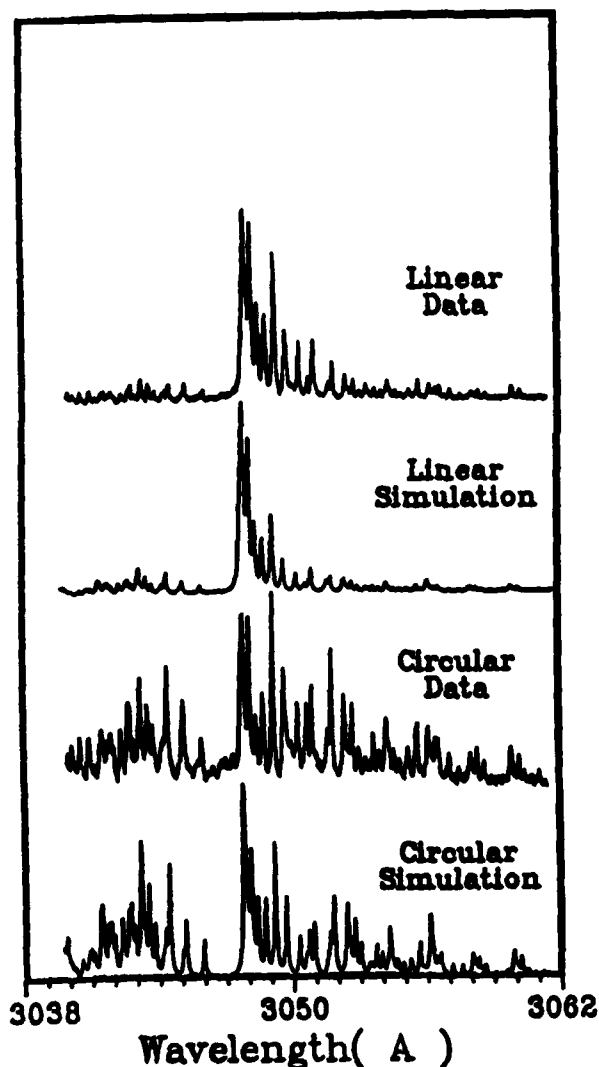
The $\tilde{\text{C}}'$ state of NH_3 has been the subject of several investigations by MPI spectroscopy. These include (3+1)^{1,2} and (2+1)³⁻⁵ REMPI.

We report results of 2+1 REMPI via the $\tilde{\text{C}}'(\text{v}_2=2)$ state that is well separated from the B state⁴ and is reported² to be unaffected by pre-dissociation. The results are compared with the formalism of McClain and Harris.⁶

UV light is focussed into a hollow-cathode discharge tube. The light has $\approx 0.2\text{\AA}$ resolution, ≈ 0.7 mJ/pulse and is the doubled output of an excimer-pumped dye-laser. Its polarization is adjusted to be either linear or circular. The focal length is 9 cm. The tube works either with a discharge (optogalvanic cell) or without (normal 300 K gas MPI cell). A computer synchronizes the laser's wavelength scan (i.e., its grating and doubler crystal) and the operation of a boxcar analyzer.

McClain and Harris⁶ provide the following results. The two-photon absorptivity δ is given by $P_0Q_0 + P_1Q_1 + P_2Q_2$, where the P's depend only on polarization and the Q's only on molecular properties. For two identical photons, linear polarization yields $P_0 = 1/3$, $P_1 = 0$, and $P_2 = 2/3$, while for circular polarization, $P_0 = 0$, $P_1 = 0$, and $P_2 = 1$, and so P_1Q_1 is zero in both cases. Further $Q_0 = 0$ unless ΔJ and ΔK are both zero (i.e., the Q_0 rotational branch) so that P_0Q_0 contributes

only to that branch and then only with linearly polarized light. Accordingly, in changing from linearly to circularly polarized light, we expect all rotational lines, except Q_Q , to gain $3/2$ in intensity. For the Q_Q , and the P_2Q_2 term will also increase by $3/2$, but P_0Q_0 will become zero. This means that a spectrum involving both Q_Q transitions and either O, P, R, or S transitions will yield a ratio of Q_0/Q_2 , which in turn leads to vibronic parameters which are otherwise difficult to obtain.



The figure at the left clearly shows the effect of changing from linear to circular polarization: there is a large decrease for the Q line intensities relative to those of the O, P, R and S line. The nine largest lines in the top spectrum (linear polarization) are Q branch. Simulations are shown using the B and C constants of reference 2. Because of experimental difficulty in maintaining constant geometry and intensity as the polarization is altered, all spectra are normalized, so that the $3/2$ factor is not seen. The ratio of Q_0/Q_2 was adjusted, in the linear simulation, to yield approximately the experimental ratio of Q-branch intensities to those of

other branches. No analogous adjustment can be made for circular light.

We checked the effect of collection voltage in the cell and of the pressure dependence of the signal: i.e., the number of detected electrons. The signal increases significantly with voltage and nearly linearly with pressure to ≈ 1.5 Torr, and then apparently saturates.

We also studied the two-photon optogalvanic effect in discharges in pure NH_3 with both linear and circular polarization. The magnitude of the signals is sometimes increased by factors as large as 10 over the no discharge case.

We thank AFOSR, ACS/PRF, and NSF for support of this work. We appreciate receiving unpublished notes written by Dr. Takayuki Ebata, Stanford, and helpful conversations with Dr. William E. Conaway, Stanford, Prof. W. Martin McClain, Wayne State, and Thomas Steelemann and Prof. Peter Andersen, MPI für Strömungsforschung, Göttingen.

1. G. C. Nieman and S. D. Colson, J. Chem. Phys. 68, 5656 (1978); 71, 571 (1979); J. H. Glowia, S. J. Riley, S. D. Colson, and G. C. Nieman, *ibid.* 72, 5998 (1980); 73, 4296 (1980).
2. M. N. R. Ashfold, R. N. Dixon, and R. J. Stickland, Chem. Phys. 88, 463 (1984).
3. A. J. Grimley and B. D. Kay, Chem. Phys. Letters 98, 359 (1983).
4. W. E. Conaway, R. J. Morrison and R. N. Zare, Chem. Phys. Letters 113, 429 (1985).
5. R. J. Stanley, O. Echt, and A. W. Castleman, Appl. Phys. B32, 35 (1983).
6. W. W. McClain and R. A. Harris, Excited States, Vol. 3 (Academic Press, New York, 1977).

REMPI SPECTRA OF LARGE THERMALLY LABILE MOLECULES
AFTER IR-LASER INDUCED DESORPTION

A. Habekost, H. Ulbrich and H. von Weyssenhoff
Institut für Physique Chemie
Universität Hannover
Federal Republic of Germany

The pulsed IR-laser induced desorption technique¹ has been employed to obtain structural and dynamical information on large thermally labile molecules by means of high resolution REMPI mass spectra in a supersonic jet. Such molecules which usually decompose during conventional thermal heating are volatilized and injected into the expanding argon jet without significant ionization or fragmentation. Resonance MPI is obtained using a tunable, frequency doubled dye laser pumped by an excimer laser. Ions are analyzed in a conventional TOF mass spectrometer.

REMPI spectra were taken for the amino acids tryptophane and phenylalanine as well as related aromatic carboxylic acids. These spectra are similar to those reported by Levy and coworkers² using thermal evaporation and thermospray techniques. There is, however, a marked difference: conventional heating yields the different possible rotational conformers of these compounds in thermal equilibrium which - after cooling - show up as well separated sharp bands. In contrast, with IR-laser induced desorption we observed only one conformer with significant intensity indicating that the desorption process produces a largely non-equilibrium distribution of conformers.

The mass spectra of some compounds also suggest the formation of hydrogen-bonded dimers in the laser desorption process. Further investigation of this effect is in progress and will be reported.

REFERENCES

1. H. von Weyssenhoff, H. L. Selzle and E. W. Schlag, *Zeits. f. Naturf.* **40A**, 672 (1986); J. Grotemeyer, U. Boesl, K. Walther and E. W. Schlag, *JACS* **108**, 4233 (1986); F. Engelke, J. H. Hahn, W. Henke and R. N. Zare, in press.
2. Y. D. Park, T. R. Rizzo, L. A. Peteanu and D. H. Levy, *J. Chem. Phys.* **84**, 6539 (1986).

**LASER-INDUCED FLUORESCENCE LIFETIME OF RUBRENE
BY TWO PHOTON EXCITATION AT 1064 NM**

Fuat Bayrakçeken
Ankara University, Faculty of Sciences
Department of Engineering Physics
06100 Tandoğan, Ankara, Turkey

In recent years it has been shown that two-photon excitation spectra (TPES) can provide valuable information on dipole forbidden transitions not observable in conventional UV absorption. Of the limited number of molecules studied by this technique over a wide spectral range, rubrene has not been investigated.

Rubrene has a center of symmetry and therefore the principle of mutual exclusion holds for one and two photon allowed transitions. It has been found possible to excite the upper singlet state of rubrene with two photon of 1.06 micron light from the YAG Laser. The fluorescence decay time is found to be 48 ns., in toluene at room temperature as compared with 16 ns., in single photon excitation appears to be a low lying vibrational level of the first excited singlet.

PRESSURE EFFECTS IN ORGANOMETALLIC MPD/MPI EXPERIMENTS

Jeanne M. Hossenlopp and J. Chaiken

Department of Chemistry

Syracuse University

Syracuse, New York 13244-1200

There has been much recent interest in pressure related effects on the measured ion yields in bulk gas multiphoton dissociation/ionization (MPD/MPI) experiments. We have measured the effects of added buffer gas on the MPI signal of various arene chromium tricarbonyls (ACT's) and $\text{Cr}(\text{CO})_6$. Using basic gaseous electronics theory and experimental results on ion multiplication behavior in pure gases, we have found a simple method for quantitative analysis of ion signal multiplication effects in MPI systems. For various buffer gases and ion collection electric fields, the multiplication model successfully models the pressure dependence of total ion signal in most of the wavelength regions studied, indicating that the measured ion signal is directly proportional to the initial MPI yield. This is of crucial importance for MPI studies where product branching ratios are being determined.

In certain spectral regions, the pressure dependence of the measured ion signals deviated dramatically from the expected multiplication behavior. We have measured the pressure dependence of vacuum ultraviolet (VUV) emission in order to determine the nature of processes which compete with ion formation in bulk gas experiments.

MECHANISM OF THE INFRARED MULTIPHOTON DECOMPOSITION OF ETHANOL

D. K. Evans, J. W. Goodale, M. J. Ivanco, Robert D. McAlpine
 Atomic Energy of Canada Research Company
 Chalk River Nuclear Laboratories
 Chalk River, Ontario, Canada
 KOJ 1PO

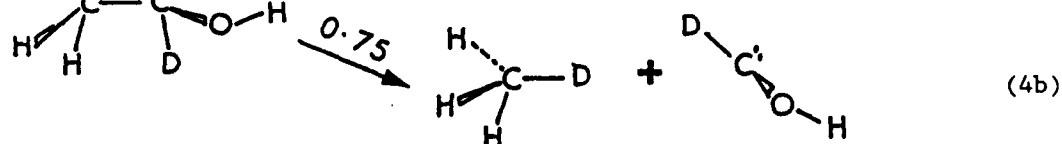
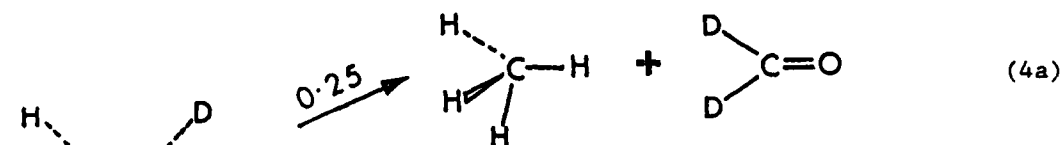
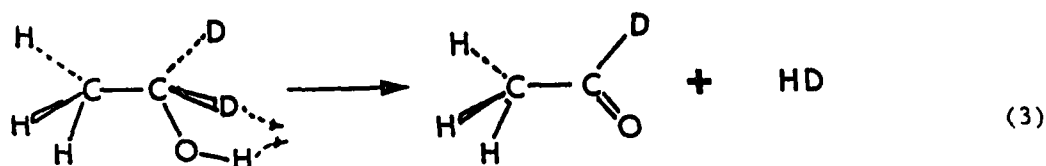
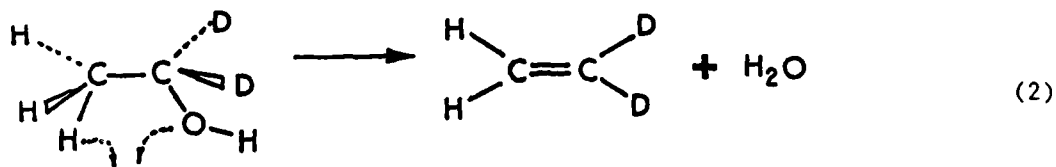
Infrared laser induced multiphoton decomposition (IRMPD) experiments on $\text{CH}_3\text{CD}_2\text{OH}$ and $\text{C}_2\text{H}_5\text{OD}$ and on normal ethanol with iodine as a free radical scavenger are reported. Irradiations were performed using a temporarily smooth 60 ns FWHM CO_2 laser pulse¹ and measurement of reagent depletion and product appearance was done using a GC/MS. Measurements were made for a range of ethanol pressure (67-1333 Pa) and laser fluences ($3\text{-}15 \text{ J/cm}^2$). There were only small effects on channel ratios and no observable dependence of the mechanism over the ranges studied. In previously reported work^{2,3} the following reactions have been suggested as the major channels:



In experiments on $\text{C}_2\text{H}_5\text{OH}$ with the addition of the very efficient free radical scavenger, I_2 ,⁴ there is little, if any, change in the production of C_2H_4 , CH_3CHO and CH_4 or in the depletion of $\text{C}_2\text{H}_5\text{OH}$. However, production of C_2H_6 was totally suppressed, indicating that it arises by reaction (1c) followed by recombination of two methyl radicals.

Further information about the decomposition mechanism is seen from consideration of the following primary photochemical reactions with no

I₂ present:



The only form of ethene from the IRMPD of CH₃CD₂OH was CH₂CD₂, indicating that the elimination of proceeds as shown by the arrows in reaction (2) and the hydroxyl group combines with a C₂-hydrogen atom. Production of acetaldehyde is entirely by reaction (3). The hydroxyl hydrogen atom combines with a hydrogen atom from C₁ to form hydrogen as shown by the arrows and there is no involvement of the methyl hydrogens. Methane is mainly produced by the molecular channel, reaction (4b). About three times as much CH₃D as CH₄ is formed in the IRMPD of CH₃CD₂OH. Similar conclusions come from corresponding experiments on CH₃CH₂OD indicating that there is no intramolecular isotope effect on the mechanism of this channel. The methyl group favors combination with a hydrogen atom from C₁ and not with the hydroxyl hydrogen. These experiments have shown that reactions (1a)-(1c) but not (1d) are major channels in the IRMPD of ethanol. In addition we have determined that several products such as methane are formed from concerted molecular reactions and not from free radical paths.

References

1. A. W. Pasternak, D. J. James, J. A. Nilson, D. K. Evans, R. D. McAlpine, H. M. Adams and E. B. Selkirk, *App. Opt.* **20**, 3849 (1981).
2. A. Gandini and R. A. Back, *J. Photochem.* **18**, 241 (1982).
3. R. A. Back, D. K. Evans, R. D. McAlpine, E. M. Verpoorte, M. Ivanco, J. W. Goodale, and H. M. Adams, to be published.
4. J. G. Calvert and J. N. Pitts Jr., Photochemistry (Wiley: New York, 1966), pp. 601-602.

UV LASER MULTIPHOTON IONIZATION STUDY OF FORMALDEHYDE

Liu Houxiang, Li Shutao, Han Jingcheng and Wu Cunkai

Laboratory of Laser Spectroscopy

Anhui Institute of Optics and Fine Mechanics

Academia Sinica

Hefei, China

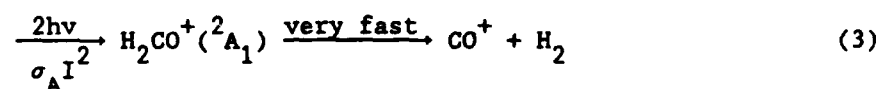
Multiphoton ionization of formaldehyde at 308 nm has been studied under diffusive beam conditions. The ion peaks appearing at $m/e=30$ and 28 are assigned to H_2CO^+ and CO^+ , originating from 2+1 and 2+2 photoionization, respectively.

Formaldehyde is of importance to chemistry, medicine, astrochemistry and environmental science, but only a experiment of its two-step photoionization have been done¹ by Letokhov. We present here, for the first time, a MPI investigation of H_2CO under diffusive beam conditions using a XeCl excimer laser.

The H_2CO molecular beam is crossed at right angles with the focused excimer laser (70 mJ/pulse, 10 ns FWHM, 5Hz) in the photoionizing region of a quadrupole mass spectrometer. The pressure during the experiments is in the range of $7 \times 10^{-6} \sim 7 \times 10^{-5}$ torr. The measured ion peaks are at $m/e=30$ and 28, and have been assigned to H_2CO^+ and CO^+ , respectively. The dependence of the ion signals on laser intensity and pressure are measured, giving the laser intensity indices of 2.32 and 3.66 to H_2CO^+ and CO^+ , the pressure indices of 0.88 ± 0.3 and 0.71 ± 0.3 to H_2CO^+ and CO^+ , respectively.

The ionization potential of H_2CO is 10.87 eV which is lower than the three photon energy (12.03 eV) of 308 nm light. The dissociation from the first excited state ($^2\text{B}_1$) of H_2CO^+ into $\text{CO}^+ + \text{H}_2$ requires energy of 13.98 eV which is lower than the four photon energy (16.04 eV) of 308 nm light. The $^2\text{B}_2 - ^2\text{B}_1$ transition of H_2CO^+ for C_{2v} symmetry is forbidden and can be neglected. So we present a dominant mechanism for MPI of H_2CO at 308 nm as follows:





The population of H_2CO^+ (N_P^+) and CO^+ (N_F^+) is given by the approximate solution for a set of rate equations from formulae (1) - (3) as

$$N_P^+ = \sigma \sigma_B I^3 N_0 T / (\sigma_B I + \gamma) \quad (4)$$

$$N_F^+ = \sigma \sigma_A I^4 N_0 T / (\sigma_B I + \gamma) \quad (5)$$

where γ is a nonradiative relaxation rate of $\tilde{\text{C}}$ state of H_2CO , N_0 is the population of $\text{H}_2\text{CO}(\tilde{\text{X}}, \text{}^1\text{A}_1)$ and T is the laser pulse duration. Based on Eqs. 4 and 5 we explain our experiment result.

REFERENCES

1. V. S. Antonov, V. S. Letokhov et al. Zh. Eksp. Teor. Fiz. (Russian) 73, 1325 (1977).

MECHANISM OF MULTIPHOTON IONIZATION AND FRAGMENTATION OF ALKYL IODIDES

Han Jingcheng, Liu Houxiang, Gu Jianping, Li Shutao, Wu Cunkai
Laboratory of Laser Spectroscopy
Anhui Institute of Optics and Fine Mechanics
Academia Sinica, P. O. Box 25
Hefei, China

In the course of a few years, the field of Multiphoton Ionization-Dissociation Mass Spectroscopy (MIDMS) has developed into a mature branch of research. The MIDMS has been proven to be a very useful tool for understanding the dynamics of fragmentation of polyatomic molecules. Multiphoton ionization-fragmentation patterns have been reported for six alkyl iodides in the 400-360 nm region.¹ The significant differences on the MPIMS patterns of tert-butyl iodide and n-butyl iodide are thought to be attributed to differences in the spectroscopic and dynamic properties of the first-formed fragment ion in the MPI-Fragmentation process. MPI studies of methyl iodide were also performed in the 7100-5300 Å and 3550-2650 Å regions to look into the nature of the $\sigma^* + n$ A-band system and its photochemistry.²

In this paper the MPI mass spectra are reported for C_2H_5I and $n-C_3H_7I$ under the action of XeCl excimer laser by using quadrupole mass spectrometer. In one-photon absorption, the A-band continuum begins at approximately 32000 cm^{-1} for each of these molecules. The dissociation rate in the A-band excited state is significantly larger than the up-pumping rate. One-photon frequency of XeCl excimer laser approaches and is just beyond the A-band threshold, whereas two-photon excitation are obviously different for these molecules. The motivation for this study is in the understanding of the effect of one-photon dissociation and two-photon resonance via Rydberg states on MPI process of alkyl iodides.

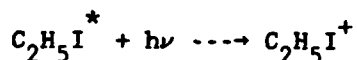
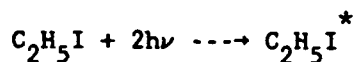
The experimental setup of MPI mass spectrum of C_2H_5I and $n-C_3H_7I$ consists of three parts: a XeCl excimer laser, a molecular beam device, a modified quadrupole mass spectrometer and signal processing system.

For MPI mass spectrum of C_2H_5I molecule, three mass peaks are observed, which belongs to $C_2H_5^+$, I^+ , $C_2H_5I^+$, whereas other mass peaks are too small to be observed. For MPI mass spectrum of $n-C_3H_7I$ molecule, four mass peaks are stronger, which belongs to $n-C_3H_7^+$, I^+ , $C_2H_5^+$ and $C_2H_3^+$.

The dependences of all ionic yields on the parent molecule pressure are found to be linear, as to be expected, indicating that the formation of all ions is an unimolecular process.

The power data are measured for seven ions. For MPI of C_2H_5I , the slopes of the plots of lag ionization current versus lag optical power for $C_2H_5^+$, I^+ , $C_2H_5I^+$ and total ion at low power are 3.88, 3.17, 3.27 and ~3.5 respectively, whereas they become 1.57, 3.17, 1.60 and ~2 at high power, respectively. For MPI of $n-C_3H_7I$, the power indexes of I^+ , $n-C_3H_7^+$, $C_2H_5^+$, $C_2H_3^+$ and total ion at low power are 3.25, 4.15, 3.99, ~5 and ~4, respectively, whereas these indexes are 3.25, 1.63, 1.21, 1.92 and ~2 at high power, respectively.

The experimental results are analyzed in terms of population rate equations for various mechanisms. It is shown that the MPI of C_2H_5I molecule is mainly determined by the two competitive channels



Then neutral fragments C_2H_5 and the I atoms undergo further photo-absorption and ionization. The $C_2H_5^+$ and I^+ ions also come from further absorption and dissociation of parent ions. But the former channel is predominant. For the $n-C_3H_7I$ molecule interacting with XeCl laser radiation, dissociation followed by ionization is the most probable mechanism. It is unlikely that the parent molecule is ionized prior to dissociation.

When C_2H_5I and $n-C_3H_7I$ molecules are irradiated by a XeCl excimer laser beam at 308 nm, one-photon frequency just approaches the A-band

threshold of these molecules, whereas two photons are only resonant with the transition to Rydberg state of C_2H_5I molecule. Therefore MPI-fragmentation mechanisms are obviously different for the two molecules.

References

1. D. H. Parker and R. B. Bernstein, J. Phys. Chem. 86, 61 (1986).
2. A. Gedanken, M. B. Robin and Y. Yafet, J. Chem. Phys. 76, 4798 (1982).

Molecular Model of Multiple-Photon Absorption through
Chaotic and Bistable Steady States

John C. Englund* and Charles M. Bowden

Research Directorate, AMSMI-RD-RE-QP
Research, Development, and Engineering Center
U.S. Army Missile Command
Redstone Arsenal, Alabama 35898-5248

and

Frederic A. Hopf

Optical Sciences Center, University of Arizona
Tucson, Arizona 85721

A simple model¹⁻³ of the multiple-photon excitation of a single molecule has been successful in yielding the experimentally observed fluence dependence of laser-light absorption by SF₆ prior to dissociation. Interestingly, this regime is associated with chaotic dynamics of the molecular modes.

It can be shown that this model also contains time-independent steady-state solutions. We have found by a linear stability analysis that these are either unstable or neutrally stable (centers). In the former case, the chaotic states result. However, in the latter, perturbations give rise to periodic responses (see Fig. 1); hence, the molecular absorption is likewise periodic, and fluence dependence is not predicted. This behavior may also be seen when the molecule is initially in an unexcited state, with periodicity most likely if the unexcited state is near a center. Thus, the model predicts two distinct types of absorption, with that observed dependent upon the system parameters (e.g., the laser frequency).

This model is structurally unstable, however. That is, if an arbitrarily small dissipative term is added, the qualitative nature of the solutions is changed (e.g., centers become nodes). To remedy this, we have investigated a model that differs in having a phenomenological dissipative term in the pump-mode dynamical equation. Among the consequences of this extension are the appearance of stable nodes and limit cycles (see Fig. 2) in place of neutrally stable states. This gains in significance when we consider the time-independent response curve (Fig. 3). The Duffing-like nonlinearity of the model is responsible for the multivalued regions seen here, while the existence of multiple resonances with the background molecular modes is responsible for there being a series of such regions. We have found that these can support hysteresis cycles in the response of the molecule, and hence in its absorption characteristics⁴. This contrasts with the original model, in which the absence of a relaxation mechanism prevents hysteresis from occurring.

The extended model, like the original, exhibits chaotic states (though these are presumably associated with a strange attractor). However, the parameter ranges over which chaos is predicted are narrowed, and may disappear entirely with sufficient dissipation. As was the case before, chaos becomes more likely to occur as the time-independent steady states become farther away from the initial molecular state. Hence, referring again to Fig. 3, we find windows of chaotic behavior between each resonance.

*Work supported by a National Research Council-(MICOM) Research Associateship. Present Address: Department of Physics, Southern Methodist University, Dallas, TX 75275

1. J.R. Ackerhalt, H.W. Galbraith, and P.W. Milonni, Phys. Rev. Lett. 51, 1259 (1983).
2. J.R. Ackerhalt, P.W. Milonni, and M.-L. Shih, Phys. Reports 128, 205 (1985).
3. J.R. Ackerhalt and P.W. Milonni, Phys. Rev. A 34, 1211 (1986).

4. J.C. Englund, C.M. Bowden, and F.A. Hopf, in Optical Chaos, SPIE Vol. 667 (1986).

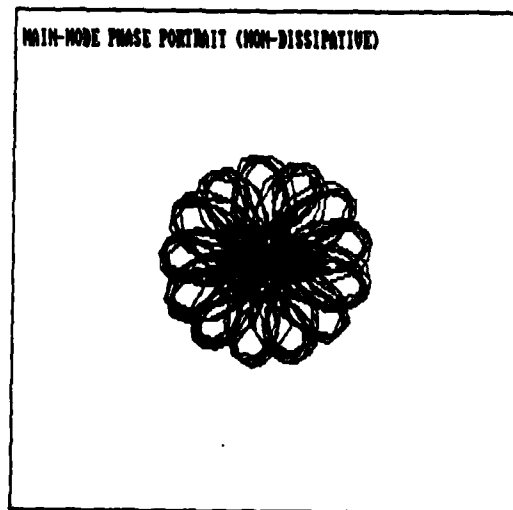


Fig. 1

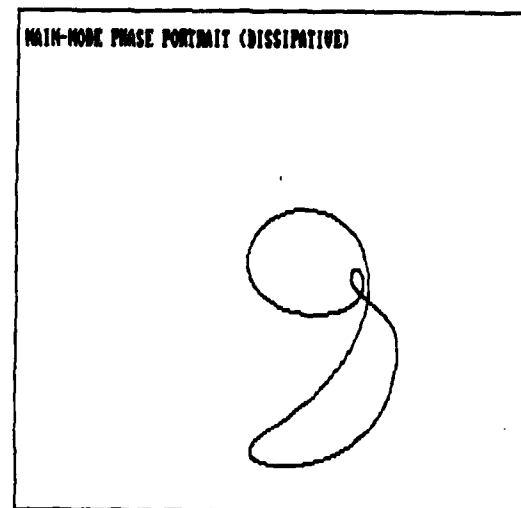


Fig. 2

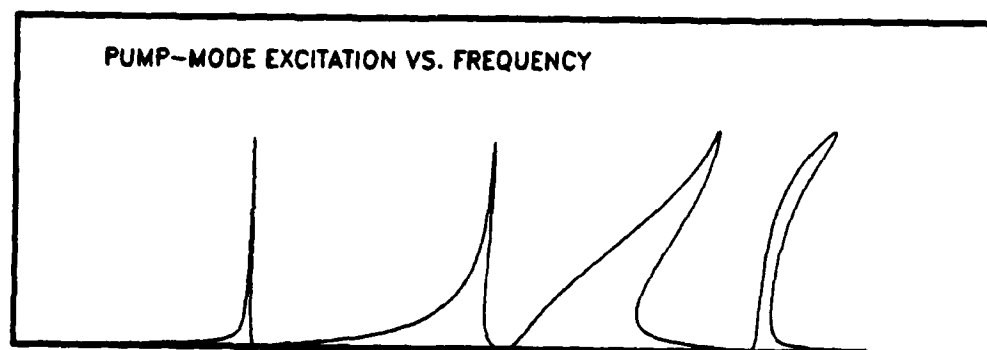


Fig. 3

CLASSICAL TRAJECTORY STUDIES OF IR MULTIPHOTON ABSORPTION
IN DIATOMIC MOLECULES: DESTRUCTION OF COHERENCE BY ROTATION

Robert Parson

Joint Institute for Laboratory Astrophysics, University of Colorado
and National Bureau of Standards, and Department of Chemistry,
University of Colorado, Boulder, CO 80309-0440

In polyatomic molecules, infrared multiphoton absorption is characterized by a rapid destruction of phase coherence between the molecular vibration and the driving field.¹ This accounts for the success of semiphenomenological schemes based upon master equations,^{1,2} which do not, however, address the detailed mechanisms that bring about destruction of coherence. Much theoretical^{3,4,5} evidence confirms the intuitive expectation that molecular rotation plays a crucial role.

The present study is directed towards a simple system motivated by the preceding considerations: a rotating heavy diatomic molecules (IBr) in a strong single-mode field. While this is a caricature of a polyatomic, it is a system which can be analyzed in great detail. Some of the qualitative dynamics should be useful in understanding more complicated systems. The system may also be of experimental interest in its own right.

The Hamiltonian representing IBr in a laser field is:

$$H = \frac{p_r^2}{2\mu} + \frac{L^2}{2\mu r^2} + U(r) + \lambda\mu(r) \cos\omega t \cos\theta \quad (1)$$

where θ is the angle between the field polarization axis and the internuclear axis, L is the total angular momentum, r and p_r the vibrational coordinate and conjugate momentum, and ω the field frequency. $U(r)$ is modelled as a Morse oscillator. At low field strengths the energy and angular momentum oscillate in a correlated fashion. At higher fields intermittent bursts of irregular behavior interrupt this pattern, leading to randomization of the relative phase after a few rotational periods. (The dynamics of a driven non-rotating diatomic at these energies is very regular.)

The results can be interpreted using a nonlinear resonance analysis⁶ of the classical phase space. The familiar first-order selection rule $\Delta m_L = \pm 1$ points to the importance of resonance zones in which the angular momentum changes in lock-step with the vibrational energy; surface-of-section analysis reveals the structure of these zones. The major resonance centers are separated by twice the rotational frequency, so that overlap, and the possibility of chaos, can occur at modest field strengths. In essence, the mechanism reduces to overlap of power-broadened vibration-rotation absorption lines.

Further analysis identifies the irregular bursts with passage of trajectories across a broken-up multidimensional separatrix. The rate at which coherence is destroyed can be related to the frequency at which trajectories encounter the stochastic layer and the time they spend inside it.⁷

The mechanism identified here involves an interplay between vibrational anharmonicity and the nonlinearity implicit in the molecule-field coupling; it resembles "modulational diffusion."⁶ In polyatomics, distinct mechanisms involving vibrational angular momentum have been identified by others.⁴ Future work will assess the relative importance of these processes. Quantum effects, including dynamical tunnelling between vibration-rotation resonances, are also under investigation.

References

1. P.A. Schultz, A.S. Sudbo, D.J. Krajnovich, M.S. Kwok, Y.R. Shen, and Y.T. Lee, *Ann. Rev. Phys. Chem.* **30**, 374 (1979).
2. S. Mukamel, *Adv. Chem. Phys.* **47**, Part I, 507 (1981); D.S. King, *Adv. Chem. Phys.* **105** (1982); M. Quack, *Adv. Chem. Phys.* **50**, 395 (1982).
3. C.D. Cantrell and K. Fox, *Opt. Lett.* **2**, 151 (1978).
4. H.W. Galbraith, J.R. Ackerhalt, and P.W. Milonni, *J. Chem. Phys.* **79**, 5395 (1983).
5. J. Chang and R.E. Wyatt, *J. Chem. Phys.* **85**, 1840 (1986).
6. A.J. Lichtenberg and M.A. Lieberman, Regular and Stochastic Motion, Springer, NY, 1983.
7. M.J. Davis and S.K. Gray, *J. Chem. Phys.* **84**, 5389 (1986).

Acknowledgment: This work was supported by the National Science Foundation under Group Grant PHY-8604504.

EFFECTS OF STRONG E.M. FIELDS IN THE CONTINUUM OF HELIUM ATOM

A. Lami,^{*} N. K. Rahman[†] and P. Spizzo^{*}

^{*}Istituto di Chimica Quantistica ed Energetica Molecolare del C.N.R.
Via Risorgimento 35, 56100 Pisa, Italy

[†]Dipartimento di Chimica e Chimica Industriale, Sezione Chimica-Fisica
Via Risorgimento 35, 56100 Pisa Italy

Double resonance with two discrete states coupled to an autoionizing (or predissociating) state for an atom (or molecule) provides notable features that have been studied theoretically by us.^{1,2}

We now integrate our previous work with ab initio calculations for the helium atom. The two discrete states are the ground state and the 2p3p, the 2p4p or the 2p5p state (all 1P). Each of these three lies far above the ionization threshold but for our purposes can be considered to be discrete states (spin-orbit effects being weak in helium, these states have lifetimes long enough to be considered as discrete states). The resonance lies 2.30653 atomic units from the ground state and therefore, the e.m. fields necessary would be normally a synchrotron source and a laser. All the atomic parameters are calculated utilizing extended configuration interactions and are of the state-of-the-art accuracy.³ We shall be reporting results of our calculations which include ionization probabilities and field-induced structures in the continuum.

1. A. Lami and N. K. Rahman, Phys. Rev. A 34, 3908 (1986) and references therein.
2. A. Lami and N. K. Rahman, in Photons and Continuum States of Atoms and Molecules, eds. N. K. Rahman, C. Guidotti and M. Allergrini (Springer-Verlag, 1987).
3. R. Moccia and P. Spizzo, J. Phys. B: Atom. Molec. Phys. (1987), in press.

COUPLED LOGISTIC MAP AS A MODEL FOR PHOTON ABSORPTION
IN MULTIMODE SYSTEMS

A. Ferretti and N. K. Rahman

Dipartimento di Chimica e Chimica Industriale, Sez. di Chimica-Fisica,
Università di Pisa, Via Risorgimento 35, 56100, Pisa, Italy

Absorption of energy for a molecular system from an extended electromagnetic field have various implications. One of these is that for the energy close to the dissociation threshold, the dynamics is that of chaos. One technique for studying chaotic dynamics involves study of discrete mapping. An application of discrete mapping will be reported which explains why dissociation of molecules will occur at much lower threshold of external field intensities when two modes of a molecule are simultaneously coupled by two external electromagnetic fields. New calculations for coupled logistic map involving Lyapunov exponent, power spectra and spacing distribution will be presented.¹

1. A. Ferretti, N. K. Rahman, Chem. Phys. Lett., (1987), in press.

CLASSICAL COUNTERPARTS OF MULTIPHOTON PHENOMENA

Qi-Chang Su and J. Javanainen
Department of Physics and Astronomy
University of Rochester
Rochester, NY 14627

To elucidate the nature of "quantum chaos", extensive comparisons of the classical and quantum-mechanical dynamics in microwave ionization of hydrogen have been carried out^{1,2}. For higher photon frequencies, quantum mechanical numerical simulations of multiphoton ionization and above-threshold ionization (ATI) have recently been begun.^{3,4} In this work we investigate the possible classical counterparts of multiphoton phenomena.

In analogy to our quantum calculations⁴ we use the classical Hamiltonian

$$H = \frac{p^2}{2} + V(x,t)$$

$$V(x,t) = -\frac{1}{\sqrt{1+x^2}} + xE \sin \omega t. \quad (1)$$

We integrate Newton's equations of motion for particles with various initial energies, including the ground-state energy of the corresponding quantum system $W = -0.6699$. The angular frequency of the classical orbit of such an electron is $\nu = 2.490$.

In the limit of low field frequencies the electron adjusts itself adiabatically to the slowly-varying instantaneous potential $V(x,t)$. Starting from the quantum ground-state energy, the electron can escape from the local minimum of the potential around the origin only if the field strength is $E > 0.12$; see the Figure. However, in the quantum-mechanical system with $\omega = 0.07$ and $E = 0.07$, 10-photon ionization takes place at the finite rate of $2 \times 10^{-2} \omega$. For such parameters multiphoton ionization is a quantum phenomenon with no classical counterpart.

If the driving frequency is increased keeping the field strength fixed, the field forces the electron to execute fast quivering motion around the unperturbed cyclic orbit, but the

electron remains bounded. It is easy to choose parameters such that there is no classical analog of the quantum-mechanical one-photon ionization either.

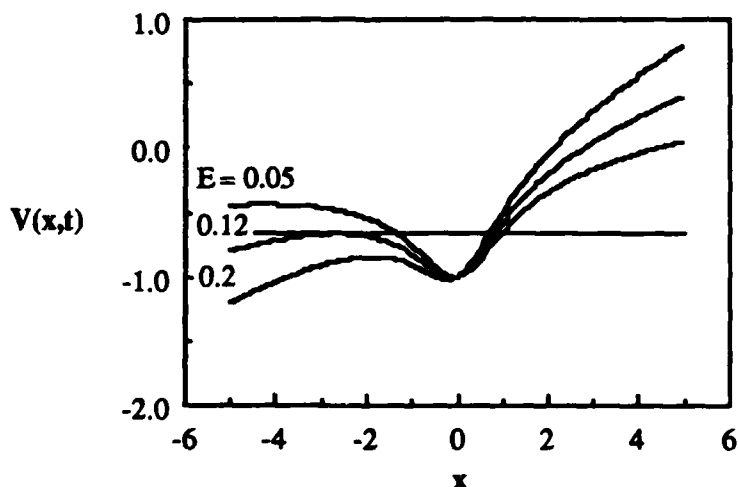


Fig. 1. The effective potential $V(x,t)$ at time $t = \pi/2\omega$ when the time-dependent part is at its steepest, for the three field strengths $E = 0.05, 0.12$ and 0.2 . The horizontal line denotes the ground-state energy $W = -0.6699$. If the potential were static, a particle with this energy could leave the neighborhood of $x = 0$ only for $E > 0.12$.

When the ionization starts from the ground state, classical and quantum-mechanical results have little in common. The situation is known to be different for higher initial energies^{1,2} where the classical motion becomes chaotic for certain field strengths and frequencies. We discuss the intermediate zone between ATI and chaotic microwave ionization.

References:

1. G. Casati, B. V. Chirikov, D. L. Shepelyansky, and I. Guarneri, Phys. Rev. Lett. **57**, 823 (1986).
2. R. V. Jensen, Phys. Rev. A **30**, 386 (1984).
3. K. Kulander, XV IQEC (1987), invited paper FFF3; and private communications.
4. J. Javanainen and J. H. Eberly, submitted for publication.

Multiphoton Dynamics and Quantum Diffusion in Rydberg Atoms*

Shih-I Chu and K. Wang

Department of Chemistry, University of Kansas, Lawrence, KS 66045

We report the first three-dimensional (3D) quantum-mechanical study¹ of the multiphoton dynamics and quantum diffusion phenomena in the microwave-driven Rydberg hydrogen atoms near the onset of classical chaos, using the Floquet theory² and artificial intelligence algorithms.³ The 3D calculations reveal new results which are significantly different from the conventional one-dimensional (1D) quantal calculations⁴ with regard to quantum diffusion phenomena and ionization pathways.

Figure 1 depicts a schematic diffusion pattern at the initial time from the quantum state $n=66$ ($n_1=65$, $n_2=0$ in the parabolic coordinates). Note that the 1D calculations include only the $n_2=0$ ladder, whereas the 3D calculations allow for $n_2 \neq 0$ ladders as well. Figure 2 shows the comparison of 1D and 3D results for the case ω (field freq. in a.u.) = $0.8/n_0^3$, and F (field strength) = $0.025/n_0^4$ ($n_0=66$) for the average quantum number $\langle n(t) \rangle$ as a function of time (from $t=0$ to 50τ (optical cycles)). Note the 1D results mimic very well the 3D results for $t < 15\tau$, but deviation occurs at larger times. Fig. 3 shows the comparison for the total flux (probability) flowing into $n \geq 100$ states, a measure of the ionization probability (field parameters same as Fig. 2). It is seen that apart from the first few optical cycles, the 1D model significantly underestimates the ionization flux at larger times. The most notable result is the dominance of the diffusion flux into the $n_2 = 1$ ladder. The quantum diffusion pattern is shown in more details in Fig. 4, where the populations for each quantum state (n) are plotted at two different times (field parameters same as Fig. 2). These results indicate that except for short times when the main flux remains in the initial $n_2 = 0$ ladder, the flux diffuses quickly into the $n_2 \neq 0$ ladders only a few optical cycles after the field is turned on and that ionization occurs mainly through the $n_2 = 1$ ladder at this frequency and field strength. More detailed results about the frequency and intensity dependent dynamical evolution of Rydberg states will be presented at the conference. Comparison with experimental data⁵ will also be made.

* Supported by D.O.E.

References

1. S.-I. Chu and K. Wang, Phys. Rev. Lett. (submitted).
2. S.-I. Chu, Adv. At. Mol. Phys. **21**, 197 (1985); Adv. Chem. Phys. (1987).
3. J.V. Tietz and S.-I. Chu, Chem. Phys. Lett. **101**, 446 (1983).
4. G. Casati, B.V. Chirikov, I. Guarneri, and D.L. Shepelyansky, Phys. Rev. Lett. **56**, 2437 (1986) and references therein.
5. J.E. Bayfield and L.A. Pinnaduwage, Phys. Rev. Lett. **54**, 313 (1985) and references therein.

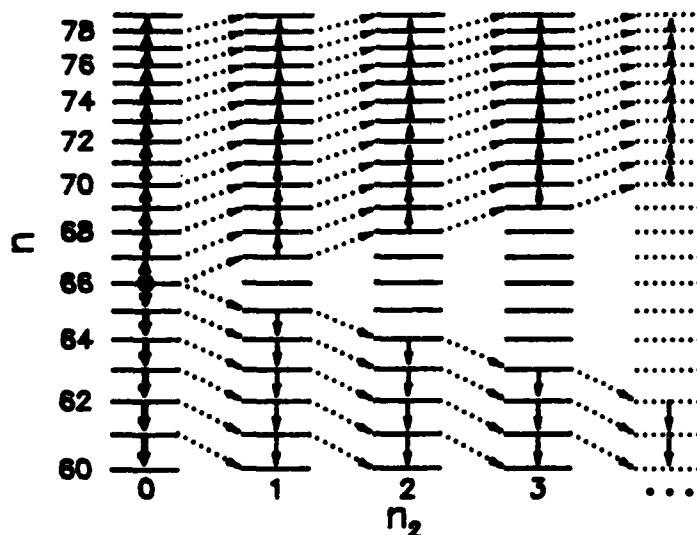


Figure 1

Quantum diffusion pattern at initial times. The initial state is at $n=66$ (principle quantum number) or $n_1=65$, and $n_2=0$.

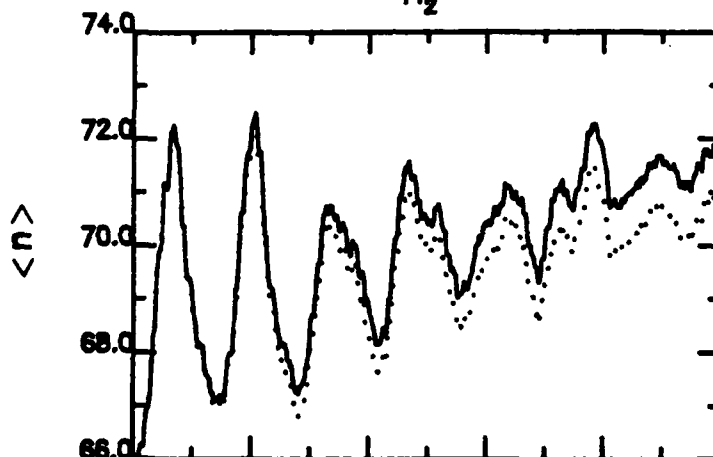


Figure 2

Average quantum number $\langle n(t) \rangle$ as a function of time (0 to 50 optical cycles):

— 3D results
..... 1D results

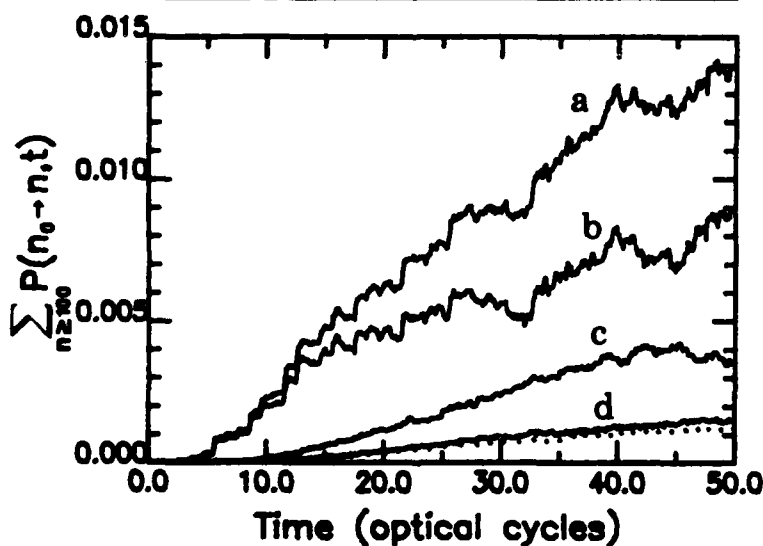


Figure 3

Ionization probability as a function of time. Curve notation :

..... 1D ($n_2=0$ only),
curve a: 3D (total),
curve b: 3D ($n_2=1$),
curve c: 3D ($n_2=2$),
curve d: 3D ($n_2=0$).

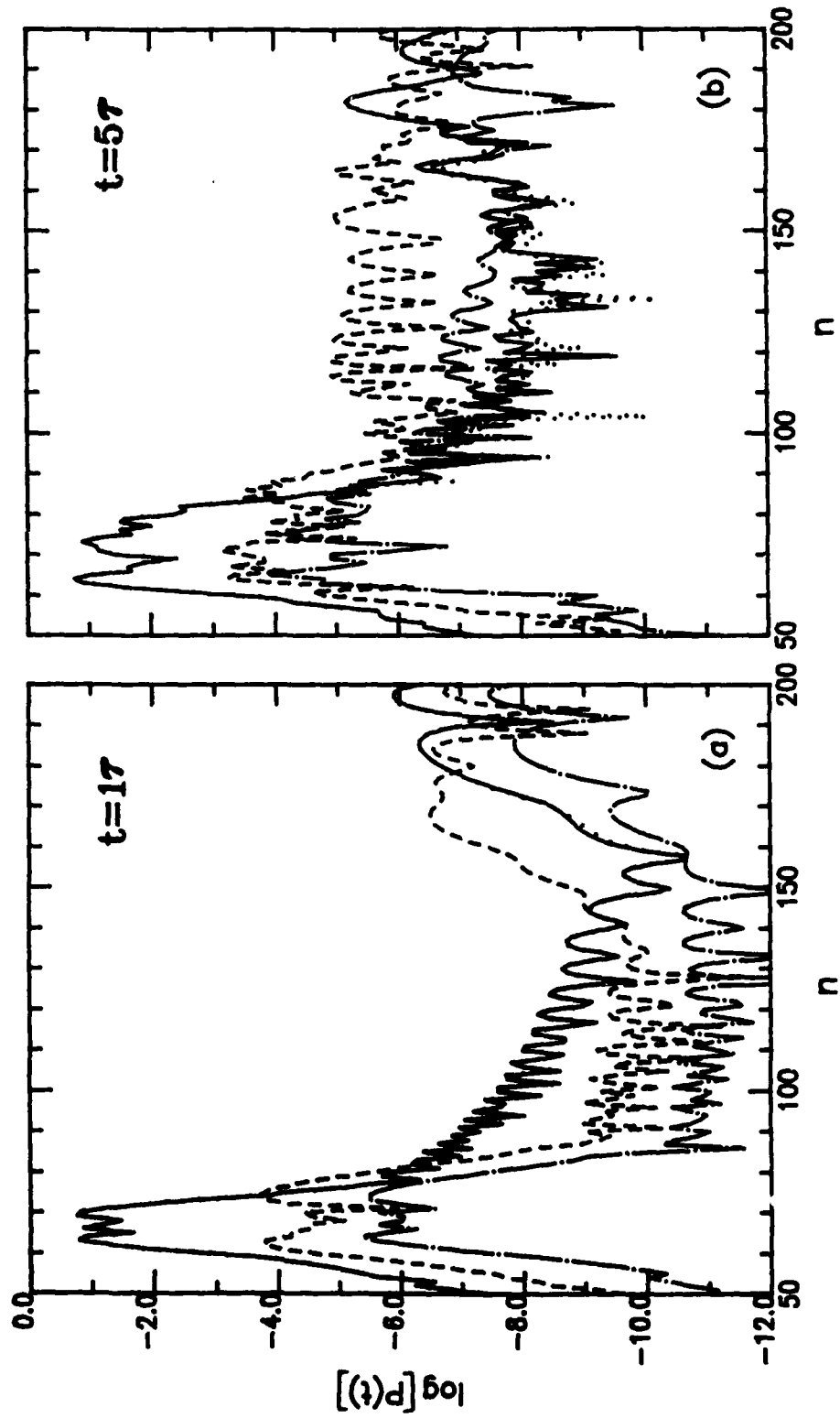


Figure 4. Time-dependent population $P_n(t)$ as a function of quantum number n .

Curve notation: 1D ($n_2=0$ only); — 3D ($n_2=0$);
 ----- 3D ($n_2=1$); —·—·—· 3D ($n_2=2$).

IONIZATION OF ATOMS IN A MAGNETIC FIELD:
THE EFFECT OF CLOSED CLASSICAL ORBITS ON QUANTUM SPECTRA

M. L. Du and J. B. Delos*

Joint Institute for Laboratory Astrophysics
University of Colorado and National Bureau of Standards
Boulder, Colorado 80309-0440

The behavior of quantum systems in which classical motion is irregular or chaotic is poorly understood, and the whole field of "quantum chaos" is marked by confusion and controversy. Important insight comes from experimental measurements of the absorption spectrum of atoms near the ionization threshold.¹ If the atom is placed in a magnetic field, then the absorption spectrum shows sinusoidal oscillations superimposed on a smooth background. These oscillations are correlated with periodic orbits in the system: the "wavelength" (or peak-to-peak energy spacing ΔE_n) of each oscillation corresponds to the period T_n of a classical periodic orbit of the system through the relationship $\Delta E_n = 2\pi \hbar / T_n$. Computational evidence indicates that these systems are classically chaotic, with only isolated, unstable periodic orbits. Why do these orbits produce such phenomena?

We have developed a quantitative theory showing the relationship between closed orbits and the observed oscillations in the spectrum. The theory and calculations are based upon two approximations. (1) Close to the nucleus ($r \lesssim 50$), the effect of the magnetic field is neglected, and the electron wave function corresponds to zero-energy scattering in a Coulomb field. (2) Far from the nucleus ($r \gtrsim 50$) a semiclassical approximation is used. These approximations lead to a simple physical picture. When the atom absorbs a photon, the electron goes into a near-zero energy Coulomb outgoing wave. This wave propagates away from the nucleus to large distances. For $r \gtrsim 50 a_0$ the outgoing wave fronts propagate according to semiclassical mechanics, and

*1986-87 JILA Visiting Fellow. Permanent address: Physics Dept.
College of William and Mary, Williamsburg, VA 23185.

they are correlated with outgoing classical trajectories. Eventually the trajectories and wave fronts are turned back by the magnetic field; some of the orbits return to the nucleus, and the associated waves (now incoming) interfere with the outgoing waves to produce the observed oscillations.

Spectral measurements observe the average oscillator strength density: the transition dipole moment averaged over the small range of energy corresponding to the experimental resolution,

$$\overline{Df}(E) = \left(\frac{2m}{\hbar}\right) \int |\langle \psi_f | D | \psi_i \rangle|^2 (E_f - E_i) \rho(E_f) g(E_f - E) dE_f \quad (1)$$

From the above ideas, we have shown that the observed oscillator strength can be written as a smooth, slowly varying background term plus a sum of sinusoidal oscillations:

$$\overline{Df}(E) = Df_0(E) + \sum_n A_n(E) \sin\left(\int_0^E T_n(E') dE' + \alpha_n\right) \quad (2)$$

The background term $Df_0(E)$ is the oscillator strength density that would be obtained in the absence of an external field. Each oscillatory term in (2) corresponds to a closed orbit of the electron in the combined Coulomb and magnetic fields. Each closed orbit begins and ends at the atomic nucleus. $T_n(E)$ is the transit time for the electron on this orbit. If the spectrum is measured at low resolution, then only the orbits of shortest duration contribute to this sum; orbits of longer duration produce rapidly oscillating terms that average to zero. With increasing resolution, more and more terms become significant, and the spectrum oscillates wildly.

The amplitudes and phases of the oscillations depend upon: (1) the initial state of the system; (2) the polarization of the absorbed light; (3) the initial and final directions of the orbit, as it leaves and returns to the nucleus; (4) the relative stability of the closed orbit, i.e., the divergence of adjacent trajectories from the central closed orbit; (5) the classical action integral $\int \vec{p} \cdot d\vec{q}$ on the orbit, and phase corrections associated with caustics through which the orbit passes.

We show our first results. Because the spectrum itself is wildly oscillatory, direct comparison between theoretical and experimental oscillator strengths is unhelpful. More appropriate for comparison is the Fourier transform of the spectrum, which was obtained in Ref. 1. We show their result compared to our calculated amplitudes in Fig. 1. Very pleasing agreement is obtained for the short-period orbits ($T/T_c \lesssim 4.6$).

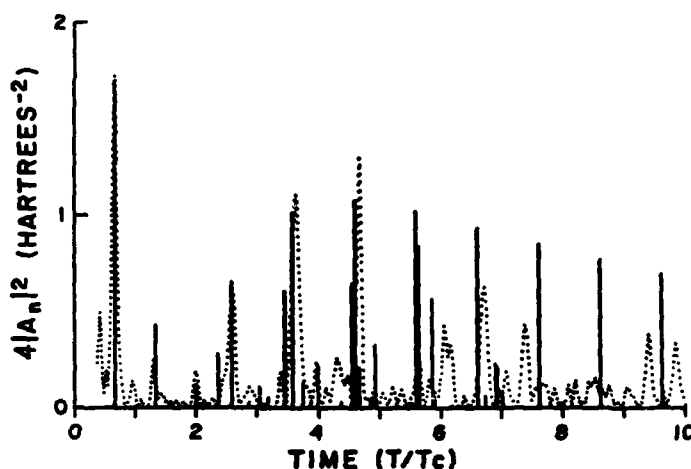


Fig. 1. Heavy lines: amplitudes $|A_n|^2$ associated with closed orbits of duration T_n . Dotted line: Fourier transform of measured absorption spectrum ($1s + 2p_z + \text{ionization}$).

Conclusion. Stable and orderly properties of a quantum chaotic system are associated with closed classical orbits of the system. In particular, observed oscillations in the absorption spectrum of an atom in a magnetic field can be understood quantitatively from properties of these orbits.

This work was supported by NSF.

- ¹K. T. Lu, F. S. Tomkins, and W. R. S. Garton, Proc. Roy. Soc. (London) A 362, 421 (1978). A. R. Edmonds, J. Phys. (Paris) Colloque 31, 71 (1970). A. Holle, G. Wiebusch, J. Main, B. Hager, H. Rottke, and K. H. Welge, Phys. Rev. Lett. 56, 2594 (1986); J. Main, G. Wiebusch, A. Holle, and K. H. Welge, *ibid.*, 57, 1789 (1986).

AUTHOR INDEX

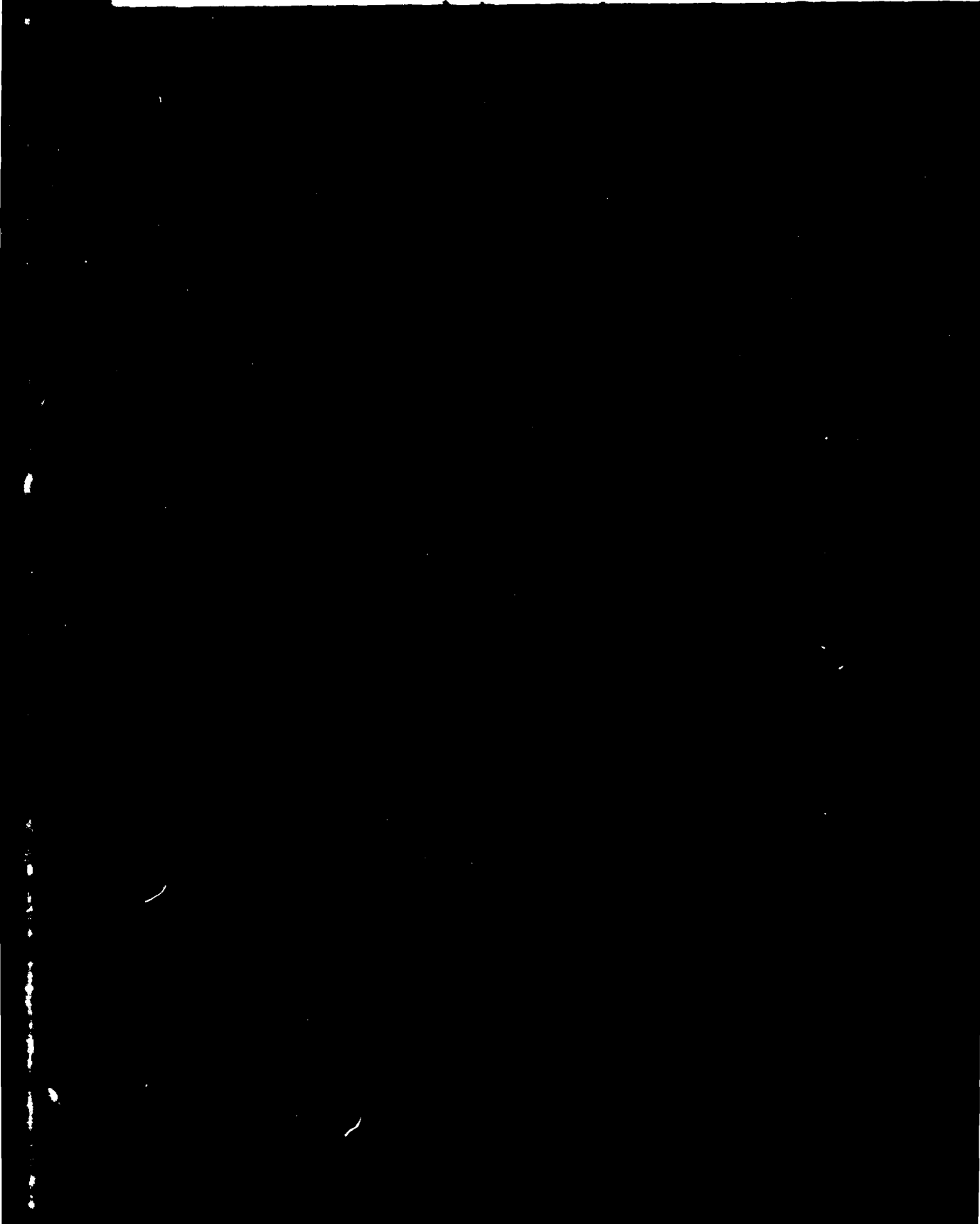
Agarwal, G. S.	137	Codling, K.	63
Agostini, P.	256, 257	Colson, S. D.	13
Alber, G.	213, 216, 278	Compton, R. N.	111, 263, 266
Alford, W. J.	275	Cooke, W. E.	134
Angelie, C.	154	Cooper, J.	278
Appling, J. R.	16	Crance, M.	166
Arnett, K.	84		
Ashfold, M. N. R.	38	Dai, B.	263, 286
		Darack, S.	253
Bachau, M.	172	Dehmer, J. L.	33, 260, 302
Bajic, S. J.	111	Dehmer, P. M.	33, 260, 302
Bandrauk, A.	62	de Lange, C. A.	307
Baravian, G.	221	Delos, J. B.	344
Barker, J. R.	147	Dimou, L.	66
Bashkansky, M.	72	Dixit, S. N.	35
Basile, S.	230	Dodhy, A.	266
Bayfield, J. E.	53	Drabe, K. E.	307
Bayrakceken, F.	322	Dressler, R.	117
Beaudoin, Y.	283	Du, M. L.	344
Beck, K. M.	142	Dubs, R. L.	35
Becker, W.	30		
Bernstein, E. R.	110	Eberly, J. H.	24
Bérsons, I. J.	3	Edwards, M.	233
Bhatt, R.	189	Ehlotzky, F.	192
Biernacki, D. T.	13	Elliott, D. S.	84
Bittner, J.	297	Englund, J. C.	332
Bowden, C. M.	332	Esherick, P.	275
Boyd, R. W.	129	Esposito, F.	313
Brown, T. C.	147	Evans, D. K.	150, 324
Bruzzese, R.	313	Ewart, P.	278
Bucksbaum, P. H.	72	Eyler, E. E.	13
Bunge, C. F.	96		
Burnett, K.	103, 123, 189 190	Faisal, F. H. M.	66, 241
		Fan, J. Y.	305
Campbell, E. M.	78	Fedorov, M. V.	23
Campos, F. X.	10	Fedoseyev, V. N.	89
Capitini, R.	154	Feldmann, D.	18
Casati, G.	58	Feng, B-H	93
Casperson, D. E.	81	Ferrante, G.	69, 230
Chaiken, J.	119, 323	Ferretti, A.	338
Chanda, A.	259	Pink, M. G. J.	163
Chariton, A.	278	Potakis, C.	269, 305
Chen, B.	241	Frasinski, L. J.	63
Chen, K-H	144	Fredin, S.	218
Chewter, L. A.	310	Freeman, R. R.	1, 253
Chin, S. L.	153, 250, 283	Fridell, E.	120
Christian, W.	266, 280	Friedmann, H.	205
Chu, S.-I	236, 341	Fujimura, Y.	42

Ganguly, S.	295	Kaminski, J. Z.	194
Garrett, W. R.	124, 272	Kielich, S.	202
Gauthier, D. J.	129	Kiermeier, A.	107
Gauyacq, D.	218	Knight, P.	155, 211
Gavrila, M.	47, 50, 194, 196	Koenders, B. G.	309
Geusic, M.	253	Kohse-Höinghaus, K.	297
Girard, P.	154	Kompa, K. L.	175
Giusti, A.	169	Körmendi, F. F.	240
Glab, W. L.	300	Koshi, M.	142
Golub, I.	283	Kühlewind, H.	107
Goodale, J. W.	324	Kukliński, R.	90
Gordon, R. J.	142	Kulander, K. C.	158
Grant, E. R.	10	Kupersztych, J.	256
Greenfield, A. C.	123	Kyrälä, G. A.	81
Greenland, P. T.	123, 208, 209	Kyrölä, E.	224
Grobe, R.	7	Lambropoulos, P.	132, 172, 181
Gu, J.	329		257, 263, 266
			286, 289
Habekost, A.	321	Lami, A.	337
Haber, K. S.	10	Landen, O. L.	78
Hadley, G. R.	275	Lane, A. M.	209
Hamilton, M. W.	84	Lau, A. M. F.	87
Han, J.	327, 329	Lee, H. W. H.	139
Han, Q-S	93	Lee, P. H. Y.	81
Harris, S. E.	176	Lee, S.-P.	318
Hart, D. J.	114	Lengyel, V. I.	102
Hatherly, P.	63	Leone, S. R.	117
Hayashi, M.	42	Leónski, W.	202
Heideman, H. G. M.	97	Lewenstein, M.	247
Henle, W. A.	216	L'Huillier, A.	160, 257
Hepburn, J. W.	114	Li, S.	327, 329
Hessler, J. P.	300	Lin, S. H.	42
Hopf, F. A.	332	Lindberg, M.	224
Horani, M.	218	Liu, H.	327, 329
Hossenlopp, J. M.	323	Lompre, L. A.	256
Hou, M-Y	93	Lutz, H. O.	71, 241
Huang, H.	24		
		Malakian, Yu. P.	128
Ivanco, M.	150, 324	Malcuit, M. S.	129
		Maquet, A.	196
Jacobs, V. L.	291	Matthias, E.	120
Janjušević, M.	44	Mazur, E.	144
Javanainen, J.	4, 339	McAlpine, R. D.	150, 324
Jetzke, S.	241	McCurdy, C. W.	47
Johnson, W. R.	163	McKoy, V.	35
Jones, L. A.	81	Meacher, D.	278
Judish, J. P.	272	Meier, U.	297
Jungen, Ch.	218	Mercouris, T.	239
Just, Th.	297	Messina, G.	69

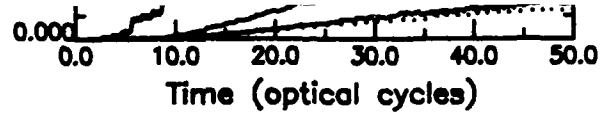
Meyer, H.	117	Rudolph, H.	35
Milchberg, H.	253	Ryabov, E. A.	61
Milomni, P. W.	56	Rzatewski, K.	7, 90
Mittleman, M. H.	44		
Moore, M. A.	272	Sacks, R.	92
Mostowski, J.	90, 104	Sander, M.	310
Mourou, G. A.	178	Sapers, S.	316
Muller, H. G.	20	Scanzano, P.	241
Müller-Dethlefs, K.	310	Schappert, G. T.	81
		Schlag, E. W.	107
Naaman, R.	316	Schlicher, R. R.	30
Needels, J.	236	Schumacher, D. W.	72
Neusser, H. J.	39, 107	Scully, M. O.	30
Nicolaides, C. A.	239	Semmler, O.	120
Nielsen, H. B.	120	Sha, G.	175
Nomura, Y.	42	Shah, M.	190
		Shakeshaft, R.	233
Offerhaus, M. J.	50	Shao, Y-L	93
O'Halloran, M. A.	33, 302	Shi, Y-B	93
Olsen, T.	266	Shore, B. W.	92, 226
Oostwal, M. G.	307	Smith, A. V.	275
		Smith, S. J.	84
Parker, J.	229	Solimeno, S.	313
Parson, R.	335	Spinelli, N.	313
Patsilinacou, E.	305	Spizzo, P.	337
Payne, M. G.	272	Spong, J. K.	176
Perry, M. D.	78	Stockdale, J. A. D.	111, 263, 266
Petite, G.	2, 256, 257		269
Pindzola, M. S.	263	Story, J. G.	134
Piroux, B.	69, 189, 211	Stroud, C. R. Jr.	229
Pont, M.	47, 50	Su, Q.-C.	339
Pratt, S. T.	33, 260, 302	Sultan, G.	221
Proch, D.	175	Szöke, A.	75, 78
Proctor, M. J.	269		
		Tanas, R.	202
Radmore, P.	155	Tang, X.	132, 233, 257
Rahman, N. K.	337, 338		289
Rai Dastidar, K.	292, 295	Tarzi, S.	155
Rai Dastidar, K. T.	292	Taylor, A. J.	81
Rapoport, L. P.	157	Tepper, P.	120
Ravi, S.	137	Tomkins, F. S.	33
Reck, G. P.	318	Trippenbach, M.	7, 104
Reif, J.	120	Trombetta, F.	69, 230
Reiss, H. R.	27, 199		
Rhodes, C. K.	179	Ulbrich, H.	321
Riedle, E.	39		
Ritsch, H.	216	Vaida, V.	316
Rosen, A.	120	Van, C. L.	104
Roso-Franco, L.	24	van de Ree, J.	194
Rothe, E. W.	318	van Linden van den	
Rottke, H.	18	Neuvell, H. B.	20
Rozsnyai, B. F.	291	Van Woerkom, L. D.	134

Varró, S.	192
Veniard, V.	196
Verma, R. D.	259
von Weyssenhoff, H.	321
Walet, N.	47
Waller, I. M.	114
Walther, H.	177
Wang, J.	144
Wang, K.	341
Watanabe, S.	99
Welge, K. H.	18, 180
Wenhöner, M.	18
Wendin, G.	160
Wessel, J. E.	139
Westin, E.	120
White, M. G.	16
Wiedmann, R. T.	10
Wieringa, D. M.	307
Wilson-Gordon, A. D.	205
Wódkiewicz, K.	30, 82
Wolff, B.	18
Wu, C.	327, 329
Wunderlich, R. K.	272
Wyatt, R. E.	60
Wynne, J. J.	125
Yergeau, F.	256
Yerram, M.	147
Yin, R. Y.	236
Young, J. F.	176
Zakrzewski, J.	244
Zei, D.	263
Zellweger, J.-M.	147
Zhu, Q-S	93
Zoller, P.	163, 169, 213
	216
Zwanziger, J. W.	10
Zyczkowski, K.	244

DATE
FILMED
3-8

3. K. Kulander, XV IQEC (1987), invited paper FFF3; and private communications.
 4. J.Javanainen and J. H. Eberly, submitted for publication.
- 

- (1987).
3. J.V. Tietz and S.-I. Chu, Chem. Phys. Lett. 101, 446 (1983).
 4. G. Casati, B.V. Chirikov, I. Guarneri, and D.L. Shepelyansky, Phys. Rev. Lett. 55, 2437 (1986) and references therein.
 5. J.E. Bayfield and L.A. Pinnaduwa, Phys. Rev. Lett. 54, 313 (1985) and references therein.



curve d: $3D (n_2=0)$.

$\log[P(t)]$

0
-2
-4
-6
-8
-10
-12

1986-87 JILA Visiting Fellow. Permanent address: Physics Dept.
College of William and Mary, Williamsburg, VA 23185.

